Navigating Global Food Networks: Resilience and Sustainability in Present and Future Food Systems

SHRUTI JAIN

Reuben College

University of Oxford

A thesis submitted for the degree of

Doctor of Philosophy

Michaelmas term, 2025

Supervised by Samuel Fankhauser and Radhika Khosla and Michael Clark

For the animals –
may this work contribute, however modestly,
to kinder food systems.

Acknowledgements

This thesis marks the end of my DPhil journey at Oxford. This work was generously supported by the Oxford–Reuben Interdisciplinary Scholarship in Environmental Change, for which I am deeply grateful, and it reflects the support of several incredible people who made the work possible.

I am immensely grateful for the invaluable support of my supervisor Sam Fankhauser. Thank you for your guidance, your clarity, and for consistently helping me find the strongest version of the argument I was trying to make. Throughout the DPhil, you were generous with detailed comments on my drafts and thoughtful feedback that sharpened both the structure and substance of the work. You were also consistently supportive of my broader development as a researcher, sharing opportunities, encouraging collaboration, and backing me when I explored new projects, roles, and directions. There were moments during this DPhil when I questioned whether I had what it takes, and your steady encouragement during those times helped me regain confidence and keep moving forward.

I am equally grateful to my supervisor Michael Clark, who was always generous with his time and support. Your expertise has been invaluable to this research, and you were always willing to share it openly. Thank you for being so engaged with my work – offering feedback when it was most needed, connecting me with collaborators and co-authors, and creating opportunities for me to contribute my own expertise. I also want to thank Radhika Khosla for being part of my supervisory team and for the perspective you brought.

I am grateful to Saher Hasnain and Jasper Verschuur for their friendship and mentorship. Saher, I am thankful for the care you took as my college advisor and beyond, including our walks where we talked through everything from research to the practicalities of being in the UK. Jasper, thank you for the brainstorming

sessions at the start of the DPhil; one of those conversations directly sparked the idea that became my third paper, and I remain grateful for your generosity with your time and ideas.

I am also grateful to my co-authors, Jim Hall, Savka Akester, Joe Kennedy, E.J. Milner-Gulland, Mike Rayner, Ricki Runions, and Peter Scarborough, for their collaboration, which shaped key parts of this work. I also want to acknowledge Monica Zurek, Douglas Gollin, and Paul Behrens, each of whom engaged with my work at different points of my DPhil. Thank you for reading carefully, asking incisive questions, and offering feedback that strengthened the thesis.

I'm grateful to the friends and colleagues who helped me find community at Oxford and made the experience richer. Vrinda, Yi Fan, Pippa, Liam, Dasom, Mark, Jess, Ben, Xiang, Poornima, Min, Hayden, Pam, Fulvia, Sugandha, thank you for the conversations, the solidarity around deadlines, and the informal check-ins that mattered more than they probably seemed. I am also grateful to the Sustainable Food Systems research cluster and the Future of Food network for the camaraderie they provided. Working alongside others grappling with related questions made the research feel far less solitary, and I valued the steady exchange of ideas, feedback, and encouragement that helped sustain momentum throughout the DPhil.

I would also like to express my gratitude to the administrative staff and faculty members at the School of Geography and the Environment and at Reuben College. Your support and guidance have been invaluable in navigating the DPhil.

During the final, and at times particularly intense, stages of writing up, I was fortunate to be supported by colleagues in my postdoctoral role, Oliver Taherzadeh, Aysegül Çelik, and Hongyi Cai, thank you for the kindness, flexibility, and encouragement you showed while I was finishing the thesis alongside the postdoc. That support made a tangible difference to getting this over the line.

Long before the DPhil began, and throughout it, I benefited from mentors who encouraged me to believe that a doctorate was within reach. I am especially grateful to Solomon Hsiang, who first urged me to pursue research and consider applying for a doctoral program during my master's, and whose encouragement has

stayed with me ever since. I also want to thank David Lobell and Karen Byrnes, for their mentorship in the years leading up to the doctorate, and to Talip Kilic and Sydney Gourlay for the opportunity to work alongside them during my DPhil, which provided perspective, collaboration, and support as the thesis came together.

I also owe deep thanks to Purnima, a friend of many years. Thank you for your constancy, perspective, and quiet encouragement over the years, long before this thesis existed and throughout the process of completing it. Your presence has been a steady reminder of who I am beyond the work.

I am profoundly grateful to my mother, Seema, and my father, Sushil. Your belief in me never wavered, even when the path I was taking felt uncertain or distant. Everything I have been able to do rests on the love, sacrifices, and values you have given me, and I carry that with me in all that follows.

Finally, I dedicate this work to Saurabh and Coffee. Saurabh, thank you for being my partner throughout this journey, for being my loudest cheerleader, and for the everyday acts of care that sustained me through the most demanding stages of the DPhil. And my sweetest dog Coffee, thank you for the comfort, routine, and joy you brought to every day – your presence made even the hardest moments feel lighter.

Abstract

Global food systems face mounting pressures from climate change, evolving dietary preferences, and shifting trade policies, all of which threaten food security. Understanding how food moves from production to consumption, and identifying the vulnerabilities and environmental impacts embedded in these distribution networks, is essential for building resilient and sustainable food systems. Despite this necessity, there remains substantial empirical uncertainty around the structure of food flows at fine spatial scales, the environmental footprints of the foods we consume, and how future changes in diets, climate, and trade policy may reshape global food systems. In this doctoral thesis, I present three papers that advance this understanding.

In Paper 1, I develop a novel methodological framework to map global cereal flows at subnational scales across 3,536 regions in 195 countries, revealing substantial heterogeneity in regional dependencies and identifying concentration patterns that expose vulnerabilities in cereal flow networks. In Paper 2, I estimate the environmental footprints of approximately 475,000 retail food products across 74 countries, demonstrating that the relative ranking of food categories by environmental impact is consistent across regions – with products containing animal-derived ingredients, coffee, and nuts consistently exhibiting the highest footprints – but that ingredient sourcing can also meaningfully affect a product's footprint. In Paper 3, I model how bilateral trade flows for 32 crops across 153 countries may evolve through 2050 under alternative dietary, climate, and trade policy scenarios, finding that accommodating large-scale dietary transitions under climate change would require substantial restructuring of global food trade, and that more liberalized trade regimes increase reliance on a smaller set of foreign suppliers alongside efficiency gains.

Overall, I argue that more informed decision-making amid the coupled challenges of climate mitigation and food systems transformation requires attention to several

interrelated dimensions of food systems. Among these are the balance between local self-sufficiency and global connectivity; the fact that environmental impacts are driven largely by what is consumed, but also by how food is produced; and the ways in which dietary, climate, and policy pathways may reshape global food flows.

Contents

List of Figures

List of Tables

1 Introduction

Global food systems lie at the heart of the sustainability and climate crisis. On one hand, climate related extremes are increasingly disrupting agricultural productivity and food supply chains, with more frequent production losses undermining food security (Skea et al., 2022). On the other hand, the global food system is itself a major driver of climate and environmental change, accounting for up to a third of anthropogenic greenhouse gas emissions (Crippa et al., 2021; Foley et al., 2011). Furthermore, globalization and agricultural trade mean that a shock to food production in one region can rapidly propagate across borders (Centeno et al., 2015; Wellesley et al., 2017), while dietary transitions, whether driven by rising incomes or by health and sustainability goals, would reshape both demand patterns and supply chain configurations (Gouel & Guimbard, 2019; Pingali, 2007; Willett et al., 2019). These interconnected dynamics, where food systems are simultaneously vulnerable to climate change and a cause of it, create both challenges and opportunities for building resilient and sustainable food futures.

Addressing this dual challenge requires understanding how food moves from where it is produced to where it is consumed. International food trade has more than doubled in the last two decades and is now critical to global food security (FAO, 2022). For many countries, trade is the primary mechanism through which food deficits are met (Kinnunen et al., 2020). Trade can buffer local production

shocks and serve as an adaptation mechanism under climate change (Janssens et al., 2020). Yet trade networks can also transmit and amplify shocks through geopolitical disruptions, extreme weather events, and disease outbreaks, especially when disruptions occur in key producing regions (Centeno et al., 2015; Puma et al., 2015; Wellesley et al., 2017). Understanding the structure of food flows, i.e., where food comes from, where it goes, and which links are most critical, is therefore essential for identifying vulnerabilities and building resilience.

Yet our understanding of food flows remains limited. Most prior research on food trade has focused on international trade at national scales (Sartori & Schiavo, 2015; Vishwakarma et al., 2022; Y.-T. Zhang & Zhou, 2022), but this perspective obscures substantial heterogeneity within countries (Lin et al., 2019; Pandit et al., 2023). Subnational resolution can enable a more accurate assessment of local exposure to supply disruptions, and allocation of consumption-related environmental impacts. The first paper of this thesis addresses this gap by developing a novel methodological framework to map global cereal flows at subnational scales, revealing the hidden geography of food distribution and its implications for resilience.

Alongside the structure of food flows, we must also understand the environmental burdens these impose. The environmental footprint of food systems spans greenhouse gas emissions, land use change, water use, nutrient pollution, and biodiversity loss (Foley et al., 2011). The environmental cost of producing the same goods can be highly variable, indicating substantial mitigation opportunity on the production side (Poore & Nemecek, 2018). At the same time, even the lowest-impact animal products typically have higher impacts than those of plant-based substitutes, suggesting that dietary change on the consumer side can have substantial positive effects (Poore & Nemecek, 2018). A critical question then, is whether impacts are driven primarily by what people eat or by where and how its ingredients are sourced.

Answering this question requires rigorous data on the environmental footprints of food products, accounting for both product composition and ingredient sourcing. Such data would enable retailers to compare products consistently, procurement teams to set evidence-based targets, policymakers to design effective regulation,

and consumers to make informed choices (El Bilali & Allahyari, 2018). Yet most research has quantified footprints of agricultural commodities rather than the multi-ingredient packaged foods that dominate many modern retail environments (Clark et al., 2022; Poore & Nemecek, 2018; Sala et al., 2017). The second paper of this thesis addresses this gap by estimating the environmental footprints of 475,000 retail food products across 74 countries, and assessing the contribution of product composition and ingredient sourcing to these impacts.

Beyond current patterns, food flows will be reshaped by forces already in motion, such as climate change, population growth, urbanization, land-use competition, and evolving dietary preferences (Godfray et al., 2010; Nelson et al., 2014; Springmann et al., 2018; Tilman et al., 2011). Climate change will unevenly affect regional crop productivity (Gaupp et al., 2019; Rezaei et al., 2023). Simultaneously, socio-economic growth across emerging economies towards more diverse diets that often include greater consumption of animal products (Pingali, 2007), or global transitions towards healthier and more sustainable diets (Willett et al., 2019) would reallocate demand across commodities. Trade policy regimes will further shape how production and consumption are spatially distributed and how efficiently surpluses reach deficit regions.

The interaction between these forces will determine the future geography of food production and trade. Yet the literatures on climate impacts on agriculture (Gaupp et al., 2019; Havlík et al., 2014; Rezaei et al., 2023; Robinson et al., 2015), dietary transitions (Gouel & Guimbard, 2019; Springmann et al., 2018; Willett et al., 2019), and trade as an adaptation mechanism under climate change (Gouel & Laborde, 2021; Janssens et al., 2020) have largely proceeded separately. The third paper of this thesis addresses this gap by developing an integrated modelling framework that projects bilateral trade flows for 32 crop groups across 153 countries through 2050, under alternative combinations of dietary transitions, climate pathways, and trade policy regimes.

Together, these three papers provide a comprehensive examination of global food systems across spatial scales, food system activities, and temporal dimensions. The

first paper reveals the hidden structure of food flows, identifying where vulnerabilities lie. The second paper quantifies the environmental burdens these flows carry, decomposing impacts into actionable components. The third paper projects how these systems may evolve, identifying the forces that will matter most. The thesis moves from diagnosis to prognosis, from understanding the current state of food systems to anticipating their future trajectories (Figure 1.1).

To pursue these questions, I employ a range of quantitative approaches including machine learning and network analysis to capture the topology of food flows, life-cycle assessment and Monte Carlo analysis to measure environmental burdens through supply chains, and partial equilibrium modelling to simulate trade patterns under future scenarios. These methods allow me to move beyond aggregate statistics to reveal the spatial heterogeneity, supply chain complexity, and scenario-dependent uncertainty that characterise global food systems.

Together, these three papers offer complementary perspectives on global food systems. Paper 1 reveals that national-level statistics obscure substantial subnational heterogeneity in food flows, with implications for how we assess vulnerability. Paper 2 shows that while dietary composition is the primary driver of environmental footprints, sourcing decisions matter enough to warrant attention from supply chain interventions. Paper 3 finds that achieving dietary transitions under a changing climate requires global food trade to reshape significantly over the coming decades, and that trade liberalization involves trade-offs between efficiency and concentration. While each paper addresses a distinct question, these findings underscore the need for integrated approaches that align dietary guidelines, agricultural investment, and trade policy to build equitable and sustainable food futures.

1.1 Thesis outline

In Chapter 1, I outline the overall motivation of my doctoral thesis. I discuss why understanding global food flows and their implications is crucial for building resilient and sustainable food systems. After this outline, I present a review of the relevant

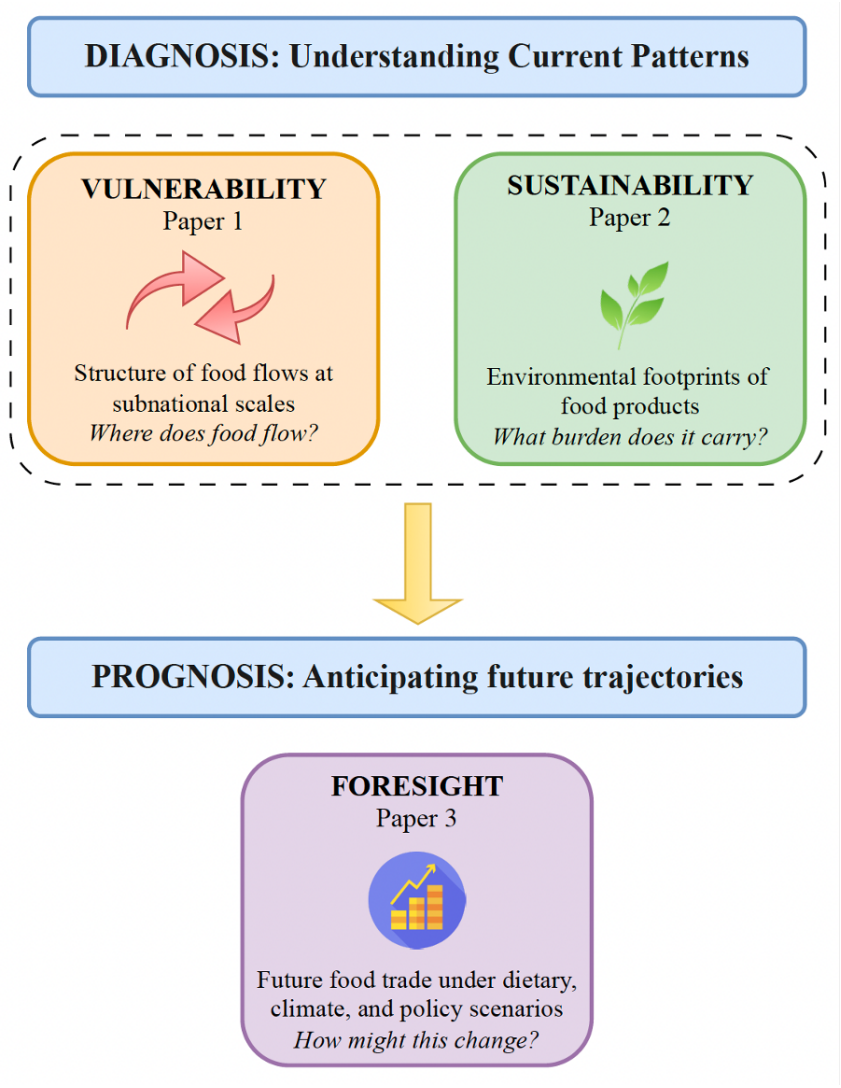

Figure 1.1: Structural overview of doctoral thesis

literature that situates the three papers within broader scholarly debates on food systems resilience, environmental impacts of food, and future food system scenarios.

In Chapters 2, 3, and 4, I present three individual pieces of research that tackle different facets of the food systems challenge. Paper 1 has been submitted to *Environmental Research: Food Systems*. Paper 2 is ready to be submitted to *Proceedings of the National Academy of Sciences*. Paper 3 will be submitted to *Nature Food* after incorporating co-author feedback.

In **Paper 1**, I present a paper that develops a novel methodological framework integrating machine learning and data harmonisation algorithms to map global cereal flows at subnational scales. The paper models international and domestic cereal

flows across 3,536 first-level administrative regions in 195 countries, identifies critical nodes and links in cereal distribution networks, and quantifies concentration patterns that reveal vulnerabilities to production and market shocks. The analysis reveals substantial heterogeneity in regional dependencies on domestic versus international food flows, with implications for food systems resilience.

In **Paper 2**, I present a co-authored paper that estimates the environmental footprints of approximately 475,000 retail food products across 74 countries. The paper combines machine learning-based product categorisation, ingredient composition estimation, and life cycle assessment data weighted by supply chain sourcing patterns to quantify impacts across five environmental indicators: land use, greenhouse gas emissions, biodiversity loss, eutrophication, and water stress. The analysis demonstrates that ingredient composition remains the dominant driver of environmental impacts – with products containing animal-derived ingredients, coffee, and nuts consistently exhibiting the highest footprints – but that ingredient sourcing can also meaningfully affect a product's footprint, suggesting supply chain interventions can complement dietary shifts.

In **Paper 3**, I present a co-authored paper that models how bilateral trade flows for 32 crops across 153 countries may evolve through 2050 under alternative dietary transitions, climate pathways, and trade liberalization regimes. The paper employs a spatial price equilibrium model to project future production, consumption, and bilateral trade flows under 20 scenario combinations. The analysis finds that accommodating large-scale dietary transitions would require substantial restructuring of global food trade, and that this restructuring interacts with climate impacts on yields and trade policy regimes in complex ways. Trade liberalization, meanwhile, involves trade-offs between efficiency gains and increased import concentration.

Finally, in Chapter 5, a brief Conclusion is presented where I summarise the main insights that the collective work of this thesis has yielded. The individual pieces of work combined in this thesis illustrate that there is significant value in examining food systems across multiple scales and dimensions. The thesis demonstrates that

building resilient and sustainable food systems requires understanding the interplay between local self-sufficiency and global connectivity, recognising that environmental impacts are shaped primarily by what we eat but also by how it is produced, and coordinating dietary guidelines with trade policy to navigate the restructuring of global food networks that dietary transitions will entail.

1.2 Literature Review

This literature review situates the three papers within the broader scholarly context, organised around three themes that correspond to each paper. Each section reviews the relevant literature, identifies gaps, and explains how the corresponding paper addresses them.

Before proceeding, it is useful to define the key concepts that frame this thesis. *Food systems* include all activities associated with food production and utilization as seen in Figure 1.2 (Woodhill & Quak, 2019). These activities are influenced by the institutional norms they operate within, and by activities conducted under any supporting sectors such as logistics or communication. Moreover, they are influenced by their natural, social, and economic environments, referred to as drivers. At the same time, food systems generate outcomes such as food security, environmental and economic impacts. This framework demonstrates the interconnected nature of food systems activities, drivers, and outcomes.

Food systems are responsible for 21-37% of anthropogenic greenhouse gas emissions, with agricultural production accounting for the majority of this, and other activities in the food system such as processing and transport accounting for the remainder (Crippa et al., 2021; Van Berkum et al., 2018). At the same time, environmental conditions significantly impact food systems activities. Rising temperatures, changing rainfall patterns, extreme weather events such as droughts and floods, and increased pests and diseases, can negatively impact crop production (Baas et al., 2015; Fisher et al., 2002; Lesk et al., 2016; Rosenzweig et al., 2001). Extreme humidity can have a negative impact on food while it is in storage; floods can damage transport networks that distribute food, which in turn can increase

price volatility in markets and cause consumers to seek food substitutes (Davis et al., 2021). From a socio-economic perspective, agri-food is the world's largest economic sector with more than 2 billion people working in the food system. In emerging and developing countries in particular, agriculture continues to be an important livelihood and social safety net. Hence, as the demand for food grows due to rising populations amid economic development and urbanization, achieving food security in a sustainable manner requires food systems to increase the supply of safe, healthy food, in an inclusive manner, while staying within environmental limits (Van Berkum et al., 2018).

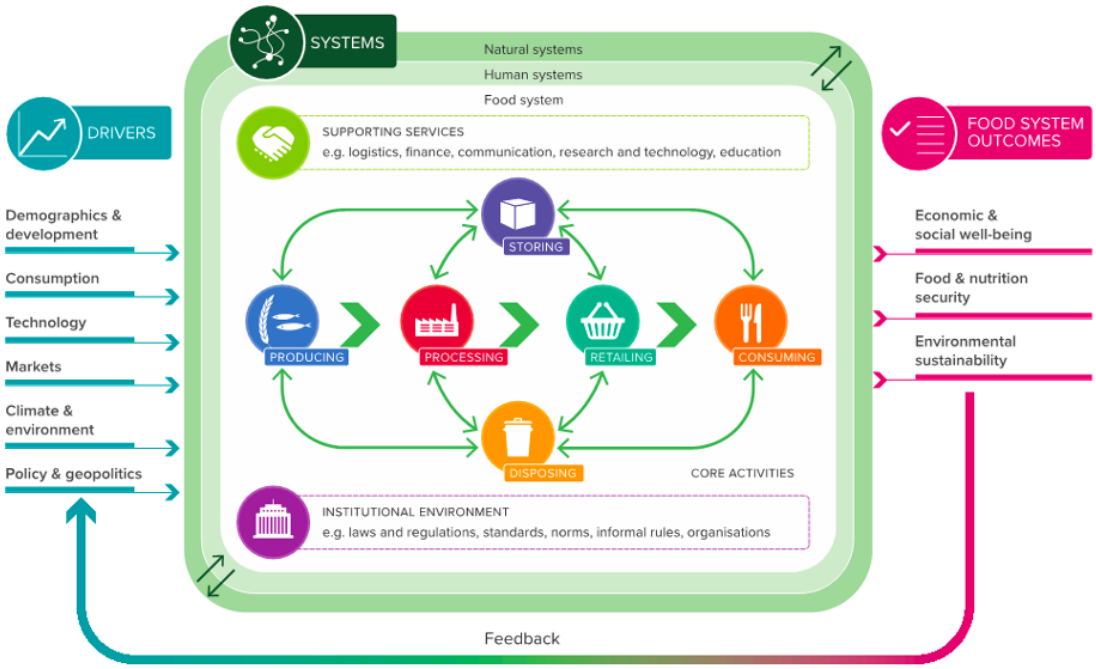

Figure 1.2: Food systems framework as defined by Woodhill and Quak (2019)

Food systems resilience can be defined as the capacity of a food system to provide sufficient, appropriate, and accessible food to all in the face of various and even unforeseen disturbances (Tendall et al., 2015). This definition encompasses the complexity of food systems and discourages enhancing resilience at the expense of negative outcomes like food insecurity or environmental degradation (Zurek et al., 2022). Food systems face two types of threats: shocks, which are abrupt events such as extreme weather, disease outbreaks, or geopolitical disruptions; and stresses,

which are longer-term drivers such as climate change, demographic shifts, and biodiversity loss (Ingram & Zurek, 2019; Zurek et al., 2022). These threats can interact and propagate through interconnected supply chains.

This thesis addresses both types of threats. Paper 1 examines resilience to shocks by mapping the current structure of food flows and identifying concentration patterns and dependencies that could amplify or transmit disruptions. Paper 3 examines resilience to stresses by exploring how food systems may need to transform under long-term drivers including climate change, dietary transitions, and trade policy shifts. Paper 2 complements the two by quantifying the environmental burdens embedded in current food flows, burdens that sustainability concerns may require us to reduce.

Food systems sustainability refers to the capacity of food systems to deliver food security and nutrition without compromising the economic, social, and environmental bases that generate food security for future generations (Nguyen, 2018). Sustainability thus requires managing the environmental footprint of food systems, including greenhouse gas emissions, land use, water consumption, nutrient pollution, and biodiversity loss, while continuing to meet nutritional needs.

Additionally, this thesis uses several trade-related concepts in a specific, operational sense. *Concentration* refers to the degree to which trade flows within a network are unevenly distributed across a limited number of nodes, and is quantified using standard concentration metrics applied to bilateral trade flows. Import concentration denotes this property from the perspective of the importer, capturing the extent to which a country or region relies on a narrow set of external suppliers. Concentration risk describes the potential vulnerability that may arise when high concentration increases exposure to supply disruptions affecting key trading partners. *Trade liberalization*, as used in this thesis, does not represent specific policy instruments such as tariffs or trade agreements, but rather a modelling assumption about the degree of freedom in international sourcing. Low trade liberalization constrains countries to maintain higher self-sufficiency and caps reliance on individual exporters,

while high trade liberalization allows production and trade patterns to adjust more freely to comparative advantage.

1.2.1 Vulnerability: Mapping food distribution

Food systems are vulnerable to a range of shocks that can disrupt the flow of food from production to consumption. Climate-related extremes like droughts, floods, and heatwaves are increasingly affecting agricultural productivity, with evidence suggesting that the frequency and intensity of such events is rising under climate change (Skea et al., 2022). Critically, production shocks are not independent across regions. Gaupp et al. (2017) found that historically observed wheat yield deviations in five major breadbaskets (United States, Argentina, India, China, and Australia) were interdependent, meaning that shocks in one region often coincide with shocks in others. Beyond climate, food systems face shocks from disease outbreaks, geopolitical conflicts, trade policy disruptions, and financial market volatility. The COVID-19 pandemic and the Russia-Ukraine war demonstrated how shocks can cascade through global food supply chains, disrupting trade flows, spiking prices, and threatening food security in import-dependent regions (Laborde et al., 2020; Lang & McKee, 2022; Salih et al., 2020).

The role of trade and transport in food distribution

Studies have examined the extent to which populations depend on trade and transport infrastructure to access food. Kinnunen et al. (2020) found that only 11-28% of the global population can fulfil their demand for specific crops (such as maize, rice, and temperate cereals) within a 100-kilometre radius, with significant variation across regions and crops. Their analysis computed distances to these crops in the absence of trade, based on friction surfaces derived from transport networks. This study highlighted that satisfying food demand with only local production is not feasible for most of the world's population.

Building on this work, Kotavaara et al. (2021) combined proxies of regional supply and demand with transport network information, concluding that global

accessibility of grains varies significantly in space, with lowest accessibility in central Africa, central South America, and the Arabian Peninsula. The FAO used flood simulations to understand the fragility of food delivery transport networks in Nigeria and Pakistan, finding that breakdown of critical transport routes causes significant detours, affecting food accessibility and causing food loss (Torero, 2021).

Z. Sun et al. (2020) evaluated the link between global consumption and local production hotspots, tracing the supply chains of 40 primary crops and 6 kinds of livestock using road networks to allocate supply between domestic consumption and exports. They found that high-income countries outsource agricultural production significantly to low-income countries with lower production costs, whereas low- and middle-income countries have greater self-sufficiency, partly driven by lower per-capita consumption. Although this study provided high-resolution analysis of production hotspots, there remains scope to extend it by incorporating all modes of transport (ports, rail, roads) and by building high-resolution networks linking both producers and consumers at subnational scales.

Evolution and structure of international trade networks

The literature on international food trade networks has evolved considerably. Sartori and Schiavo (2015) analysed the evolution of global trade over the years 1986–2010 and concluded that while the world has become more interconnected, it is not necessarily less stable due to rising global trade. The dissipation of shocks through networks provides sufficient benefits to outweigh the potential costs of shock propagation and magnification. However, some nodes are critically important owing to a few very strong relationships responsible for much of world trade.

Y.-T. Zhang and Zhou (2022) applied network analysis to the evolution of international trade networks for maize, rice, and soybean from 1993 to 2018, finding that all networks grew with more participants and larger trade values, becoming tighter (more interconnected with higher clustering) and more similar across crop types over time. Traverso and Schiavo (2020) examined global food trade from a nutritional perspective, specifically proteins, carbohydrates, and lipids, finding that

macronutrient trade has more than doubled since 1996, improving macronutrient availability and aggregate food access in low-income countries.

Collectively, these studies show that global food trade networks have become denser and more integrated over time, with important consequences for systemic resilience, vulnerability to shocks, and the distribution of food and nutrients across countries.

Trade shocks and propagation

Studies have also examined how shocks propagate through trade networks and their implications for food security. Grassia et al. (2022) used a network model of shock diffusion to understand the role of trade in mitigating versus propagating shocks to domestic agricultural production. They found that low-income and food-insecure countries were most exposed to external shocks and were also unable to fully leverage international trade to shield themselves from domestic production shocks.

Distefano et al. (2018) examined shock propagation empirically, using drops in exports for wheat, maize, rice, and soybeans during 1986-2011. This study also found that developing countries absorbed most trade shocks, bearing disproportionately larger drops in food imports. Income per capita was a key determinant, as wealthier countries could pay higher prices and leverage greater bargaining power to maintain their import levels. Furthermore, they found that food prices and quantities traded were weakly correlated, suggesting that food flows contain more information than prices alone in the context of trade shocks.

The gap: subnational resolution

Most prior research on food trade has focused on international flows at national scales (Sartori & Schiavo, 2015; Vishwakarma et al., 2022; Y.-T. Zhang & Zhou, 2022). This perspective, while valuable, obscures substantial heterogeneity within countries. Agricultural production is not evenly distributed across national territories; some regions produce far more than they consume, while others depend heavily on inflows from elsewhere. A country that appears self-sufficient at the

national level may contain regions that are highly dependent on distant suppliers, while a country that appears trade-dependent may contain breadbasket regions that anchor both domestic and international supply chains. Subnational resolution would therefore enable more accurate assessment of local exposure to supply disruptions, identifying which populations are most vulnerable to shocks in specific source regions. Furthermore, since the environmental impact of producing the same commodity varies substantially across regions (Poore & Nemecek, 2018), detailed sourcing information can help allocate environmental impacts to consumption more accurately.

The analysis of spatially resolved food distribution networks remains limited to select geographies. Lin et al. (2019) modelled food flows between counties in the United States. Harris et al. (2020) examined interstate cereal flows within India. Pandit et al. (2023) analysed spatially detailed agricultural trade between China and the United States. While these studies demonstrate the value of subnational analysis, a globally consistent framework for mapping food flows at subnational scales has been lacking.

Paper 1 contribution

Paper 1 addresses this gap by developing a novel methodological framework that integrates machine learning and data harmonisation algorithms to map global cereal flows at subnational scales. The focus on cereals reflects their importance as the foundation of global food security. They form the most important source of calories for a majority of the world's population, either directly or indirectly via animal feed (Awika, 2011). By modelling international and domestic flows across 3,536 first-level administrative regions in 195 countries, the paper identifies critical nodes and links in subnational cereal flow networks, and quantifies concentration patterns that expose vulnerabilities obscured by national-level statistics.

1.2.2 Sustainability: Environmental Impacts of Food Systems

The environmental footprint of food systems is substantial and spans multiple dimensions. Food systems account for 21-37% of global greenhouse gas emissions (Crippa et al., 2021), and they also have significant impacts on land use, freshwater consumption, nutrient cycling, and biodiversity (Foley et al., 2011). As the global population grows and diets shift, particularly towards greater consumption of animal products in emerging economies, the environmental pressures from food systems are expected to intensify (Tilman & Clark, 2014).

Drivers of environmental impacts

Evidence from farms producing diverse agricultural goods around the world suggests that the environmental cost of producing the same goods can be highly variable, indicating substantial mitigation opportunity on the production side (Poore & Nemecek, 2018). This landmark study, synthesising life cycle assessment data from approximately 38,700 farms and 1,600 processors across 119 countries, quantified cradle-to-retail impacts spanning production, processing, packaging, and transport. The study found that impacts can vary by a factor of 50 among producers of the same product, indicating substantial mitigation opportunity across supply chains. However, this research also found that the impacts of even the lowest-impact animal products typically exceed those of plant-based substitutes, suggesting that dietary change on the consumer side can have substantial positive effects. For example, the lowest-impact beef still generates more greenhouse gas emissions than the highest-impact plant protein sources.

The EAT-Lancet Commission proposed dietary benchmarks explicitly aimed at promoting human health and environmental sustainability (Willett et al., 2019). Research has demonstrated that replacing animal-source foods with plant-based alternatives could improve nutrient levels, lower premature mortality, and substantially reduce greenhouse gas emissions (Springmann et al., 2018). Esteve-Llorens et al. (2019), evaluated the Atlantic diet using a life cycle analysis methodology,

and found that it was beneficial both in terms of its nutritional and environmental impacts. Clark et al. (2020) showed that food system emissions alone could preclude achieving the 1.5°C and 2°C climate change targets if current dietary trends continue, underscoring the importance of dietary shifts for climate mitigation.

The role of transport and sourcing

The role of food transport in overall food system emissions has received increasing attention. Li et al. (2022) estimated that transport accounts for about 19% of total food-system emissions when the entire upstream supply chain is considered, including transport of fertilizers, machinery, and feed. This finding is particularly pronounced for fruits and vegetables, where transport accounts for approximately 36% of their total footprint, nearly twice the emissions from their production. However, roughly half of these emissions stem from upstream input transport rather than the movement of food from farm to retail. Estimates focusing on the latter suggest a smaller share of around 6% on average, where upstream processes are allocated to production rather than transport (Poore & Nemecek, 2018).

Even where transport of food itself is substantial, the relationship between food miles and environmental impact is not straightforward. Production conditions vary substantially across regions, meaning that food produced locally under energy-intensive conditions may have higher impacts than food transported from regions with more favourable growing conditions (Weber & Matthews, 2008). This complexity makes it difficult to provide simple guidance on whether consumers should prioritise local sourcing or focus primarily on dietary composition.

The gap: packaged food products

Information on environmental impacts of foods sold at retail stores remains vital for transitioning to sustainable food systems (El Bilali & Allahyari, 2018), but such information remains sparse, fragmented, and non-standardized (Deconinck et al., 2023). Scalable estimation and clear, consistent communication of these

impacts are critical to support evidence-based purchasing, procurement, reporting, and target-setting, by consumers, retailers, producers, and policymakers.

Yet most research has focused on the environmental footprints of raw agricultural commodities, such as grains, fruits, meats, rather than the multi-ingredient packaged foods that dominate modern retail environments (Poore & Nemecek, 2018; Sala et al., 2017). Some recent work has begun to address this gap. Clark et al. (2022) estimated the environmental impacts of approximately 57,000 food products in the United Kingdom and Ireland, finding that nutrition and environmental sustainability are broadly compatible. However, food products vary substantially in their recipes and regional sourcing patterns across geographies, and it remains crucial to develop a global, standardized assessment of retail foods.

Another remaining question is whether environmental impacts are driven primarily by what people eat or by where ingredients are sourced. If composition is dominant, then dietary guidelines and product reformulation are the primary levers for reducing impacts. If sourcing is dominant, then supply chain interventions, such as shifting procurement towards lower-impact producers, become equally important. Answering this question requires product-level data on environmental footprints, linked to information on both composition and sourcing. A systematic analysis of how composition and sourcing jointly shape footprints across a wider range of countries and products remains limited.

Paper 2 contribution

Paper 2 addresses this gap by estimating the environmental footprints of approximately 475,000 retail food products across 74 countries. By combining machine learning-based product categorisation, ingredient composition estimation, and life cycle assessment data corresponding to supply chain sourcing patterns, the paper quantifies impacts across five environmental indicators: land use, greenhouse gas emissions, biodiversity loss, eutrophication, and water stress. The analysis demonstrates that ingredient composition remains the dominant driver of environmental impacts, with products containing animal-derived ingredients, coffee, and

nuts consistently exhibiting the highest footprints across regions, but that ingredient sourcing accounts for meaningful variation within product categories, suggesting that supply chain interventions can complement dietary shifts. This decomposition enables a more direct assessment of where intervention opportunities lie.

1.2.3 Foresight: Understanding How Food Systems May Evolve

Food systems are not static. Several forces are already reshaping, and will continue to reshape, global food production and trade over the coming decades. Understanding how these forces interact is essential for anticipating future challenges and identifying policy pathways that promote resilience and sustainability.

Climate impacts on agricultural production

Climate change will unevenly affect regional crop productivity. Some regions will see yields decline due to heat stress, water scarcity, and increased pest pressure, while others may benefit from longer growing seasons or shifting agroclimatic zones (Rezaei et al., 2023). Research has shown that these impacts will not be uniformly distributed: tropical and subtropical regions face the greatest risks, while some temperate regions may experience short-term gains before negative impacts emerge (Rosenzweig et al., 2014; Tubiello et al., 2007).

Some studies have quantified how yield losses may evolve under future climate scenarios. Leng and Hall (2019) estimated yield loss risk from future drought severity, focusing on wheat, maize, rice, and soybeans. They found that yield loss risk grows non-linearly with increasing drought severity and is projected to increase substantially in the future. Research on global breadbasket regions has examined how climate change may increase the risk of simultaneous production failures. Gaupp et al. (2019) examined simultaneous breadbasket failures for maize, wheat, and soybeans under 1.5°C and 2°C warming scenarios, finding that projected yield losses increase disproportionately between the two warming levels, with wheat showing the highest simultaneous climate risk increase, followed by maize and

soybean. Gaupp et al. (2020) quantified the changing risk of simultaneous global breadbasket failure, finding increasing risk for wheat, maize, and soybean, while rice showed decreasing risk due to solar radiation changes that favour rice growth.

The implications for trade are significant. As climate change alters the geography of comparative advantage in agriculture, production may need to shift towards regions with more favourable conditions, and trade will play a crucial role in connecting areas of surplus to areas of deficit. At the same time, the increasing risk of simultaneous production failures across major breadbasket regions could overwhelm the capacity of trade to buffer shocks.

Dietary transitions

Socio-economic growth across emerging economies is already driving shifts towards more diverse diets that often include greater consumption of animal products, fruits, and vegetables (Pingali, 2007). Gouel and Guimbard (2019) documented how rising incomes reshape the structure of food demand, with consumers shifting from starchy staples towards animal-source products, fats, and sweeteners as incomes rise

These demand shifts matter not only because they change what people eat, but also because they set the trajectory of future environmental impacts, and reshape the mix of commodities and ingredients moving through domestic and international supply chains. While historical income-driven transitions tend to increase the consumption of resource and emissions-intensive foods, alternative pathways aligned with health and sustainability oriented dietary benchmarks, such as those proposed by the EAT-Lancet Commission, could bend this trajectory toward lower impacts (Willett et al., 2019). Modelling studies suggest that such shifts could deliver substantial reductions in greenhouse gas emissions alongside health co-benefits (Springmann et al., 2018; Tilman & Clark, 2014). Z. Sun et al. (2022) further show that, in the European Union and United Kingdom, similar dietary transitions could help offset supply deficits linked to geopolitical disruptions, while improving outcomes related to water use, greenhouse gas emissions, and carbon sequestration.

Whether dietary change continues to follow historical patterns or is steered toward healthier and more sustainable alternatives will therefore have major consequences for environmental footprints and for future agricultural trade patterns.

Trade as adaptation

A growing body of research has examined the potential of international trade to serve as an adaptation mechanism under climate change.

Janssens et al. (2020) analysed combinations of trade scenarios and climate futures, finding that current levels of trade could lead to up to 55 million additional undernourished people in 2050 under climate change. Without adaptation through trade, this number could reach 73 million, while reductions in tariffs and barriers could decrease it to 20 million. Adaptation through trade was found to positively impact import-dependent regions the most, though at the expense of domestic food availability in exporting regions. Janssens et al. (2022) assessed the combined impacts of continental free trade and agricultural development in Africa, finding that this combination could almost eliminate undernourishment in Africa by 2050 with modest increases in greenhouse gas emissions.

Gouel and Laborde (2021) examined the crucial role of both domestic and international market-mediated adaptation to climate change, finding that trade flexibility is essential for efficient adaptation but that its benefits depend on the trade policy environment. Vishwakarma et al. (2022) analysed the international wheat trade network from 2005 to 2014, finding that countries with larger differences in extreme weather stress and synchronous yield variations tend to be trade partners with higher trade volumes. This counterintuitive finding calls for improved trade policies to enhance the adaptive capacity of trade networks.

Modelling approaches

Global models have been developed to project how climate change, dietary shifts, and policy changes may affect food systems. International Food Policy Research Institute's (IFPRI) IMPACT model (Robinson et al., 2015) integrates

climate projections with economic responses to assess food security outcomes under alternative scenarios. GLOBIOM (Havlík et al., 2014) and MAgPIE (Dietrich et al., 2019) are partial equilibrium models that link land use, agriculture, and environmental outcomes, and have been used to explore pathways for climate change mitigation through agricultural transitions. Integrated assessment models such as REMIND-MAgPIE have been used to explore how dietary shifts could contribute to achieving climate targets (Humpenöder et al., 2024). These modelling exercises demonstrate that the interaction between production-side and demand-side changes will determine the overall environmental trajectory of food systems.

The gap: limited integration across literatures

Despite this progress, the literatures on climate impacts on agriculture, dietary transitions, and trade as an adaptation mechanism, have developed with limited integration. Studies examining climate impacts on trade have typically held diets constant; studies of dietary transitions have often assumed static trade patterns or ignored climate effects on production; and trade models have rarely incorporated both climate-driven yield shocks and demand-side dietary shifts simultaneously.

This separation limits our understanding of several important questions. How dietary transitions and climate-driven changes in regional productivity jointly reshape the geography of trade and reconfigure critical exporters and importers, remains unclear. Similarly, whether trade liberalization can enhance allocative efficiency without concentrating import dependence among fewer suppliers is not well understood. Addressing these questions requires frameworks that integrate all three forces simultaneously.

Paper 3 contribution

Paper 3 addresses this gap by developing an integrated modelling framework that projects bilateral trade flows for 32 crops across 153 countries through 2050. By combining dietary transition scenarios with climate impact projections and alternative trade policy regimes, the paper explores how these forces interact to reshape global

food trade under 20 scenario combinations. The analysis finds that accommodating large-scale dietary transitions would require substantial restructuring of global food trade, and that this restructuring interacts with climate impacts on yields and trade policy regimes in complex ways. Trade liberalization, meanwhile, involves trade-offs between efficiency gains and increased import concentration. The scenario-based approach allows for systematic comparison of how different pathways affect trade patterns, import concentration, and the distribution of production across regions.

2

Mapping Global Cereal Flow at Subnational Scales Unveils Key Insights for Food Systems Resilience

Shruti Jain[1]

[1]*Smith School of Enterprise and the Environment, University of Oxford, UK*

Abstract

Strengthening food systems resilience requires a comprehensive understanding of global food distribution networks, especially amid escalating climate and geopolitical challenges. This research maps spatially resolved networks of global cereal flows across 3,536 subnational regions in 195 countries employing machine learning and harmonization algorithms to downscale national cereal flow data. The study identifies pivotal exporting and importing regions in both domestic and international distribution networks. Almost half of net importing countries contain surplus regions that supply grain both domestically and internationally, while nearly every net exporting country retains deficit regions that rely on inflows. Major cereal producers such as the United States, Russia, and India demonstrate substantial domestic self-sufficiency, whereas Southeast Asia and Europe rely on both domestic and international sources. The study also identifies significant concentrations within cereal distribution networks, highlighting vulnerabilities to potential disruptions. These findings offer critical insights into the spatial complexities of global cereal trade, providing a foundation for targeted policy interventions aimed at enhancing global food security and resilience.

2.1 Introduction

Agricultural trade has more than doubled between 1995 and 2018 (FAO, 2022), accounting for 19% of globally consumed calories (Martin & Laborde Debucquet, 2018), which has allowed the flow of food from regions with surplus to those with deficit (Janssens et al., 2022; Suweis et al., 2015). Trade can serve as an adaptation mechanism under climate change (Janssens et al., 2020), and as resources like land and water become limited with climate change, the role of trade in distributing food will become even more important. At the same time, these distribution networks can further geopolitical, environmental, and climate related vulnerabilities in the form of food production, exchange, and transport disruptions (Centeno et al., 2015; Wellesley et al., 2017). With regional specialization, major breadbaskets have become sole suppliers of agricultural commodities to other nations (Puma et al., 2015), and such structural food dependence of food deficit countries can be disadvantageous if food surplus countries decide to impose international trade restrictions (Paillard et al., 2011). For example, a small set of Asian exporters dominate global rice trade (FAO, 2023), such that when India and Vietnam imposed export restrictions during the 2007-2008 food crisis, import-dependent countries faced sharp price spikes and food security pressures (Headey, 2011). Overall, the potential of trade to enhance food systems resilience can only be realized if the associated risks of increased exposure to geopolitical and environmental stresses are minimized (Brown et al., 2017).

It is crucial to evaluate these food trade networks to improve our understanding of vulnerabilities in food supply chains and of their associated environmental impacts. While past research has extensively examined international trade networks (Sartori & Schiavo, 2015; Vishwakarma et al., 2022; Y.-T. Zhang & Zhou, 2022), spatially resolved analyses of food distribution networks have received comparatively less attention and remain largely limited to select geographies, such as the United States and China (Croft et al., 2018; Pandit et al., 2023). Subnational analyses of food distribution are critical for an improved understanding of the heterogeneity in vulnerabilities and resilience of food systems to natural and demographic threats

(Kummu et al., 2020; Stokeld et al., 2020), and for accurately assessing the environmental footprints of global food supply chains (Li et al., 2022).

The vulnerabilities and resilience of food systems play out at the subnational scale because both domestic and international supply channels are vulnerable to disruption, and regions within the same country are exposed to these disruptions to differing degrees (Porkka et al., 2017; Stokeld et al., 2020). Domestic distribution networks can be severed by extreme weather events, as illustrated by the 2022 floods in Pakistan (Qamer et al., 2023), or by labour and political mobilisations, as illustrated by the 2018 Brazilian truckers' strike that triggered food shortages (Lopes et al., 2019; Schlindwein & Ison, 2020). International supply chains also carry risks, including disruptions at maritime chokepoints (Wellesley et al., 2017), and supply shocks from conflict in major producing regions, as illustrated by the disruption to global wheat markets following Russia's 2022 invasion of Ukraine (Devadoss & Ridley, 2024). A country may appear adequately supplied at the national level either because its regions are individually self-sufficient, or because its aggregate balance relies on fragile distribution arrangements – a few internal corridors moving grain from surplus to deficit regions, or a narrow set of overseas suppliers. National-level statistics cannot tell these situations apart.

To address this gap, this research models international and domestic cereal flows at subnational scales and provides insights into their implications for the resilience of food systems. Specifically, global cereal flows are estimated between the first level administrative regions in all countries, both domestically and internationally. These 'flows' explicitly link the region of production with the final destination of import, and hence provide an accurate estimate of regional import dependencies. Cereal grains were chosen for this work given that they form the most important source of calories for a majority of the world's population, either directly or indirectly via animal feed (Awika, 2011). The estimated cereal flows are used to – i) identify the most crucial nodes and links in cereal flow networks, ii) understand the heterogeneities in regional reliance on domestic vs international inflows, and iii) quantify the overall concentration and diversification of cereal flows, both internationally and

domestically. This analysis is a step towards evaluating global food trade at different spatial scales, which is crucial for unraveling the dual role of trade as both a promoter and a detractor of food system resilience – an outcome that depends on specific contexts and scales (Kummu et al., 2020).

2.2 Methods

This study estimates the flow of cereals between 3,536 subnational regions in 195 countries by downscaling available data on the bilateral flow of cereals at national scales. The modelling pipeline comprises three main components: i) pre-processing the production and bilateral trade data from the FAO and other sources, ii) training machine learning models on the national-scale data and a small subset of available subnational flow observations, to predict the existence of food flow links and the volume of food flows on links at subnational scales, and iii) harmonizing the subnational scale predictions using the national-scale food flow data – to ensure that the aggregated subnational predictions align with the reported national scale food flows, and that each subnational region can meet its estimated consumption Supplementary Figure B.1.

2.2.1 Pre-processing production and trade data

The primary data inputs in this study were the FAO's national-scale statistics on the production, distribution, and consumption for 15 cereal commodities - barley, buckwheat, canary seed, fonio, maize, millet, mixed grain, oats, quinoa, rice, rye, sorghum, triticale, wheat, other. This data was pre-processed to address the following discrepancies – i) the trade volumes reported by the importing countries did not always match those reported by the exporting countries, and ii) the total reported exports from some countries exceeded the volumes produced and imported together, because of misreported transactions or countries reporting re-exported imports as their exports. Discrepancies between the volume of cereal trade reported by the importer and exporter were resolved using a reliability index approach similar to the one outlined by (Gehlhar, 1996) (Supplementary Methods B.3.1).

Furthermore, to resolve the second issue, a re-export algorithm developed by Croft et al. (2018) was used to obtain cereal 'flows'. This algorithm ensures that the total exports from a country never exceed its production and total imports; and it also links the source of production with the destination of import (Supplementary Methods B.3.2). These two processing steps were implemented separately for each crop and year, and the processed trade data was then merged first, for each year separately, summing the trade data for all the cereal commodities, and then second, averaging the total annual processed cereal trade data for the years 2017-2021 to smooth out inter-annual variability in trade partners and volumes.

In addition to the FAO's national level bilateral trade statistics, subnational flow estimates were incorporated where available. Domestic cereal movements between 35 Indian states in 2011-12, as estimated by Harris et al. (2020), were aggregated across individual commodities (e.g., wheat, maize) to derive total interstate cereal flows. Subnational cereal transfers among 51 U.S. states and 31 Chinese provinces in 2017, as estimated by Pandit et al. (2023), were likewise included. Although both sources consist of modelled estimates rather than direct observations, they capture subnational flow patterns absent from the FAO data, providing useful nuance to the machine learning models.

2.2.2 Machine learning to predict cereal flow links and volumes

A machine learning approach was employed to deal with the complexity due to the number of flow links rising exponentially from ~38k at the national level to ~12.5 million at the subnational level. It is important to note that the validity of this approach relies on the assumption that a machine learning model trained on primarily national scale data can be used to make subnational food flow predictions. The justification of this assumption is based on previous research that identified similar structural properties across food flow networks at the global, national, and village levels in the United States (Konar et al., 2018). This insight has been leveraged by other studies to estimate spatially explicit food flows using machine

learning models trained on food flows at aggregate spatial scales in the United States and China (Karakoc et al., 2022; Lin et al., 2019; Pandit et al., 2023). The strength of this assumption may vary across regions, depending on differences in market institutions, transport infrastructure, and trade governance; this is discussed in full in Supplementary Methods B.3.6.

Several factors determine the flow of food between regions, including production, consumption preferences, storage facilities, transport infrastructure, and socio-political factors (Venkatramanan et al., 2017). Subnational cereal production and area estimates were derived from the GAEZ+ 2015 global gridded dataset (Grogan et al., 2022), which provides crop-specific harvested area, yield, and production at 5-minute (~10 km) resolution for the year 2015. GAEZ+ 2015 builds on the Global Agro-Ecological Zones (GAEZ v4) model (Fischer et al., 2021), which downscales national-scale FAOSTAT crop statistics to grid cells using a sequential rebalancing procedure that draws on cropland and irrigation distribution maps, soil and climate data, livestock and population layers, and observed crop calendars. The gridded production values were aggregated to first-level administrative boundaries and proportionally scaled so that the sum across all subnational regions in each country matches the FAO-reported national production total averaged over 2017-2021. The limitations of this dataset and approach are discussed in Supplementary Methods B.3.6.

The remaining input datasets, including gridded livestock counts, population characteristics, and transport data, were used as proxies for the other factors listed above and are described in Supplementary Table B.1. These datasets serve as the best available globally consistent sources for these variables at subnational scales. Producer prices from the FAO were also incorporated, see Supplementary Methods B.3.3 for how this data was processed. These datasets were used as predictors or covariates in the machine learning pipeline. A classification model was used for identifying cereal flow links, and a regression model was used for predicting flow volumes. These models learned the relationship between the features and the

observed cereal flows, and the trained models were then used to make predictions for expected cereal flows at subnational scales.

The machine learning models achieved strong performance for predicting link presence, and a moderate performance for flow volume prediction – the best classification model achieved an out-of-sample accuracy of 94%, and the best regression model achieved an out-of-sample R-squared of 0.52 on the linear scale and 0.68 on the log scale. Performance metrics are averaged over five model runs with distinct train-test splits to account for sampling variation. Regression model performance in this analysis remained poorer than its counterparts in data-rich geographies such as the United States (Karakoc et al., 2022), but was modest given the quality of data available for training. Supplementary Tables B.5 and B.7 report the out-of-sample performance of different classification and regression models tested, across datasets. The best performing classification model, a gradient-boosting classifier achieves consistently high out-of-sample accuracy (exceeding 90%), precision (exceeding 85%), recall (exceeding 90%), and MCC (exceeding 0.75) scores, across national-scale international flows from the FAO, domestic cereal flows within India, and subnational-scale international flows between USA and China (FAO, 2023; Harris et al., 2020; Pandit et al., 2023). In case of flow volume prediction, gradient boosting regressor and a neural network deliver the strongest results – both models provide consistent performance across datasets (R-squared exceeding 0.35 on the linear scale and 0.65 on the log scale) demonstrating that non-linear methods can effectively capture cereal flow volume patterns at different scales. The best performing models were used to predict cereal flows for each subnational region. See Supplementary Methods B.3.4 for more details on these models.

2.2.2.1 Rationale for modelling cereal flows in aggregate

Flows were estimated for cereals in aggregate rather than by individual crop (e.g., wheat, rice, maize) for two reasons. First, models predicting total cereal flows generally outperformed those for individual cereals (Supplementary Table B.9). Second, disaggregating by cereal type would also require estimating subnational

consumption for each cereal crop to harmonize its flows, which would require much stronger assumptions about each subnational region's crop-specific preferences. Subnational consumption is estimated based on the relationship in Supplementary Equation B.3.5.1 (Supplementary Methods B.3.5), which is derived from national-scale consumption values. By treating cereals as an aggregated commodity, these assumptions apply to the cereal bundle rather than to each cereal type individually. Furthermore, national-scale regressions for estimating consumption of individual cereals yielded lower R-squared than for the aggregate commodity (Supplementary Table B.10). To demonstrate that the predictions for total cereal flows still respect individual cereal flows, out-of-sample Pearson correlations were computed between i) observed total cereal flows and observed disaggregated cereal flows, and ii) predicted total cereal flows and observed disaggregated cereal flows (Supplementary Table B.11). Although correlations between observed and predicted total flows against individual cereal flows dipped modestly in some cases (e.g., wheat from 0.74 to 0.56; maize from 0.76 to 0.56), all cereals maintained positive correlations with total flow predictions. Any shifts in relative ordering were small, and no cereal experienced a disproportionately large change, indicating that the aggregate model preserves the key spatial flow patterns of each grain.

2.2.3 Harmonizing the predicted flows

The estimates of cereal flows from machine learning models do not always satisfy national-scale aggregates and local consumption demands. Hence, a harmonization algorithm was applied to adjust the predicted flows to ensure that: i) the final subnational flow network reconciles with known national cereal trade statistics, ii) each subnational region has a supply of cereals (from production and inflows) that is sufficient to meet its demand, and iii) no subnational region exports more cereal than it produces. Previous work has applied post-prediction harmonization of machine learning estimates to ensure consistency with known national or subnational scale statistics, e.g. mass balancing of predicted commodity flows (Karakoc et al., 2022; Lin et al., 2019), and calibrating satellite-based high-resolution agricultural

maps (Jin et al., 2019; Kluger et al., 2021). See Supplementary Methods B.3.5 for more details on the harmonizing procedure.

2.2.3.1 Sensitivity analysis

Robustness of the harmonization procedure was evaluated via a comprehensive sensitivity analysis across parameter combinations listed in Supplementary Table B.12. For each combination, the harmonization algorithm was re-executed, and the resulting subnational flow matrices were compared by computing pairwise Pearson correlation coefficients; the complete correlation matrix is shown in Supplementary Figure B.8. In all cases, correlations exceeded 0.95, demonstrating that the final harmonized flows remain highly stable under reasonable variations in threshold values, iteration limits, and scaling factors.

2.3 Results

2.3.1 Key links and nodes in cereal flow networks

An overview of the disaggregated flows is presented in Figure 2.1 below. Figure 2.1 panel *a* shows the cereal flows at national scales, as obtained after processing production and bilateral trade data from the FAO. The width of the links indicates the volume of trade flows, and the color indicates the exporting region. Figure 2.1 panel *b* show the top 5% of the cereal flows at subnational scales. Panel *c* shows the domestic flow of cereals in 6 select countries – Spain, Colombia, Ethiopia, United States, New Zealand, and India. These 6 countries were chosen to display the importance of domestic flows in different regions around the world. International flows of cereals scales sum up to about 455 million tonnes and account for 16.5% of global production, and global domestic flows make up a total of about 730 million tonnes which is 26.5% of global production. 1568 million tonnes of cereals, i.e. ~57% of total global production, are consumed within the regions they are produced.

It is vital to identify the key links and nodes in cereal flow networks for a deeper understanding of resilience and vulnerabilities to production and market shocks. Both national and subnational flows followed a right-skewed distribution – most

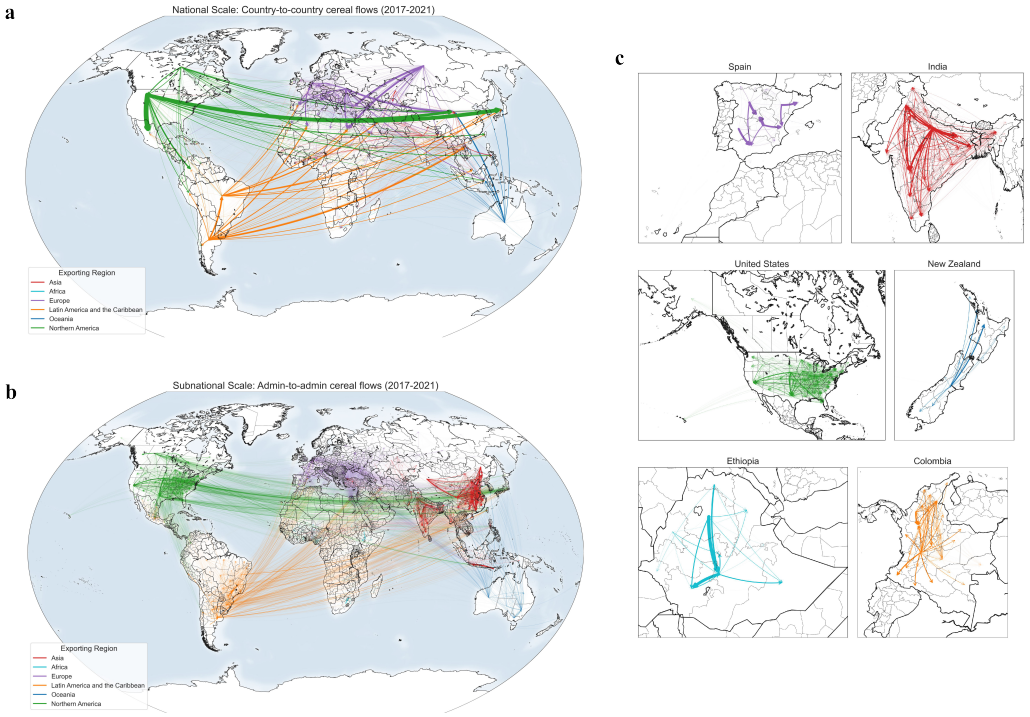

Figure 2.1: National and subnational cereal flows (annual, averaged over 2017-2021). **a** Cereal flows at national scales. **b** Top 5% of cereal flows at subnational scales. **c** Domestic flows in 6 select countries.
The width of arrows representing flows in Figures 2.1*a* and 2.1*b* are plotted at the same scale. However, the flows in Figure 2.1*c* are all plotted at different scales for better visibility of domestic flows.

flows were small, with a few very large flows. Table 2.1 shows the 10 links with largest flow volumes at national scales and subnational scales. Both international and domestic flows at subnational scales are presented. India and China have some of the largest domestic cereal flows, but these countries do not show up in the largest international subnational links, which means that these countries have a greater reliance on domestic flows as compared to international flows. United States and Argentina have some of the largest international outflows, both at national and sub-national scales. At subnational scales, the largest domestic links carry about three times larger cereal flows as compared to the largest international links. This distinction between domestic and international flows highlights the varying degrees of dependency on international trade versus domestic production in different countries.

Table 2.1: Largest cereal flows at national and subnational scales (annual, averaged over 2017-2021)

Scale	**Exporting region**	**Importing region**	**Cereal flow (million tonnes)**
National	United States	Mexico	19.3
	United States	Japan	15.1
	United States	China	11.2
	Russia	Egypt	7.3
	Russia	Turkey	7.2
	Argentina	Vietnam	6.5
	Ukraine	China	6.5
	Argentina	Brazil	6.0
	United States	Colombia	5.4
	United States	South Korea	5.4
Subnational (international)	Texas, United States	Nuevo León, Mexico	1.6
	Bahia, Brazil	Taiwan, Taiwan	1.2
	Buenos Aires, Argentina	Lima Province, Peru	1.0
	Mendoza, Argentina	Región Metropolitana de Santiago, Chile	0.9
	Texas, United States	Coahuila, Mexico	0.9
	Rio Grande do Sul, Brazil	Cataluña, Spain	0.9
	Hauts-de-France, France	Vlaanderen, Belgium	0.8
	Buenos Aires, Argentina	Johor, Malaysia	0.8
	Buenos Aires, Argentina	Selangor, Malaysia	0.7
	California, United States	Baja California, Mexico	0.7
Subnational (domestic)	Uttar Pradesh, India	Bihar, India	5.2
	Nusa Tenggara Timur, Indonesia	Jawa Barat, Indonesia	4.6
	Nebraska, United States	Texas, United States	3.8
	Heilongjiang, China	Jilin, China	3.4
	Uttar Pradesh, India	Maharashtra, India	3.0

Table 2.1 continued from previous page

Scale	Exporting region	Importing region	Cereal flow (million tonnes)
	Nebraska, United States	California, United States	2.9
	Heilongjiang, China	Liaoning, China	2.9
	Anhui, China	Guangdong, China	2.8
	Henan, China	Sichuan, China	2.7
	Anhui, China	Zhejiang, China	2.7

Flows aggregated by exporting and importing regions can help identify key exporters and importers in international and domestic markets. Figure 2.2 shows total inflows into and outflows from all regions at national and subnational scales, with the subnational outflows and inflows broken down into international and domestic flows. Table 2.2 highlights regions with the largest outflows and inflows at both national and subnational scales.

In subnational international markets, outflows concentrate in agriculture-intensive regions, e.g. Texas and Illinois (USA), and Buenos Aires (Argentina), and largest inflows land in major gateway regions, such as Gyeonggi-do (South Korea) and Guangdong (China). At the domestic level, a similar split appears between production and consumption hubs. Domestic outflows peak in top-producing states and provinces, while inflows cluster in populous, industrialized regions. In the United States, international export activity is concentrated in states adjacent to Gulf and Great Lakes ports, whereas domestic redistribution hinges on the High Plains. China's eastern provinces drive domestic outflows, while coastal, industrial centers and inland hubs lead inflows. India's northern breadbasket dominates outflows, with southern states driving inflows. Notably, Texas and Guangdong play dual roles – Texas exports nearly 20 Mt internationally yet imports nearly 18 Mt domestically, reflecting its large-scale production and port operations, while Guangdong ranks among the top importers in both international and domestic flows. Although the

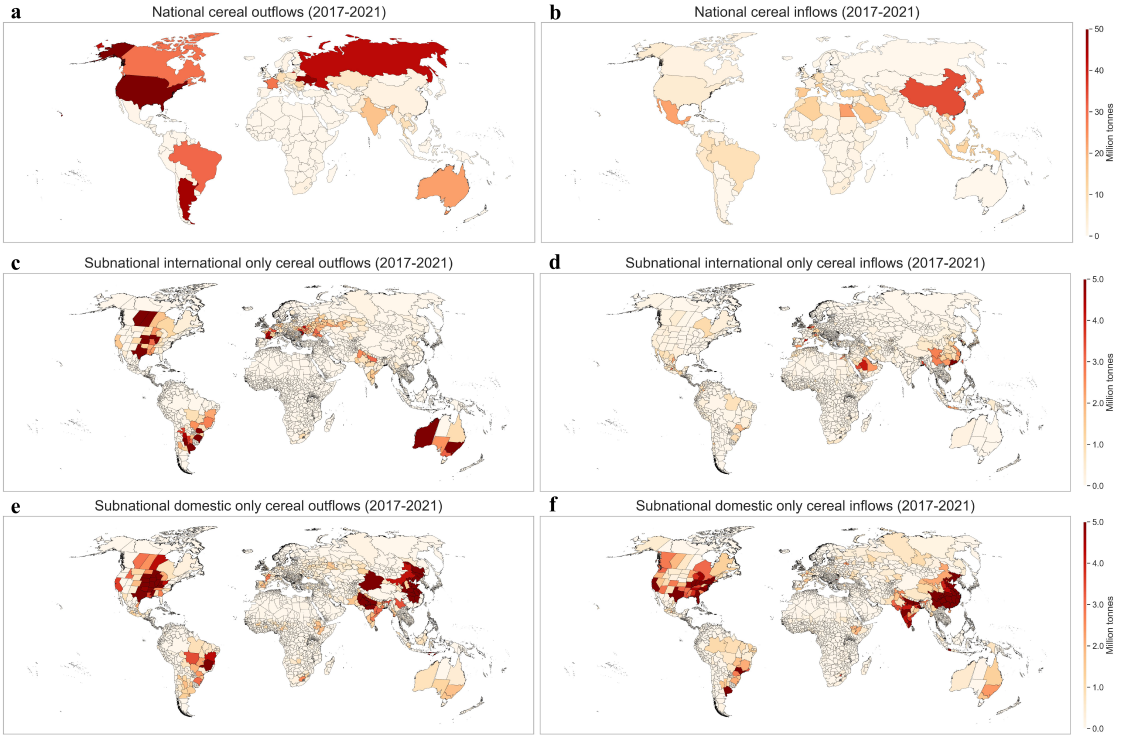

Figure 2.2: Total outflows and inflows at national and subnational scales (annual, averaged over 2017-2021). **a** National outflows. **b** National inflows. **c** Subnational outflows, international only. **d** Subnational inflows, international only. **e** Subnational outflows, domestic only. **f** Subnational inflows, domestic only.

harmonization algorithm ensures exports never exceed local production, residual re-export artifacts can persist when a region both produces and imports large volumes, so some of Texas's estimated international outflows likely reflect re-exports.

Table 2.2: Regions with the largest outflows and inflows at national and subnational scales (annual, averaged over 2017-2021)

Scale	**Flow**	**Region**	**Value (million tonnes)**
National	Outflows	United States	89.7
		Ukraine	47.5
		Argentina	45.7
		Russia	42.4
		Brazil	30.8
	Inflows	China	34.1
		Japan	24.0
		Egypt	22.4
		Mexico	22.0
		South Korea	15.6
Subnational (international)	Outflows	Texas, United States	19.8
		Buenos Aires, Argentina	17.6
		Illinois, United States	14.9
		Rio Grande do Sul, Brazil	14.7
		Saskatchewan, Canada	13.8
	Inflows	Gyeonggi-do, South Korea	5.4
		Guangdong, China	5.2
		Vlaanderen, Belgium	4.7
		Cataluña, Spain	4.1
		Ar Riyad, Saudi Arabia	4.0
Subnational (domestic)	Outflows	Nebraska, United States	24.8
		Shandong, China	23.6
		Uttar Pradesh, India	23.3
		Anhui, China	22.3
		Henan, China	20.6
	Inflows	Guangdong, China	20.8
		Texas, United States	17.8
		Sichuan, China	17.5
		Florida, United States	13.8
		California, United States	13.8

It is also useful to explore net flows to pinpoint surplus and deficit regions – nearly half of all net importing countries contain surplus regions with net domestic

and international outflows, while virtually every net exporting country retains deficit regions that receive net domestic and international inflows. Substantial subnational heterogeneity exists in both domestic and international flows from surplus and into deficit regions, respectively (Figure 2.3).

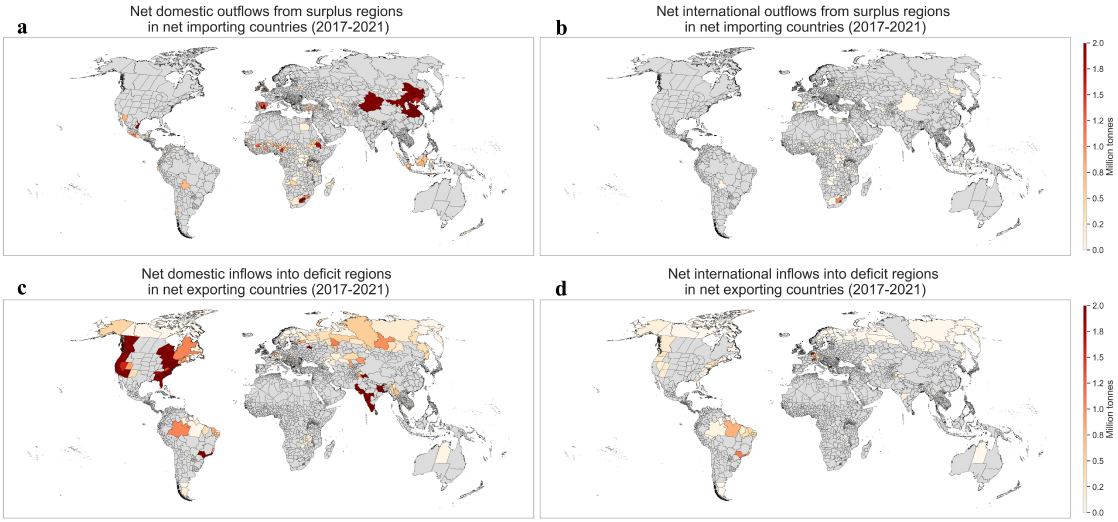

Figure 2.3: Net cereal flows by surplus and deficit regions in net importing and exporting countries, respectively (annual averages, 2017–2021). **a** Net domestic outflows from surplus regions in net importing countries. **b** Net international outflows from surplus regions in net importing countries. **c** Net domestic inflows into deficit regions in net exporting countries. **d** Net international inflows into deficit regions in net exporting countries.

Figure 2.3 panel *a* shows that in several net importing countries, some breadbasket regions still generate internal surpluses. For example, subnational regions in China such as Shandong, Shaanxi, and Jilin, ship significant volumes to the country's south and east; Spain's Castile-La Mancha, Indonesia's Nusa Tenggara Timur and Mexico's Tamaulipas likewise feed domestic shortfalls; and in sub-Saharan Africa, Ethiopia's Amhara, Nigeria's Taraba and South Africa's Free State account for net internal exports. By contrast, Figure 2.3 panel *b* shows that very little of these surpluses is exported internationally. Figure 2.3 panels *c* and *d* mirror the pattern in net exporters. Within the United States, New England and the Pacific Northwest import from domestic heartlands; India's western states and Brazil's northern provinces depend on their national breadbaskets (Figure 2.3 panel *c*). International

imports into these deficit zones remain less prominent, but are significant in a few cases, including Brazil, Denmark, and Germany (Figure 2.3 panel *d*).

2.3.2 Implications for food systems resilience

This section examines food system resilience through the lens of cereal trade flows – first by comparing regional self-sufficiency and trade dependency, and then by evaluating the concentration of cereal flow networks.

Assessing the balance between local self-sufficiency and connectivity with regional and global networks is crucial, given its impact on food security and food systems resilience (Kummu et al., 2020; Wood et al., 2023). Reliance on food inflows allows for a more diverse food supply, increases resilience to local production shocks, and leads to more efficient global production systems (Kearney, 2010; Liu et al., 2019; Seekell et al., 2017). On the other hand, global food flow networks can increase the vulnerability of importing regions to market shocks in exporting regions (Cottrell et al., 2019). Hence, reliance on international inflows must be met with strengthened domestic food flow networks to promote food sovereignty, and to secure food availability (Béné, 2020; Kummu et al., 2020).

To understand the balance between self-sufficiency and trade dependency, Figure 2.4 compares the international and domestic flow patterns in 20 countries. These countries have the largest totals of the three types of cereal flows in the data – international inflows, international outflows, and within country domestic flows. The figure shows that countries in Africa and Asia generally have higher inflows and domestic flows and smaller outflows. In Europe, Latin America and the Caribbean, North America, and Oceania, outflows are higher than or comparable with inflows and domestic flows, with a few exceptions. The volume of domestic flows is highly correlated with the country's population, with a correlation coefficient of 0.80. It is not possible to assess the resilience of cereal flow networks based on flow volumes alone. Hence, domestic and international flows were also evaluated relative to consumption, as described below.

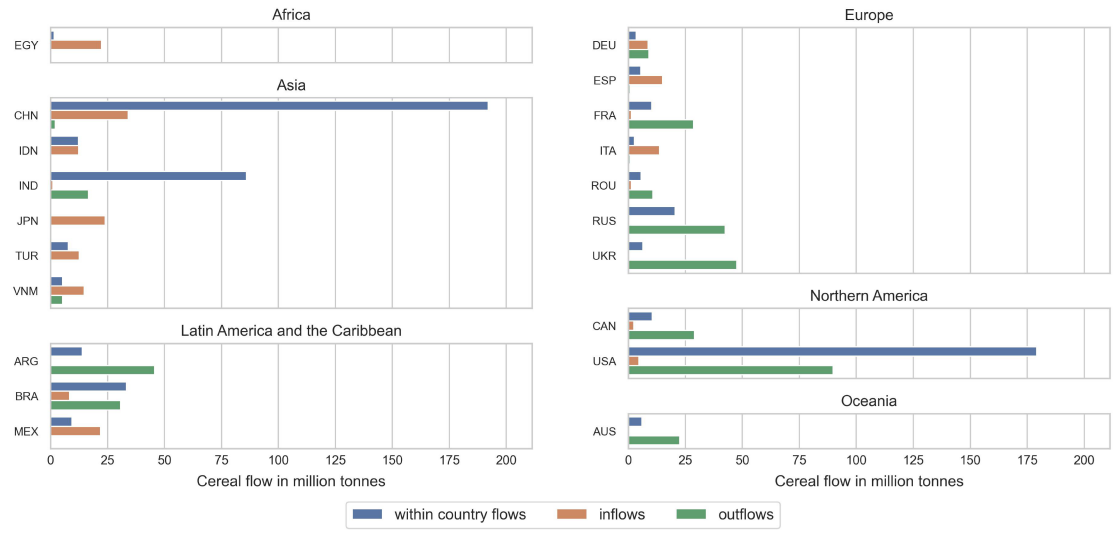

Figure 2.4: A comparison of inflows, outflows, and within country flows for a select 20 countries (2017-2021).

Figure 2.5 quantifies, for each subnational unit, the share of cereal consumption covered by domestic versus international inflows (Panels a and b, respectively). While some regions heavily rely on domestic inflows to meet their consumption, there are others that depend on international inflows, and the two are generally mutually exclusive. Regions along the coastlines in Latin America and Africa, for example, exhibit a greater dependence on international inflows compared to their inland counterparts. Although the cereal flow allocation model explicitly minimizes re-exports, residual onward shipments may still blur the distinction between port-entry and true consumption nodes, and this may partly contribute to elevated import shares along coastlines. Several countries including the United States, Canada, and India, display higher levels of self-sufficiency, with domestic inflows playing a dominant role in meeting consumption demands. Parts of Southeast Asia and Europe show a mixture of reliance on both domestic and international inflows, reflecting complex trade dynamics. Several remote regions such as those in Middle East and North Africa, Northern Canada, and Northern Europe, have domestic or international inflows approaching proportions of 1. These regions have lower consumption levels, which means their absolute inflows are not exceptionally large, but these modest inflows cover nearly 100% of their demand.

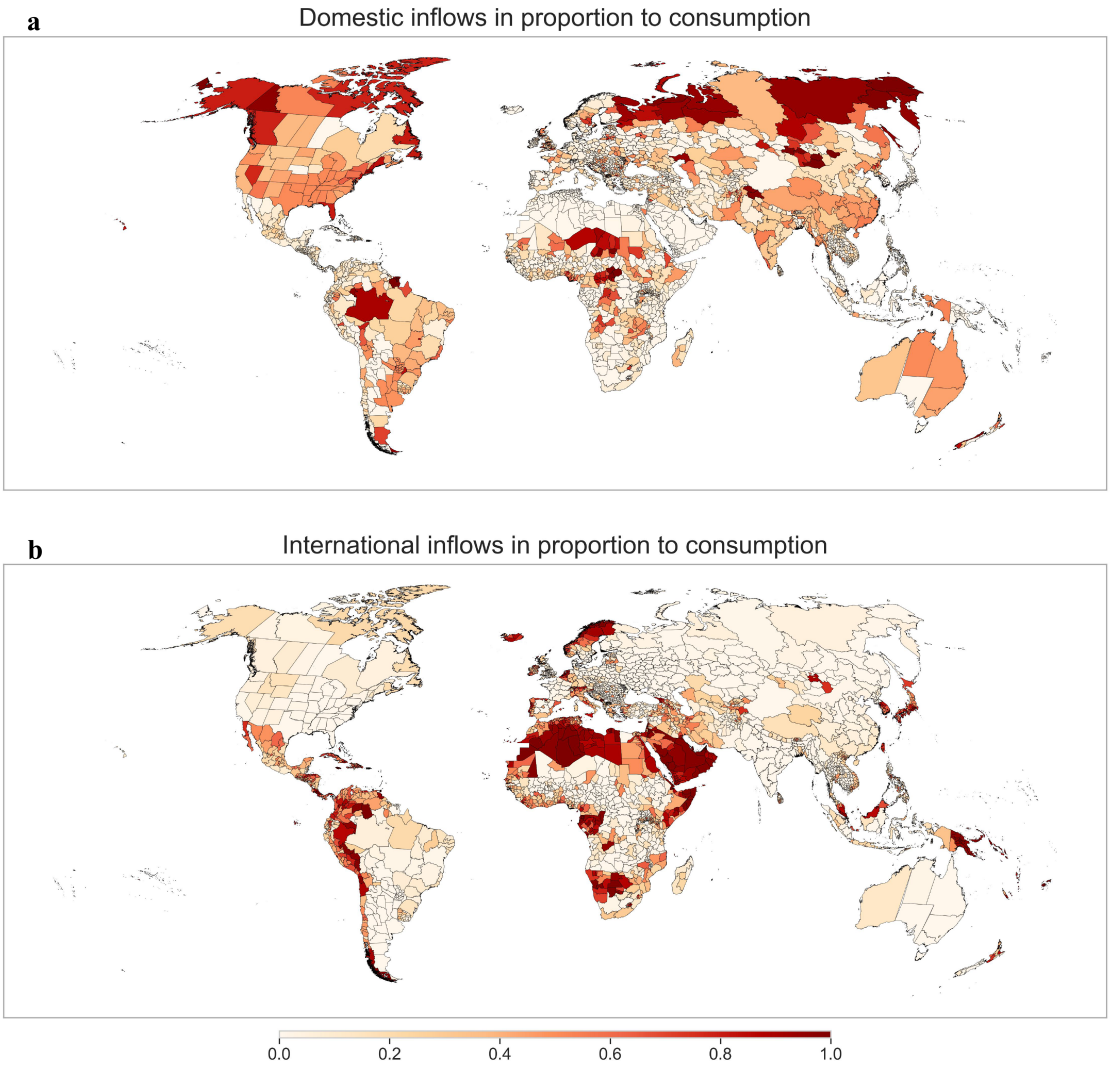

Figure 2.5: Regional inflows in proportion to consumption (2017-2021). a Proportion met by domestic inflows. **b** Proportion met by international inflows. Colors run from 0 (no coverage) to 1 (100% of consumption covered). Subnational cereal consumption is calculated as *subnational production + subnational inflows – subnational outflows*. The sum of the two shares can never exceed 1, i.e. total inflows never exceed consumption.

Globally, international and domestic flows contribute to 16.56% and 26.53% of cereal consumption. Supplementary Figure B.2 shows a breakdown of the contribution of these flows to consumption by continent, with international inflows further broken down into inter- and intra-regional flows, i.e. international inflows originating outside and within the continent respectively. Domestic flows are the most prominent in Northern America and the least in Africa. International inflows are the most prominent in Africa and Latin America and the Caribbean, and

the least in Northern America. Majority of the international inflows into Africa, Asia, and Latin America and the Caribbean, originate from outside the continent. On the other hand, most international inflows into Europe come from within the continent, which can be attributed to the common market and agricultural policy of the European Union.

Food systems resilience also depends on the concentration in food flow networks – lower concentration allows for greater resilience to regional shocks to production (Q. Sun et al., 2022; C. Zhang et al., 2021). In this work, the concentration of cereal flow networks at national and subnational scales is measured using the Herfindahl–Hirschman Index (HHI) and the four-partner concentration ratio (CR4)[1]. Karakoc and Konar (2024) show that national cereal import portfolios with lower HHI consistently exhibit lower price-volatility risk, empirically validating the use of HHI to measure concentration in cereal flow networks. Hernández et al. (2023) demonstrate rising concentration in the agrifood industry using both HHI and CR4, and this research extends their firm-level focus to highlight concentration in cereal flows between countries.

At the national level, the cereal flow network exhibits moderate concentration – the HHI is under 0.10 for both exporters and importers, and CR4 sits at 0.49 for exporters and 0.22 for importers. In other words, a handful of countries account for a large share of global exports, but no one nation dominates, and import destinations are comparatively more varied. While concentration remains moderate overall, greater regional concentration exists. Most countries rely on a limited set of partners for their imports and exports – the median HHI for both imports and exports is roughly 0.27, while the median CR4 exceeds 0.80 in both directions, meaning that for several countries, the top four suppliers provide over 80 percent of their cereal imports and the top four buyers absorb over 80 percent of their

[1]The HHI measures the relative size of firms within an industry and serves as an indicator of market competitiveness. This index ranges from 0 to 1, with 0 representing a highly competitive market and 1 indicating a monopoly. An HHI<0.15 indicates a competitive market, and HHI between 0.15 and 0.25 indicates moderate concentration, and an HHI>0.25 indicates high levels of market concentration. The CR4 measures the market share of the four largest firms and should generally be less than 0.4 for the market to be considered competitive.

exports (Supplementary Figure B.3). These findings echo Kummu et al. (2020), who show import dependency rose and the number of partners fell between 1987-2013, and Fanelli and Giglio (2021), who document that agri-food trade flows are highly concentrated among a small set of country-pairs.

At the subnational level, the global cereal flow network does not exhibit concentration – the HHI is under 0.01 for both exporters and importers, and CR4 is under 0.10 – reflecting the presence of multiple exporting areas within major cereal producing countries, and vice versa. However, this aggregate picture masks pronounced pockets of concentration at finer scales, both within and between nations. Within many countries, domestic cereal distribution is dominated by just a handful of regions (Supplementary Figure B.4). In Bolivia, Ghana and New Zealand, for instance, domestic flows exceed 10,000 tonnes (more than 20% of national consumption), yet only a few key domestic exporters account for these flows (HHI>0.60). The CR4 for these countries approaches 1, but that is less meaningful for domestic networks, since the total number of subnational units is relatively smaller for within country flows.

Considering both international and domestic flows at subnational scales, many administrative regions depend on only a handful of partners, making them particularly vulnerable to local and global production or market shocks (Supplementary Figure B.5). For example, Ayacucho in Peru, where cereal inflows exceed 10,000 tonnes (around 60% of regional consumption), obtains over 70% of its inflows from its top four source regions, and has an HHI of ~0.25. Conversely, Sinop in Turkey, exporting more than 10,000 tonnes (about 60% of its production), primarily sells its grains to a handful of regions (HHI=0.52, CR4=0.80). These findings demonstrate how cereal flow concentration occurs at multiple spatial scales, both between and within countries, with direct implications for the resilience of cereal supply chains.

2.4 Discussion and Conclusions

This study evaluates global cereal flows at spatially resolved scales, providing a detailed analysis of global food supply chains and the vulnerabilities inherent in

food flow networks. The research highlights substantial heterogeneity in subnational cereal flows and identifies pivotal nodes and links within the cereal flow networks. The study underscores the importance of both domestic and international flows for regional food security. With approximately 17% of global cereal consumption met through international flows and 27% through domestic flows, the critical balance between local self-sufficiency and trade dependency in enhancing food systems resilience becomes apparent. Regions that source most of their consumption from domestic inflows enjoy greater insulation from international market volatility but remain vulnerable to local production shocks and domestic transport disruptions. Conversely, regions reliant on international inflows are more exposed to price spikes, export restrictions, and supply chain disruptions in exporting countries. Furthermore, the study reveals regional concentration in cereal inflows and outflows at country and administrative levels, highlighting a need for both strengthening local production capacities and ensuring diversified, efficient trade networks to minimize potential vulnerabilities.

This study's second contribution lies in its innovative modelling approach, which integrates machine learning, data processing and calibration algorithms, to effectively downscale national cereal flow data to a more granular, subnational level. Crucially, despite modest prediction performance, these models help establish a foundational understanding of cereal distribution dynamics.

The modelling pipeline in this research relies on some key assumptions – concerning the spatial accuracy of gridded production data, the estimation of subnational consumption from national-scale relationships, the structural similarity of flow networks across spatial scales, the representativeness of the predictor variables, and the harmonization parameters. These assumptions are enumerated and discussed in full in Supplementary Methods B.3.6. Modelled flows can inherit errors from input data; for example, in the United States, spatial misallocations in the gridded crop production layer overestimate cereal output in Texas and California and underestimate it in Corn Belt states like Iowa and Illinois, producing modest deviations from reported cereal flow patterns. In future work, richer

input datasets, for both predictor and target variables, could improve prediction performance and produce better estimates of cereal flows with less reliance on post-prediction adjustments.

This global, subnational cereal flow analysis fills a critical gap in food systems resilience research, and its findings can support policies aligned with the United Nations' SDG 2 (Zero Hunger) and SDG 13 (Climate Action), while also informing regional initiatives such as EU's Common Agricultural Policy and the Comprehensive Africa Agriculture Development Programme (Commission, n.d. Nations, n.d. Union, n.d.). This research can support future work to build a comprehensive resilience index that balances local self-sufficiency with trade reliance, and can underpin scenario analyses of regional vulnerabilities to climate shocks affecting global breadbaskets. Going forward, integrating these insights into policymaking and scenario planning can guide targeted strategies that bolster food systems resilience.

Data availability This study relies on publicly available datasets as inputs. The data outputs of this study are included with the paper as supplementary information. Any additional data related to this paper may be requested from the corresponding author.

Code availability The code needed to analyse the data and reproduce the figures from this study is publicly available via GitHub.

3

The Environmental Footprint of Retail Foods at Scale: A Multi-Country Analysis

Shruti Jain[1], Savka Akester[1], Joe Kennedy[2], E.J. Milner-Gulland[3], Mike Rayner[4], Ricki Runions[2], Peter Scarborough[5], Michael Clark[1]

[1]*Smith School of Enterprise and the Environment, University of Oxford, UK*
[2]*Global Academy of Agriculture and Food Systems, University of Edinburgh, UK*
[3]*Department of Biology, University of Oxford, UK*
[4]*Nuffield Department of Population Health, University of Oxford, Oxford, UK*
[5]*Nuffield Department of Primary Care Health Sciences, University of Oxford, UK*

Abstract

Understanding the environmental impacts of food products is essential for a sustainable food systems transformation. While there has been extensive characterisation of specific agricultural commodities such as fruits, grains, and meats, there has been much less work on the impacts of multi-ingredient retail foods. Here we analyse around 475,000 products across 74 countries, with especially large samples from North America and Europe. We use machine learning to categorize products into standardized food categories across countries, to help identify product compositions by parsing ingredient lists. By pairing identified ingredients with Life Cycle Assessment (LCA) databases and their supply chain information, we quantify impacts on land use, greenhouse gas emissions, biodiversity loss, eutrophication, and water stress. We find that the relative order of category-level environmental impacts is consistent across different countries, with the highest impacts observed in categories such as animal products, coffee, nuts and seeds, and the lowest in fruits, vegetables, and beverages. However, the absolute impacts of products within categories vary across geographies due to differences in product composition and ingredient sourcing patterns. For some products, sourcing differences across countries can result in

substantially higher or lower footprints, sometimes outweighing their compositional differences – highlighting the potential for targeted supply chain interventions. The findings indicate that sufficient data exist to produce robust, comparable estimates of product-level environmental impacts, that can support policies aimed at shifting demand toward foods with lower environmental footprints.

3.1 Main

The food system is a major contributor to global environmental challenges, including climate change, land-use change, biodiversity loss, freshwater depletion, and the pollution of aquatic and terrestrial ecosystems (Foley et al., 2011). There is an urgent need to transition to sustainable food systems, as even substantial improvements in other sectors will be insufficient to counteract the escalating environmental damage if current food production and consumption practices remain unaltered (Clark et al., 2020; Springmann et al., 2018). Information on environmental impacts of foods sold at retail stores remains vital for this transition, as retail purchases account for the majority of food consumed in many countries (Clark et al., 2022; El Bilali & Allahyari, 2018). Yet such information remains sparse, fragmented, and non-standardized (Deconinck et al., 2023). Scalable estimation and clear, consistent communication of these impacts are critical to support evidence-based purchasing, procurement, reporting, and target-setting, by consumers, retailers, producers, and policymakers.

While numerous studies have quantified the environmental footprints of agricultural commodities such as grains, fruits, and meats (Poore & Nemecek, 2018; Sala et al., 2017), less attention has been paid to the multi-ingredient food products that dominate many modern retail environments. Clark et al. (2022) addressed this information gap by estimating the environmental impacts of retail food products in the United Kingdom through integrating ingredient-level Life Cycle Assessment (LCA) data with parsed product composition information. However, food products vary substantially in their recipes and regional sourcing patterns across geographies, and it remains crucial to develop a global, standardized assessment of retail foods. This research provides a foundation for such standardization by analyzing the environmental impacts of retail food products across a broad geographic scope while

integrating ingredient-level sourcing information, thereby enabling a comprehensive and precise assessment of product-level environmental impacts.

We evaluate the environmental impacts of around 475,000 food products from 74 countries. Our dataset is particularly detailed for Europe and North America; therefore, the findings should be considered representative of product availability only in these regions, while additional data are required to improve product representation in other regions. Nonetheless, the analysis offers valuable insights into the impacts of the specific products included. Through this multi-national lens, our research illuminates both the commonalities and differences in product-level environmental footprints across geographies.

Our analysis reveals that environmental impacts follow consistent trends across regions, with animal products, coffee, nuts and seeds, emerging as some of the highest-impact product categories. Differences in where ingredients are sourced across countries generally have a limited effect on impact estimates for most ingredients and products. However, in some cases, similar products in different countries source ingredients from markedly different production systems, leading to substantially higher or lower impacts – sometimes exceeding differences attributable to product composition. Importantly, these differences reflect variation in production conditions at the source, rather than the geographic proximity between production and consumption. By highlighting these cross-country consistencies and variations, our study provides the evidence base for assessing the role of producer, retailer and consumer behavior in driving food-system impacts, and to identify opportunities for targeted supply chain interventions.

3.2 Results

3.2.1 Estimating the Environmental Impacts of Food Products Across Geographies

The overall environmental footprint of a multi-ingredient food product is determined by aggregating the environmental impacts of its individual ingredients, each weighted by its respective quantity (Figure 3.1). However, the information about ingredient

composition is scarce, and it varies by country. For example, while in United Kingdom and the European Union, food labelling regulations mandate that certain ingredients' percentages be listed on retail foods, in countries like the United States only the rank order of ingredients is required to be listed. Across the entire dataset of foods in this analysis, the percent composition was provided for about 8% of all ingredients, i.e. for about 400k of a total of 5.21 million ingredients. This varied from 1.5% of ingredients in USA & Canada to 13% in France. Percentage composition for all ingredients in a product was listed for only ~14k products in our dataset (~3% of products). On average, the composition of 19% of the product by mass was provided in ingredient lists, which varied from 1.6% in USA & Canada to 29% in UK & Ireland. Accordingly, prior to estimating environmental impacts, we imputed ingredient-level percentage shares for approximately 90% of ingredients, which on average accounted for 80% of total product composition by mass.

This required us to first classify food products into a consistent shared set of food categories that span across countries, using natural language processing and machine learning (see Methods). The categorization scheme was based on the three-tier categories used in the UK National Diet and Nutrition Survey (Supplementary Table C.1). We used a pretrained language model, Sentence-BERT (Reimers & Gurevych, 2019), to obtain contextual representations (embeddings) that capture the semantic meaning of product names and ingredient lists. We then used these embeddings as features in machine learning models to classify each of the ~475k products into one of 104 food categories. This categorization enabled us to leverage known composition information from functionally similar products, to estimate the composition of the ingredients where composition was not provided. This assumes that products within a food category, e.g. white breads, tend to have similar ingredient profiles across supermarkets and countries. Overall, the food categorization models achieved ~90% overall accuracy across all products, ranging from 88% to >95% across product types (Supplementary Tables C.2 and C.3). Classification accuracy was highest for the 'miscellaneous', and 'sugar, preserves, and confectionery' food categories, and lowest for the 'fat spreads' and 'non-alcoholic beverages' categories. This

variation likely reflects differences in semantic separability of categories in the embedding space – categories with distinctive product names and ingredient lists are easier to distinguish than others. For example, low-fat, reduced-fat, and full-fat spreads are less separable due to similar product names and ingredients. By contrast, chocolate confectionery and sugar confectionery might have similar names but often differ in ingredients (i.e. presence/absence of cocoa derivatives), hence improving separability. In addition, products that we call 'edge cases', which could be appropriately allocated into multiple categories, were also challenging for the models, e.g., a 'pasta dish with beef' could be included in both the 'pasta' and 'beef and veal' categories. Supplementary Figure C.2 visualizes the predicted product categories, and Supplementary Table C.4 shows product counts by category.

We next estimated each product's ingredient composition from the ingredient lists using an algorithm developed and tested by Clark et al. (2022). This process estimates the composition of each ingredient in each product, using the known ingredient percentages as provided, and employing a series of algorithms to estimate composition of the remaining ingredients. Missing quantities were estimated based on known ingredient percentages from similarly categorized products with comparable ingredients, with matches restricted to the same country or region to avoid gap-filling with products sold in dissimilar food environments. This ensured that, for example, German products were gap-filled with composition information from other similar products available in Germany and Western Europe, rather than with products from Asia.

We paired the composition estimates with environmental databases that quantify cradle-to-retail impacts of food production systems across five indicators – land use, greenhouse gas emissions, biodiversity loss, eutrophication, and water stress. Environmental data were drawn from Poore and Nemecek (2018) and Blue Food Assessment (Gephart et al., 2021). We used publicly available trade data from FAOSTAT (FAO, 2023) and FishStat (FAO, 2024b) to determine ingredient sourcing, enabling us to use region-specific LCA data for each ingredient. To estimate the possible range for a product's impacts after accounting for its plausible supply chain

pathways, we then conducted a Monte Carlo analysis with 3,000 simulations per product, where each simulation corresponds with a possible supply chain for that product. These simulations yielded distributions of the potential environmental impacts for each product, which we used to derive mean environmental-impact estimates and associated variances for each indicator. To summarize the five indicators, we created a composite metric by first normalizing each indicator to a 0-100 scale (where 0 equals lowest observed impact; 100 equals highest), then averaging those scores with equal weights, and finally re-scaling the result back to 0-100. Expressed per 100 g of product, this composite provides a single metric for comparing products, e.g., a score of 20 indicates that a product's overall impact is 20% of that of the highest impact product. Note that reporting impacts per 100 g rather than per kg is a presentation choice and does not affect the relative comparison of products, but mass-based normalisation differs meaningfully from nutrition-based normalisation (e.g., per 1,000 kcal or per gram of protein), which can produce different impact estimates for the same product.

Although we approximated ingredient sourcing using country-average supply chains, the absence of product-specific sourcing information remains a limitation. The Monte Carlo simulations described above quantify the resulting uncertainty in product-level footprints. For individual foods, the median simulated footprint was, on average, 98% higher than the 5^{th} percentile value and 36% higher than the 25^{th}, whereas the 75^{th} and 95^{th} percentiles exceeded the median by 32% and 138%, respectively. Across products, the median difference between the 5th (lower-impact sourcing) and 95th (higher-impact sourcing) percentile simulated footprints was 1.5 composite units, though it exceeded 30 units for some products. This implies that supply-chain uncertainty typically has only a small effect on estimated footprints, but it can be substantial for a subset of products.

Finally, we computed a confidence score for each product, indicating the robustness of its environmental impact estimate (see Figure 3.2). We define the score as the product of three components: (i) classification model certainty; (ii) the share of ingredient composition provided on the package; and (iii) geographic

coverage of LCA data for the product's likely supply chains (see Supplementary Methods C.3.8). Confidence varies across geographies and categories because ingredient composition is unevenly reported across regions, and the LCA databases are skewed toward commodities and practices common in high-income countries. Products from European countries generally have higher confidence scores, due to more complete composition information and better LCA data coverage. In North America, confidence is lower despite strong LCA data coverage, primarily due to limited composition information. In Asia and Oceania, available composition information is comparable to Europe, but overall scores are lower because of gaps in LCA coverage. Classification model certainty is consistently high across regions and categories (Supplementary Figure C.4).

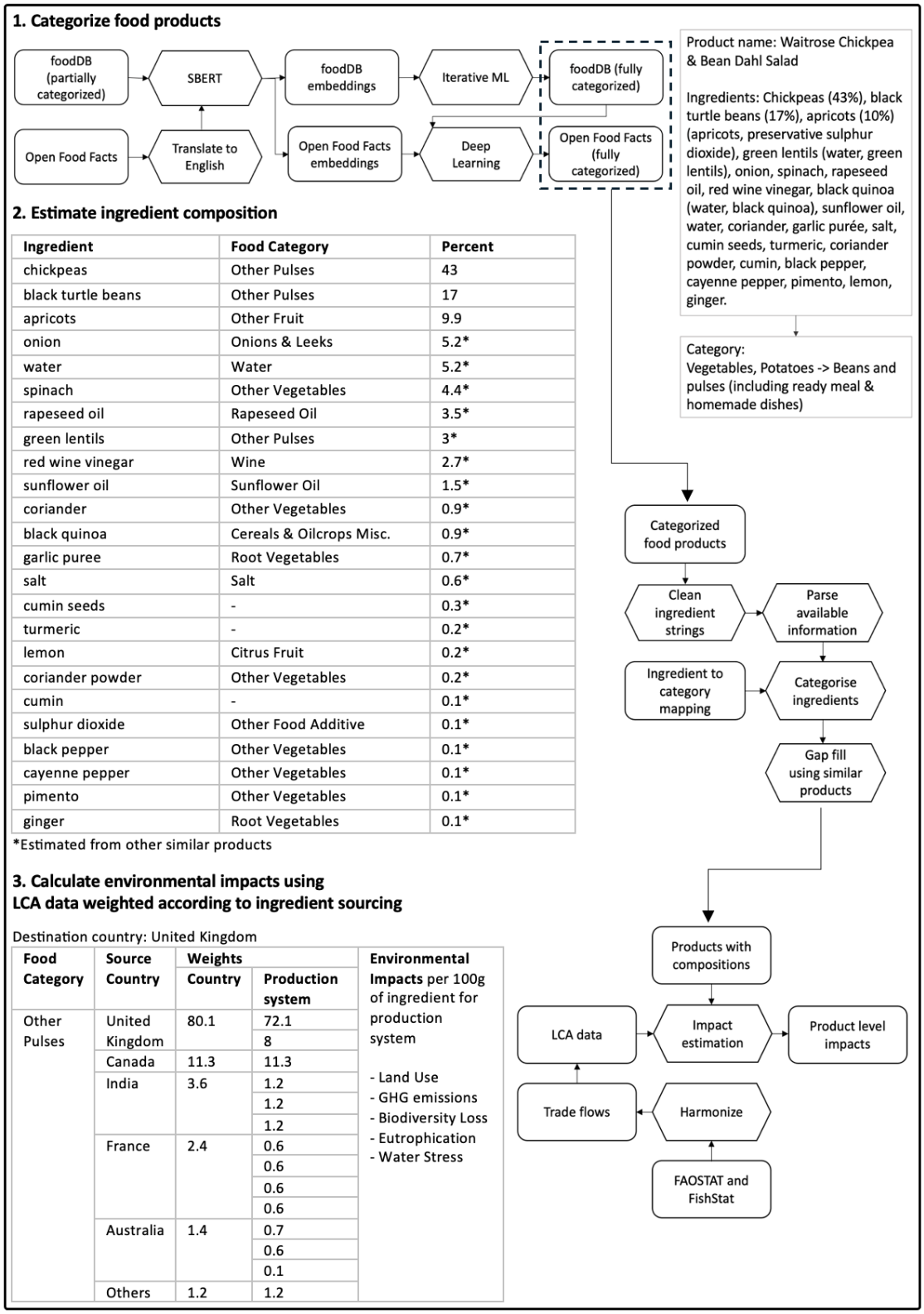

Figure 3.1: Workflow to estimate the environmental impacts of food products across countries, with illustrative examples. Products were sourced from two databases – foodDB (Harrington et al., 2019) and Open Food Facts (world.openfoodfacts.org/data). See Methods and Supplementary Information C.3 for more details.

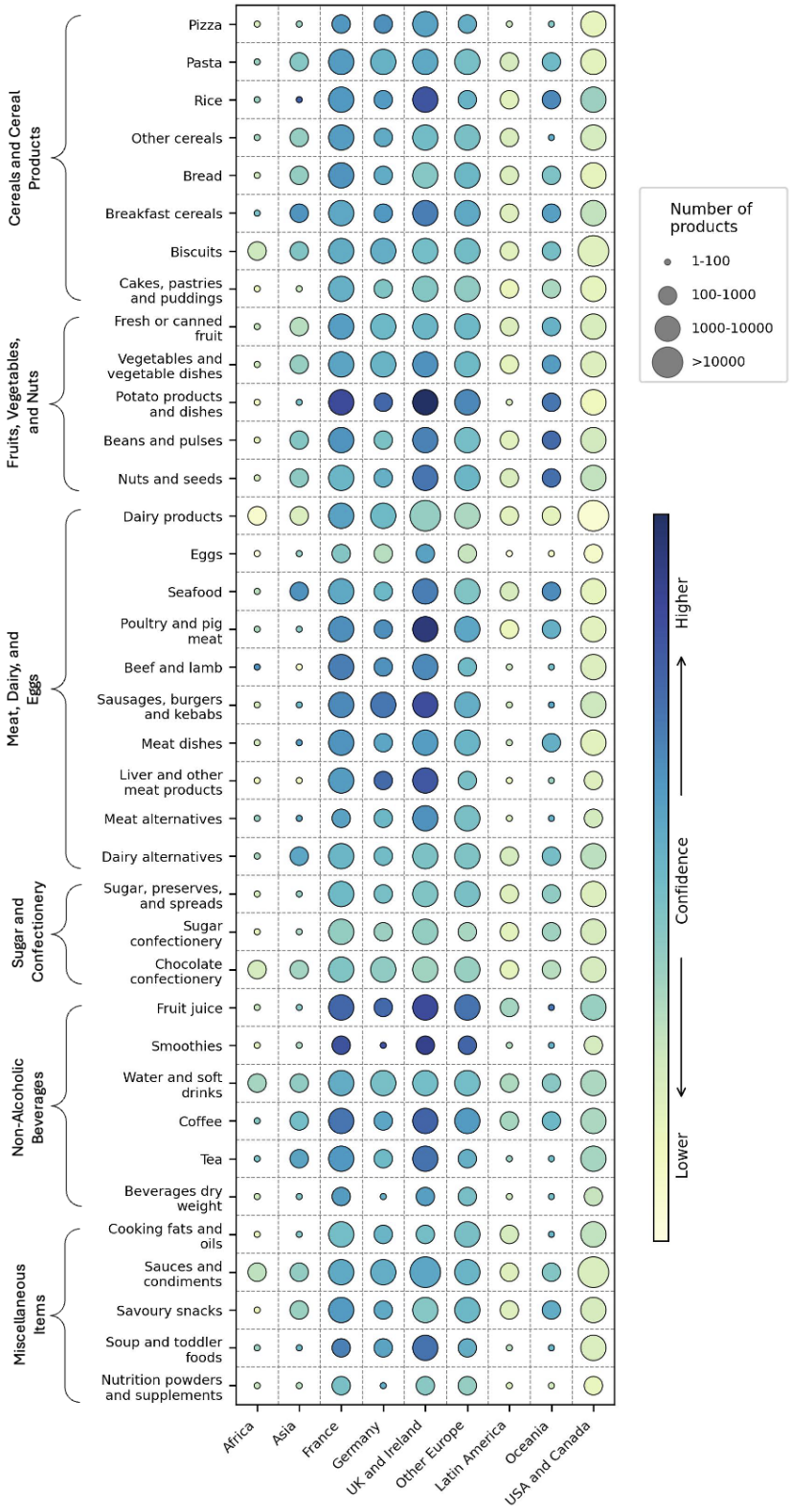

Figure 3.2: Confidence in environmental impact measures across geographies and categories. For plotting, some categories were condensed for visibility and clarity. For instance, white and brown breads were combined into a single 'Bread' group. See Supplementary Methods C.3.8 for details.

3.2.2 Distribution of Environmental Impacts Across Food Products

We estimated environmental footprints for 474,955 products spanning 74 countries. Coverage is concentrated in North America (USA & Canada, 30.8%) and UK & Ireland (25.6%). Within continental Europe, France contributes 19.3%, Germany 5.3%, and other European countries 14.5%. The remainder comes from Latin America & the Caribbean (1.7%), Oceania (1.5%), Asia (0.9%), and Africa (0.4%). Retail category shares vary by region (Supplementary Figure C.5). We report shares only for the five regions with adequate sample sizes, where the product set is likely indicative of products available at retail stores. Across regions, cereals and animal products account for the largest proportion of products available, with processed foods such as biscuits, savoury snacks, sauces and condiments also accounting for a sizable share. In our sample, continental Europe shows a smaller proportion of miscellaneous items (10–13%) than UK & Ireland and USA & Canada (15–18%). USA & Canada have fewer animal products (21%) than Europe (25–29%), while UK & Ireland have fewer fruits, vegetables, and nuts (13% vs. 17–21% elsewhere). These shares provide a plausible proxy for product availability and could be suggestive of the environmental footprints of national dietary patterns.

We find that product-level environmental impacts are highly right-skewed across all countries, with a small subset of products accounting for disproportionately large impacts (Figure 3.3, Supplementary Figure C.6). While most food products have relatively lower footprints on a comparative scale, this does not imply that their impacts are environmentally negligible or that they are sustainable; rather, it reflects the presence of a long upper tail of products with exceptionally high impacts. For the overall distribution of product-level environmental impacts, the 5^{th}, 25^{th}, 50^{th} (median), 75^{th}, and 95^{th} percentiles are 0.2, 0.8, 1.6, 3.6, and 11.7, respectively, meaning that 95% of products have less than one-eighth the impact of the highest impact product. The gap between the 95th percentile and the median is 7.7 times larger than the gap between the median and the 5th percentile, and the individual environmental indicators are similarly right-skewed – again highlighting that a

small subset of products has disproportionately large impacts. The highest impact products are those with high proportions of beef (Supplementary Figure C.7), while the lowest impact products are those with high water content, such as soft drinks. In fact, for products with over 30% beef content, the 10th-percentile footprint is roughly 40% higher than the 90th-percentile footprint of all beef-free products. The highest impact beef-free products, (i.e. those above the 90th percentile) typically contain high proportions of animal products, nuts, tea, coffee, and rice.

Figure 3.3 compares the estimated environmental impacts of food products across categories and geographies, showing that the relative ordering of categories from highest to lowest impact is consistent across regions. Animal-based foods, especially beef, lamb, sausages, burgers and kebabs, consistently exhibit the highest impacts, while fruits, vegetables, and beverages show lower environmental footprints. Tea, coffee, nuts and seeds tend to have higher environmental impact scores per 100g than many other plant-based foods, sometimes even reaching levels comparable with some animal products. Meat alternatives show substantially lower footprints compared with their conventional counterparts, with reductions typically exceeding 60% across regions, while dairy alternatives reduce environmental impacts relative to dairy products by approximately 20-65% across most regions. Within the dairy group, cheeses impose markedly higher burdens than milks, yogurts, or butters (Supplementary Figure C.8). Among cereals-based products, processed foods like bread, pizza and pasta have lower impacts, whereas rice products have higher impacts.

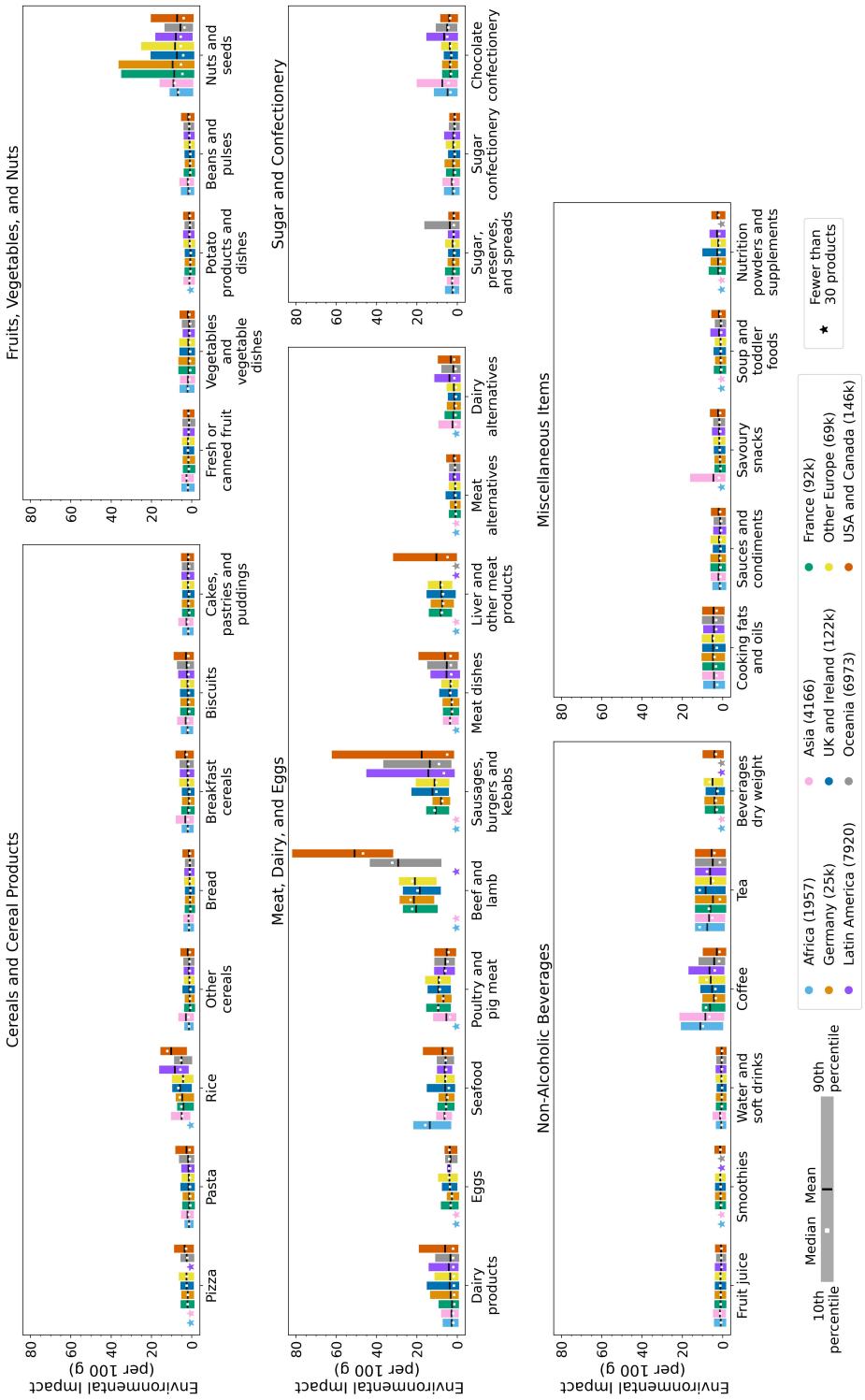

Figure 3.3: Environmental impact of food categories across geographies (per 100 g). For each category, the bars span the 10^{th} to 90^{th} percentile impacts of food products; the mean (black line) and median (white dot) impacts for each category are overlaid. For each product, the impact is given by the mean of its Monte Carlo simulation outputs. Categories with fewer than 30 products are omitted and instead indicated by star markers.

While rank ordering of categories is broadly consistent across regions, the absolute impacts of comparable products can vary considerably between countries. In USA & Canada, 'beef and lamb' and 'sausages, burgers, and kebabs' exhibit especially high impacts. Smaller but meaningful regional deviations also appear for 'rice', 'nuts and seeds', 'dairy products', 'seafood', 'poultry and pig meat', 'meat dishes', 'chocolate confectionery', and 'coffee'. For example, on our composite scale, the average beef jerky product scores roughly 15 in France but ~38 in USA & Canada; chicken and rice dishes average ~4 in UK & Ireland but ~2 in Oceania; pork sausages average ~12 in France versus ~5 in USA & Canada; and chocolate and hazelnut products average around 4 across Europe and North America, but ~7 in Asia.

Crucially, while the composite metric summarizes patterns across regions, it can mask important environmental trade-offs – for example, rice cultivation produces substantial greenhouse gases, yet has comparatively low land use impacts (Poore & Nemecek, 2018). Pairwise correlations among the five indicators range from $r = 0.1$ (biodiversity vs. water stress) to $r = 0.8$ (land use vs. eutrophication), indicating that biodiversity loss and water-stress impacts are largely decoupled, whereas products requiring extensive land conversion also tend to have high eutrophication impacts (Supplementary Table C.9). To unpack these differences, we examine the five indicators separately. Figure 3.4 disaggregates the composite into its five components across the five regions with adequate sample sizes. We focus the main text on nine food categories (rice, nuts and seeds, dairy products, seafood, beef and lamb, dairy alternatives, chocolate confectionery, coffee, and cooking fats and oils) because they span a wide range of composite environmental impacts and exhibit distinct trade-offs across the five component indicators. Comprehensive results for all categories are provided in Supplementary Figure C.9. For beef and lamb products, all indicators except water use lie toward the upper end of their distributions and thus drive the composite; GHG emissions dominate dairy; and water use dominates rice products and nuts and seeds. Dairy alternatives improve substantially on land use, GHG emissions, biodiversity, and eutrophication relative to dairy products, but show comparable or slightly higher water footprints in some regions. The relative

importance of indicators in the composite is consistent across regions for most food types. However, beef and lamb products exhibit substantially higher land use, biodiversity, and eutrophication impacts in USA & Canada than in other regions, but somewhat lower GHG emissions and similar water use footprints. Our impact estimates also enable product-level comparisons across indicators. As an illustration, Supplementary Figure C.10 plots GHG emissions against scarcity-weighted water use for 100 randomly selected products per category across the nine categories.

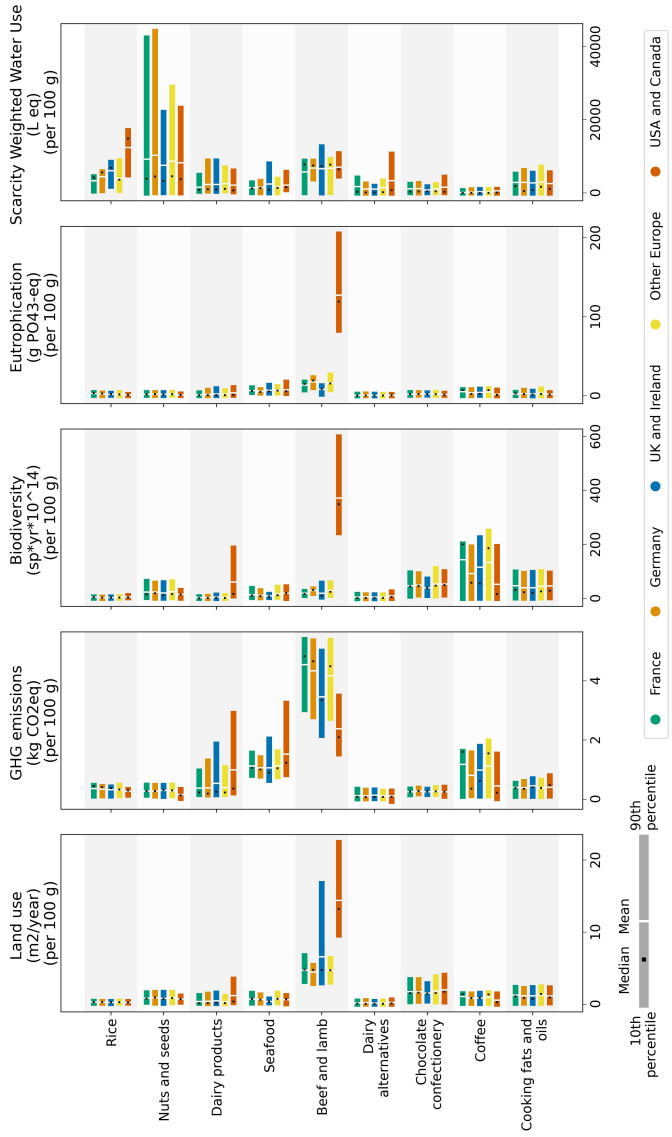

Figure 3.4: Environmental footprints of six food categories across five regions, disaggregated by five impact metrics – land use, GHG emissions, biodiversity loss, eutrophication, water use.

3.2.3 Drivers of Regional Variation in Footprints of Comparable Products

The observed differences in the environmental impacts of certain food products across geographies highlight the need for further investigation. We examine two potential sources of variation in impacts of similar products – differences in ingredient mix (the types and proportions of ingredients), and differences in ingredient sourcing (the production systems from which ingredients are obtained) – to understand how each of these contribute to region-level differences in impacts.

To examine how ingredient mix of similar food products varies between countries, we expressed each product's composition as the proportion of its ingredients falling into five ingredient groups, from lowest to highest ingredient-level impacts. Supplementary Figure C.11 presents these proportions aggregated by food category, capturing the typical ingredient mix within each category across regions. We limit this comparison to the five regions with sufficiently large product samples, which are likely indicative of retail product availability. We find that ingredient mix for similar products sold in different regions is often similar but there are a few exceptions. For example, products in USA & Canada often contain a smaller proportion of the highest impact ingredients (such as bovine meat, nuts, cheese, crustaceans) in the beef and lamb category compared to similar products in other countries, but a higher proportion of high impact ingredients in products in the seafood category. Importantly, these findings are not simply an artifact of our approach to filling in missing ingredient data. Missing ingredient proportions are estimated using products where the same ingredient appears in the same position in the ingredient list, drawing only from products within the same category and country group (see Methods and Supplementary Information C.3.3). Moreover, category-level aggregation captures not just individual product compositions but also differences in the mix of product types available in each region. These patterns indicate that differences in ingredient mix across regions among comparable products are insufficient to fully explain the observed footprint differences, particularly

the differences in mean category-level impacts between regions, motivating an examination of differences in ingredient sourcing.

To understand the effect of ingredient sourcing on product-level impacts, we computed an alternative set of footprints using global average supply chains, ignoring regional sourcing patterns (Methods and Supplementary Information C.3.4). Figure 3.5 compares these to our primary sourcing adjusted estimates. Differences are reported as (global average – sourcing adjusted) per 100g on the composite scale. Positive values indicate products with higher impacts when global average (rather than sourcing-adjusted) supply chains are used to calculate product impacts. Using global average supply chains raises average footprints for beef and lamb products by ~20 units in France and UK & Ireland (over 40 unit increases for some products), but lowers them by ~20 units on average in USA & Canada (up to 40 unit decreases in some cases). Similarly, global average assumptions lower average footprints for seafood in Africa (~7 units), savoury snacks in Asia (~3), rice products in Latin America & the Caribbean (~3) and in USA & Canada (~6), and poultry and pig meat products in UK & Ireland (~2). In contrast, using global average supply chains raises average impacts for dry-weight beverages (~10 units) and chocolate confectionery (~5 units) in Germany, France, Other Europe, and UK & Ireland. These alternative impacts (assuming global average supply chains) are presented in Supplementary Figure C.12. Despite shifts across geographies, the rank ordering of food categories remains broadly similar to that in Figure 3.3, i.e. incorporating sourcing information changes the absolute impacts of a product, but is unlikely to change the relative order of impacts between products. Cross-regional variation among comparable products is smaller when global average supply chains are used, consistent with differences in ingredient mix across regions.

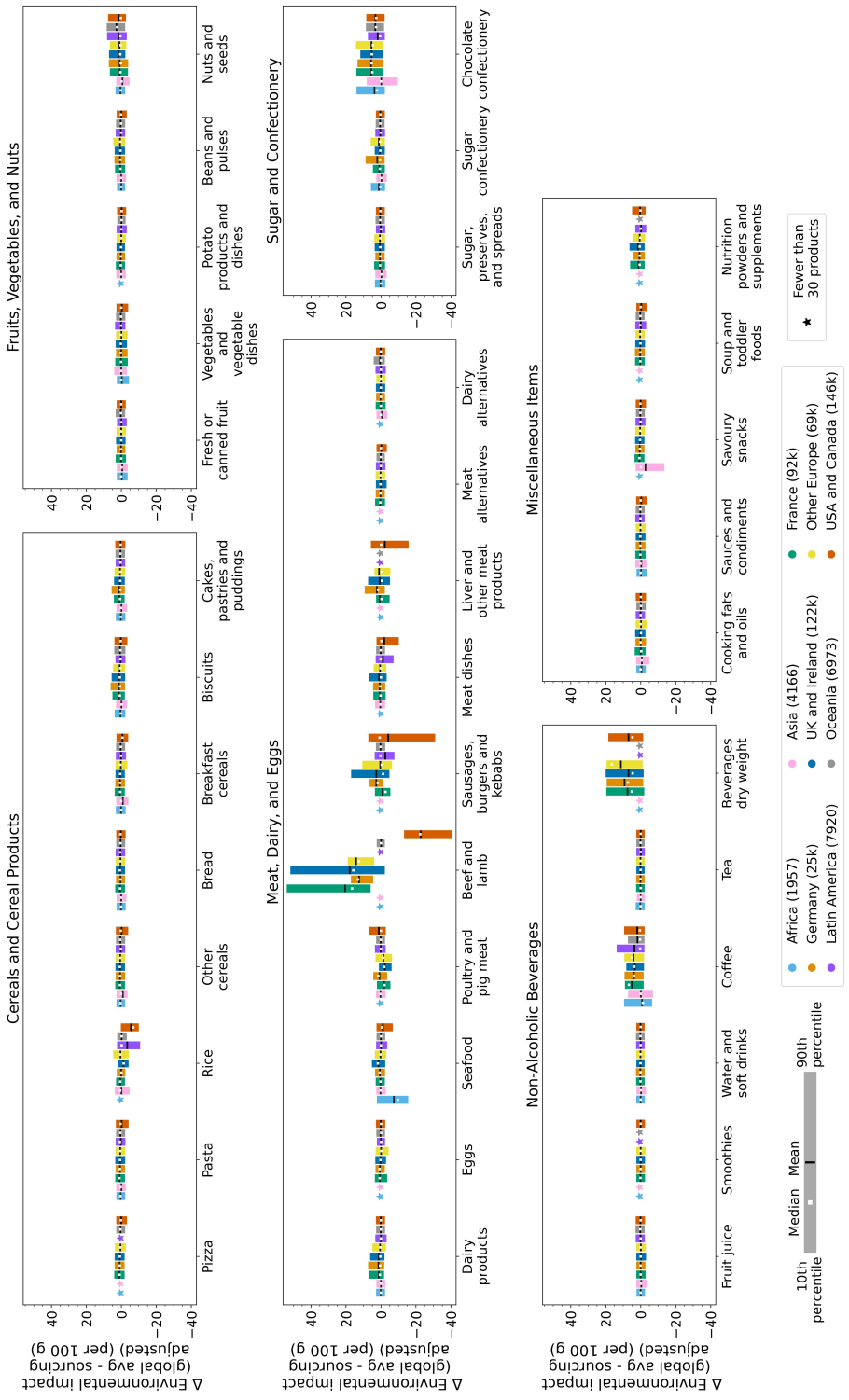

Figure 3.5: Differences in environmental footprints (per 100g) of food categories across geographies, when computed excluding vs including ingredient sourcing. For each category, the bars span the 10^{th} to 90^{th} percentile of product-level differences; the mean (black line) and median (white dot) differences of each category are overlaid. Categories with fewer than 30 products are omitted and instead indicated by star markers.

To further quantify how much of the variation in product-level impacts is attributable to ingredient sourcing, we computed the Pearson correlation between our two sets of estimates (those computed with and without accounting for ingredient sourcing) across all products. The correlation is $r = 0.80$, indicating that approximately 64% of variation in product impacts is explained by factors other than sourcing, i.e. product composition (r^2), while the remaining 36% reflects sourcing-related differences ($1 - r^2$). The importance of sourcing differs markedly by category, e.g., it is minor for dairy products, nuts and seeds, and tea ($r > 0.95$; sourcing $< 10\%$), but substantial for rice, dry-weight beverages, chocolate confectionery, and especially beef and lamb (r = 0.10; sourcing = 99%). The low correlation for beef and lamb does not mean that products in this category have identical compositions – these products vary widely in their share of highest-impact ingredients (40% to 100%), as also reflected in the large 10th-90th percentile impact bars for these products across all regions in Figure 3.3. Rather, it reflects the fact that sourcing differences can outweigh compositional differences, e.g. a product containing 50% beef sourced from high-impact production systems can have a larger footprint than a product containing 90% beef sourced from lower-impact systems (Supplementary Figure C.7). However, this does not imply that sourcing decisions are more important than ingredient choice for reducing impacts, as products with substantial beef content remain among the highest-impact products regardless of sourcing, even if sourcing decisions shift their relative ranking. The contribution of sourcing also differs by indicator – overall, it explains roughly 17% of variation for water scarcity ($r = 0.91$), 31% for GHG emissions ($r = 0.83$), 51% for land use ($r = 0.70$), 56% for eutrophication ($r = 0.66$), and 68% for biodiversity loss ($r = 0.57$). Supplementary Table C.10 presents the full set of correlations across all food categories and indicators.

3.3 Discussion

This study presents a global, multi-indicator, product-level assessment of the environmental footprints of nearly half a million food products and establishes

a scalable impact-estimation framework for multi-ingredient retail foods across geographies. By bridging commodity-level LCA and product-level analysis, together with information on ingredient sourcing, our work advances the literature and enhances the granularity of environmental assessments.

Our analysis confirms that, consistent with commodity-level studies, animal-based products carry substantially higher environmental footprints compared to plant-based and processed foods. While overall trends in environmental impacts are similar across regions, notable differences emerge upon closer inspection. These variations are explained partly by product composition, and partly by ingredient sourcing. When we omit sourcing information, impact profiles change markedly for some products and categories, highlighting the sensitivity of certain food categories to sourcing practices. Our findings suggest that the most reliable gains come from shifting demand away from highest-impact categories and toward lower-impact alternatives (e.g., replacing ruminant meat with poultry or plant-based options), and that supply-chain interventions can complement such shifts, particularly where the data show large sourcing effects (e.g., beef and lamb products, rice dishes, etc.). Crucially, even the best-sourced beef and lamb products exceed the footprints of meat alternatives or beans and pulses – underscoring that while sourcing matters, dietary shifts remain the primary lever for reducing food-system impacts.

Even where supply-chain interventions are warranted, regional sourcing information is necessary but not sufficient as a policy lever. Consumer-driven shifts toward lower-impact sources face structural limits: lower-impact production systems often cannot scale to meet aggregate demand, and price-sensitive consumers may continue purchasing from higher-impact sources. Achieving genuine reductions requires combining sourcing transparency with mechanisms that change production practices at the source, including price incentives such as carbon pricing or differentiated input subsidies, supply-side regulation of high-impact production systems, investment in lower-impact farming techniques, and trade policies that internalise environmental externalities. Sourcing information at the product level provides the evidence base for these systemic interventions, but the interventions themselves must operate

through the political and economic structures that shape how food is produced – not only through individual consumer choice.

The approach demonstrated here uses an open and transparent algorithm to estimate the environmental impact of a food product by connecting its ingredients with a dataset of LCAs. The pipeline here has been developed using LCA data from Poore and Nemecek (2018), but the modular approach means that this can be replaced with other LCA datasets where necessary. This provides a mechanism whereby we can estimate the environmental impact of any food product with an ingredients list. Of course, this approach is limited by the amount of information that is available on an ingredients list – if manufacturers have more specific information about the contribution of ingredients to the composition of the product and the sourcing of those ingredients, then a more refined estimate can be reached. This approach is analogous to how nutrition labelling regulations are applied in the UK and elsewhere, where estimates of the nutritional content of food is based on linking ingredients with nutritional data from Food Composition Tables, e.g. McCance and Widdowson (2014). These estimates are used as the baseline but can be superseded by chemical analyses of specific food products if needed. Nutritional data estimated in this way are the bedrock of public health regulations worldwide – adapting an analogous approach for environmental metrics could open the doors to policies and regulations that support more sustainable diets. Our pipeline can be used and adapted to support ecolabelling schemes like France's "Planet Score" (Hélias et al., 2022) and voluntary carbon-footprint labels in Japan (Potts et al., 2014), by calculating and analyzing per-product impacts at scale. The pipeline, and outputs from it, can also be integrated into decision-support tools that link environmental footprints with nutrient profiles and affordability to guide healthier, lower-impact choices (Willett et al., 2019), and it can power manufacturer and retailer scorecards that compare performance across multiple environmental dimensions (Thøgersen & Nielsen, 2016).

The analysis also highlights research and data priorities. First, while our LCA database encompasses data from over 40,000 food production systems, these are

skewed toward commodities and production systems prevalent in high-income regions. As a result, environmental data for some origin regions may be sparse or unavailable, necessitating the substitution of data with available proxies. Similarly, the food product datasets used in our analysis favor markets in Europe and North America. Consequently, our findings are most robust for developed markets and may not fully capture consumption patterns or production practices in under-sampled regions. Closing these data gaps is urgent as global targets call for halving food-system emissions by 2030 (Nkonya, 2019). Our analysis reveals geographic and category-level heterogeneity in data coverage, pinpointing regions where LCA inventories and ingredient composition records remain sparse. Our research can be used to identify environmental hotspots, calibrate context-specific interventions, and monitor progress toward the twin goals of nutritional security and climate mitigation (Springmann, Godfray et al., 2016).

3.4 Methods

There were three main elements in the approach to estimate food product impacts across geographies (Figure 3.1). First, we developed a machine learning pipeline to categorize food products into standardized categories across countries. Second, with the categorized products, we used the previously developed algorithm that estimates product ingredient composition by leveraging known ingredient lists, with similarly categorized products used to gap fill missing composition information (Clark et al., 2022). And last, we used publicly available information on trade flows to determine sourcing of identified ingredients, and the composition and sourcing information was combined with LCA databases to estimate the environmental impacts of food products. A brief description of these steps is provided below, see Supplementary Methods C.3 for more details.

We estimated the environmental impacts of food products from two large-scale datasets - foodDB (Harrington et al., 2019) and Open Food Facts (homepage). FoodDB is a web tool which systematically scrapes major UK and Irish retailer

websites. Open Food Facts is a publicly available dataset, which relies on crowd-sourcing to collect information about food products available around the world. We obtained 262,711 products from foodDB and 961,989 products from Open Food Facts. Nearly two-thirds Open Food Facts entries were non-English, and we deployed automated language detection followed by machine-assisted translation to English. After all products were categorized, ingredient text was cleansed via regular expressions to strip extraneous content, such as allergen warnings, sourcing statements, or promotional claims, and standardized into a uniform format. Products whose lists could not be reconciled to this uniform structure were excluded, and composition was estimated for the rest of the products. Products whose identifiable ingredient mass fell below a predefined completeness threshold of 75%, were also excluded. This multi-stage cleaning pipeline yielded just under half a million food products covering over seventy countries and multiple retail contexts, for which environmental impacts were estimated.

3.4.1 Automated product categorization

We first allocated all food products into a set of shared food categories. This allowed us to a) estimate composition of ingredients where this is not provided in ingredient lists, and b) to compare the environmental impacts of similar products that are sold in different countries. For the food categories, we adopted the hierarchical categorization system followed by the UK National Diet and Nutrition Survey (Amoutzopoulos et al., 2025). This categorization system organizes foods into broad parent categories (such as cereals, dairy, fruits, vegetables, meats and fish), further divided into detailed main (such as bread, and cheese) and subcategories (such as white bread and cheddar cheese). We made a few adjustments to this system to remove redundancies (e.g., merging homemade and manufactured pasta categories into one), and added a category to capture non-food items in our dataset, which resulted in a total of 18 parent categories, 53 main categories, and 104 subcategories.

To categorize products, we developed a supervised machine learning approach, where we trained classification models to predict food categories based on product

descriptions. To train these models, we assembled a labelled dataset of ~60,000 products from foodDB, by combining fuzzy-matching techniques, annotation via a large-language-model API with researcher review, and direct manual labelling (Kennedy et al., 2025). The classifiers used product descriptions, i.e. product names and listed ingredients, as model features. For each product, we concatenated the product name with ingredient string, and then generated vector representations using the Sentence-Bert model (Reimers & Gurevych, 2019). This approach captures both semantic nuance and contextual cues in a fixed-length embedding, enabling classification without intensive domain-specific tuning.

Our categorization pipeline works in two stages. First, a parent model assigns each product to one of the 18 parent categories, simplifying the classification problem. Second, specialized subcategory models refine each item's label within its parent category, i.e., they allocate products in each parent category (such as milk and milk products), into one of the potential subcategories (such as whole milk, skimmed milk, cheese, yogurt). We began with a labelled dataset of products from foodDB, which we used to categorize the entire foodDB collection. Our goal was to achieve highly accurate foodDB classifications so that these category assignments could then serve as reliable and representative training data for categorizing products from other datasets, such as Open Food Facts.

To accomplish this, we followed an iterative process – training machine learning models on the labelled data, predicting on the unlabelled portion of foodDB, and then manually correcting and expanding the labels to retrain improved models. This cycle was repeated until manual evaluations showed both strong overall accuracy and consistently high precision across all categories. During this phase, we primarily used Random Forest classifiers. Although we also tested alternative models – including linear discriminant analysis, k-nearest neighbours, and histogram gradient boosting – all achieved comparable out-of-sample accuracies (approximately 85% to over 95% at the parent and most subcategory levels). However, Random Forests produced more reliable results on previously unlabelled products, making them our model of choice.

Once we achieved robust category predictions on foodDB, we scaled up by training deep learning classifiers on the larger dataset of roughly 260,000 foodDB products. These models were then applied to classify approximately 960,000 products from Open Food Facts in a single pass, with no additional manual correction required.

3.4.2 Ingredient parsing and composition estimation

Deriving accurate ingredient breakdowns from ingredients lists is challenging because of inconsistent formatting, nested sub-lists, and the need to estimate percent composition for most ingredients in a product. For this work, we built on the methodology of Clark et al. (2022), extending it to accommodate the greater variability in our dataset across multiple geographies. The Clark et al. (2022) approach proceeds in three steps. First, ingredients text is parsed to identify individual ingredients and their percent composition, when reported. Second, these ingredients are mapped to one of 110 agricultural commodities to enable i) estimation of ingredient composition when unknown, and ii) integration with environmental databases (Gephart et al., 2021; Poore & Nemecek, 2018). For example, shiitake mushrooms are mapped to 'Mushrooms', and organic peanut butter to 'Groundnuts'. Third, a series of algorithms estimate the composition of ingredients with unknown shares by drawing on the composition of similar ingredients in similar positions across comparable products. The final output is adjusted to comply with food regulations, ensuring that ingredient shares sum to 100% and that each ingredient accounts for at least as much mass as the one listed after it.

We extended this methodology in two ways. First, we standardized ingredient strings across products from both foodDB and Open Food Facts. Ingredients were separated by commas, percentages (when available) placed in brackets after the ingredient name, and sub-ingredient lists nested within brackets following the same format. Second, whereas Clark et al. inferred missing composition from products stocked on the same supermarket shelf, aisle, or department, we gap-filled missing composition using products from the same classification category and

geographic cluster (e.g., Western Europe, Southeast Asia; Supplementary Table C.5). This ensured that product composition was imputed using similar products available in comparable food contexts.

Through this process, we estimated compositions for ~4.81 million of the 5.21 million ingredient entries, covering approximately 80% of the total ingredient mass in our dataset.

3.4.3 Linking compositions to environmental impacts

To translate ingredient compositions into environmental footprints, we linked each ingredient to its environmental impacts under different production systems, as reported in LCA databases. Because production systems vary geographically, and countries source ingredients from these regions in varying proportions, we weighted the LCA data by real-world sourcing shares derived from bilateral trade data from FAOSTAT (FAO, 2023) and FishStat (FAO, 2024b). The trade data were first harmonized using algorithms from Gehlhar (1996) and Croft et al. (2018) to resolve two reporting discrepancies – i) import volumes reported by importing countries often differed from those reported by exporters, and ii) total reported exports from some countries exceeded the sum of production and imports, reflecting misreporting or re-exports counted as exports. Using the harmonized dataset, we estimated, for each country, the share of each commodity in the LCA database that was sourced from different supplier countries. When a supplier lacked country-specific data for a commodity, we substituted it with corresponding regional averages.

For each product, we conducted a Monte Carlo analysis with 3,000 simulations, repeatedly sampling production-system footprints for each ingredient in proportion to its sourcing probabilities. This yielded distributions for five environmental indicators (land use, greenhouse gas emissions, eutrophication potential, biodiversity loss, and water scarcity), from which we calculated their expected values. We also computed ingredient-level shares of each product's impact by pooling across draws. For each indicator, we summed each ingredient's impact over the 3,000 draws and divided by the pooled product-level total.

In parallel, we ran another set of simulations that ignored trade flows, allowing us to isolate the effect of sourcing patterns on overall footprints. For these simulations, we weighted each ingredient's LCA data for different production systems by their share in global production rather than by specific regional sourcing.

To communicate product-level environmental impacts, we normalized each indicator relative to the global distribution of observed values and averaged the five indicators into a single composite impact score. This composite score was further normalized on a 0-100 scale, enabling direct comparison among foods with diverse compositions and sourcing patterns. For the sourcing-agnostic analysis, indicators and scores were normalized using the minimum and maximum values from the sourcing-informed results to ensure comparability between the two approaches.

3.4.4 Computing sourcing-adjusted ingredient footprints and summarizing product composition

For each indicator, we estimated sourcing-adjusted ingredient footprints (per 100 g) by dividing an ingredient's contribution to a product's total impact by its percentage in that product. Ingredient composite scores were then computed using the same five-indicator aggregation as for product-level footprints, with indicator values normalized to the same min-max bounds as for products to ensure comparability. Because an ingredient can appear in multiple products, and each product's Monte Carlo draws sample different sourcing pathways, its estimated footprint varies across instances, yielding a sourcing-dependent distribution of ingredient impacts.

To group ingredients, we averaged each ingredient's composite score across all products in which it appeared, ranked ingredients by their mean footprint, and split them into five equal-sized impact groups (from lowest to highest). To enable comparison of composition across geographies and food categories, each product's composition was then expressed as the proportion of its ingredients falling into these five groups, yielding a common five-variable representation.

3.4.5 Quantifying the confidence in each product's environmental impact estimate

We quantified confidence in each product's environmental impact estimate as the product of three components: classification certainty, composition completeness, and LCA data coverage. Classification certainty reflected the reliability of product categorization. All foodDB products were assigned a high baseline certainty given extensive validation, while Open Food Facts products were assigned variable certainties depending on the classification models' probability scores at the parent and subcategory levels. Composition completeness captured the proportion of a product's ingredients identified by weight on the label, with higher completeness corresponding to greater confidence. LCA data coverage represented the geographic resolution of environmental data available for each ingredient – country-level data contributing most to confidence, and regional or global averages contributing less. Additional details on these calculations are provided in the Supplementary Methods C.3.8.

Data Availability The data used in this study will be partially available after publication. All data for products obtained from Open Food Facts will be made publicly available via a research archive. Product-level data from foodDB cannot be made publicly available due to privacy and proprietary reasons. Access to this data will be available upon request by email to fooddbaccess@ndph.ox.ac.uk.

Code Availability All code used for this study will be made publicly available after publication, via a GitHub repository.

4

The Impact of Dietary Transitions, Trade Policy and Climate Change on Food Production and Import-dependence through to 2050

Shruti Jain[1], Michael Clark[1], Jim Hall[2], Jasper Verschuur[3]

[1]*Smith School of Enterprise and the Environment, University of Oxford, UK*
[2]*Environmental Change Institute, University of Oxford, UK*
[3]*Faculty of Technology, Policy and Management, Delft University Technology, NL*

Abstract

International food trade is critical for global security yet faces compounding pressures from climate change, evolving dietary preferences, and shifting trade policies. We quantified how these forces jointly reshape global food networks by modelling bilateral trade for 32 crops across 153 countries through 2050, integrating climate pathways, dietary scenarios, and trade liberalization regimes. We find that dietary transitions are the dominant driver of future agricultural production and trade patterns. Climate pathways exert comparatively modest effects under our model setup, though this finding assumes continued technological progress to offset climate-induced productivity losses; under more pessimistic adaptation scenarios, climate effects could be substantially larger. Traditional commodity corridors, particularly grain and soybean flows from the Americas to Asia, weaken substantially under plant-forward scenarios, while trade in fruits and vegetables intensifies. Major producing countries face uncertain futures depending on which pathway materializes. While dietary choices primarily dictate regional supply requirements, trade policy remains a critical determinant of export dynamics. Furthermore, trade liberalization

consistently increases both import dependence and concentration across crop groups, suggesting that while open markets may improve efficiency, they also concentrate risk among fewer suppliers. Vulnerability profiles vary markedly across regions, with some facing heightened dependence while others see reduced risk. These results underscore the need for strategic coordination of dietary guidelines and trade policy to ensure dietary transitions deliver both environmental and food security benefits.

4.1 Main

International food trade has more than doubled in the last two decades (FAO, 2022), and is critical to ensuring global food security. Trade enables linking surplus regions to deficit ones and can serve as an adaptation mechanism under climate change (Janssens et al., 2020; Suweis et al., 2015). Yet, trade networks can also transmit geopolitical and environmental shocks and concentrate food production, exchange, and transport risks (Centeno et al., 2015; Grassia et al., 2022; Wellesley et al., 2017).

Several forces will determine the evolution of food trade over the coming decades. Socio-economic growth across economies will create changes in the demand for food products, especially in emerging economies (Pingali, 2007). Climate change will unevenly affect regional crop productivity (Gaupp et al., 2019; Rezaei et al., 2023). Efforts to promote healthier or more sustainable diets, with the potential to reduce environmental impacts of food systems (Clark et al., 2020; Poore & Nemecek, 2018; Springmann et al., 2018) would reallocate demand across commodities (Springmann, Mason-D'Croz et al., 2016; Willett et al., 2019). Additionally, trade policy regimes can further shape how production and consumption are spatially distributed and how efficiently surpluses reach deficit regions. Present-day trade networks already exhibit structural vulnerabilities, with over a third of countries unable to achieve self-sufficiency for most essential food groups, and low self-sufficiency coupled with dependence on a limited number of exporters constraining national capacities to absorb global shocks (Stehl et al., 2025). How climate change, dietary transitions, and trade policy regimes may jointly reshape bilateral flows, self-sufficiency, and import concentration (reliance on few exporters) remains poorly understood, yet is essential for anticipating emerging food security risks.

4. The Impact of Dietary Transitions, Trade Policy and Climate Change on Food Production and Import-dependence through to 2050

We address this gap by modelling future scenarios that couple projections of climate change and socio-economic pathways with dietary transition pathways and alternative trade policy regimes. Diet transitions are represented using benchmarks from the EAT-Lancet Commission that target human health and environmental sustainability (Willett et al., 2019). These are linked with country-level yield trajectories that reflect climate impacts and technological progress, in a modelling approach that solves for market-clearing quantities, prices, and trade under alternative trade-liberalization regimes. Here, trade liberalization refers to the degree to which countries can flexibly source imports from global markets, rather than the removal of specific tariffs or quotas. Covering 153 countries and 32 vegetal commodities (all major food crops except tea, coffee, cocoa, and spices) from 2020 to 2050, we quantify changes in total demand, import dependence, and bilateral trade flows, and assess how concurrent shifts in climate and diets reshape the geography and concentration of global trade.

We find that dietary transitions emerge as the dominant driver of future agricultural production and trade patterns, with trade policy modulating spatial distribution and climate pathways exerting comparatively modest effects. These demand shifts trigger a restructuring of bilateral trade networks and introduce new vulnerabilities. Import concentration increases across most crop groups by 2050, especially under freer trade scenarios, suggesting that trade liberalization may enhance efficiency but concentrate risk among fewer suppliers. Country-level production trajectories prove highly scenario-dependent, with major producers facing substantial uncertainty depending on which dietary and trade pathway materializes. Together, these findings reveal that realizing dietary transitions are likely to demand considerable adjustment in how food is produced and traded globally, underscoring the need for coordinated dietary and trade policy for building equitable and resilient food futures.

4.2 Results

We used a multi-country partial-equilibrium model to project crop-level demand, supply, and bilateral trade for 32 crops across 153 countries through 2050. The model was calibrated to baseline trade flows observed during 2018-2022, incorporating country-specific production and bilateral trade costs. For each scenario, the model jointly solves for supply, demand, consumer and producer prices, and bilateral trade flows in five-year intervals from 2020 to 2050, using forward projections of diets, yields, and demand and supply elasticities. On the demand side, dietary pathways include benchmark, flexitarian, pescatarian, vegetarian, and vegan trajectories, with per-capita consumption translated to country totals using population and food/feed/other shares. On the supply side, yields evolve along climate-affected trajectories (RCP 2.6 and RCP 7.0) overlaid on technological progress. Trade policy is varied through 'low' and 'high' liberalization regimes (see Methods and Supplementary Methods D.3). The full factorial design (diet × climate × trade, 2020-2050) yields equilibrium projections from which we summarize changes in total demand, import reliance, and bilateral flows relative to 2020, and characterize scenario-driven uncertainty.

Figure 4.1 presents projected global market-clearing quantities and trade fractions for six major crop groups from 2020 to 2050 under varying diet, climate, and trade liberalization scenarios. Production trajectories diverge substantially across dietary pathways, with the most pronounced differences observed in grains and soybeans. Plant-forward diets (vegetarian and vegan) reducing production demand for both grains and soybeans, while animal-protein-rich diets (benchmark, flexitarian, pescatarian) maintain or increase production levels. Fruits and vegetables demonstrate consistent growth across all scenarios, but particularly for vegan diets, rising from 2,000 to about 3,500 million tonnes. Trade fractions reveal distinct patterns by crop group. Grains, soybeans, oil crops and sugar crops maintain relatively high trade shares, while roots and tubers and fruits and vegetables remain predominantly locally consumed. Trade liberalization regimes significantly influence trade intensity, with high liberalization scenarios generally exhibiting

greater trade fractions. Climate pathways exert more modest effects compared to diet and trade policy. Overall, dietary transitions emerge as the dominant driver of future agricultural production patterns, with trade policy modulating the spatial distribution of production and consumption.

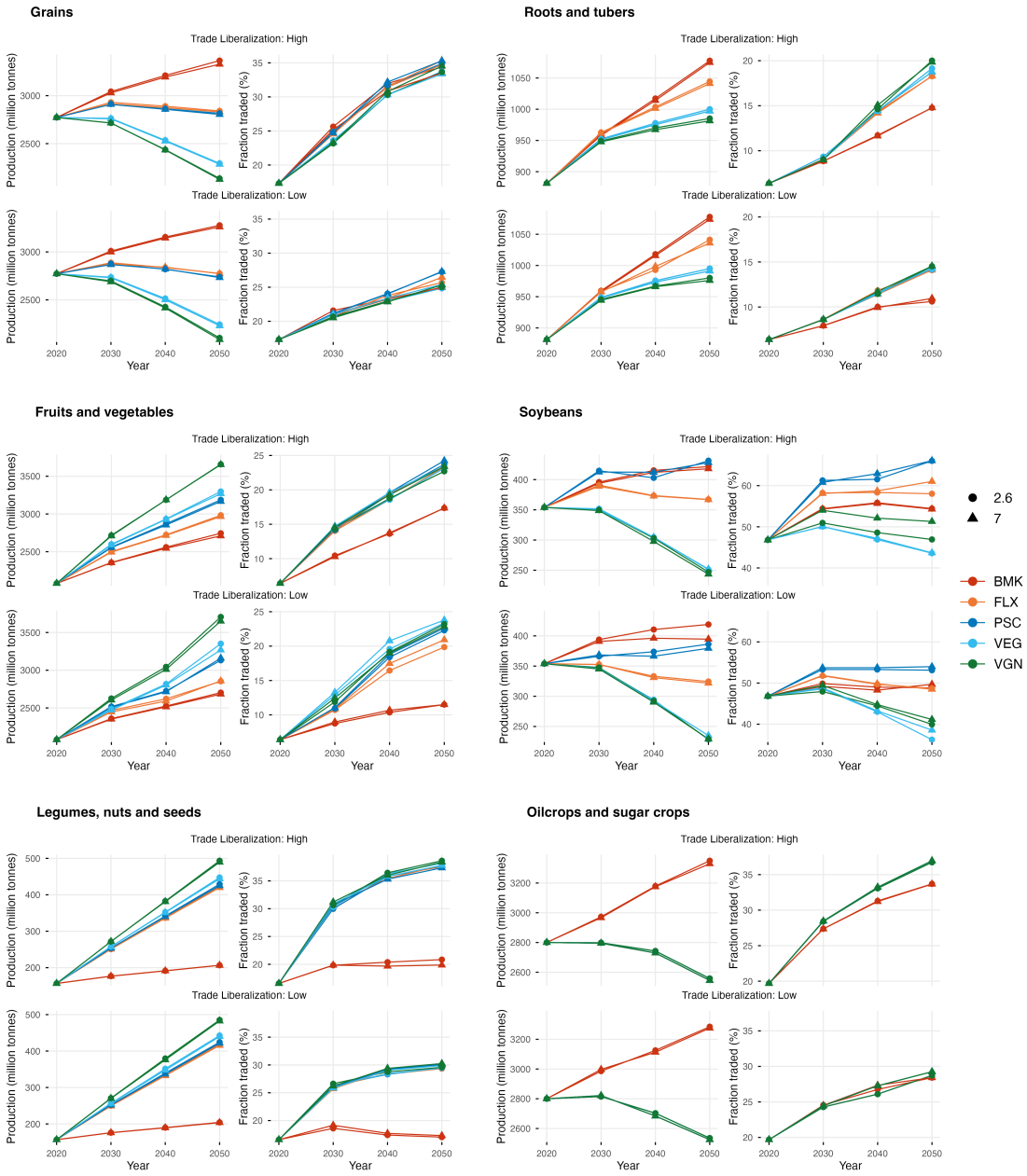

Figure 4.1: Global production and trade fraction trajectories by crop group, 2020–2050. Line colours indicate dietary pathways; markers distinguish climate pathways; rows compare trade liberalization scenarios.

Global agricultural trade networks reshape over time, with dietary transitions

producing variable changes in regional bilateral trade flows by 2050 relative to 2020 patterns (Figure 4.2 presents results for low trade liberalization and RCP 2.6). Grains show a restructuring of trade networks, even under the benchmark scenario, as the model eliminates present-day inefficiencies in grain networks over time. Europe emerges as an increasingly important grain exporter across most scenarios, with strengthened flows to Africa, Asia, and within Europe. On the contrary, flows from Northern America and Latin America to Asia experience reductions across most dietary pathways, suggesting shifts in regional production capacity and import dependencies. Fruits and vegetables exhibit the most widespread trade intensification, especially under non-benchmark dietary scenarios, with notable increases within Africa, Europe, and Latin America, and expanded flows from multiple exporting regions to Asia across all diet pathways. Dietary transitions produce markedly different trade patterns for soybeans. Under plant-forward scenarios (VEG, VGN), soybean exports from Northern America and Latin America to Asia decline substantially, indicating diminished demand for animal feed in these regions. Conversely, benchmark, flexitarian, and pescatarian diets maintain or intensify these traditional trade corridors. Oil crops and sugar crops display complex, region-specific responses with both increases and decreases across trading pairs, particularly between Africa, Asia, and Latin America. Results under high trade liberalization and RCP 2.6 (Supplementary Figure D.3) reveal consistent patterns of trade network evolution across scenarios, though with greater intensification of trade flows, particularly for grains and fruits and vegetables. These patterns demonstrate that while trade networks undergo temporal restructuring, dietary transitions modulate these changes distinctly, especially with respect to feed-oriented commodity flows.

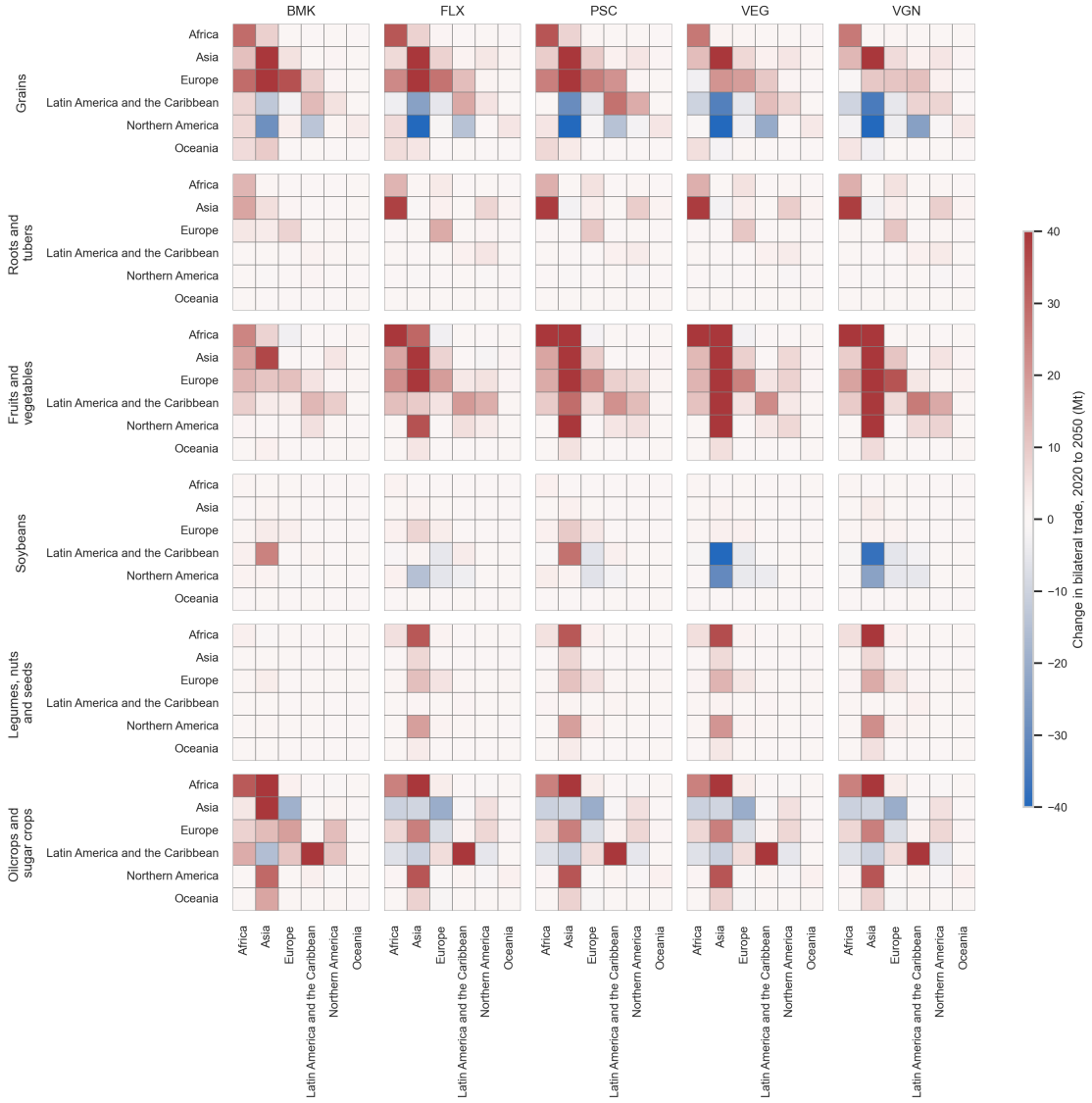

Figure 4.2: Change in bilateral trade by 2050 relative to 2020 under low trade liberalization and RCP 2.6. Panels are organized by crop group and diet scenario, and values are aggregated to regions. In each panel, rows are exporting regions and columns are importing regions.

Both import dependence and supplier concentration evolve by 2050, providing insights into changing trade vulnerability patterns across crop groups and dietary scenarios (Figure 4.3 compares 2050 projections with 2020 baseline under RCP 2.6). Import dependence reflects the inverse of self-sufficiency, while the Herfindahl-Hirschman Index (HHI) measures import concentration, i.e. the inverse of supplier diversification. Most crop groups in 2050 are characterized by increased import concentration along with variable changes in import dependence. Soybeans display

the highest vulnerability, maintaining elevated import dependence, and an HHI of around 0.5 under most scenarios. Fruits and vegetables, and roots and tubers, experience notable increases in import concentration along with modest changes in import dependence, suggesting consolidation of import sources. Grains and legumes show relatively moderate changes, maintaining concentration near baseline levels while experiencing small increases in import dependence. Trade liberalization consistently increases import concentration across crop groups, with high liberalization scenarios pushing HHI values higher than low liberalization counterparts, indicating that freer trade may enhance efficiency but concentrate risk among fewer supplier countries. Dietary transitions produce more nuanced effects, with plant-forward diets generally reducing import dependence for animal feed crops like soybeans and increasing import dependence for fruits and vegetables, while having minimal impact on diversification. Regional disaggregation (Supplementary Figure D.4) reveals substantial heterogeneity in vulnerability profiles. For instance, Oceania exhibits increasing import dependence and higher concentration compared to baseline for several crop groups, while Latin America shows reducing vulnerability for grains and soybeans, with both import dependence and concentration reducing under several scenarios, indicating different risk profiles across regions and food groups.

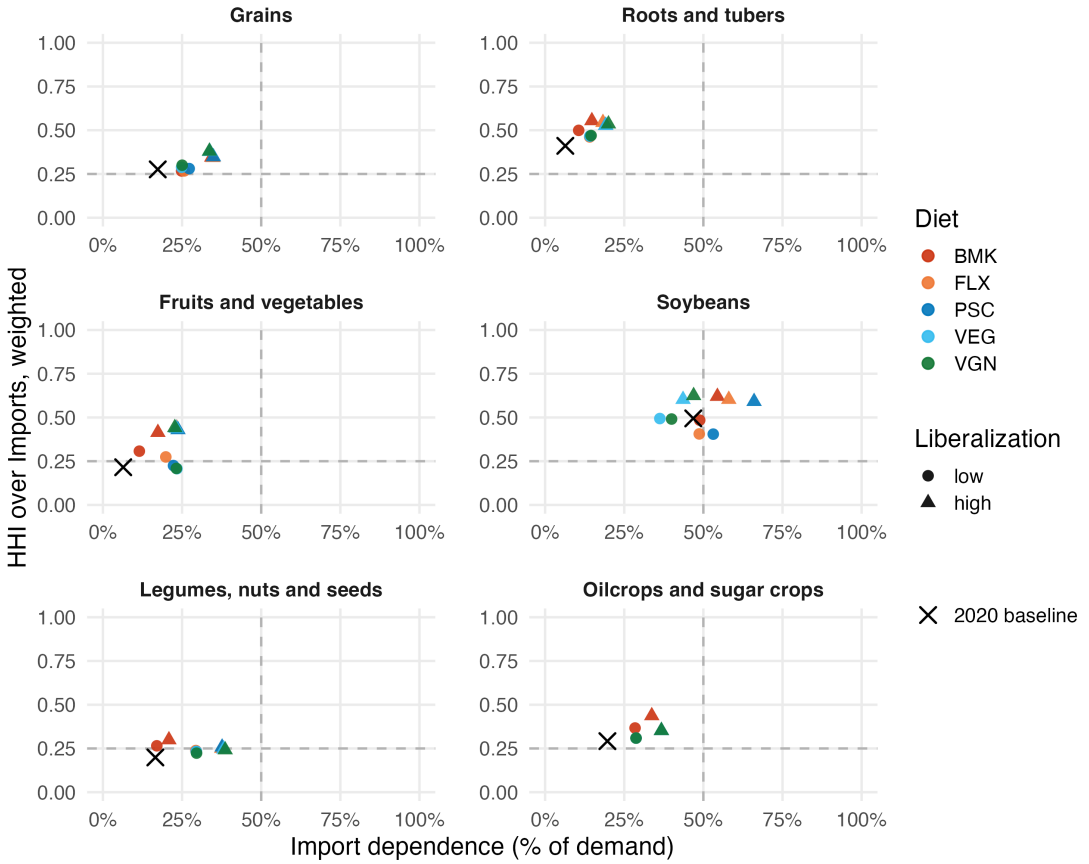

Figure 4.3: Global import dependence vs. supplier concentration by crop group in 2050. Concentration is measured using HHI over imports, weighted by importer size. Points represent dietary and trade liberalization scenarios under RCP 2.6; 2020 baseline shown for comparison.

Country-level supply requirements vary substantially across scenarios, with different dietary, climate, and trade pathways demanding divergent production trajectories from major producers. Figure 4.4 plots mean supply changes from 2020 to 2050 against across-scenario variation measured as the interquartile range. Large variations across scenarios indicate that the countries' production roles depend heavily on which dietary, climate, and trade scenario materializes. For grains, China exhibits particularly high scenario sensitivity, with production requirements ranging from substantial declines to near-baseline levels depending on the scenario. India and Ukraine both show moderate positive mean changes with substantial uncertainty, and the United States shows moderate negative mean changes with uncertainty, while several mid-sized producers cluster near stable trajectories. For roots and

tubers, most major producers, including Nigeria and Democratic Republic of Congo, and excluding China, show positive mean changes but with varying degrees of scenario dependence, suggesting stable growth requirements across most pathways but with some sensitivity to dietary transitions. For Fruits and vegetables, China shows near-zero mean change but extremely wide scenario variation. Besides China, many countries, including India, Brazil, and the United States, show moderate to high mean growth in production with moderate uncertainty across scenarios. Soybeans reveal stark differences across scenarios. Traditional exporters like the United States and Brazil show large mean reductions but with substantial variation across scenarios, likely reflecting reduced feed demand under plant-forward diets versus sustained or increased demand under animal-protein-rich scenarios. Other producers like Argentina and India show small positive changes in production but with moderate uncertainty. For legumes, nuts and seeds, nearly all countries demonstrate modest positive changes with low variation across scenarios, suggesting consistent demand growth across dietary pathways. Oil crops and sugar crops exhibit large reductions across several major producers like Brazil, India, Indonesia and Malaysia, and small increases in some countries including China, but all with moderate to high cross-scenario uncertainty. Overall, future production geographies remain highly scenario-dependent, with the magnitude and even direction of changes varying dramatically across dietary, climate, and trade pathways.

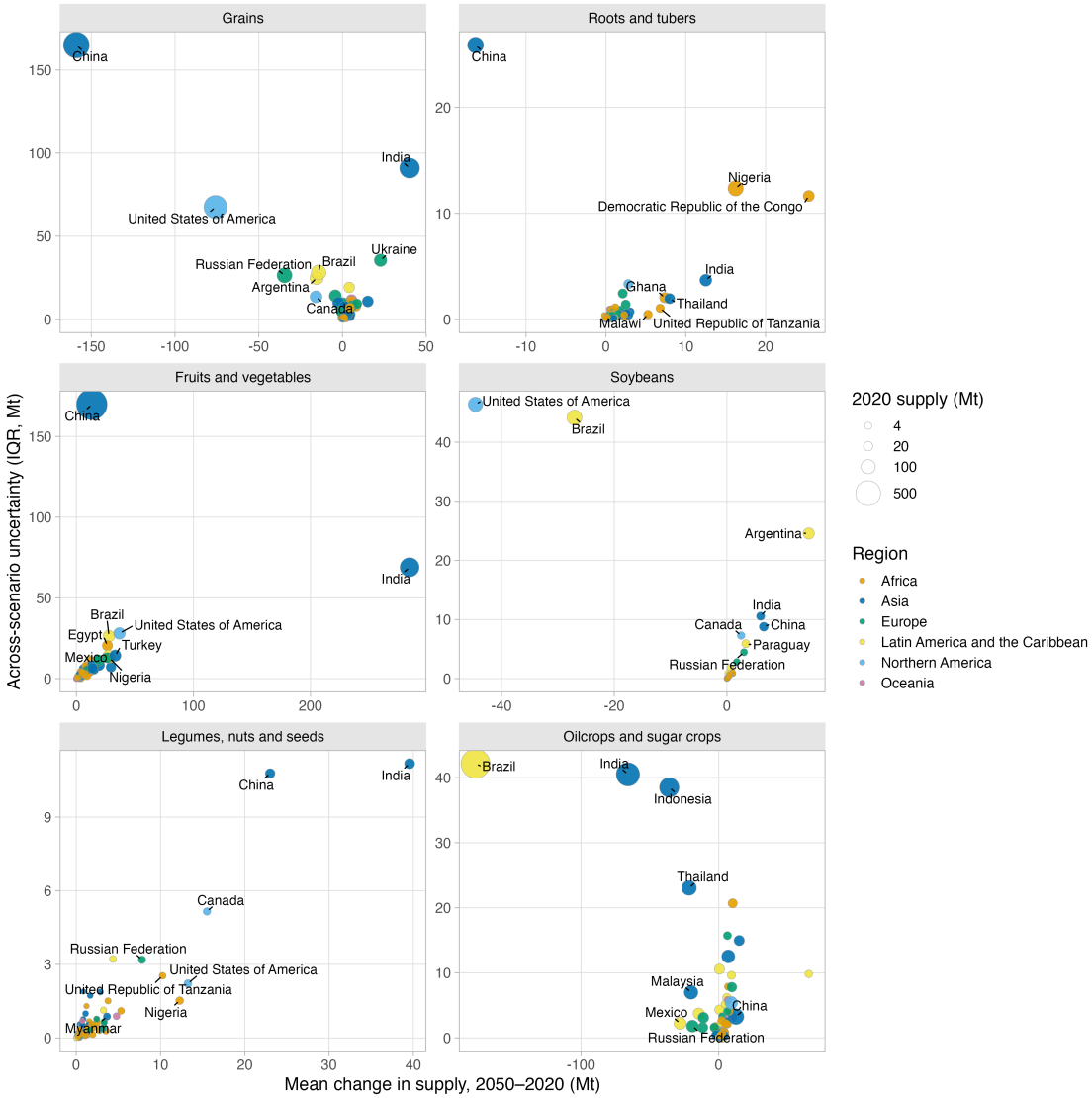

Figure 4.4: Country-level supply shifts and uncertainty by crop group. Each panel shows, for the indicated crop group, the mean change in supply from 2020 to 2050 versus the across-scenario interquartile range. Point size is 2020 supply and colour denotes region.

To understand the sources of future uncertainty, we decompose the variance in supply projections across the three scenario dimensions, i.e., dietary transitions, climate pathways, and trade liberalization (Figure 4.5). Variance increases substantially from 2030 to 2050 across all crop groups and regions, reflecting the compounding effects of scenario divergence over time. In the short term, variance is driven primarily by dietary transitions and trade liberalization, with relatively balanced contributions between the two depending on crop and region. Climate

pathways contribute minimally to variance in both the short and long term. By 2050, dietary transitions emerge as the dominant source of variance for most crop groups and regions. Trade liberalization continues to contribute meaningfully but is overshadowed by dietary effects in the long term. Variance patterns also differ across crop groups. Fruits and vegetables exhibit the highest variance, particularly in Asia, followed by grains in Asia and Northern America, and oil crops in Asia and Latin America. Soybeans show high variance concentrated in the Americas, while roots and tubers display modest variance in Asia and Africa. Legumes show the lowest variance across regions. Generally, regions and crops with higher mean production levels also exhibit higher variance, though the relative contribution of each scenario dimension varies. Variance decomposition for projected exports (Supplementary Figure D.5) reveals distinct patterns from supply variance, with trade liberalization playing a proportionally larger role. While dietary transitions remain important for exports, liberalization contributes more substantially to export variance than to supply variance across most crops and regions, reflecting its direct influence on trade policy and flow patterns. This indicates that while diets predominantly reshape production requirements, trade policy more directly governs the magnitude and direction of international commodity movements.

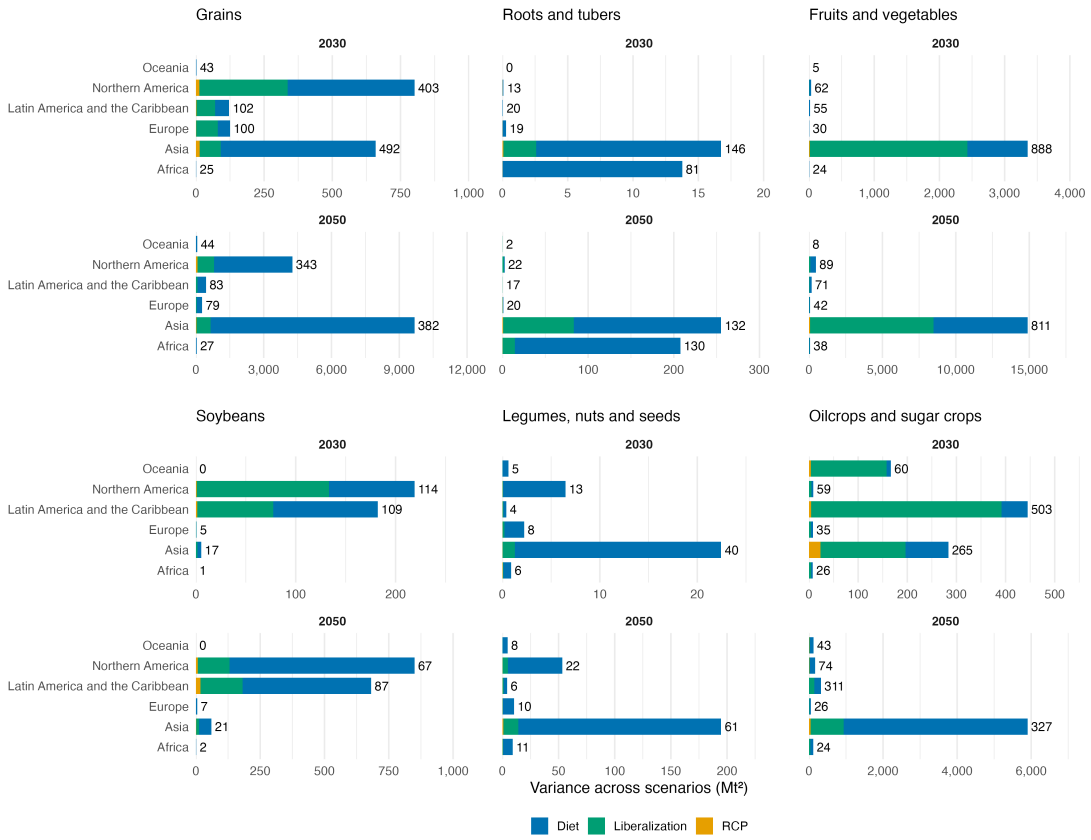

Figure 4.5: Variance decomposition of projected supply by crop group for 2035 (top) and 2050 (bottom). Bars show the total variance across scenarios (Mt^2) partitioned by dietary, trade, and climate drivers. Annotations show regional mean supply (Mt). Regional statistics are computed as variance-weighted averages of country-level values. See Supplementary Information for decomposition details.

4.3 Discussion

The global food system is increasingly pressured by interrelated challenges such as climate variability, population growth, urbanization, land-use competition, and evolving dietary preferences (Godfray et al., 2010; Nelson et al., 2014; Springmann et al., 2018; Tilman et al., 2011). This study is among the first to jointly model how climate change, dietary transitions, and trade policy regimes interact to reshape bilateral food trade networks. We find that dietary transitions are the primary driver of future agricultural production and trade patterns. Traditional commodity corridors, particularly the flows of grains and soybeans from the Americas to Asia, weaken substantially under plant-forward scenarios, while trade in fruits

and vegetables intensifies across most regions and scenarios. At the country level, major producers like China, Brazil, and the United States face wide uncertainty in future supply requirements, with the magnitude and even direction of changes varying dramatically across scenarios. One caveat to these findings is that the alternative dietary scenarios assume global convergence to 2,500 kcal/day, combining compositional shifts with elimination of undernutrition, whereas the benchmark scenario carries existing country-specific dietary patterns forward. The projected differences between scenarios therefore partly reflect changes in caloric quantity alongside composition. Running the model with the benchmark diet calibrated to 2,500 kcal/day would reduce projected global demand as our benchmark scenario averages around 2,700 kcal/day globally in 2050. How this plays out would likely vary substantially across overconsuming and undernourished regions. Disentangling composition and quantity effects is a useful direction for future work.

Reorientation of trade networks can also introduce new vulnerabilities. Fruits, vegetables, and roots and tubers show rising import concentration by 2050, and regions increasingly reliant on external supply for these commodities may face elevated exposure to production shocks or trade disruptions. Trade liberalization, on one hand, enhances allocative efficiency by enabling production to concentrate in regions with comparative advantage. On the other hand, it consistently increases import concentration across crop groups, suggesting a trade-off between efficiency and diversification. This aligns with longstanding debates in food security scholarship about the risks of trade openness (Grassia et al., 2022; Wellesley et al., 2017). Regional heterogeneity in vulnerability profiles underscores the need for differentiated policy responses. Oceania, for instance, faces increasing import dependence and supplier concentration for several crop groups, while Latin America shows reduced vulnerability for grains and soybeans under multiple pathways. The optimal policy mix to mitigate concentration risks will therefore vary across regions depending on their production potential and trade relationships.

Our finding that climate pathways exert modest effects relative to dietary transitions warrants careful interpretation. Our yield trajectories come from the

IMPACT model (Robinson et al., 2015), in which climate impacts are layered onto exogenous productivity growth assumptions. Climate-induced yield losses are therefore partially offset by assumed technological gains. Recent empirical work suggests this assumption may be optimistic: Hultgren et al. (2025) estimate a global crop production decline of approximately 5.5×10^{14} kcal per 1°C of global mean surface temperature rise, and project that even after accounting for adaptation and income growth, substantial residual losses remain for all staples except rice, with damages concentrated in modern-day breadbaskets. If realised yields follow trajectories closer to those projected by Hultgren et al. (2025), the climate effect on production and trade would be larger than our model suggests.

Furthermore, offsetting climate-induced yield losses through 2050 could require hundreds of billions of dollars in additional public R&D investment globally (Baldos et al., 2020). For the United States alone, sustained annual R&D spending growth of 5-8% may be necessary to avoid productivity declines (Ortiz-Bobea et al., 2025). These investments face significant time lags between expenditure and productivity gains, so realising the productivity gains assumed by our model requires sustained policy commitment to agricultural R&D. In a counterfactual scenario where this investment stagnates, climate impacts on production would be substantially larger, and regions projected by our model to expand production – often those most vulnerable to climate change – might be unable to do so. For example, parts of sub-Saharan Africa appear in our results as candidates for expanded production and exports of legumes, nuts and seeds under plant-forward scenarios, but these regions are also among the most exposed to climate change and the least equipped to absorb productivity shocks. Future iterations of this analysis could draw on empirically-grounded climate damage estimates to estimate the range of plausible climate impacts on global food production and trade.

Other limitations also apply to our modelling framework (See Supplementary Methods D.3.8). First, the model solves for each crop independently rather than jointly, potentially overstating the feasibility of production shifts that would compete for the same land or resources. Second, the model focuses on long-run

trajectories and does not incorporate short-term shocks such as pest outbreaks, droughts, or geopolitical disruptions, all of which can significantly affect short-term production and trade patterns (Cottrell et al., 2019; Lesk et al., 2016). Third, elasticities derived from benchmark dietary projections may not accurately represent consumer/producer behaviour under alternative dietary regimes, causing the model to underestimate achievable demand for some scenarios and commodities. Fourth, the partial equilibrium framework relies on linear demand and supply curves and does not capture economies of scale or cross-sectoral linkages. Future work could integrate these dynamics through coupling with computable general equilibrium models or agent-based approaches.

Despite these limitations, our findings offer actionable insights for policymakers and stakeholders navigating the intersection of diet, climate, and trade. Strategic alignment across dietary guidelines, agricultural investment, and trade policy will be essential for managing emerging trade dependencies and supporting vulnerable regions. Dietary change offers substantial leverage for reducing food system emissions (Clark et al., 2020; Springmann et al., 2018), and the urgency of these considerations is underscored by evidence that rapid dietary transitions away from animal-source foods may be necessary to keep the food system within its carbon budget (Hale et al., 2025). Choices made in the coming decades about what the world eats will shape not only emissions trajectories but also the geography of production and structure of trade dependencies.

4.4 Methods

We developed a Spatial Price Equilibrium Model (SPEM) to project bilateral trade flows, prices, production, and consumption for 32 crops across 153 countries from 2020 to 2050. The model builds previous research analysing short-term supply chain shocks (Verschuur et al., 2024) but is adapted here for scenario-based projections of future food systems. We first calibrated the model to reproduce current observed trade patterns, then projected forward under 20 scenario combinations representing alternative dietary transitions (5 scenarios), climate pathways (2 scenarios), and

trade policy regimes (2 scenarios). Each crop is modelled independently, with the model solving for equilibrium prices, quantities, and bilateral flows that satisfy supply-demand balance across all countries. A brief overview of the methodology is provided below, see Supplementary Methods D.3 for more details.

4.4.1 Baseline model calibration

SPEM is a multi-region partial equilibrium model that links producers and consumers across countries through domestic supply and international trade (Takayama et al., 1984; Takayama & Judge, 1964). Producers in each country supply a certain quantity to the market, which they sell at a price determined by their supply curve. Consumers have demand for the commodity and purchase at a price determined by their demand curve. Countries can trade with any other country, subject to bilateral trade costs, including transportation, tariffs, border and custom compliance. In equilibrium, trade occurs between two countries if the consumer price in the importing country equals the producer price in the exporting country plus trade costs. The model solves for the set of bilateral trade flows, production quantities, consumption quantities, and prices that satisfy these equilibrium conditions.

The SPEM framework offers several advantages for analysing future food trade. It explicitly captures bilateral trade flows, which is not standard in many global food system models. It allows for trade diversion and the establishment of new trading partners as relative costs change. It captures directional trade flows, meaning countries can both import and export the same product. While Verschuur et al. (2024) adapted the SPEM framework for short-term shock analysis, SPEM models are traditionally designed for longer-term partial equilibrium simulations under changing trade costs or policy regimes (Janssens et al., 2022; Mosnier, 2014). Our application aligns with this traditional use, projecting how bilateral trade networks evolve under scenarios of dietary change, climate impacts, and trade policy over a 30-year horizon.

The model is calibrated independently for each of the 32 crops. At baseline, the SPEM assumes that sourcing decisions are determined by cost differentials between

total landed cost of producing and shipping crops. In practice, non-cost factors also influence where countries source from. To capture both cost and non-cost determinants of bilateral trade, the model is calibrated on observed trade data to reconcile modelled flows with observed bilateral trade patterns (Jansson & Heckelei, 2009). Calibration performance is reported in Supplementary Table D.6.

Baseline production and bilateral trade data come from FAOSTAT, averaged over 2018-2022 to smooth inter-annual variability. Raw trade data were harmonised using a reliability index approach (Gehlhar, 1996) to reconcile discrepancies between importer- and exporter-reported quantities, then processed through a re-export algorithm (Croft et al., 2018) to ensure mass balance and link production origins to consumption destinations. We aggregated ~120 FAO commodities into 32 categories corresponding to International Food Policy Research Institute's (IFPRI) IMPACT model crop classifications (Robinson et al., 2015) (Supplementary Table D.1). Processing factors convert between raw commodities (e.g., oil palm fruit) and derived products (e.g., palm oil) where necessary. Producer prices were obtained from FAOSTAT and gap-filled using a regression model relating log price per hectare to GDP, production volume, yield, and region fixed effects (see Supplementary Methods D.3.4). Transport and trade costs were obtained from Verschuur et al. (2023), and bilateral tariff rates from MAcMap-HS6 (Guimbard et al., 2012).

4.4.2 Demand-side scenarios

Dietary scenarios were derived from the EAT-Lancet reference diet framework (Willett et al., 2019), which specifies recommended per capita consumption per day of 21 food groups, including both plant and animal foods. We modelled five dietary trajectories: a benchmark scenario representing continuation of current dietary patterns, and four alternative scenarios (flexitarian, pescetarian, vegetarian, and vegan), reflecting progressively greater shifts away from animal-source foods. We assume gradual adoption, with diets remaining at benchmark levels through 2020 and transitioning linearly to reach full adoption of the target diet by 2050.

Total quantity is estimated for each country, year, food group, and dietary scenario, including demand for food, feed, and other uses. Food demand is calculated by multiplying scenario-specific per capita consumption by population projections. While animal products weren't modelled in this analysis, their consumption was used to estimate feed corresponding requirements. Feed demand is estimated using livestock-specific feed conversion ratios from Herrero et al. (2013) for terrestrial animals and Tilman and Clark (2014) for aquaculture, accounting for the crop composition of feed rations. We incorporate trade in animal products when allocating feed requirements across countries, assigning feed demand to the country where livestock production occurs. Other uses (industrial, seed, waste) are held at baseline levels, derived from FAOSTAT food balance sheets and supply utilization accounts.

The EAT-Lancet dataset provides projections for 13 vegetal food groups, whereas we model 32 crop groups. Each of the 32 crops is mapped to one of the 13 EAT-Lancet food groups (Supplementary Table D.1). For each food group, diet, country, and year, we calculate demand change ratios from the EAT-Lancet projections, i.e. projected demand divided by 2020 demand. These ratios are then applied to the calibrated 2020 demand values (which are based on observed FAOSTAT data) to project future demand for each of the 32 crop groups. This approach preserves the relative changes implied by dietary scenarios while maintaining consistency with observed baseline demand patterns.

4.4.3 Supply-side scenarios

Climate scenarios follow Representative Concentration Pathways RCP 2.6 and RCP 7.0, which affect agricultural yields through temperature, precipitation, and CO2 fertilization effects. Future crop yields under climate change are derived using projections from the IMPACT model (Robinson et al., 2015), which provide year, region and crop specific yields and yield change factors under each RCP. IMPACT incorporates projected technological progress through assumptions about future yield gains from improved inputs, seeds, and management practices, calibrated using historical yield trends. Climate impacts on yields are then layered on top of these

productivity trajectories, meaning that climate-induced yield losses in our scenarios are partially offset by assumed technological gains. A no-R&D counterfactual is not included in our scenario set, but would be a useful direction for future work.

The IMPACT model also provides future projections for region and crop specific supply, assuming benchmark demand. These trajectories are used to shift the supply curve and production prices for each year, region and crop. We calculate the ratio of projected supply/yield to 2020 supply/yield from IMPACT, and apply these ratios to calibrated 2020 values based on observed FAOSTAT data. This approach preserves the relative yield and supply changes implied by climate scenarios while maintaining consistency with observed baseline production patterns. Since IMPACT uses the same 32 crop categories that we model, no aggregation or disaggregation is required for supply-side projections.

4.4.4 Scenario modelling for projecting forward

After calibration, the model is run forward with scenario-specific parameters. Demand curves shift according to dietary and population projections, and supply curves shift according to climate-driven yield changes. Trade policy scenarios vary constraints on self-sufficiency and supply diversification. The 'high trade' scenario permits greater reliance on imports (self-sufficiency must remain at least 30% of 2020 levels; no single trading partner may supply more than 70% of imports), while the 'low trade' scenario restricts import dependence (self-sufficiency at least 70% of 2020 levels; no partner exceeds 30% of imports). For existing trade links, import shares are constrained to the maximum of the current share or the scenario threshold, under both 'low' and 'high' scenarios.

Demand and supply elasticities are also drawn from the IMPACT model, which are used to determine the shapes of demand and supply curves. Demand elasticities vary by region, crop and year, while supply elasticities vary by region and crop. The model solves for projected equilibrium prices, bilateral trade flows, and domestic production and consumption at five-year intervals from 2020 to 2050. Note that the model does not include stocks and solves each crop and time period independently.

4.4.5 Outcome metrics

We assess several outcome metrics to characterise future food trade patterns. First, we examine global aggregated equilibrium production and import dependence (defined as total traded quantity divided by total production) across scenarios and time periods (Figure 4.1). Second, we analyse bilateral trade flows aggregated to the regional level to identify shifts in the geography of food trade (Figure 4.2). Third, we compute import dependence and import concentration at both global and regional scales; import concentration is measured using the Herfindahl-Hirschman Index (HHI) across trading partners, weighted by import volumes. Fourth, we quantify mean changes in domestic supply across scenarios and the interquartile range (IQR) to characterise uncertainty in supply trajectories. Finally, we conduct variance decomposition to attribute variation in projected supply and exports to dietary, climate, and trade policy drivers. In all results and figures, the 32 crop categories are aggregated into six groups to improve clarity (see Supplementary Methods D.3.7).

5
Conclusion

Building resilient and sustainable food systems requires a comprehensive understanding of how food moves from production to consumption, what environmental burdens these flows carry, and how they may need to transform under long-term pressures. Yet our collective understanding of these dynamics has been hampered by a reliance on national-level aggregates that obscure subnational heterogeneity, by environmental assessments focused on raw commodities rather than the packaged foods that dominate modern retail, and by scenario analyses that treat climate impacts, dietary transitions, and trade policy as separate concerns. These gaps matter as without spatially resolved data on food flows, we cannot identify which populations are most vulnerable to supply disruptions; without product-level environmental footprints, we cannot guide consumers and policymakers toward lower-impact choices; and without integrated scenario frameworks, we cannot anticipate how the forces reshaping food systems will interact.

The relevance of addressing these gaps is immense. Food systems account for up to a third of global greenhouse gas emissions while simultaneously facing mounting pressures from climate change. International trade has more than doubled in recent decades and now plays a critical role in connecting surplus regions to deficit ones, yet trade networks can also transmit and amplify shocks. Dietary transitions are reshaping demand across commodities, with profound implications

for both environmental footprints and the geography of production. Understanding these interconnected dynamics is essential for designing policies that enhance food security without exacerbating environmental degradation.

The literature on food systems has advanced significantly in recent years. Network analyses have revealed the structure and evolution of international food trade. Life cycle assessments have quantified the environmental footprints of agricultural commodities across diverse production systems. Scenario models have projected how climate change and policy interventions may affect agricultural production and trade. These advances have provided a foundation for understanding food systems at global scales.

In this thesis, I have made contributions to this literature by addressing several key gaps. In Paper 1, I developed a novel methodological framework integrating machine learning and data harmonisation algorithms to map global cereal flows at subnational scales across 3,536 regions in 195 countries, revealing substantial heterogeneity in regional dependencies that national statistics obscure. In Paper 2, I estimated the environmental footprints of approximately 475,000 retail food products across 74 countries, bridging the gap between commodity-level life cycle assessment and the multi-ingredient packaged foods that consumers regularly purchase. In Paper 3, I developed an integrated modelling framework that projects bilateral trade flows through 2050 under alternative combinations of dietary transitions, climate pathways, and trade policy regimes, addressing the separation that has characterised these literatures.

This thesis has demonstrated that examining food systems across multiple scales and dimensions yields insights that aggregate analyses miss. The subnational mapping in Paper 1 revealed that nearly half of all net importing countries contain surplus regions with net outflows, while virtually every net exporting country retains deficit regions dependent on inflows – patterns invisible at national scales. The product-level assessment in Paper 2 showed that while ingredient composition remains the dominant driver of environmental impacts, ingredient sourcing accounts for approximately 36% of variation in footprints, with particularly pronounced effects

for certain product categories – nuance lost when focusing only on producer-side impacts of raw commodities. The scenario analysis in Paper 3 found that large-scale dietary transitions would necessitate substantial restructuring of global food trade – a dynamic obscured when dietary and trade literatures proceed separately.

Overall, I argue that building resilient and sustainable food systems requires understanding the interplay between local self-sufficiency and global connectivity, recognising that environmental impacts are shaped primarily by what we eat but also by how it is produced, and coordinating dietary guidelines with trade policy to navigate the restructuring of global food networks that dietary transitions will entail. The findings of this thesis underscore the need for integrated approaches that align interventions across scales and domains. Dietary change offers substantial leverage for reducing food system emissions, but the trade reconfigurations it would trigger must be anticipated and managed. Subnational heterogeneity means that national policies may have uneven effects across regions. Supply chain interventions must complement dietary shifts for specific product categories where sourcing effects are pronounced.

Several limitations warrant acknowledgment. The subnational flow analysis relied on machine learning models with moderate predictive accuracy for flow volumes, and estimating regional consumption required assumptions about subnational preferences that could not be validated against observed data. The analysis focused on cereals, but does not capture flows of other commodities such as oilseeds, fruits, vegetables, or animal products, which may exhibit different network structures. The product-level environmental assessment used estimated ingredient compositions rather than verified formulations, and the underlying life cycle assessment databases are skewed toward production systems in high-income regions. Similarly, the product datasets favour markets in Europe and North America, so findings may not fully capture consumption patterns in under-represented regions. The scenario model solved for each crop independently rather than jointly, potentially overstating the feasibility of production shifts that would compete for the same land or resources. Yield projections reflected climate trends but did not account for discrete shocks such as

pest outbreaks, droughts, or geopolitical disruptions, and the model also did not incorporate the risk of simultaneous production failures across breadbasket regions. Elasticities drawn from the literature may not adequately capture structural breaks that could occur under large-scale dietary transitions. These limitations point toward methodological priorities including closing data gaps in life cycle assessment coverage for low and middle-income countries, validating subnational consumption estimates, and incorporating joint optimisation across crops in trade models.

This thesis also highlights several avenues for future research that build directly on its contributions. First, the subnational cereal flow framework developed in Paper 1 could be extended to additional commodities, particularly perishable foods, to assess whether vulnerabilities and concentration patterns differ across food groups with distinct storage and transport characteristics. Second, the framework developed in Paper 2 could be used to explore counterfactual scenarios: what if countries sourced ingredients from the best or worst performing origins, or adopted formulations typical of other markets? Such analyses could quantify potential gains from supply chain optimisation and reformulation. Finally, the trade projections in Paper 3 highlight the need to coordinate dietary guidelines with trade policy. How such coordination might occur – through international trade negotiations, national food strategies, or other policy pathways – remains an open question for future research.

As global targets call for halving food system emissions while safeguarding food security for a growing population, the need for granular, integrated analysis will only intensify. The approaches developed in this thesis offer a means of navigating uncertainty and trade-offs, supporting more informed decision-making amid the coupled challenges of climate mitigation and food systems transformation.

Appendices

A

Contribution Statement

This section outlines my specific contributions to each paper to enable examiners to gain a clear understanding of my independent work.

Paper 1 is single-authored; I was responsible for all aspects of the research and writing.

In Paper 2, I developed the food classification model based on natural language processing and machine learning, processed large volumes of product-level data including language translation, incorporated ingredient sourcing information accounting for country-specific supply chains, conducted comparative assessments of product-level footprints across food categories and geographies, and decomposed the relative effects of ingredient sourcing and product composition. The methods for estimating product composition and implementing Monte Carlo analysis for product-level footprints were developed by Clark et al. (2022) and further refined by Michael Clark. Joe Kennedy, Ricki Runions, and Savka Akester assembled large datasets of categorized food products that were used to train the machine learning classification models. Interpretation of results and writing were carried out with support from all co-authors.

In Paper 3, I processed trade, production, consumption, and producer price data from FAOSTAT; constructed demand-side scenarios incorporating food, feed, and other uses; defined the scope of analysis including the set of demand, supply, and

trade scenarios; and implemented the Spatial Price Equilibrium Model (SPEM). The SPEM used in this work was originally developed by Verschuur et al. (2024) and further modified jointly by myself and Jasper Verschuur. Interpretation of results and writing were carried out with support from Jasper Verschuur, Michael Clark, and Jim Hall.

B

Supplementary Material for "Mapping Global Cereal Flow at Subnational Scales Unveils Key Insights for Food Systems Resilience"

Contents

B. Supplementary Material for "Mapping Global Cereal Flow at Subnational Scales Unveils Key Insights for Food Systems Resilience"

B.1 Supplementary Figures

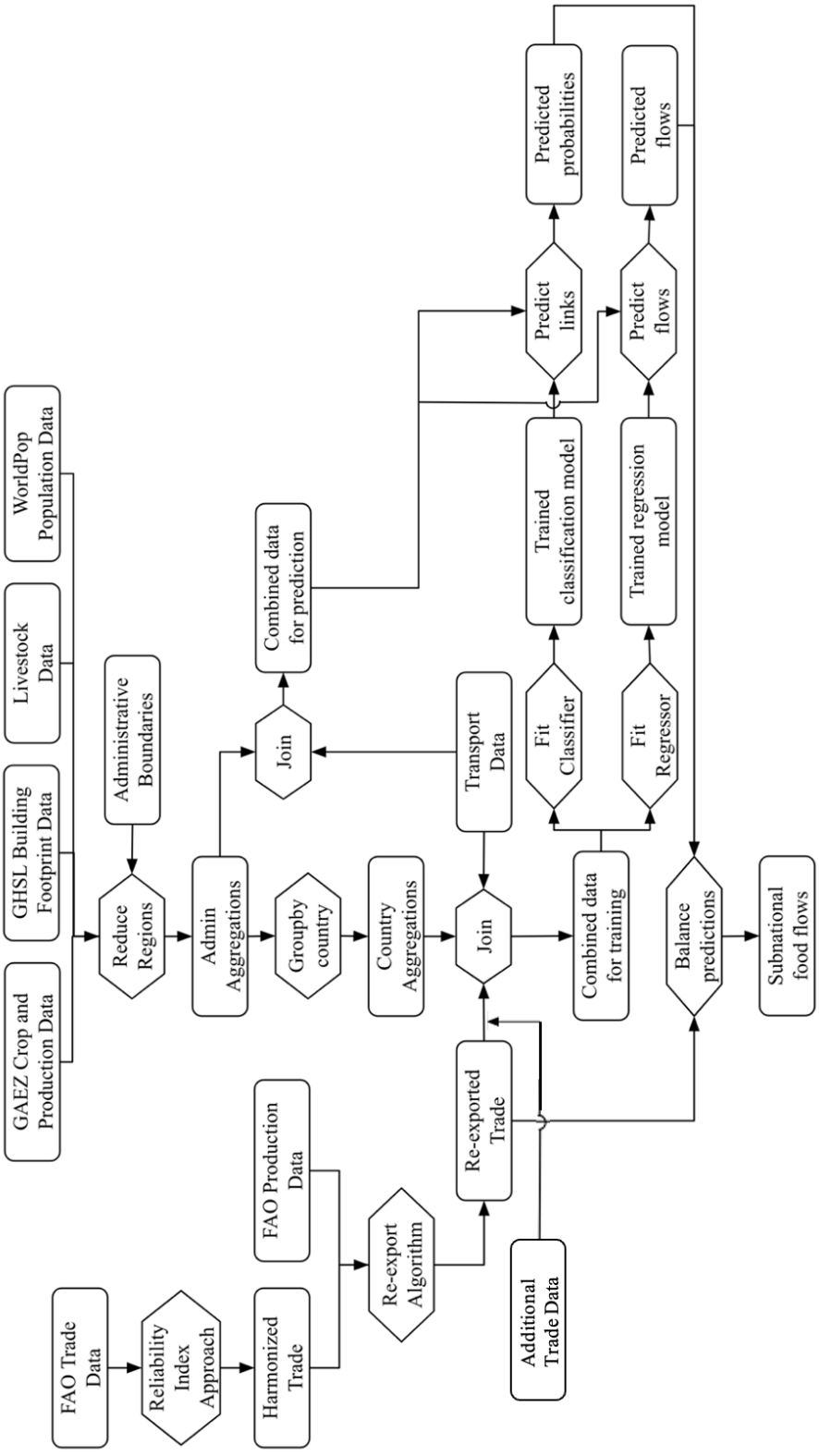

Figure B.1: Modelling pipeline.

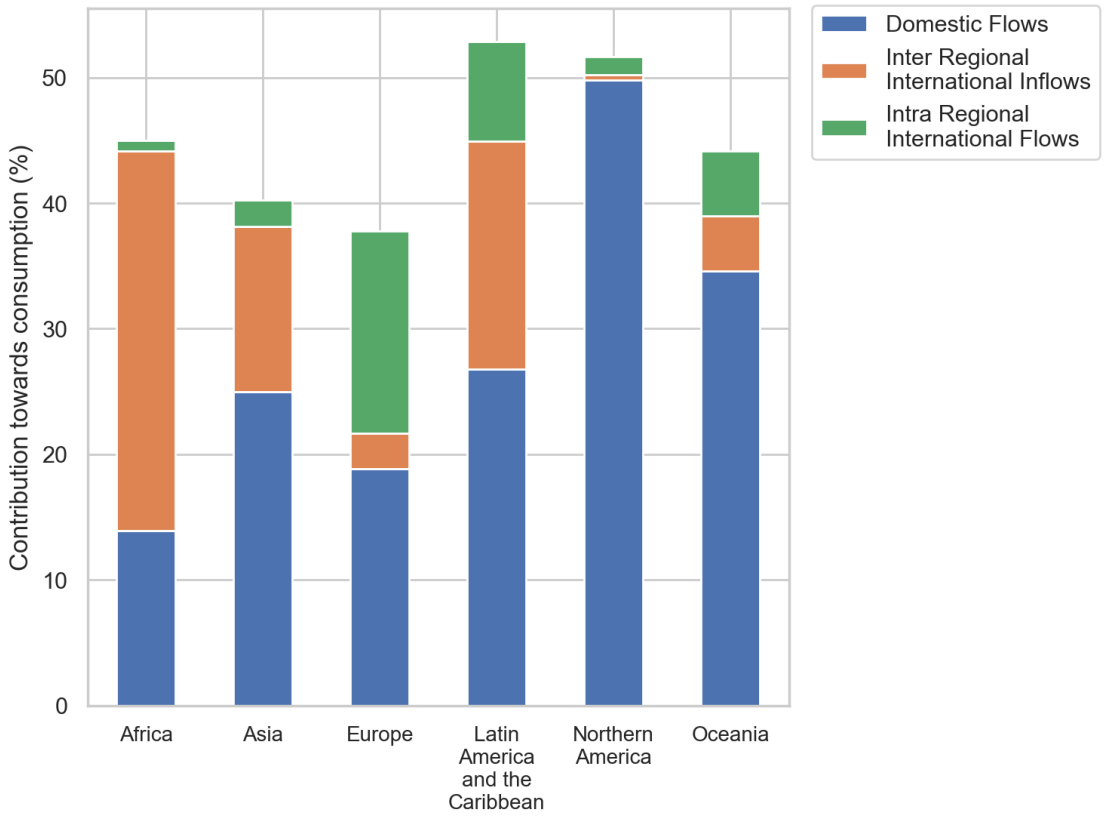

Figure B.2: Contribution of cereal flows to consumption, by continent (2017-2021). Note that continental groupings differ widely in country count and scale; these bars are descriptive and should not be read as strictly comparable efficiency metrics.

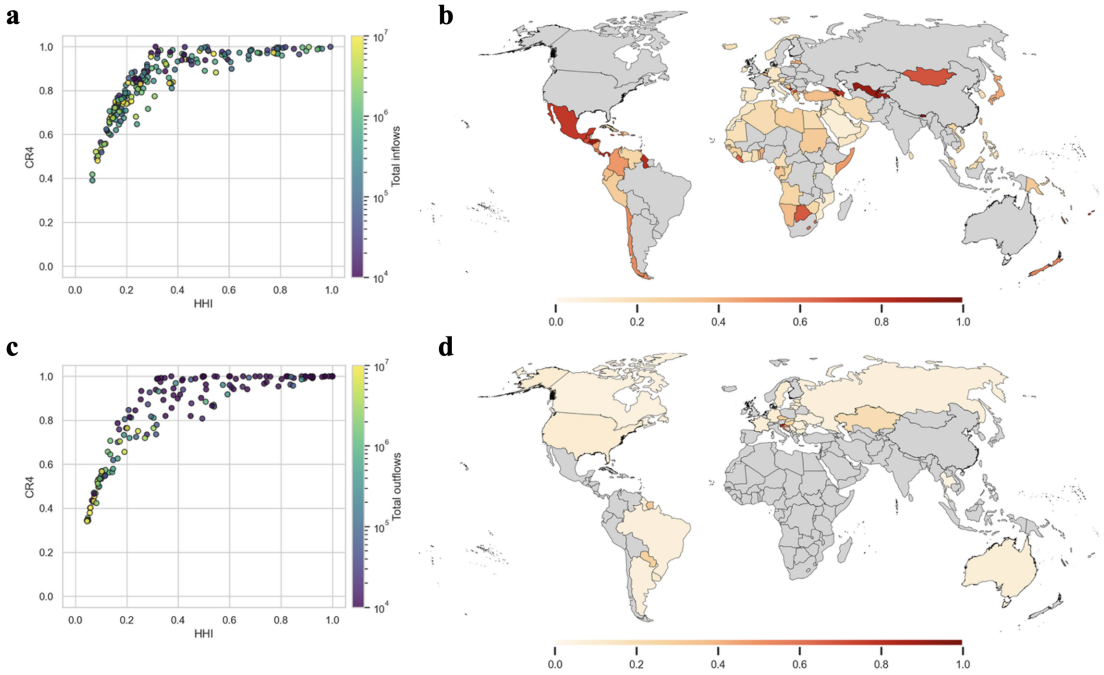

Figure B.3: Concentration of national scale international cereal flows. **a** Comparison of HHI and CR4 for cereal inflows, by importing country. **b** HHI over inflows, by importing country (showing only countries where international inflows exceed 20% of national consumption). **c** Comparison of HHI and CR4 for cereal outflows, by exporting country. **d** HHI over outflows, by exporting country (showing only countries where international outflows exceed 20% of national production).

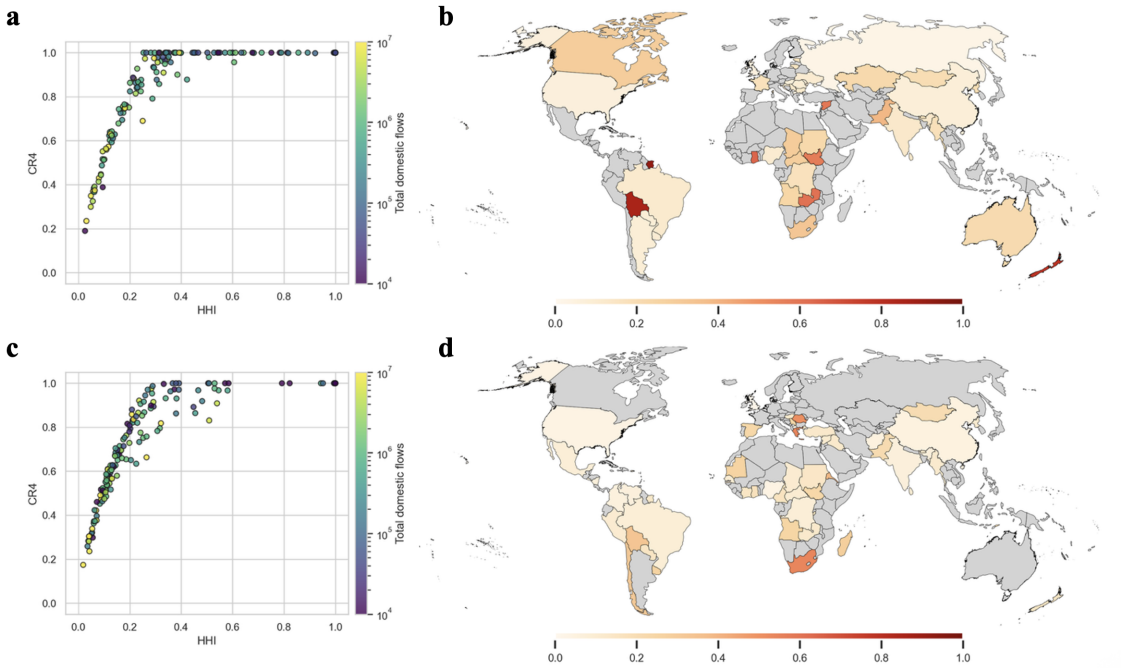

Figure B.4: Concentration of subnational scale domestic cereal flows. **a** Comparison of HHI and CR4 for cereal exporters, by country. **b** HHI over exporters, by country (showing only countries where domestic flows exceed 20% of national consumption). **c** Comparison of HHI and CR4 for cereal importers, by country. **d** HHI over importers, by country (showing only countries where domestic exceed 20% of national production).

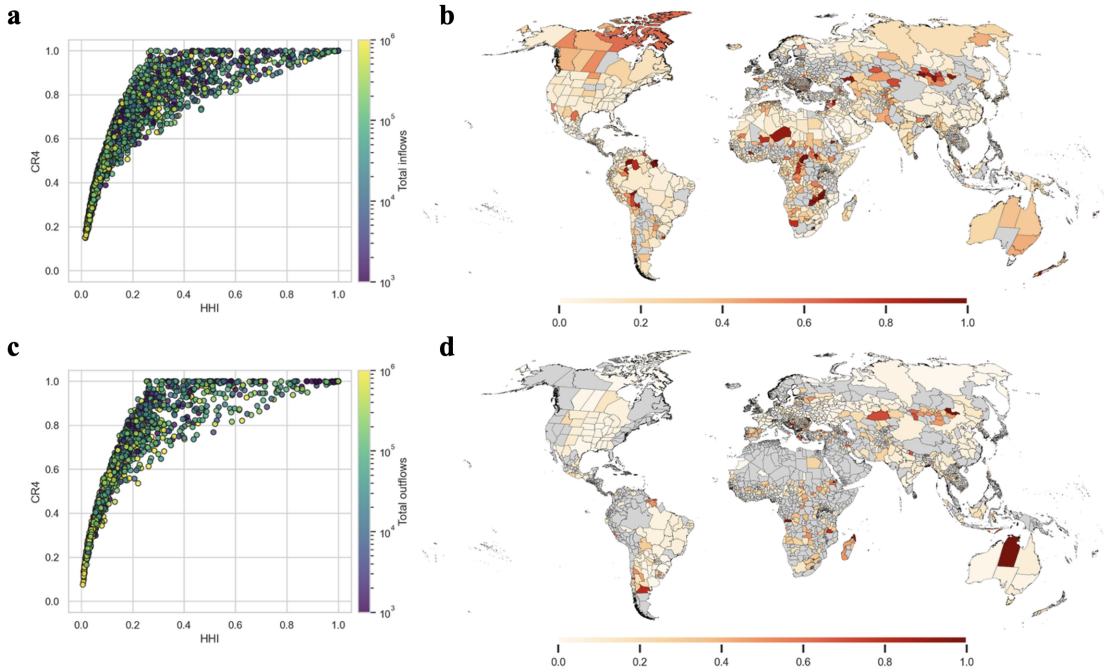

Figure B.5: Concentration of subnational scale cereal flows (both domestic and international). **a** Comparison of HHI and CR4 for cereal inflows, by importing administrative region. **b** HHI over inflows, by importing administrative region (showing only regions where total inflows exceed 20% of regional consumption). **c** Comparison of HHI and CR4 for cereal outflows, by exporting administrative region. **d** HHI over outflows, by exporting administrative region (showing only regions where international outflows exceed 20% of regional production).

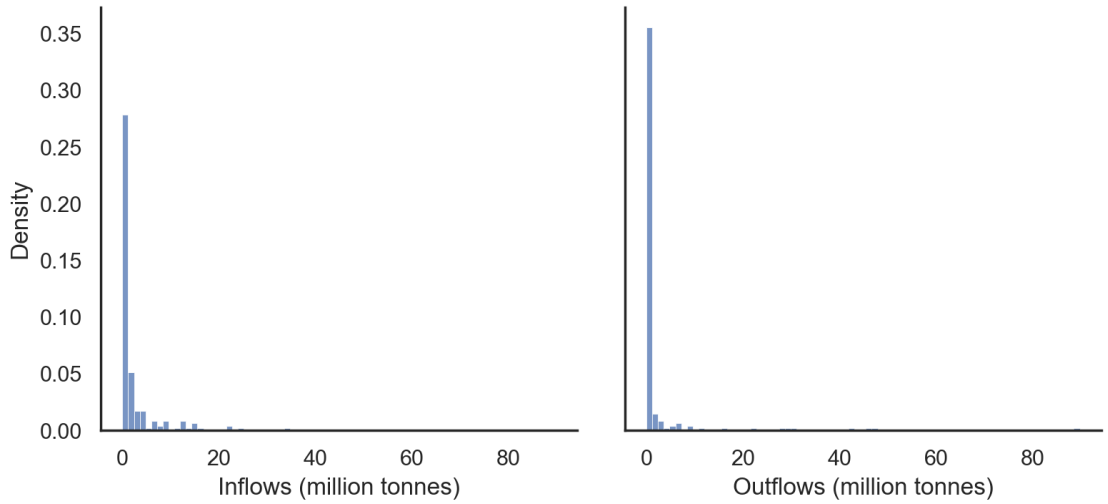

Figure B.6: Distribution of country-level total inflows and total outflows.

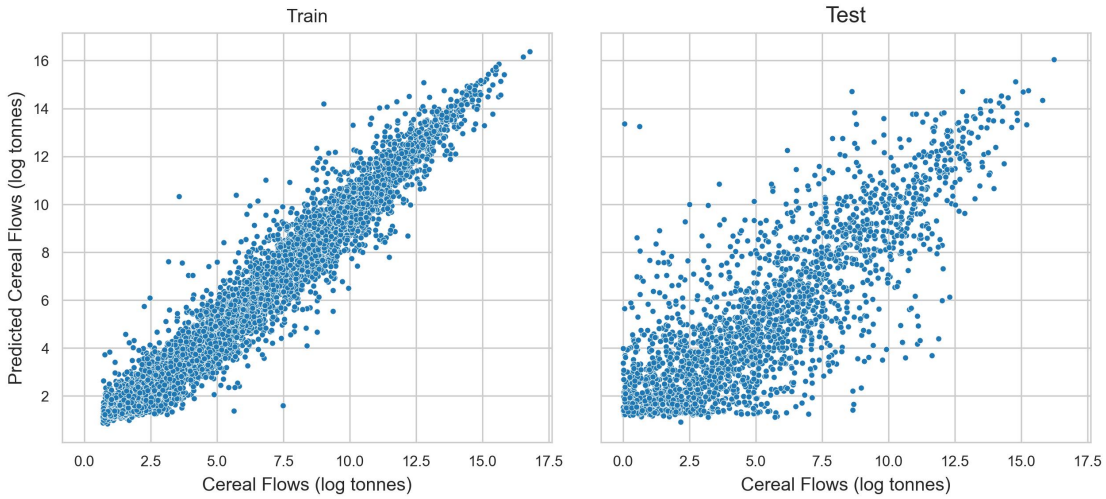

Figure B.7: Predicted vs observed national-scale cereal flows in log tonnes for train ($\mathbf{n = 7,959}$) and test sets ($\mathbf{n = 2,026}$).

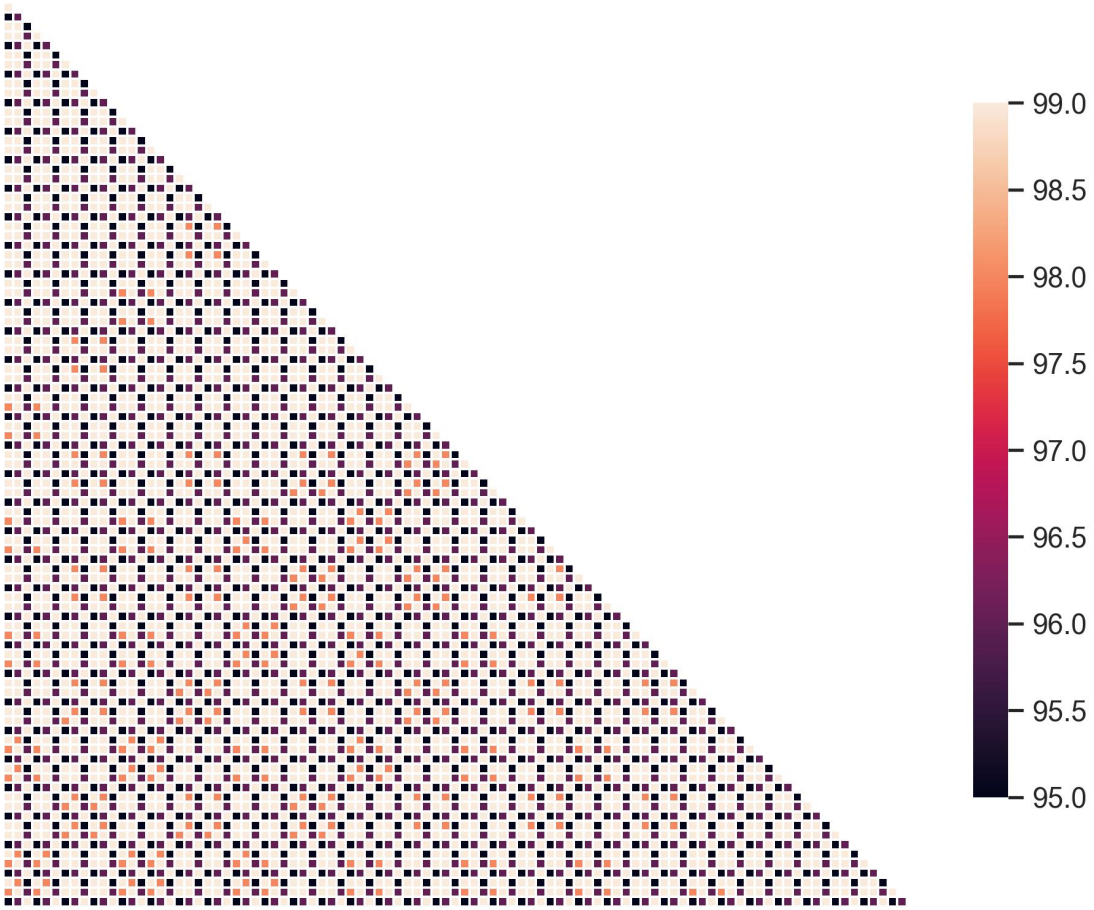

Figure B.8: Pairwise Pearson correlations among subnational cereal flow estimates generated under 96 different harmonization-parameter settings.

B.2 Supplementary Tables

Table B.1: Datasets used in the modelling pipeline.

Data	Database	Year(s)	Details
Political boundaries	Global Administrative Areas Database (GADM)		195 countries, 3,536 subnational primary administrative regions
Production	FAOSTAT (FAO, 2023)	2012	Crops included: barley, buckwheat, canary seed, fonio, maize, millet, mixed grain, oats[b], quinoa, rye, rice[c], sorghum, triticale, wheat, other cereals[d]
		2017	
		2017-21[a]	
Producer prices	FAOSTAT (FAO, 2023)	2010-21	
Yield	FAOSTAT (FAO, 2023)	2010-21	Spatial resolution: National scale
Bilateral trade	FAOSTAT (FAO, 2023)	2017-21	
	Harris et al. (2020)	2012	Domestic cereal flow in India
	Pandit et al. (2023)	2017	Subnational international flows between USA and China
Global gridded crop areas	Global Agro-Ecological Zones (GAEZ) + 2015 Annual Crop Harvest Area and Production (Frolking et al., 2020a; 2020b)	2015	Crops included: barley, maize, millet, rice, sorghum, wheat, other cereals Spatial resolution: ∼10 km
Global gridded crop production		2015	
Gridded livestock counts	Gridded Livestock of the World 2015 (Gilbert et al., 2022a; 2022b; 2022c; 2022d; 2022e; 2022f; 2022g; 2022h)	2015	Animals included: buffaloes, cattle, chickens, ducks, goats, horses, pigs, sheep Spatial resolution: ∼10 km
Global gridded building footprint	Global Human Settlement Layer (GHSL) Built-up Volume (Schiavina et al., 2022)	2020	Spatial resolution: 100 m
Global gridded population	WorldPop (n.d.)	2020	Spatial resolution: 1 km
Global gridded GDP	Wang and Sun (2022)	2005	Spatial resolution: 1 km
Transport	Verschuur et al. (2023)		Includes cost, distance, and time variables for transporting commodities between any two subnational regions
Tariff	MAc-MAP-HS6 (Guimbard et al., 2012)	2019	Bilateral tariff data

[a] This five-year window was the most recent period with complete reporting for all countries at the time of this analysis. Historical trade trends from the FAO were not used, because this study aims to generate a single cross-sectional snapshot of subnational flows, and most predictor covariates are only available at one point in time rather than as time-series. Although this interval includes the COVID-19 pandemic, it remains representative of typical global cereal flows, as the literature reports no significant impact of the pandemic on global cereal grain trade (Arita et al., 2022).

Table B.1: Datasets used in the modelling pipeline (continued).

[b] Oats trade includes rolled oats as well.
[c] For rice, bilateral trade for the 'milled equivalent' category was used. For consistency, the rice production data from the FAO was scaled by a factor of 0.7, to estimate the milled equivalent rice production (Bodie et al., 2019).
[d] 'Other cereals' corresponds to FAOSTAT's 'Cereals, n.e.c.' (not elsewhere classified).

Table B.2: Global production, country-to-country trade, and flows for 15 cereal commodities. Production data comes from the FAO, trade data is obtained after harmonizing the FAO bilateral trade data (Gehlhar, 1996), and flows data is the output of the re-export algorithm (Croft et al., 2018).

Commodity	**Global Production (million tonnes)**	**Global Trade (million tonnes)**	**Global Flows (million tonnes)**	**Correlation between country-to-country trade and flows**	
				Linear scale	**Log scale**
Barley	150.34	37.74	36.35	0.99	0.89
Buckwheat	2.01	0.18	0.12	0.94	0.69
Canary seed	0.25	0.20	0.17	0.99	0.68
Fonio	0.65	0.00	0.00	0.99	0.87
Maize	1154.94	183.23	177.31	0.99	0.89
Millet	29.91	0.47	0.38	0.96	0.82
Mixed grain	3.36	0.07	0.01	0.27	0.59
Oats	23.80	4.45	4.06	0.99	0.84
Quinoa	0.16	0.10	0.08	0.98	0.62
Rice	535.07	44.96	42.56	0.99	0.84
Rye	12.96	1.63	1.49	0.99	0.89
Sorghum	58.92	7.23	7.16	0.99	0.89
Triticale	14.17	0.81	0.78	0.99	0.97
Wheat	759.29	191.62	184.11	0.99	0.86
Other	7.82	0.37	0.11	0.44	0.51
Total	**2754.09**	**471.44**	**455.92**	**0.99**	**0.89**

Table B.3: Predictor variables used by the classification and regression models.

Predictor variable	**Description**	**Obtained from dataset**
from_barley_area from_maize_area from_millet_area from_rice_area from_sorghum_area from_wheat_area from_other_cereals_area to_barley_area to_maize_area to_millet_area to_rice_area to_sorghum_area to_wheat_area to_other_cereals_area	Cereal cultivation areas in exporting and importing regions (on log scales)	GAEZ + 2015 Annual Crop Harvest Area
from_barley_production from_maize_production from_millet_production from_rice_production from_sorghum_production from_wheat_production from_other_cereals_production to_barley_production to_maize_production to_millet_production to_rice_production to_sorghum_production to_wheat_production to_other_cereals_production	Cereal production in exporting and importing regions (on log scales). Subnational production figures were adjusted to align with national totals by applying scale factors based on the corresponding national-level production data (2012 for the India data, 2017 for the US-China dataset, and 2017–21 for all 3,536 regions for which flows are to be estimated), thereby ensuring that aggregated subnational outputs matched the observed country-level production.	GAEZ + 2015 Annual Crop Production
from_buffaloes from_cattle from_chickens from_ducks from_goats from_horses from_pigs from_sheep to_buffaloes to_cattle to_chickens to_ducks	Livestock counts in exporting and importing regions (on log scales)	Gridded Livestock of the World 2015

Table B.3: Predictor variables used by the classification and regression models. (Continued)

to_goats to_horses to_pigs to_sheep		
from_built_volume_total to_built_volume_total	Built up volume in exporting and importing regions (on log scales)	GHSL Built-up Volume
from_pop to_pop	Population in exporting and importing regions (on log scales)	WorldPop
from_gdp to_gdp	GDP in exporting and importing regions (on log scales)	Global gridded GDP
from_area to_area from_region to_region domestic subnational	Area of exporting and importing regions (on log scales), Regional group (Africa, Asia, Europe, Latin America and the Caribbean, Northern America, Oceania) of exporting and importing region, Dummy variables for domestic/international and for subnational/national	GADM
from_price to_price	Producer prices in exporting and importing regions (on log scales)	FAOSTAT
transport_USD_t time_h distance_km border_USD_t customs_USD_t	Cost of transporting a tonne of goods, time in hours, distance in km, and border compliance cost per tonne, customs compliance cost per tonne, going from exporting to importing region (on log scales). To aggregate transport data to the national level, a weighted average over all subnational pairings between each pair of countries was computed. The weight for each subnational pair was a product of two elements – (i) the sum of production of all cereals in the importing region, and (ii) the sum of population and livestock counts in the exporting region.	Transport
tariff	Bilateral tariff data between countries in USD per tonne (on log scales)	Tariff

Table B.4: Hyperparameter settings for all cereal flow link classification models evaluated.

Model	**Hyperparameters**
Logistic regression	maximum iterations: 500
Random forest classifier	number of trees: 200 maximum tree depth: 15 minimum number of samples required to split a node: 4 weights associated with classes: 'balanced'
Gradient boosting classifier	maximum iterations: 5000 minimum number of samples per leaf: 100 proportion of features chose in each node split: 0.8 weights associated with classes: 'balanced'
Neural network	learning rate: 0.001 number of hidden layers: 2 dropout: 0.2 dense neurons: 512 batch size: 512 epochs: 300 hidden layer activation function: 'relu' output layer activation function: 'sigmoid' loss function: 'binary cross entropy' optimizer: 'RMSprop'

Table B.5: Out-of-sample performance of cereal flow link classification models by dataset type. Metrics are averaged over five model runs with distinct train-test splits to account for sampling variation.

Model	Dataset*	Accuracy	Precision	Recall	MCC
Logistic regression	faostat	0.89	0.82	0.77	0.72
	india	0.72	0.74	0.83	0.38
	us-china	0.80	0.53	0.33	0.30
	overall	0.88	0.80	0.75	0.69
Random forest classifier	faostat	0.93	0.84	0.91	0.82
	india	0.87	0.83	0.99	0.73
	us-china	0.97	0.94	0.91	0.90
	overall	0.93	0.84	0.92	0.83
Gradient boosting classifier	faostat	0.94	0.85	0.93	0.84
	india	0.90	0.88	0.97	0.78
	us-china	0.97	0.93	0.95	0.92
	overall	0.94	0.85	0.93	0.85
Neural network	faostat	0.93	0.86	0.87	0.81
	india	0.87	0.88	0.92	0.73
	us-china	0.95	0.89	0.86	0.84
	overall	0.93	0.86	0.87	0.81

* test-split only. 'faostat': national-scale international flows (2017–2021); 'india': domestic cereal flows within India (2012); 'us-china': subnational-scale international flows between USA and China (2017); 'overall': all datasets combined.

Accuracy measures the proportion of correct predictions over all predictions. Precision measures the proportion of true positives over all predicted positives. Recall measures the proportion of all positives that are identified by the model. The MCC score provides the most balanced estimate of performance by assessing all 4 elements of the 2×2 confusion matrix, and can take values between -1 and $+1$, where $+1$ indicates perfect agreement.

Table B.6: Hyperparameter settings for all cereal flow prediction regression models evaluated.

Model	**Hyperparameters**	**Details**
Linear regression	–	Target: log(flow volume) Loss: mean squared error on log scale
Random forest regressor	number of trees: 500 maximum tree depth: 10	Target: log(flow volume) Loss: mean squared error on log scale
Gradient boosting regressor	maximum iterations: 1000 minimum samples per leaf: 100 proportion of features per split: 0.4 maximum tree depth: 8 L2 regularization: 100 loss function: 'gamma'	Target: flow volume (linear) Loss: gamma loss, which internally uses a log-link
Neural network	learning rate: 0.01 number of hidden layers: 2 dropout: 0.2 dense neurons: 256 batch size: 512 epochs: 400 hidden layer activation: 'relu' output layer activation: 'softplus' optimizer: 'RMSprop'	Target: flow volume (linear) Loss: $L(y, \hat{y}) = \alpha\, L_q(y, \hat{y}) \times 0.01 + (1 - \alpha)\, L_l(y, \hat{y}) \times 100$, where $\alpha = 0.5$, y = observed flows, $\hat{y}$ = predicted flows, $L_q(y, \hat{y})$ = quantile loss (quantile weight = 0.6), $L_l(y, \hat{y})$ = MSE between $\log(y)$ and $\log(\hat{y})$

Table B.7: Out-of-sample performance of cereal flow prediction regression models by dataset type. Metrics are averaged over five model runs with distinct train-test splits to account for sampling variation.

Model	**Dataset***	**R2 (cereal flows)**	
		Linear scale	**Log scale**
Linear regression	faostat	0.02	0.47
	india	0.04	0.46
	us-china	-0.04	0.34
	overall	0.03	0.48
Random forest regressor	faostat	0.09	0.64
	india	0.23	0.78
	us-china	0.18	0.86
	overall	0.11	0.67
Gradient boosting regressor	faostat	0.39	0.70
	india	0.52	0.83
	us-china	0.79	0.95
	overall	0.42	0.73
Neural network	faostat	0.52	0.65
	india	0.35	0.75
	us-china	0.54	0.88
	overall	0.52	0.68

* test-split only. 'faostat': national-scale international flows (2017–2021); 'india': domestic cereal flows within India (2012); 'us-china': subnational-scale international flows between USA and China (2017); 'overall': all datasets combined.

Table B.8: Out-of-sample performance of the best performing link classification models for different cereals, by dataset type. Metrics are averaged over five model runs with distinct train-test splits to account for sampling variation.

Crop (Model)	Dataset*	Accuracy	Precision	Recall	MCC
wheat (Neural network)	faostat	0.96	0.84	0.86	0.83
	india	0.96	0.85	0.97	0.88
	overall	0.96	0.84	0.86	0.83
rice (Gradient boosting classifier)	faostat	0.95	0.75	0.94	0.82
	india	0.94	0.92	0.99	0.88
	overall	0.95	0.77	0.95	0.83
maize (Random Forest)	faostat	0.95	0.73	0.85	0.76
	india	0.97	0.00	0.00	-0.01
	overall	0.95	0.73	0.84	0.75
other cereals (Random Forest)	faostat	0.94	0.72	0.86	0.75
	india	0.94	0.64	0.28	0.39
	overall	0.94	0.72	0.85	0.75
all cereals (Gradient boosting classifier)	faostat	0.94	0.85	0.93	0.84
	india	0.90	0.88	0.97	0.78
	us-china	0.97	0.93	0.95	0.92
	overall	0.94	0.85	0.93	0.85

* test-split only. 'faostat': national-scale international flows (2017–2021); 'india': domestic cereal flows within India (2012); 'us-china': subnational-scale international flows between USA and China (2017); 'overall': all datasets combined. The 'us-china' dataset is excluded from individual-cereal models because it lacks disaggregated flows by cereal type.

Accuracy measures the proportion of correct predictions over all predictions. Precision measures the proportion of true positives over all predicted positives. Recall measures the proportion of all positives that are identified by the model. The MCC score provides the most balanced estimate of performance by assessing all 4 elements of the 2×2 confusion matrix, and can take values between -1 and $+1$, where $+1$ indicates perfect agreement.

Table B.9: Out-of-sample performance of the best performing flow prediction regression models for different cereals, by dataset type. Metrics are averaged over five model runs with distinct train-test splits to account for sampling variation.

Crop (Model)	**Dataset***	**R2 (cereal flows)**	
		Linear scale	**Log scale**
wheat (Neural network)	faostat	0.45	0.64
	india	0.36	0.70
	overall	0.45	0.65
rice (Neural network)	faostat	0.33	0.61
	india	0.44	0.87
	overall	0.36	0.67
maize (Neural network)	faostat	0.29	0.59
	india	-0.02	-0.47
	overall	0.29	0.60
other cereals (Neural network)	faostat	0.27	0.60
	india	-0.11	-0.07
	overall	0.26	0.60
all cereals (Neural network)	faostat	0.52	0.65
	india	0.35	0.75
	us-china	0.54	0.88
	overall	0.52	0.68

* test-split only. 'faostat': national-scale international flows (2017–2021); 'india': domestic cereal flows within India (2012); 'us-china': subnational-scale international flows between USA and China (2017); 'overall': all datasets combined. The 'us-china' dataset is excluded from individual-cereal models because it lacks disaggregated flows by cereal type.

Table B.10: Goodness of fit for regression models estimating consumption for different cereals.

Crop	**R-squared between true and fitted country level consumption**		**R-squared between true country level consumption and totalled admin level consumption (estimated)**	
	Linear scale	**Log scale**	**Linear scale**	**Log scale**
Wheat	0.89	0.52	0.93	0.47
Rice	0.85	0.76	0.94	0.68
Maize	0.63	0.74	0.69	0.72
Other cereals	0.57	0.75	0.52	0.65
All cereals	0.90	0.87	0.89	0.87

Table B.11: Out-of-sample Pearson correlations of observed and predicted total cereal flows with observed disaggregated cereal flows. Metrics are averaged over five model runs with distinct train-test splits to account for sampling variation.

Model	Dataset*	Correlation between total and disaggregated cereal flows							
		wheat		rice		maize		other cereals	
		obs	pred	obs	pred	obs	pred	obs	pred
Neural network	faostat	0.71	0.59	0.20	0.11	0.82	0.57	0.57	0.52
	india	0.84	0.56	0.75	0.47	0.07	0.16	0.23	0.22
	us-china	-	-	-	-	-	-	-	-
	overall	0.74	0.56	0.31	0.15	0.76	0.56	0.54	0.51

* test-split only. 'faostat': national-scale international flows (2017–2021); 'india': domestic cereal flows within India (2012); 'us-china': subnational-scale international flows between USA and China (2017); 'overall': all datasets combined. Correlations for the 'us-china' dataset are not provided because it lacks disaggregated flows by cereal type.

Table B.12: Parameter grid used for sensitivity analysis of the harmonization algorithm.

Parameter	**Description**	**Test values**
Link probability threshold	Classification probability cutoff for retaining a predicted link.	0.40, 0.50, 0.60
Domestic quantile fallback	If no domestic link in a country exceeds the threshold, retain top X% of links by probability.	0.75, 0.80
International quantile fallback	If no international link between a trading country pair exceeds the threshold, retain top X% of links by probability.	0.75, 0.80
Iteration limit	Maximum passes in Phase I (Phase II uses twice this value).	40, 50
Scaling factor α	In Phase I, upward nudges go from α to 2α and downward nudges go from 0.5α to 1.5α; in Phase II, α denotes the fraction of total deficit (or surplus) to reallocate.	0.10, 0.20
Export cap β	Maximum share of production allowed for export in Phase I.	0.90, 0.95

B.3 Supplementary Methods

B.3.1 Reliability index approach

The reliability index approach outlined by Gehlhar (1996) is used to resolve discrepancies between the volume of cereal trade reported by the importer and exporter in the bilateral trade dataset. An accuracy level (Supplementary Equation B.3.1.1) is computed for each bilateral trading pair, and this captures the quality of match between the importer and exporter reported quantities. The value of AL should be closer to 0 for the match to be more accurate, and a threshold of 0.2 is used to separate accurate from non-accurate matches, i.e. a match is accurate only if the difference between the reported imports and exports is less than 20%. Then, for each country, it becomes possible to construct an importer reliability index (RIM), and an exporter reliability index (RIX), which are given by Supplementary Equations B.3.1.2 and B.3.1.3 respectively. An importer's reliability is measured by the proportion of total imports it reports accurately, and similarly an exporter's reliability is measured by the proportion of its total exports it reports reliably. Finally, for each bilateral trading pair, the value reported by the more reliable partner is accepted as the trade flow between those countries.

Equation B.3.1.1 calculates the accuracy level (AL) of a transaction from region r to region s, for which the value of trade reported by the importer is $M_{r,s}$ and that reported by the exporter is $X_{r,s}$:

$$AL_{r,s} = 2 \times \frac{|M_{r,s} - X_{r,s}|}{M_{r,s} + X_{r,s}} \tag{B.3.1.1}$$

Equation B.3.1.2 calculates the reliability index of import region s as:

$$RIM_s = \frac{M_s^{\mathrm{A}}}{M_s^{\mathrm{T}}} \tag{B.3.1.2}$$

where $M_s^{\mathrm{T}} = \sum_r M_{r,s}\ \forall s$, and $M_s^{\mathrm{A}} = \sum_r M_{r,s}\ \forall s$ where $AL_{r,s} \leq 0.2$.

Equation B.3.1.3 calculates the reliability index of export region r as:

$$RIX_r = \frac{X_r^{\mathrm{A}}}{X_r^{\mathrm{T}}} \tag{B.3.1.3}$$

where $X_r^{\mathrm{T}} = \sum_s X_{r,s}\ \forall r$, and $X_r^{\mathrm{A}} = \sum_s X_{r,s}\ \forall r$ where $AL_{r,s} \leq 0.2$.

B.3.2 Re-export algorithm

The bilateral trade dataset harmonized using the reliability index approach is fed into a re-export algorithm along with the production dataset from the FAO. The re-export algorithm proposed by Croft et al. (2018) ensures that the total exports from a country never exceed its production and total imports; and it also links the source of production with the destination of import. The algorithm uses the production and export matrices P and E, and applies an iterative approach to produce a domestic supply matrix D. In this study, the dimensions of P, E, and D are 195×1, 195×195, and 195×195 respectively. The non-diagonal elements of the computed domestic supply matrix D and the export matrix E were highly correlated (Supplementary Table B.2).

$$P = \begin{bmatrix} p_1 \\ p_2 \\ \vdots \\ p_n \end{bmatrix}, \quad E = \begin{bmatrix} 0 & e_{12} & \cdots & e_{1n} \\ e_{21} & 0 & \cdots & e_{2n} \\ \vdots & \vdots & \ddots & \vdots \\ e_{n1} & e_{n2} & \cdots & 0 \end{bmatrix}, \quad D = \begin{bmatrix} d_{11} & d_{12} & \cdots & d_{1n} \\ d_{21} & d_{22} & \cdots & d_{2n} \\ \vdots & \vdots & \ddots & \vdots \\ d_{n1} & d_{n2} & \cdots & d_{nn} \end{bmatrix}$$

where, p_i is the production in country i; e_{ij} are the exports from country i to j; and d_{ij} is the quantity of country j's domestic supply that originates from country i. The sum of rows of matrix D equals the countries' production, and the sum of columns equals the countries' domestic supply (or consumption). The diagonal elements correspond to the produce that stays within the countries. The non-diagonal elements of matrix D are referred to as 'flows' in this study, i.e., $d_{ij|i\neq j}$ gives the food flow from i to j. Croft et al. (2018) list all the algorithm steps and also provide MATLAB code for implementing it to obtain the domestic supply matrix D.

B.3.3 Producer prices

FAO-reported producer prices (USD/tonne) reflect farm-gate receipts and exclude post–farm-gate costs such as transport to market, storage, processing, and marketing fees. When available, prices from the three most recent years since 2010 were

averaged for each crop and country. Missing values were imputed via a linear regression (Supplementary Equation B.3.3.1), with prices first converted from per hectare to per tonne by multiplying by yields to improve model fit.

Equation B.3.3.1:

$$\log(\text{price}) = \beta_0 + \beta_1 \log(\text{GDP}) + \beta_2 \log(\text{production}) + \beta_3 \log(\text{yield}) + \text{region FE} \tag{B.3.3.1}$$

with regions as Africa, Americas, Asia, Europe, and Oceania. The primary regression was fitted using data from the 25 largest producers with available price information, to minimize noise from smaller producers. Where countries fell outside the regions covered by these top 25, a secondary regression was applied using all nations with price data. In regions lacking any observations, global averages were substituted. When fewer than 25 observations existed for a given crop, subregional, regional, and then global means were used in sequence to impute missing values, instead of the regression approach.

Finally, aggregated cereal producer prices were computed as production-weighted averages of individual commodity prices. In the absence of any subnational data on producer prices, country level price data was used at all subnational regions.

B.3.4 Machine learning to predict cereal flow links and volumes

The gridded datasets (Supplementary Table B.1) were aggregated over all 3,536 administrative regions, and over 195 countries to obtain totals of the crop areas, crop production, livestock, and population characteristics for all regions of interest. Transport data available between all pairs of subnational regions was also aggregated to the national level. Finally, all covariates were combined for both subnational scale and national scales. Supplementary Table C.3 shows a list of all predictor variables used by the machine learning models. Disaggregated area and production figures for each cereal crop (e.g., maize, wheat, rice) were included as covariates because trade flows depend on the relative abundance of individual cereals in

exporting and importing regions – aggregation into a single cereal total would result in crop-level patterns being masked and opposing flows being cancelled out. Both area and production variables were used, as they can together inform the model about crop yields. Different livestock and population counts are a proxy for demand, and the GDP and built-up volume are proxies for economic activity. Trade, tariff, and transport costs, distance and transportation time between exporting and importing regions, and producer prices in both trading regions, were used as predictors of trade relationships as well.

Cereal flow link prediction

The FAO national-scale data consists of 37,830 country pairs, India's domestic data includes 1190 state pairs, and the US-China data covers 3162 state-province pairs. In total, 42,182 pairs are used to train a classification model for link prediction. A flow threshold of 1 tonne was used to define link presence, yielding 12,490 positive links (~30% overall: 25% FAO, 65% India, 20% US-China). The full dataset was first split into a train and test sets in an 80-20 proportion. This is a standard practice for machine learning algorithms – hyperparameter tuning is performed using cross-validation on the train set and the final trained model is tested on the test set, which ensures that the tuned model does not overfit to the training data. Four model types were tested for the classification task – logistic regression, random forest classifier, gradient boosting classifier, and a neural network or deep learning model (Bentéjac et al., 2021; LaValley, 2008; Pang et al., 2020; Parmar et al., 2019). See Supplementary Table B.4 for the hyperparameter setting chosen for each of these classification models.

All models except logistic regression, which performed poorly, showed comparable performances, across datasets (Supplementary Table B.5). To remove sampling variability, the performance metrics for each model were averaged over five runs, with a different random train-test split for each run. The gradient boosting model was chosen to make predictions, as it has a marginally better MCC score, as compared to the random forest and deep learning models. The chosen classification model was

subsequently trained using all data from the train and test sets combined, and then used to make predictions for the existence of cereal flow links at subnational scales using the administrative level features – for all domestic administrative pairs, and for the international administrative pairs in countries that have known cereal flows between them. This provided classification probabilities for 5,044,255 international administrative pairs and for 135,090 are domestic administrative pairs.

Cereal flow volume prediction

The cereal flow prediction model was trained using the subset of region pairs that have existing links, i.e. 12,490 pairs. Four model types were tested for the regression task – linear regression, random forest regressor, gradient boosting regressor, and a neural network or deep learning model (Pang et al., 2020; Prettenhofer & Louppe, 2014; Segal, 2004; Weisberg, 2005). The extreme right skew of the cereal-flow distributions (Supplementary Figure B.6), in which most country-level inflows and outflows cluster at low volumes while a handful reach very large values, made it challenging to train the regression models. To mitigate this, both linear regression and random forest were trained on log transformed flow volumes. Both models exhibited a poor fit ($0 < R^2 < 0.20$) on the original linear scale, failing to capture variation among smaller flows despite achieving R-squared between 0.35-0.85 on the log scale. By contrast, both gradient boosting regressor and neural network models were trained on untransformed flow volumes. A gamma loss function, which uses a log-link, was used with the gradient boosting regressor, and a custom defined loss function, which combines losses at linear and log scales, was used with the neural network (Supplementary Table B.6). These models were able to learn patterns at both ends of the distribution and achieved superior performance across linear ($0.35 < R^2 < 0.80$) and log scales ($0.65 < R^2 < 0.95$), across datasets (Supplementary Table B.7).

The regression performance metrics for each model were also averaged over five runs, with a different random train-test split for each run. Hyperparameter tuning was performed using cross-validation on the train set from one of the train-test

splits. The neural network model was chosen to make predictions, as it has a better R-squared on linear scale, as compared to the gradient boosting regressor. Supplementary Figure B.7 shows the relationship between predicted vs observed cereal flows (in log tonnes) for the train and test sets, where the predictions are obtained from one of the five runs of the neural network model. This chosen model was then trained using all 12,490 region pairs with existing flow links. This fitted model was then used to make predictions for all domestic administrative pairs and for all international administrative pairs between countries with existing food flows.

B.3.5 Harmonizing the cereal flow estimates from ML models

Predicted subnational flow links were first filtered by their classifier estimated probabilities to obtain a sparse network of likely connections. Specifically, a probability threshold of 0.5 was applied, all predicted links with probability greater than 0.5 were retained as candidate flows. Choosing a probability threshold of 0.5 implies equal weighting of false positives and false negatives (given that the classifier was trained with balanced class weights, the optimal decision boundary lies at a probability threshold of 0.5 irrespective of class imbalance). In cases where two trading countries had no subnational link with probability over the threshold, the links with the highest 20% probabilities were selected to avoid omitting potentially real flows. The same logic was used for all pairs within countries, a threshold of 0.5 was used, but the links with the highest 20% probabilities were selected when no domestic flow links had a greater than 0.5 probability. The flow volumes on these retained links were then initialized by the regression model predictions. These flows were then harmonized in two main phases: the first involves adjusting all flows (international and domestic) to reduce surpluses and deficits between regions, while scaling international flows to align with country level totals; and the second involves adjusting flows within countries only to correct any remaining imbalances in regional consumption.

Harmonization step 0: Estimating regional production and consumption

B. Supplementary Material for "Mapping Global Cereal Flow at Subnational Scales Unveils Key Insights for Food Systems Resilience"

The 2015 global gridded crop-production data were first aggregated to administrative boundaries to yield baseline estimates of regional cereal production (Frolking et al., 2020b). To account for change (growth) in overall output between 2015 and the study period (2017–2021), these values were scaled using country-specific factors equal to the ratio of the FAO's national production totals to the 2015 gridded production estimates aggregated by country.

Subnational cereal consumption was then estimated via a log-linear gamma regression fitted at the national scale (Supplementary Equation B.3.5.1). Observed national consumption was defined as $production + inflows - outflows$, and this quantity was regressed against log-transformed regional covariates, including livestock counts (buffaloes, cattle, chickens, ducks, goats, horses), population, GDP, and cereal production. The log-linear specification was

Equation B.3.5.1:

$$\begin{aligned}\log\Big(\mathrm{E}(\mathrm{consumption}_i)\Big) = {} & \beta_1 \log(\mathrm{buffaloes}_i) + \beta_2 \log(\mathrm{cattle}_i) + \beta_3 \log(\mathrm{chicken}_i) \\ & + \beta_4 \log(\mathrm{ducks}_i) + \beta_5 \log(\mathrm{goats}_i) + \beta_6 \log(\mathrm{horses}_i) \\ & + \beta_7 \log(\mathrm{pop}_i) + \beta_8 \log(\mathrm{gdp}_i) + \beta_9 \log(\mathrm{production}_i) \quad \text{(B.3.5.1)}\end{aligned}$$

Livestock and population capture combined food and feed demand, GDP serves as a proxy for dietary preferences, and regional production serves as an indirect indicator of both local availability and unobserved industrial processing. Processing plants are frequently co-located with primary grain production areas to minimize inbound transport costs for bulky cereals (Denicoff et al., 2010; Westlake, 2005). Hence, the covariate for regional cereal production can proxy for this hidden component of demand, in the absence of a direct measure of processing at subnational scales. Pigs and sheep were omitted from the regression specification due to multicollinearity. Also note that stock variation was not accounted for while estimating production or consumption even though stocks can affect total supply. Global stock variation amounted to only ~1% of annual production over

2017-2021 (and remained below 5% for nearly all countries), making it a very small component of total supply.

The R-squared between estimated and observed consumption at national scales was 0.90. The fitted model was used to estimate consumption at subnational scales. The estimated subnational-scale consumption, when aggregated at national level, also matched well with observed national level consumption (R^2=0.89). The resulting subnational consumption estimates were also scaled so that, within each country, their sum exactly matched the FAO's reported consumption total.

Harmonization step 1: Global adjustment

The first phase of harmonization proceeds as an iterative loop of up to 50 passes. At the start of each iteration, the entire flow matrix is first re-scaled so that the sum of all subnational flows between each exporter-importer country pair exactly matches the corresponding FAO bilateral trade volume. With country totals fixed, each region's own supply and demand balance is examined. If a region's net supply falls below consumption by more than 5%, all its incoming flows are nudged upward and all its outgoing flows nudged downward. Conversely, regions in surplus have their inbound flows decreased and outbound flows increased, provided they retain sufficient production after their existing exports. The magnitude of these adjustments grows linearly over the iterations – inflow increases begin at 10 percent and rise to 20 percent, while outflow reductions begin at 5 percent and rise to 15 percent. The gradually increasing adjustment factors ensure sustained progress toward convergence, preventing premature stagnation. A larger scaling range for inflow increases was employed to avoid excessively suppressing imports into net exporting regions, many of which also could be importing cereals they do not produce. In this way, under-supplied regions progressively receive greater inflows, and oversupplied regions redistribute their excess.

After adjusting for deficits and surpluses, a production-based export cap is imposed. Exports from any region are capped at the smaller of: i) 95% of its production, and ii) the amount remaining after meeting half of its consumption

needs, that is, if production exceeds 0.5 × consumption, then at least 50% of consumption must be met locally before any export, otherwise (when production ≤ 0.5 × consumption) no exports are permitted. The 50% self-consumption threshold was chosen because FAO data show that countries that produce sufficient cereals typically cover at least half of their domestic demand from their own harvest before exporting. Wherever a region's outflows exceed this cap, all its outgoing flows are proportionally scaled back.

Thereafter, the three steps of realigning country totals, rebalancing regional consumption, and enforcing outflow caps, are repeated until changes in flows become negligibly small, or until the maximum number of iterations is reached. Finally, country totals are aligned with FAO trade volumes again, before moving on to the next phase.

Harmonization step 2: Domestic adjustment

After the first harmonization phase, some regions still faced small supply deficits while others held unused surplus. To clear these residual imbalances, a domestic-only redistribution loop was run up to 100 iterations. In this phase, the outflow constraints are relaxed to facilitate balancing, but still no region may export more than what it produces. For each country, the aggregate deficit (sum of all region shortfalls) and the aggregate available surplus (sum of each region's unused production) are computed. A reallocation budget equal to 10% of the smaller of these two pools is then established, to ensure that the algorithm never moves more grain than is available or required. The budget is shared among deficit regions in proportion to each region's share of the total deficit, and it is drawn from surplus regions in proportion to each region's share of the total surplus. After updating the flows, net balances are recomputed, and the loop is repeated until every region's deficit falls within 5% of its demand or the limit of 100 iterations is reached.

B.3.6 Key Modelling Assumptions

The modelling pipeline relies on several key assumptions, enumerated here for transparency.

Spatial accuracy of gridded production data

Subnational production is derived from the GAEZ+ 2015 dataset (Grogan et al., 2022), which downscales FAO national crop statistics to grid cells using a sequential rebalancing optimisation. The dataset is not based on remote sensing observations of cropland presence, and spatial misallocations can arise where the underlying priors – cropland and irrigation distribution maps, soil and climate data, livestock and population layers, and observed crop calendars – are inaccurate or outdated. The dataset is anchored to 2015, while this analysis covers 2017-2021; proportional scaling matches country-level totals but assumes that the within-country spatial distribution of cereal production has not changed materially between these periods. Misallocations propagate directly into flow estimates, since a region's modelled surplus or deficit is determined by the difference between its estimated production and consumption. For example, in the United States, GAEZ+ 2015 overestimates cereal output in Texas and California relative to Corn Belt states like Iowa and Illinois. In regions with limited ground-truth data, particularly sub-Saharan Africa and parts of Central Asia, spatial allocation errors may be larger but are difficult to quantify.

Subnational consumption estimation

Subnational cereal consumption is estimated from a regression model fitted at the national scale, using livestock counts, population, GDP, and cereal production as predictors (Supplementary Methods B.3.5). The fitted model is then applied at subnational scales, and the resulting estimates are scaled so that the sum across subnational regions in each country matches the FAO-reported national consumption total. This assumes that the statistical relationship between consumption and its predictors holds at subnational scales within each country. The assumption may be

less accurate in countries with large within-country variation in dietary preferences, urbanisation levels, or food distribution infrastructure.

Structural similarity of flow networks across spatial scales

The machine learning models are trained primarily on national-scale flow data and a small subset of subnational observations from the United States, China, and India, and applied to predict flows at subnational scales globally. This rests on the assumption that the structural properties of food flow networks (the distribution of flow volumes, the relationship between predictor variables and flow presence) are similar across spatial scales. Konar et al. (2018) provide direct support for this assumption, examining food flow networks at three scales – global (international trade between countries), national (the United States Commodity Flow Survey), and village (Alaska Native communities) – and finding scale-invariant statistical distributions of node connectivity and mass flux at all three scales. Network parameters (mean connectivity, mass flux, centrality) vary with scale, but the underlying distributional forms are consistent. The assumption may nonetheless be weaker in regions where market institutions, transport infrastructure, or trade governance differ substantially from those represented in the training data – for example, in countries with strong government procurement systems, substantial informal trade, or fragmented domestic markets. In such cases, the underlying statistical regularities may still hold, but the specific parameters relating predictor variables to flow patterns may differ from those learned by the model, leading to less accurate predictions.

Validity of predictor variables

The machine learning models use gridded crop areas and production, livestock counts, population characteristics, transport data, and producer prices as proxies for the factors that drive food flows. The assumption is that these variables capture sufficient variation in the true drivers of cereal flows. Some important determinants – such as storage infrastructure, domestic market prices below the national level, and

informal cross-border trade – are not directly represented in the predictor set, since globally consistent data on these variables is not available at subnational scales.

Harmonization parameters

The post-prediction harmonization algorithm adjusts machine learning outputs to satisfy national-scale mass balance constraints and observed bilateral trade volumes. The specific threshold values, iteration limits, and scaling factors used in this procedure influence the final flow estimates. Sensitivity analysis across parameter combinations (Supplementary Table B.12 and Supplementary Figure B.8) demonstrates that the final harmonized flows are stable, with all pairwise correlations between alternative harmonized outputs exceeding 0.95.

B.4 Supplementary Notes

Pseudocode for modelling pipeline can be seen below:

Inputs

- 'D_fao_trade': FAO national bilateral trade data (reporter, partner, commodity, year, volume)
- 'D_fao_prod': FAO national production data (country, commodity, year, volume)
- 'D_subnat_flows_known': Available subnational flow data (e.g., India domestic, US-China international)
- 'C_gridded': Gridded covariate datasets (crop area/production, livestock, population, GDP, building footprint etc.)
- 'A_boundaries': Administrative boundaries (national and subnational)
- 'P_prices': Producer price data
- 'T_tariffs': Tariff data
- 'T_transport': Transport data

Output

- 'F_subnational': Matrix of harmonized cereal flows between all subnational administrative units (origin_admin_unit, destination_admin_unit, flow_volume, flow_type: domestic, international)

BEGIN PIPELINE

Phase 1: Data Pre-processing and Covariate Preparation

1. **Process National Trade Data ('D_fao_trade')**:

a. FOR EACH commodity, year:

B. Supplementary Material for "Mapping Global Cereal Flow at Subnational Scales Unveils Key Insights for Food Systems Resilience"

i. **Resolve Reporter Discrepancies:**

1. Calculate accuracy level for each bilateral trade pair (importer vs. exporter reported values).

2. Compute importer and exporter reliability indices.

3. 'D_harmonized_trade' = Accept value reported by the more 0reliable partner for each bilateral pair.

ii. **Apply Re-export Algorithm:**

1. Input: 'D_harmonized_trade', 'D_fao_prod'.

2. Output: 'D_national_flows' (links production source country to final import destination country, minimizes re-exports, ensures country exports <= production + imports).

b. Aggregate 'D_national_flows' across all cereal commodities, and average over 2017-2021.

2. **Process and Integrate Known Subnational Flows ('D_subnat_flows_known'):**

a. Aggregate individual commodity flows to total cereal flows.

b. Standardize format to match (origin_admin_unit, destination_admin_unit, volume).

3. **Prepare Covariates:**

a. FOR EACH gridded covariate dataset in 'C_gridded':

i. Aggregate gridded data to 'A_subnational' (subnational administrative units).

ii. Aggregate gridded data to 'A_national' (national units).

b. Process 'P_prices', 'T_tariffs', and 'T_transport', aligning them with national/subnational units.

c. Create origin-destination pair features for all potential national-national and subnational-subnational links. Features include:

- Origin characteristics (production of specific cereals, livestock counts, population, GDP, area, region, etc.).

- Destination characteristics (similar to origin).

- Pairwise characteristics (transport cost/time/distance, border compliance costs, tariffs, etc.).

d. 'X_features_links' = Combined feature set for all potential links.

Phase 2: Machine Learning Prediction of Subnational Flows

1. **Prepare Training Data for ML:**

a. 'Data_ML_train' = Combine 'D_national_flows' and 'D_subnat_flows_known'.

b. Associate each flow in 'Data_ML_train' with its corresponding features from 'X_features_links'.

2. **Link Prediction (Classification Model):**

a. Define 'y_link_presence' = 1 if flow_volume > threshold (i.e., 1 tonne), else 0.

b. Train 'Classifier_model' (e.g., Gradient Boosting Classifier, Random Forest) on 'Data_ML_train' (features: 'X_features_links' for training pairs, target: 'y_link_presence'). Use cross-validation for hyperparameter tuning.

c. 'P_link_probabilities' = 'Classifier_model'.predict_proba('X_features_links' for all potential subnational-subnational pairs).

3. **Volume Prediction (Regression Model):**

a. 'Data_ML_regression_train' = Subset of 'Data_ML_train' where 'y_link_presence' = 1.

b. Train 'Regressor_model' (e.g., Neural Network, Gradient Boosting Regressor) on 'Data_ML_regression_train' (features: 'X_features_links' for training pairs with links, target: 'log(flow_volume)' or 'flow_volume' with appropriate loss function). Use cross-validation.

c. 'V_predicted_volumes_raw' = 'Regressor_model'.predict('X_features_links' for all potential subnational-subnational pairs).

Phase 3: Harmonization of Predicted Subnational Flows

1. **Initialize Subnational Flow Network:**

a. Filter 'P_link_probabilities': Retain links if probability > 'prob_threshold' (e.g., 0.5).

- IF for a given national trade pair (CountryX -> CountryY), no subnational links (AdminX_i -> AdminY_j) exceed 'prob_threshold', THEN retain top 'k%' of links by probability for that national pair.

- Apply similar logic for domestic links within a country.

b. 'F_subnational_initial' = For retained links, assign flow volume from 'V_predicted_volumes_raw'.

2. **Estimate Subnational Consumption ('C_subnational_demand'):**

a. Estimate subnational production ('P_subnational_supply') using subnational production covariates/proxies scaled to match national production when aggregated.

b. Regress national consumption (Production + Imports - Exports) against national-level covariates (livestock, population, GDP, production).

c. Use the fitted regression model with subnational covariates to predict 'C_subnational_demand_raw'.

d. Scale 'C_subnational_demand_raw' within each country so that sum of subnational consumption equals national consumption.

3. **Iterative Harmonization - Phase I: Global Adjustment (International & Domestic Focus)**

a. 'F_subnational_current' = 'F_subnational_initial'.

b. FOR 'iter_global' FROM 1 TO 'MAX_GLOBAL_ITERATIONS':

i. **Realign with National Totals:**

1. FOR EACH national bilateral trade pair (CountryX -> CountryY) in 'D_national_flows':

- 'Sum_current_sub_intl_flow' = SUM('F_subnational_current' for all AdminX_i -> AdminY_j).

- 'Scale_factor' = 'D_national_flows(CountryX -> CountryY)' / 'Sum_current_sub_intl_flow'.

- Multiply 'F_subnational_current' for all AdminX_i -> AdminY_j by 'Scale_factor'.

ii. **Rebalance Regional Supply/Demand:**

1. FOR EACH subnational region 'r':

- Calculate 'NetSupply_r' = 'P_subnational_supply_r' + TotalInflows_r('F_subnational_current - TotalOutflows_r('F_subnational_current').

- 'Deficit_r' = 'C_subnational_demand_r' - 'NetSupply_r'.

- IF 'Deficit_r' > 'consumption_deficit_threshold' * 'C_subnational_demand_r':

- Increase incoming flows to 'r' in 'F_subnational_current' (by 'adj_factor_inflow', possibly increasing with 'iter_global').

- Decrease outgoing flows from 'r' in 'F_subnational_current' (by 'adj_factor_outflow', possibly increasing with 'iter_global').

- ELSE IF 'NetSupply_r' > 'C_subnational_demand_r' (Surplus):

- Decrease incoming flows to 'r'.

- Increase outgoing flows from 'r' (if 'P_subnational_supply_r' allows after existing exports).

iii. **Enforce Production-Based Export Cap:**

1. FOR EACH subnational region 'r':

- 'MaxExport_r' = MIN('export_prod_cap_factor' * 'P_subnational_supply_r', 'P_subnational_supply_r' - 'self_consumption_factor' * 'C_subnational_demand_r' (if 'P_subnational_supply_r' > 'self_consumption_factor' * 'C_subnational_demand_r'), else 0).

- IF TotalOutflows_r('F_subnational_current') > 'MaxExport_r':

- Proportionally scale down all outgoing flows from 'r' in 'F_subnational_current'.

iv. IF convergence criteria met (e.g., small changes in flows), BREAK.

c. Perform final realignment of international subnational flows to 'D_national_flows' country totals.

d. 'F_subnational_after_global' = 'F_subnational_current'.

4. **Iterative Harmonization - Phase II: Domestic Adjustment (Within-Country Focus)**

a. 'F_subnational_current' = 'F_subnational_after_global'.

b. FOR 'iter_domestic' FROM 1 TO 'MAX_DOMESTIC_ITERATIONS':

i. FOR EACH Country 'C':

1. Identify 'DeficitRegions_C' and 'SurplusRegions_C' within 'C' based on current balances ('P_subnational_supply' + Inflows - Outflows vs. 'C_subnational_demand').

2. 'TotalDeficit_C' = SUM of deficits in 'DeficitRegions_C'.

3. 'TotalAvailableSurplus_C' = SUM of available surpluses in 'SurplusRegions_C' (production not yet committed to export or local consumption).

4. 'ReallocationBudget_C' = 'realloc_factor' * MIN('TotalDeficit_C', 'TotalAvailableSurplus_C').

5. FOR EACH 'deficit_region_r' in 'DeficitRegions_C':

- 'ShareToReceive' = 'Deficit_r' / 'TotalDeficit_C' * 'ReallocationBudget_C'.

- Allocate 'ShareToReceive' by creating/increasing domestic flows from 'SurplusRegions_C' (proportional to their available surplus) to 'deficit_region_r'. Update 'F_subnational_current'.

6. Ensure no region exports more than its production (relaxed constraints might be used here compared to Phase I export cap for domestic balancing).

ii. IF convergence criteria met (e.g., regional deficits < 'final_deficit_threshold'), BREAK.

c. 'F_subnational_final' = 'F_subnational_current'.

5. **Return 'F_subnational_final'**

END PIPELINE

C

Supplementary Material for "The Environmental Footprint of Retail Foods at Scale: A Multi-Country Analysis"

Contents

C.1 Supplementary Figures

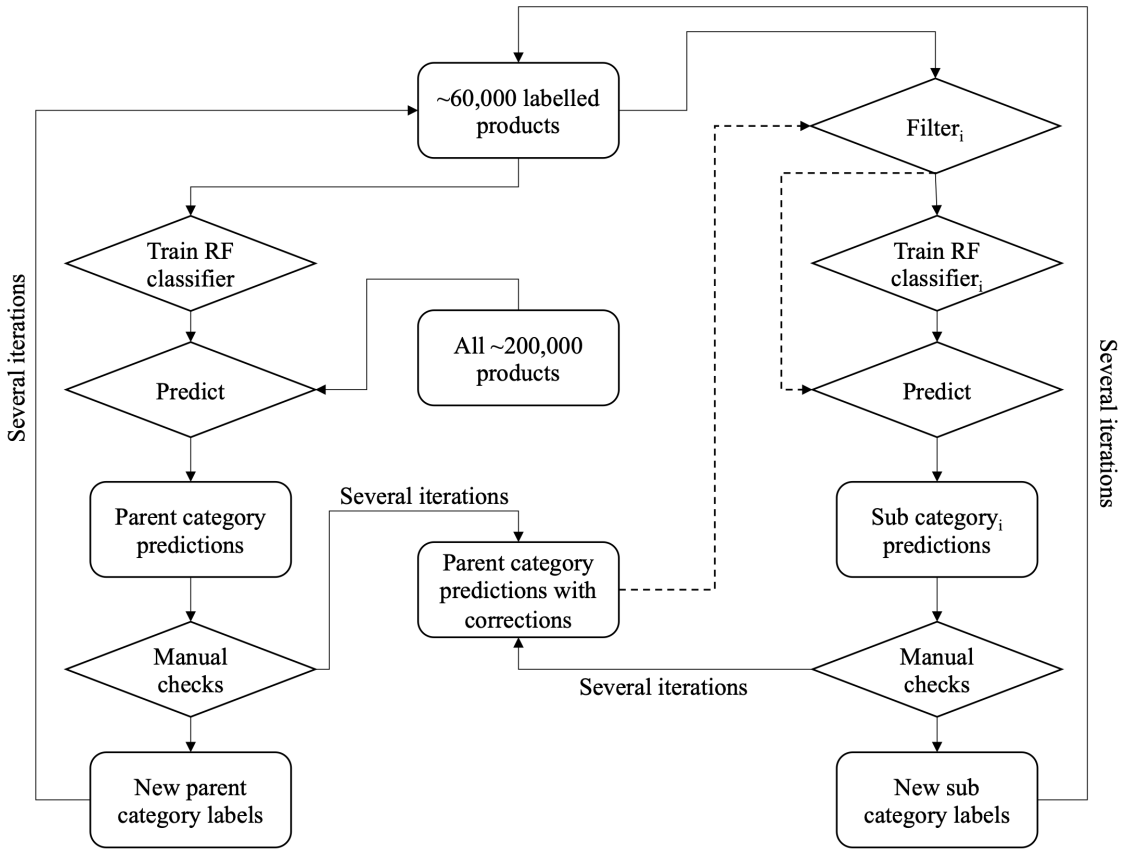

Figure C.1: Overview of Machine Learning Pipeline to Categorize Food Products in foodDB.

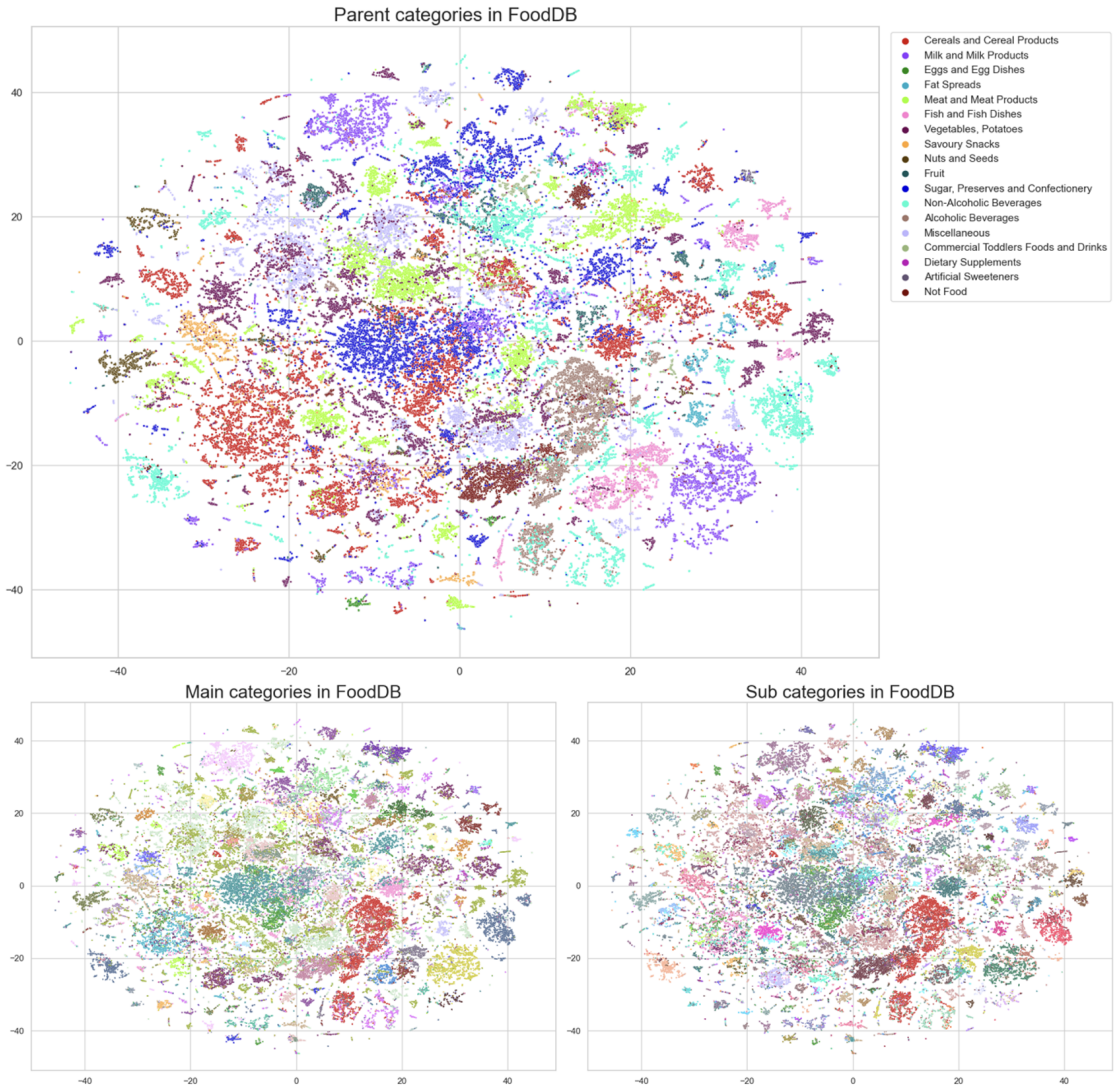

Figure C.2: Three levels of categories predicted for 262,711 products in foodDB. The t-Distributed Stochastic Neighbor Embedding (t-SNE) algorithm was used for dimensionality reduction of the original 768-dimensional feature vectors into a two-dimensional space. Given the large number of categories, only the 18 parent categories are accompanied by a legend, whereas the 53 main and 104 subcategories are presented without corresponding legends to avoid cluttering the visualization.

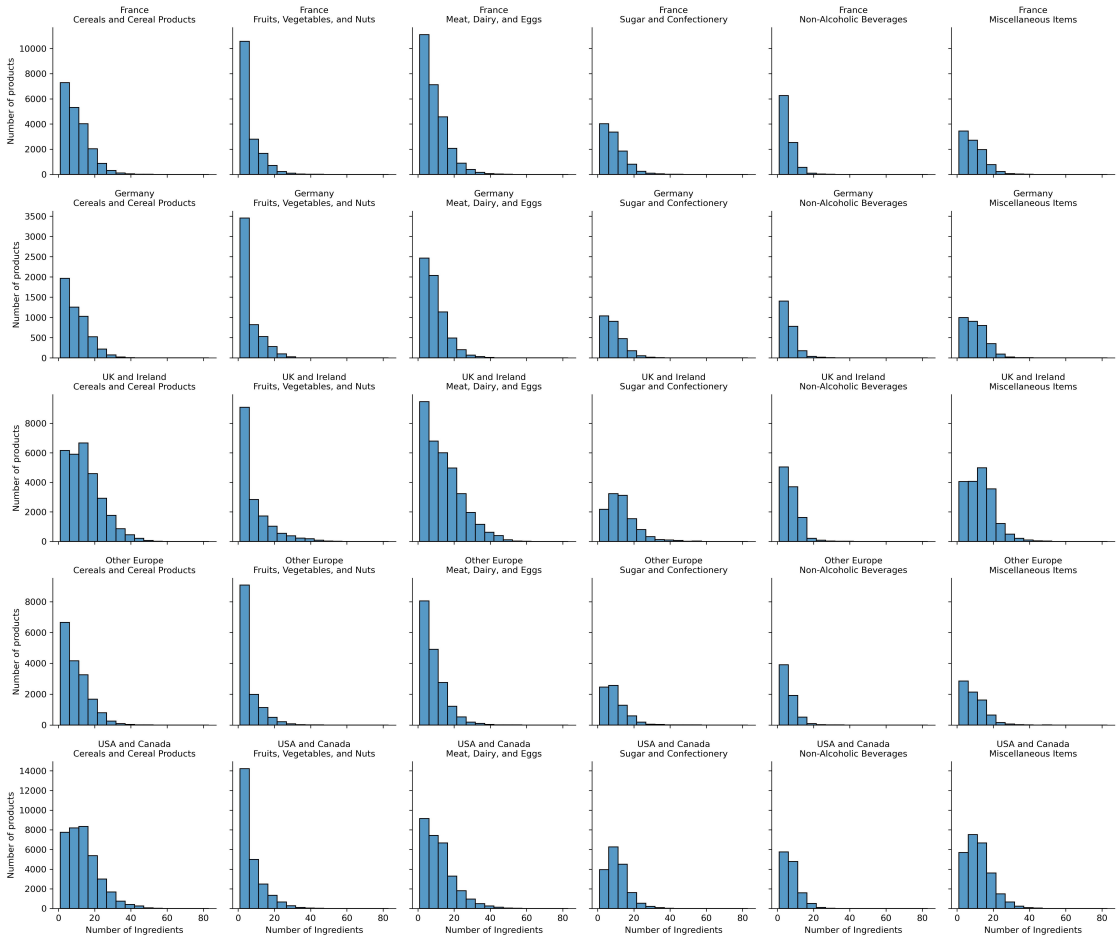

Figure C.3: Distribution of ingredient counts in food products by geography and category.

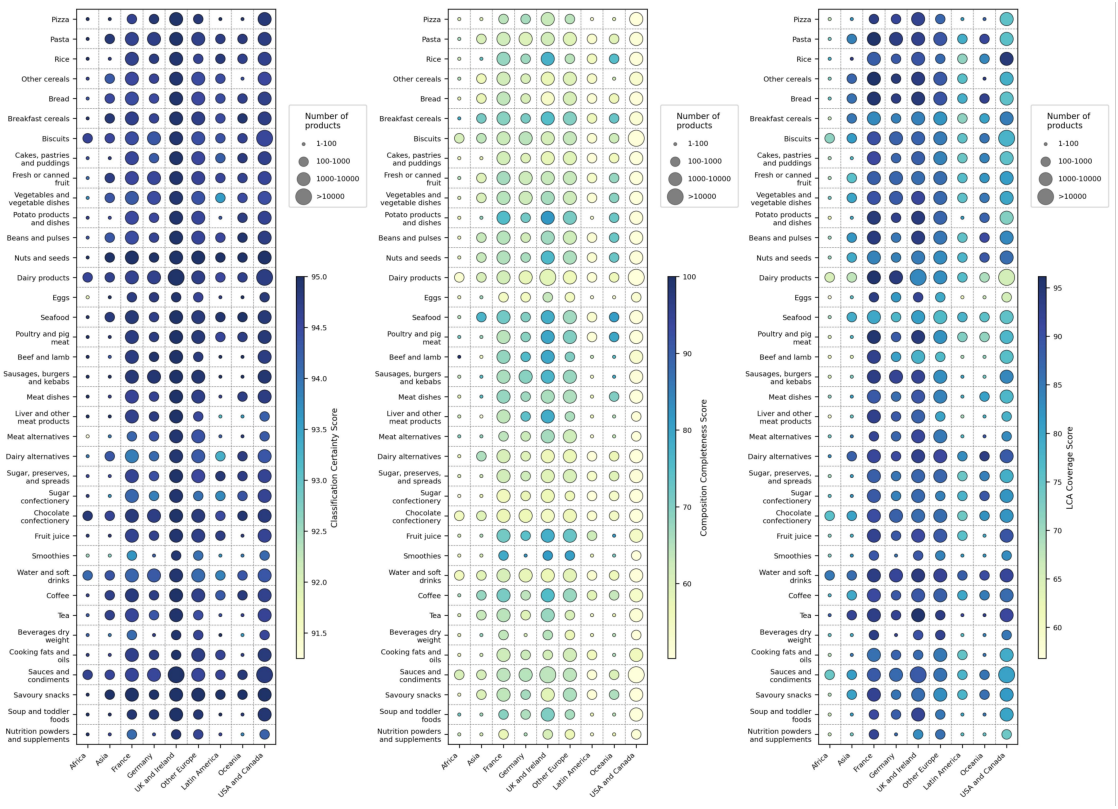

Figure C.4: Component scores used to quantify confidence in environmental impact estimates for products across geographies and categories – classification certainty, composition completeness, and LCA coverage.

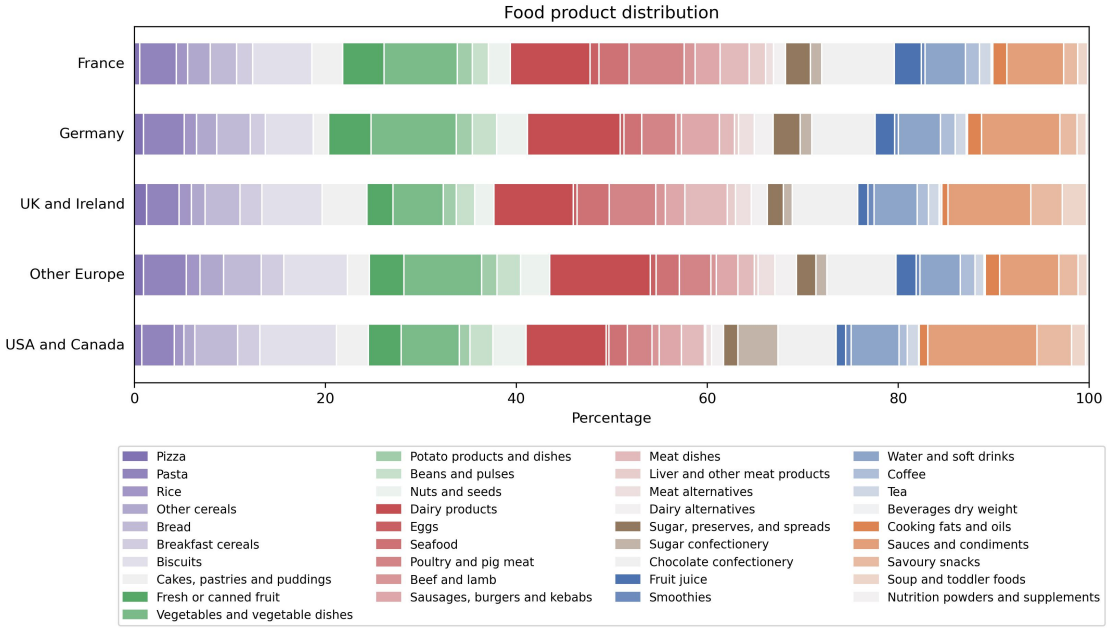

Figure C.5: Distribution of food products from different categories, only showing the five regions with sufficiently large product samples.

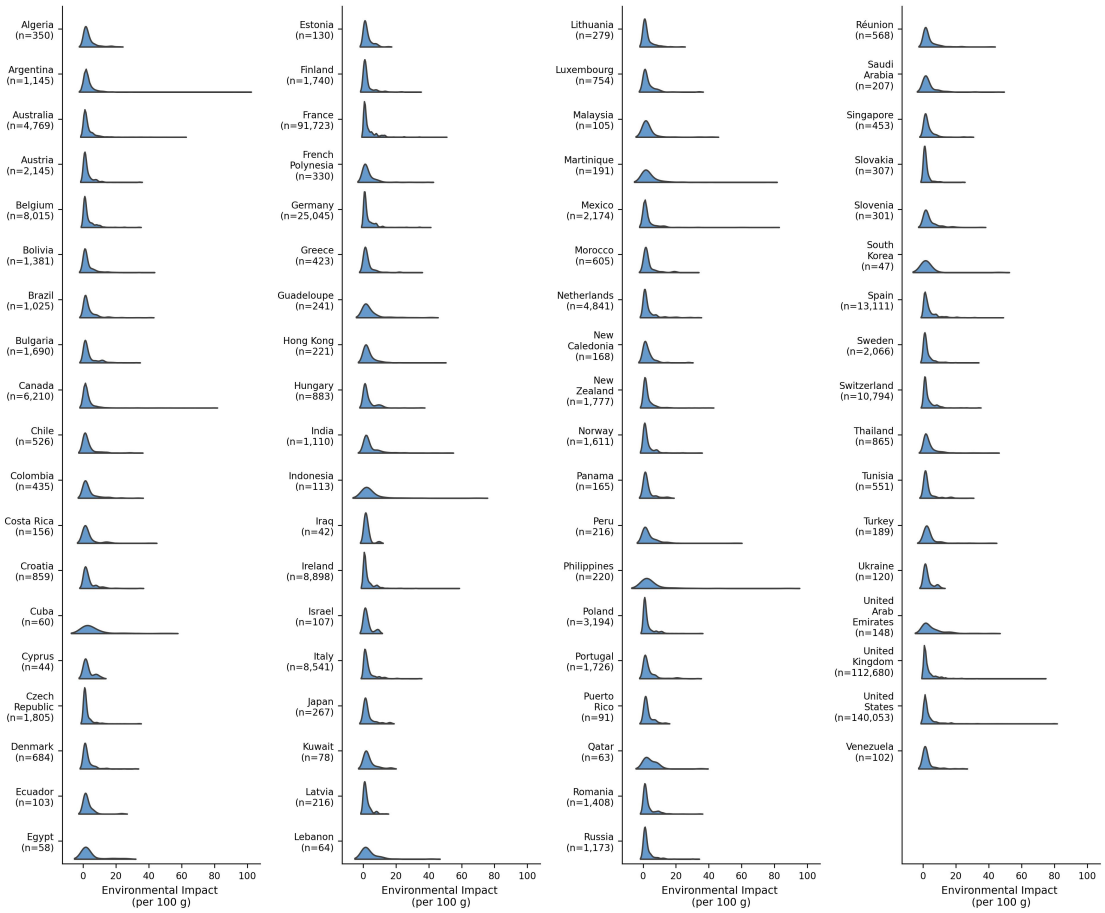

Figure C.6: Environmental impact scores per 100 g of products across countries. Each data point corresponds to the mean environmental impact across all Monte Carlo simulations for a single product.

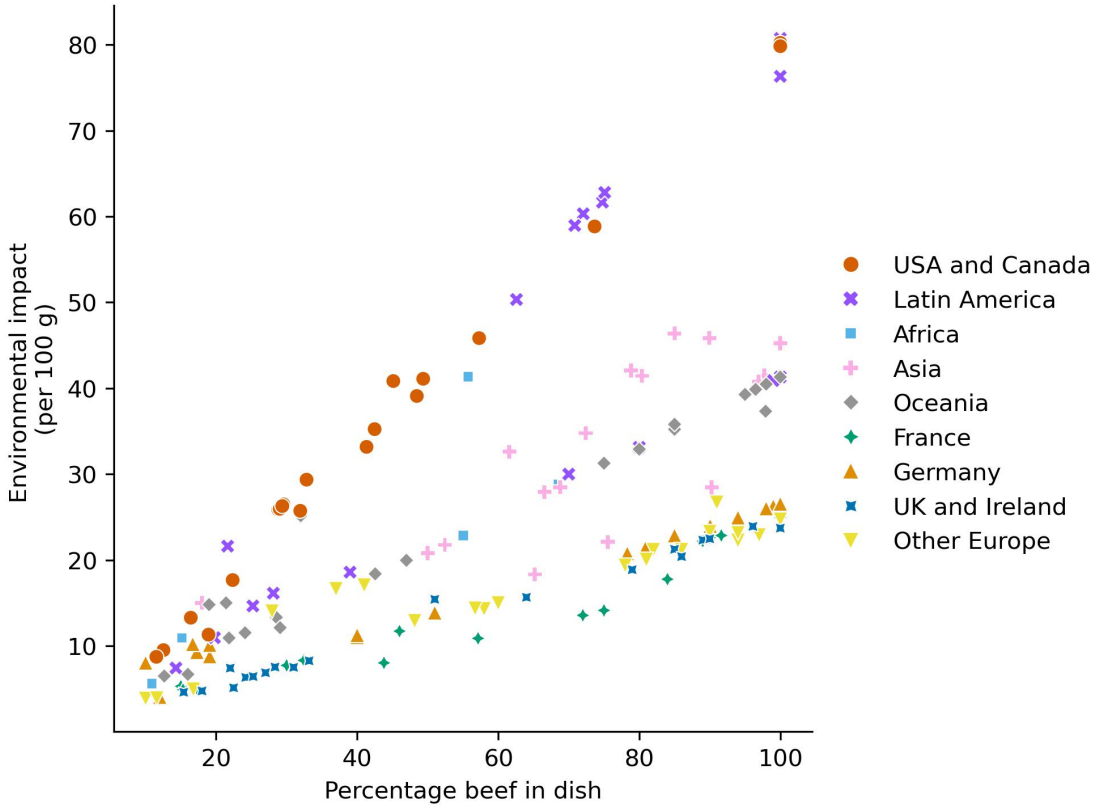

Figure C.7: Environmental impact versus beef content for a sample of beef-containing products across geographies. For each region, up to 20 products were selected at random (all 18 available Asian and 7 African items are shown). Each point represents one product, and its environmental impact corresponds to the mean of its Monte Carlo simulation outputs. The lowest-impact beef products are typically broths or stocks.

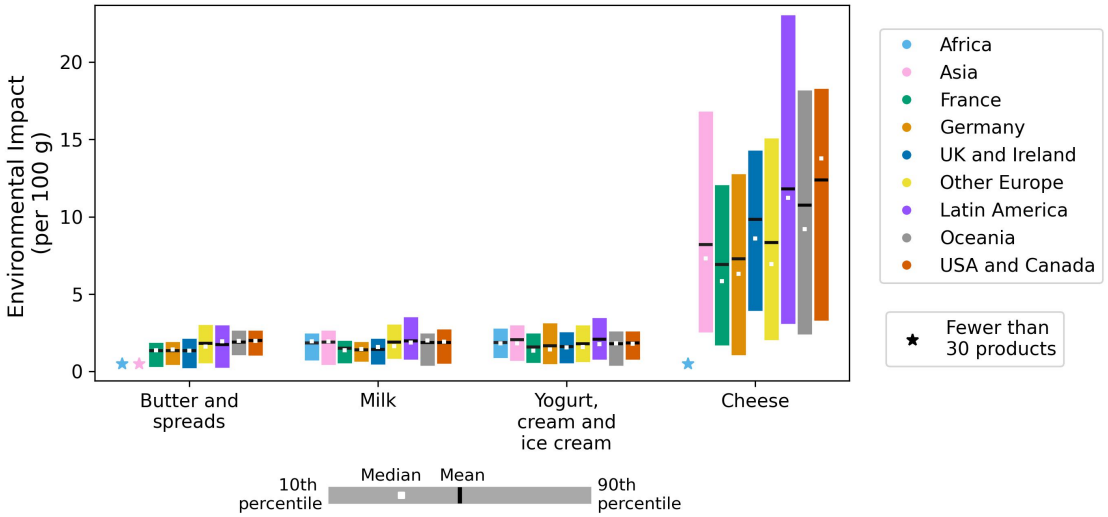

Figure C.8: Environmental impact of different types of dairy products across geographies (per 100 g). For each category, the bars span the 10th to 90th percentile impacts of food products; the mean (black line) and median (white dot) impacts for each category are overlaid. For each product, the impact is given by the mean of its Monte Carlo simulation outputs. Categories with fewer than 30 products are omitted and instead indicated by star markers.

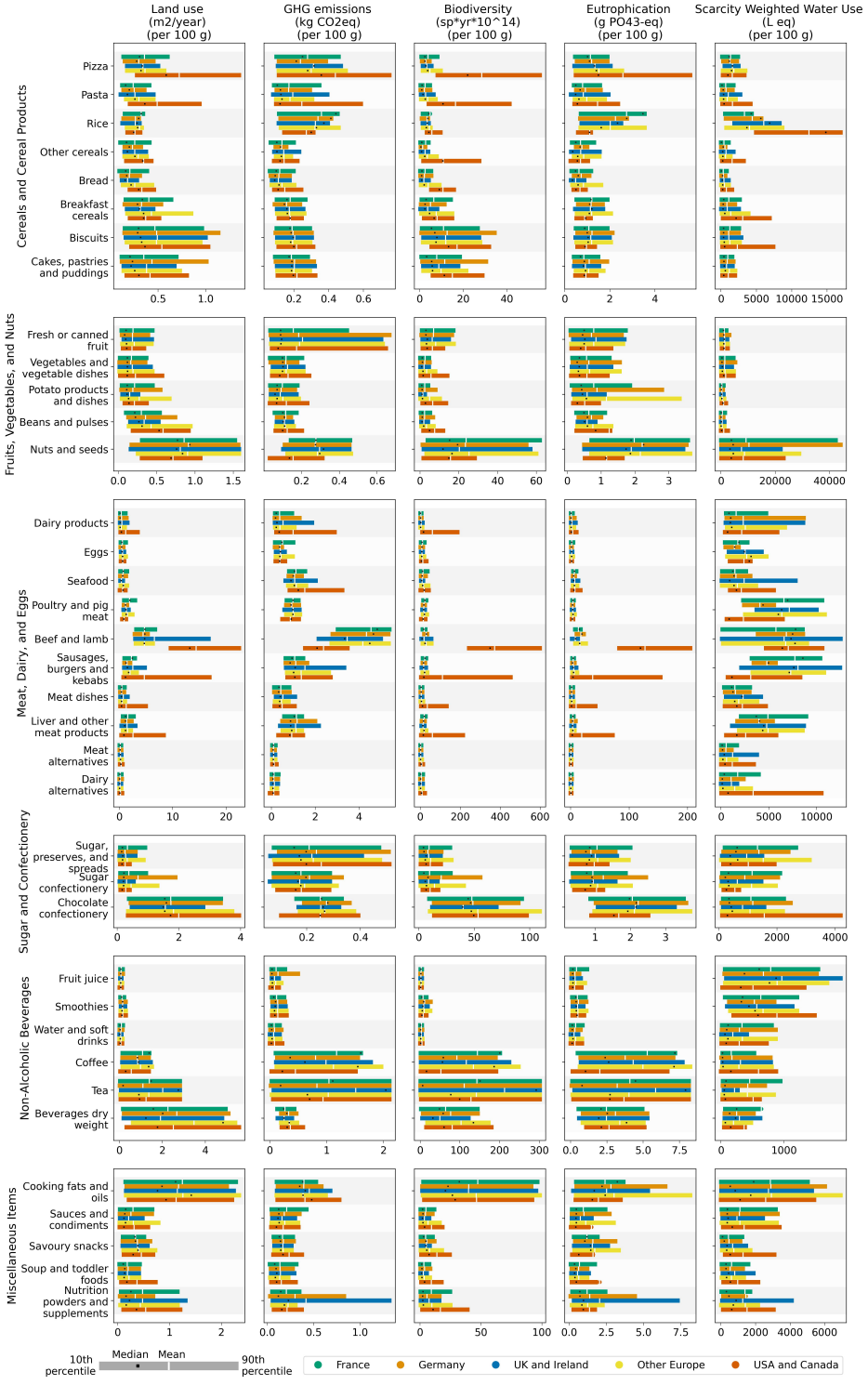

Figure C.9: Disaggregated environmental footprints by five impact metrics (land use, GHG emissions, biodiversity loss, eutrophication, water use) for all food categories across five regions. For each category, the bars span the 10^{th} to 90^{th} percentile impacts of food products; the mean (white line) and median (black dot) impacts for each category are overlaid. For each product, the impact is given by the mean of its Monte Carlo simulation outputs.

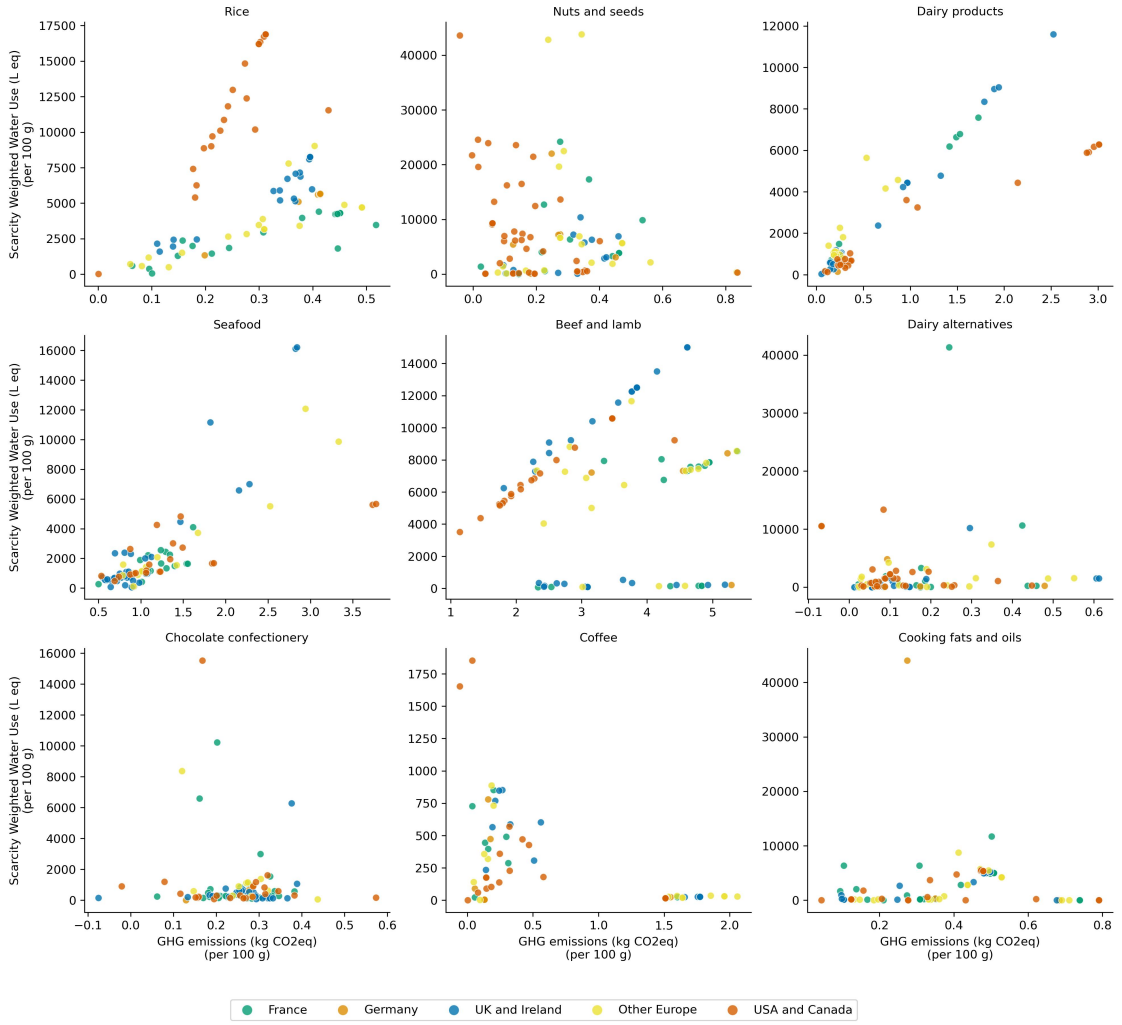

Figure C.10: GHG emissions vs. scarcity-weighted water use for 100 randomly selected products in each of nine categories (rice, nuts and seeds, dairy products, seafood, beef and lamb, dairy alternatives, chocolate confectionery, coffee, cooking fats and oils).

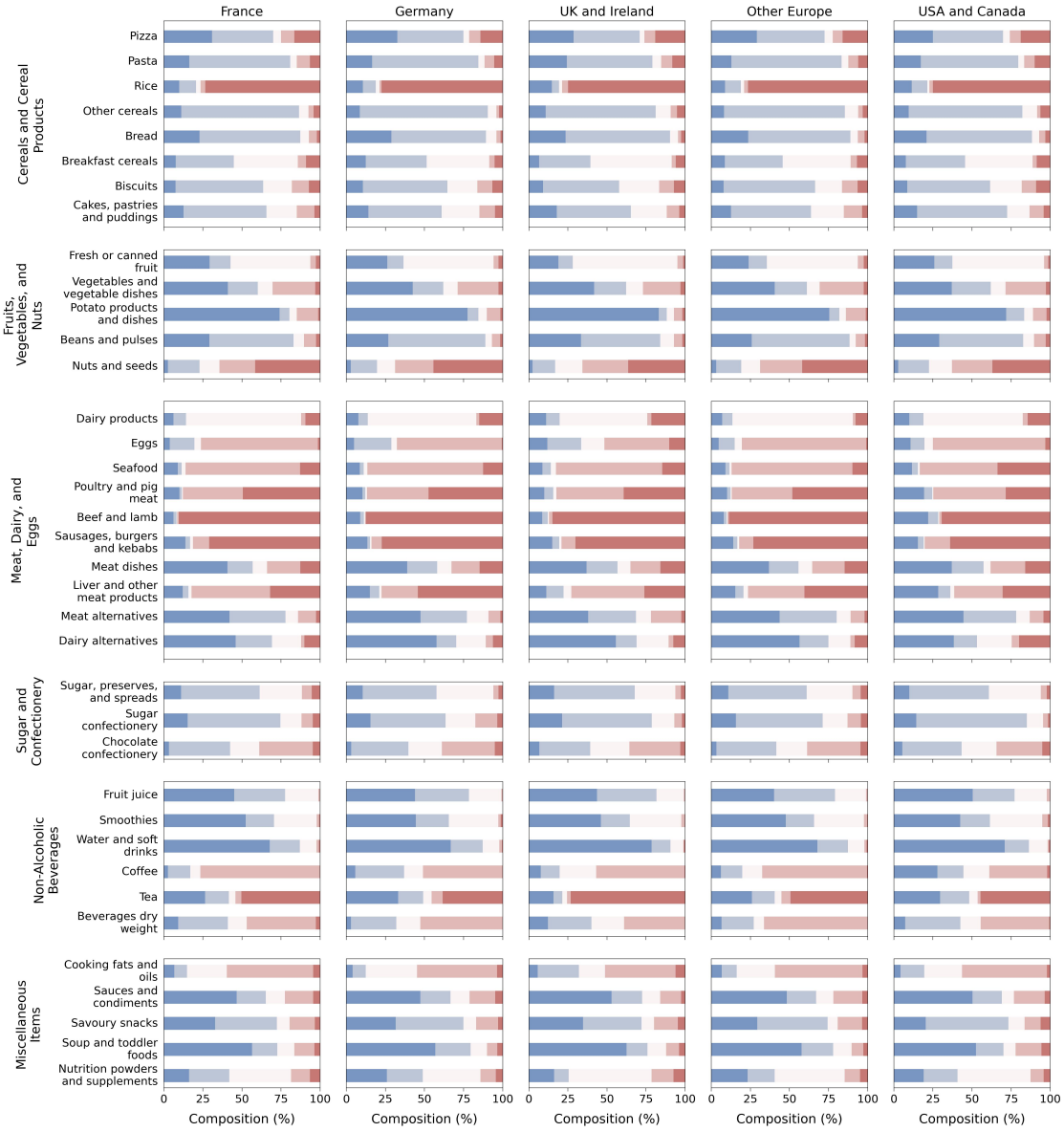

Figure C.11: Food product composition across geographies, categorized by food groups. Each bar represents the proportion of ingredients in different impact groups within a food category, where blue indicates the lowest impact ingredients, and red indicates the highest impact ingredients.

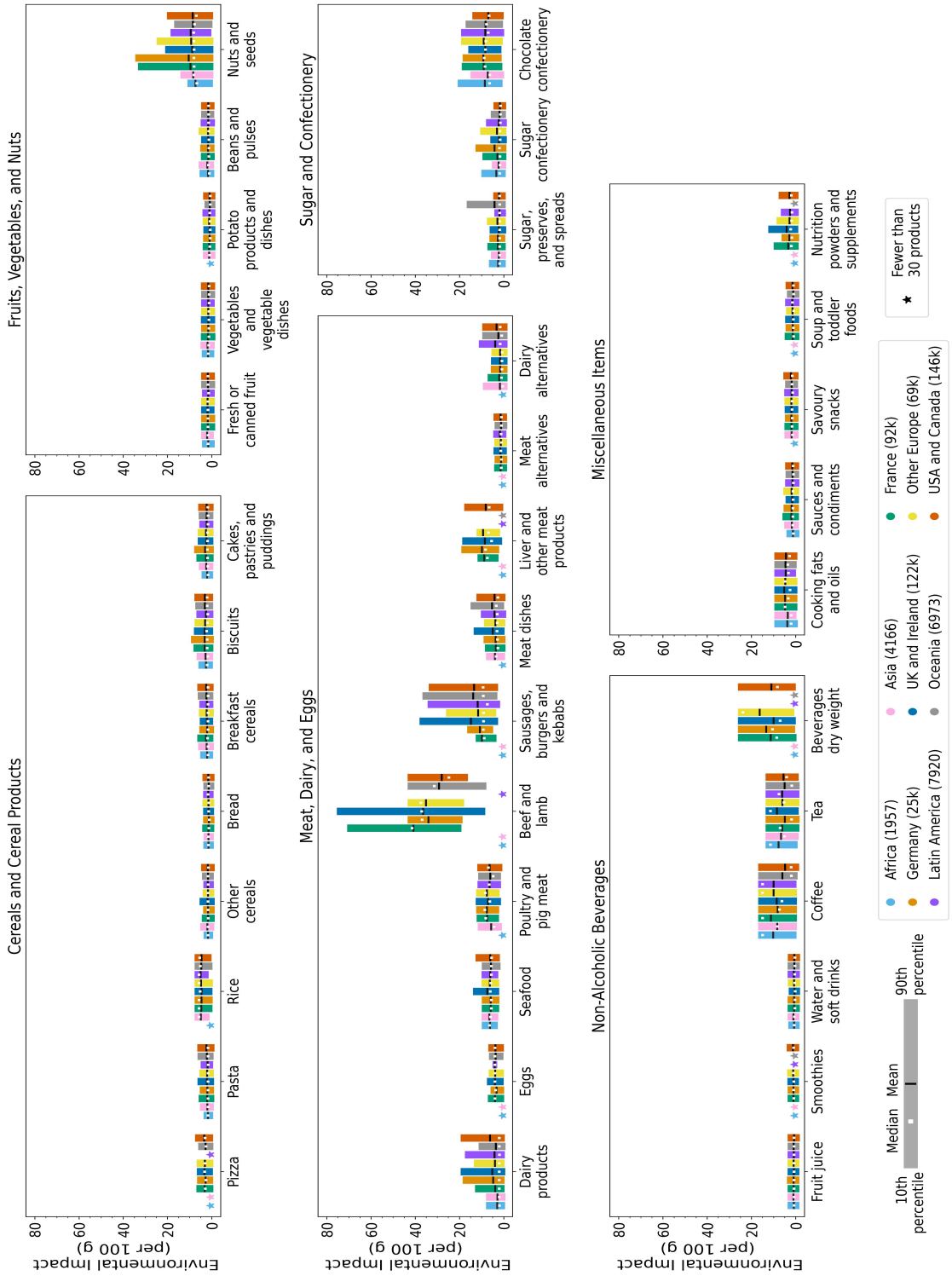

Figure C.12: Environmental impact of food categories across geographies (per 100 g), computed without accounting for ingredient sourcing. For each category, the bars span the 10^{th} to 90^{th} percentile impacts of food products; the mean (black line) and median (white dot) impacts for each category are overlaid. For each product, the impact is given by the mean of its Monte Carlo simulation outputs. Categories with fewer than 30 products are omitted and instead indicated by star markers.

C.2 Supplementary Tables

Table C.1: Categories used to classify products, derived from UK National Diet and Nutrition Survey (NDNS)

Parent category	**Main category**	**Subcategory**
Cereals and Cereal Products	Pasta, rice and other cereals	Pizza
		Pasta
		Rice
		Other cereals
	Bread	White bread (not high fibre, not multiseed bread)
		Wholemeal bread
		Brown, granary and wheatgerm bread
		Other bread
	Breakfast cereals	High fibre breakfast cereals
		Other breakfast cereals (not high fibre)
	Biscuits	Biscuits
	Buns, cakes, pastries and fruit pies	Fruit pies
		Buns cakes and pastries
	Puddings	Cereal based milk puddings
		Sponge puddings
		Other cereal based puddings
Milk and Milk Products	Whole milk	Whole milk
	Semi-skimmed milk	Semi-skimmed milk
	1% Milk	1% Milk
	Skimmed milk	Skimmed milk
	Other milk and cream	Infant formula
		Cream (including imitation cream)
		Other milk
	Cheese	Cottage cheese
		Cheddar cheese
		Other cheese
	Yogurt, fromage frais and other dairy desserts	Yogurt
		Fromage frais and other dairy desserts
	Ice cream	Ice cream
Eggs and Egg Dishes	Eggs and egg dishes	Manufactured egg products including ready meals
		Other eggs and egg dishes including homemade
Fat Spreads	Butter	Butter
	Polyunsaturated margarine and oils	Polyunsaturated margarine
		Polyunsaturated oils
	Low fat spread	Polyunsaturated low fat spread
		Low fat spread not polyunsaturated
	Margarine and other cooking fats and oils not polyunsaturated	Block margarine
		Soft margarine not polyunsaturated
		Other cooking fats and oils not polyunsaturated
	Reduced fat spread	Reduced fat spread (polyunsaturated)
		Reduced fat spread (not polyunsaturated)

Continued on next page

Table C.1: Categories used to classify products, derived from UK National Diet and Nutrition Survey (NDNS) (Continued)

Meat and Meat Products	Bacon and ham	Bacon and ham
	Beef, veal and dishes	Beef and veal
	Lamb and dishes	Lamb
	Pork and dishes	Pork
	Coated chicken and turkey	Manufactured coated chicken/turkey products
	Chicken and turkey dishes	Other chicken and turkey
	Liver, products and dishes	Liver and dishes
	Burgers and kebabs	Burgers and kebabs purchased
	Sausages	Sausages
	Meat pies and pastries	Meat pies and pastries
	Other meat and meat products	Other meat products
Fish and Fish Dishes	White fish coated or fried	White fish coated or fried
	Other white fish, shellfish and fish dishes	Other white fish
		Shellfish
		Canned tuna
	Oily fish	Oily fish
Vegetables, Potatoes	Vegetables	Carrots
		Other vegetables
		Tomatoes
		Peas
		Green beans
		Baked beans
		Leafy green vegetables
		Beans and pulses (including ready meal and homemade dishes)
		Meat alternatives (including ready meals and homemade dishes)
		Other vegetable products and dishes
	Chips, fried and roast potatoes and potato products	Chips purchased including takeaway
		Other fried/roast/baked potatoes
	Other potatoes, potato salads and dishes	Other potato products and dishes
Savoury Snacks	Crisps and savoury snacks	Crisps and savoury snacks
Nuts and Seeds	Nuts and seeds	Nuts and seeds
Fruit	Fruit	Apples and pears not canned
		Citrus fruit
		Bananas
		Canned fruit in juice
		Canned fruit in syrup
		Other fruit not canned
Sugar, Preserves and Confectionery	Sugars, preserves and sweet spread	Sugar
		Preserves
		Sweet spreads fillings and icing
	Sugar confectionery	Sugar confectionery
	Chocolate confectionery	Chocolate confectionery

Continued on next page

Table C.1: Categories used to classify products, derived from UK National Diet and Nutrition Survey (NDNS) (Continued)

Non-Alcoholic Beverages	Fruit juice	Fruit juice
		Smoothies
	Soft drinks, not diet	Soft drinks not low calorie concentrated
		Soft drinks not low calorie carbonated
		Soft drinks not low calorie, ready to drink, still
	Soft drinks, diet	Soft drinks low calorie concentrated
		Soft drinks low calorie carbonated
		Soft drinks low calorie, ready to drink, still
	Tea, coffee and water	Coffee
		Tea
		Herbal tea
		Bottled water still or carbonated
Alcoholic Beverages	Alcoholic beverages	Alcoholic beverages
Miscellaneous	Miscellaneous	Beverages dry weight
		Soup
		Nutrition powders and drinks
		Savoury sauces pickles gravies and condiments
Commercial Toddlers Foods and Drinks	Commercial toddlers foods and drinks	Commercial toddlers foods and drinks
Dietary Supplements	Dietary supplements	Dietary supplements
Artificial Sweeteners	Artificial sweeteners	Artificial sweeteners
Not Food	Not food	Not food

Table C.2: Performance of Random Forest classification models on labelled foodDB data

Categorization	**Hyperparameters**	**n**	**Classes**	**Accuracy**		**Balanced accuracy**		**F1-score (weighted)**	
				train	**test**	**train**	**test**	**train**	**test**
Parent categories	num trees: 200, min leaf samples:5, weights: balanced	68,407	18	0.99	0.91	0.99	0.89	0.99	0.91
Cereals and Cereal Products	num trees: 400, min leaf samples:4, max tree depth: 20, weights: balanced	13,999	16	0.99	0.93	0.99	0.91	0.99	0.93
Milk and Milk Products	num trees: 400, min leaf samples:10, max tree depth: 10, weights: balanced	6,348	13	0.98	0.94	0.99	0.92	0.98	0.94
Eggs and Egg Dishes	num trees: 400, min leaf samples:10, max tree depth: 20, weights: balanced	515	2	0.99	0.98	0.99	0.98	0.99	0.98
Fat Spreads	num trees: 400, min leaf samples:10, max tree depth: 20, weights: balanced	1,460	10	0.96	0.89	0.96	0.89	0.96	0.90
Meat and Meat Products	num trees: 500, min leaf samples:10, max tree depth: 20, weights: balanced	8,679	11	0.97	0.92	0.98	0.92	0.97	0.92
Fish and Fish Dishes	num trees: 500, min leaf samples:10, max tree depth: 20, weights: balanced	2,808	5	0.98	0.96	0.98	0.95	0.98	0.96
Vegetables, Potatoes	num trees: 500, min leaf samples:10, max tree depth: 20, weights: balanced	6,282	13	0.97	0.89	0.98	0.90	0.97	0.89
Fruit	num trees: 500, min leaf samples:10, max tree depth: 20, weights: balanced	1,572	6	0.99	0.94	0.99	0.90	0.99	0.94
Sugar, Preserves and Confectionery	num trees: 500, min leaf samples:10, max tree depth: 20, weights: balanced	6,141	5	0.99	0.96	0.99	0.94	0.99	0.96
Non-Alcoholic Beverages	num trees: 400, min leaf samples:10, max tree depth: 25, weights: balanced	8,042	12	0.98	0.89	0.98	0.89	0.98	0.89
Miscellaneous	num trees: 500, min leaf samples:10, max tree depth: 20, weights: balanced	5,718	4	0.99	0.98	0.99	0.98	0.99	0.98

Table C.3: Performance of Deep Learning classification models on all foodDB data

Categorization	Hyperparameters	n	Classes	Accuracy		Balanced accuracy		F1-score (weighted)	
				train	test	train	test	train	test
Parent categories	dense layers: 3, dense neurons: 512, batch size: 128, epochs: 100, dropout: 0.2	262,711	18	0.98	0.94	0.99	0.95	0.98	0.94
Cereals and Cereal Products	dense layers: 2, dense neurons: 256, batch size: 64, epochs: 100, dropout: 0.2	52,426	16	0.98	0.93	0.99	0.96	0.98	0.93
Milk and Milk Products	dense layers: 2, dense neurons: 256, batch size: 64, epochs: 100, dropout: 0.4	23,239	13	0.99	0.96	0.99	0.94	0.99	0.96
Egg and Egg Dishes	dense layers: 1, dense neurons: 32, batch size: 16, epochs: 50, dropout: 0.4	1,315	2	0.99	0.99	0.99	0.99	0.99	0.99
Fat Spreads	dense layers: 1, dense neurons: 32, batch size: 16, epochs: 50, dropout: 0.4	3,811	10	0.99	0.92	0.99	0.88	0.99	0.93
Meat and Meat Products	dense layers: 2, dense neurons: 256, batch size: 64, epochs: 100, dropout: 0.2	26,837	11	0.99	0.95	0.99	0.95	0.99	0.95
Fish and Fish Dishes	dense layers: 1, dense neurons: 64, batch size: 32, epochs: 50, dropout: 0.4	9,302	5	0.98	0.95	0.99	0.95	0.98	0.95
Vegetables, Potatoes	dense layers: 1, dense neurons: 64, batch size: 32, epochs: 50, dropout: 0.4	23,757	13	0.97	0.91	0.98	0.94	0.97	0.91
Fruit	dense layers: 1, dense neurons: 64, batch size: 32, epochs: 50, dropout: 0.4	7,343	6	0.98	0.97	0.99	0.98	0.98	0.97
Sugar, Preserves and Confectionery	dense layers: 2, dense neurons: 256, batch size: 64, epochs: 100, dropout: 0.2	25,822	5	0.99	0.98	0.99	0.97	0.99	0.98
Non-Alcoholic Beverages	dense layers: 1, dense neurons: 128, batch size: 32, epochs: 50, dropout: 0.4	25,994	12	0.97	0.91	0.98	0.91	0.97	0.91

Table C.3 continued from previous page

Categorization	Hyperparameters	n	Classes	Accuracy		Balanced accuracy		F1-score (weighted)	
				train	test	train	test	train	test
Miscellaneous	dense layers: 2, dense neurons: 256, batch size: 64, epochs: 100, dropout: 0.2	27,598	4	0.99	0.99	0.99	0.99	0.99	0.99

Table C.4: Distribution of food products in different categories, as predicted by machine learning models

Parent category	**Main category**	**Subcategory**	**foodDB**	**Open Food Facts**
Cereals and Cereal Products	Pasta, rice and other cereals	Pizza	2,324	8,609
		Pasta	7,507	31,603
		Rice	2,981	8,486
		Other cereals	3,154	14,742
	Bread	White bread (not high fibre, not multiseed bread)	4,575	23,350
		Wholemeal bread	605	1,368
		Brown, granary and wheatgerm bread	655	962
		Other bread	1,220	5,561
	Breakfast cereals	High fibre breakfast cereals	3,840	14,727
		Other breakfast cereals (not high fibre)	1,206	4,923
	Biscuits	Biscuits	13,742	63,625
	Buns, cakes, pastries and fruit pies	Fruit pies	283	839
		Buns cakes and pastries	8,126	29,991
	Puddings	Cereal based milk puddings	392	765
		Sponge puddings	429	149
		Other cereal based puddings	1,387	3,187
Milk and Milk Products	Whole milk	Whole milk	375	2,239
	Semi-skimmed milk	Semi-skimmed milk	436	1,610
	1% Milk	1% Milk	41	503
	Skimmed milk	Skimmed milk	218	557
	Other milk and cream	Infant formula	105	196
		Cream (including imitation cream)	704	4,701
		Other milk	3,368	16,341
	Cheese	Cottage cheese	120	1,258
		Cheddar cheese	1,845	3,514
		Other cheese	4,544	36,675
	Yogurt, fromage frais and other dairy desserts	Yogurt	6,166	22,402
		Fromage frais and other dairy desserts	1,381	6,055
	Ice cream	Ice cream	3,936	15,917
Eggs and Egg Dishes	Eggs and egg dishes	Manufactured egg products including ready meals	681	1,155
		Other eggs and egg dishes including homemade	634	2,917
Fat Spreads	Butter	Butter	474	2,976
	Polyunsaturated margarine and oils	Polyunsaturated margarine	78	224
		Polyunsaturated oils	424	2,677
	Low fat spread	Polyunsaturated low fat spread	133	432
		Low fat spread not polyunsaturated	19	53
	Margarine and other cooking fats and oils not polyunsaturated	Block margarine	100	416
		Soft margarine not polyunsaturated	31	48
		Other cooking fats and oils not polyunsaturated	1,972	7,532

Table C.4: Distribution of food products in different categories, as predicted by machine learning models (Continued)

	Reduced fat spread	Reduced fat spread (polyunsaturated)	225	804
		Reduced fat spread (not polyunsaturated)	355	331
Meat and Meat Products	Bacon and ham	Bacon and ham	3,042	13,396
	Beef, veal and dishes	Beef and veal	3,769	10,716
	Lamb and dishes	Lamb	996	567
	Pork and dishes	Pork	1,527	5,444
	Coated chicken and turkey	Manufactured coated chicken/turkey products	1,724	2,977
	Chicken and turkey dishes	Other chicken and turkey	7,359	20,896
	Liver, products and dishes	Liver and dishes	282	1,730
	Burgers and kebabs	Burgers and kebabs purchased	800	2,202
	Sausages	Sausages	3,275	19,653
	Meat pies and pastries	Meat pies and pastries	2,034	1,484
	Other meat and meat products	Other meat products	2,029	5,524
Fish and Fish Dishes	White fish coated or fried	White fish coated or fried	1,700	2,159
	Other white fish, shellfish and fish dishes	Other white fish	1,202	3,046
		Shellfish	1,605	6,710
		Canned tuna	882	2,801
	Oily fish	Oily fish	3,913	15,261
Vegetables, Potatoes	Vegetables	Carrots	416	2,220
		Other vegetables	4,720	18,444
		Tomatoes	1,664	6,590
		Peas	727	2,408
		Green beans	237	985
		Baked beans	700	1,011
		Leafy green vegetables	2,155	5,831
		Beans and pulses (including ready meal and homemade dishes)	3,176	16,520
		Meat alternatives (including ready meals and homemade dishes)	2,987	10,379
		Other vegetable products and dishes	4,075	22,233
	Chips, fried and roast potatoes and potato products	Chips purchased including takeaway	884	3,589
		Other fried/roast/baked potatoes	533	2,569
	Other potatoes, potato salads and dishes	Other potato products and dishes	1,483	5,796
Savoury Snacks	Crisps and savoury snacks	Crisps and savoury snacks	6,460	22,492
Nuts and Seeds	Nuts and seeds	Nuts and seeds	5,057	25,226
Fruit	Fruit	Apples and pears not canned	747	4,684
		Citrus fruit not canned	292	818
		Bananas	118	631
		Canned fruit in juice	782	3,190
		Canned fruit in syrup	227	1,855
		Other fruit not canned	5,177	17,476
Sugar, Preserves and Confectionery	Sugars, preserves and sweet spread	Sugar	1,266	4,717
		Preserves	3,828	16,040
		Sweet spreads fillings and icing	1,248	4,038
	Sugar confectionery	Sugar confectionery	5,713	33,691
	Chocolate confectionery	Chocolate confectionery	13,767	60,817

Continued on next page

Table C.4: Distribution of food products in different categories, as predicted by machine learning models (Continued)

Non-Alcoholic Beverages	Fruit juice	Fruit juice	2,623	14,169
		Smoothies	1,219	3,158
	Soft drinks, not diet	Soft drinks not low calorie concentrated	974	3,145
		Soft drinks not low calorie carbonated	5,420	17,027
		Soft drinks not low calorie, ready to drink, still	1,058	5,011
	Soft drinks, diet	Soft drinks low calorie concentrated	611	186
		Soft drinks low calorie carbonated	3,120	5,491
		Soft drinks low calorie, ready to drink, still	2,469	13,563
	Tea, coffee and water	Coffee	3,646	9,037
		Tea	2,296	7,401
		Herbal tea	1,615	5,279
		Bottled water still or carbonated	943	4,282
Alcoholic Beverages	Alcoholic beverages	Alcoholic beverages	15,150	22,295
Miscellaneous	Miscellaneous	Beverages dry weight	682	1,298
		Soup	3,590	7,861
		Nutrition powders and drinks	527	2,286
		Savoury sauces pickles gravies and condiments	22,799	75,679
Commercial Toddlers Foods and Drinks	Commercial toddlers foods and drinks	Commercial toddlers foods and drinks	2,488	1,444
Dietary Supplements	Dietary supplements	Dietary supplements	622	3,360
Artificial Sweeteners	Artificial sweeteners	Artificial sweeteners	404	1,108
Not Food	Not food	Not food	5,086	5,673
Total			**262,711**	**961,989**

Table C.5: Country groupings for product composition estimation.

Country group	Countries
1	Australia, Canada, Ireland, New Zealand, United Kingdom, United States
2	Austria, Belgium, France, Germany, Luxembourg, Netherlands, Switzerland
3	Italy, Portugal, Spain
4	Denmark, Estonia, Finland, Latvia, Lithuania, Norway, Sweden
5	Bulgaria, Croatia, Czech Republic, Hungary, New Caledonia, Poland, Romania, Russia, Slovakia, Slovenia, Ukraine
6	Algeria, Cyprus, Egypt, Greece, Israel, Lebanon, Morocco, Tunisia, Turkey
7	Argentina, Bolivia, Brazil, Chile, Costa Rica, Colombia, Cuba, Ecuador, French Polynesia, Guadeloupe, India, Iraq, Kuwait, Martinique, Mexico, Panama, Peru, Puerto Rico, Qatar, Reunion, Saudi Arabia, United Arab Emirates, Venezuela
8	Hong Kong, Indonesia, Japan, Malaysia, Philippines, Singapore, South Korea, Thailand

Table C.6: FAO commodities used to compute production and trade for all LCA food categories

LCA Food Category	**FAO Commodities Produced**	**FAO Commodities Traded**	**Notes**
Wheat Rye (Bread)	Wheat	Wheat Germ of wheat Wheat and meslin flour	Oil converted to oil crops using processing factors. Production and trade split between oil crops and oil.
	Rye	Rye Flour of rye Bran of rye	
	Millet	Millet Flour of millet Bran of millet	
	Sorghum	Sorghum Flour of sorghum Bran of sorghum	
	Buckwheat	Buckwheat Flour of buckwheat	
	Quinoa	Quinoa	
	Canary seed	Canary seed	
	Fonio	Fonio	
	Mixed grain	Mixed grain Flour of mixed grain Bran of mixed grain	
	Triticale	Triticale	
	Cereals n.e.c.	Cereals n.e.c. Flour of cereals, n.e.c. Bran of cereals, n.e.c.	
	Groundnuts, excluding shelled	Groundnuts, excluding shelled Groundnuts, shelled Prepared groundnuts Groundnut oil	
	Linseed	Linseed Oil of linseed	
	Hempseed	Hempseed	
	Safflower seed	Safflower seed Safflower-seed oil, crude	
	Sesame seed	Sesame seed Oil of sesame seed	
	Castor oil seeds	Castor oil seed Oil of castor beans	
	Cotton seed	Cottonseed oil	
	Coconuts, in shell	Coconuts, in shell Coconuts, desiccated Coconut oil	
	Mustard seed	Mustard seed Mustard seed oil, crude	
Maize (Meal)	Maize (corn)	Maize (corn) Germ of maize Flour of maize Bran of maize Cake of maize Forage and silage, maize	
Barley (Beer)	Barley	Barley Barley flour and grits Barley, pearled Bran of barley Pot barley	
Oatmeal	Oats	Oats Oats, rolled Bran of oats	
Rice	Rice	Rice, paddy (rice milled equivalent) Flour of rice	

Continued on next page

Table C.6: FAO commodities used to compute production and trade for all LCA food categories (Continued)

Potatoes	Potatoes	Potatoes Potatoes, frozen Tapioca of potatoes	Processing factors applied to convert traded commodities into equivalent quantities of crops. Tapioca of potatoes: 5
	Sweet potatoes	Sweet potatoes	
	Yams	Yams	
	Taro	Taro	
	Edible roots ad tubers with high starch or inulin content n.e.c., fresh	Edible roots ad tubers with high starch or inulin content n.e.c., fresh	
Cassava	Cassava, fresh	Cassava, dry Cassava, fresh Flour of cassava Starch of cassava Tapioca of cassava	Processing factors applied to convert traded commodities into equivalent quantities of crops. Cassava dry: 2.5 Flour of cassava: 4 Starch of cassava: 5 Tapioca of cassava: 5
Cane Sugar	Sugar cane	Sugar cane Refined sugar Raw cane or beet sugar (centrifugal only)	Sugar converted to sugar crops using processing factors Refined sugar and raw sugar flows split between sugar cane and sugar beet
Beet Sugar	Sugar beet	Sugar beet Refined sugar Raw cane or beet sugar (centrifugal only)	
Other Pulses	Bambara beans, dry	Bambara beans, dry	
	Beans, dry	Beans, dry	
	Broad beans and horse beans, dry	Broad beans and horse beans, dry	
	Lentils, dry	Lentils, dry	
	Other pulses, n.e.c.	Other pulses, n.e.c. Flour of pulses	
	Chick peas, dry	Chick peas, dry	
	Cow peas, dry	Cow peas, dry	
	Pigeon peas, dry	Pigeon peas, dry	
	Peas, dry	Peas, dry	
	Lupins		
Peas	Peas, green	Peas, green	
Nuts	Almonds, in shell	Almonds, in shell Almonds, shelled	Oil converted to oil crops using processing factors. Production and trade split between oil crops and oil.
	Cashew nuts, in shell	Cashew nuts, in shell Cashew nuts, shelled	
	Hazelnuts, in shell	Hazelnuts, in shell Hazelnuts, shelled	
	Chestnuts, in shell	Chestnuts, in shell	
	Walnuts, in shell	Walnuts, in shell Walnuts, shelled	
	Sunflower seed	Sunflower seed Sunflower-seed oil, crude	
	Brazil nuts, in shell	Brazil nuts, in shell Brazil nuts, shelled	
	Pistachios, in shell	Pistachios, in shell	
	Other nuts (excluding wild edible nuts and groundnuts), in shell, n.e.c.	Other nuts (excluding wild edible nuts and groundnuts), in shell, n.e.c.	
	Linseed	Linseed Oil of linseed	
	Hempseed	Hempseed	
	Safflower seed	Safflower seed Safflower-seed oil, crude	

Continued on next page

Table C.6: FAO commodities used to compute production and trade for all LCA food categories (Continued)

	Poppy seed	Poppy seed	
	Sesame seed	Sesame seed Oil of sesame seed	
Groundnuts	Groundnuts, excluding shelled	Groundnuts, excluding shelled Groundnuts, shelled Prepared groundnuts Groundnut oil	Oil converted to oil crops using processing factors. Production and trade split between oil crops and oil.
Soymilk	Soya beans	Cake of soya beans Soya beans Soya curd Soya paste Soya sauce Soya bean oil	Production and trade split between oil crops and oil.
Tofu	Soya beans	Cake of soya beans Soya beans Soya curd Soya paste Soya sauce Soya bean oil	Production and trade split between oil crops and oil.
Soybean oil	Soya beans	Cake of soya beans Soya beans Soya curd Soya paste Soya sauce Soya bean oil	Production and trade split between oil crops and oil.
Palm oil	Oil palm fruit	Palm oil	Oil converted to oil crops using processing factors
Sunflower oil	Sunflower seed	Sunflower seed Sunflower-seed oil, crude	Oil converted to oil crops using processing factors Production and trade split between oil crops and oil.
Rapeseed Oil	Rape or colza seed	Rape or colza seed Rapeseed or canola oil, crude	Oil converted to oil crops using processing factors
Olive oil	Olives	Olives Olives preserved Olive oil	Oil converted to oil crops using processing factors Production and trade split between oil crops and oil.
Tomatoes	Tomatoes	Paste of tomatoes Tomato juice Tomatoes Tomatoes, peeled (o/t vinegar)	
Onions Leeks	Onions and shallots, green	Onions and shallots, green	
	Onions and shallots, dry (excluding dehydrated)	Onions and shallots, dry (excluding dehydrated)	
	Leeks and other alliaceous vegetables	Leeks and other alliaceous vegetables	
Root Vegetables	Carrots and turnips	Carrots and turnips	
Brassicas	Cabbages	Cabbages	
	Cauliflowers and broccoli	Cauliflowers and broccoli	
	Cucumbers and gherkins	Cucumbers and gherkins	
	Pumpkins, squash and gourds	Pumpkins, squash and gourds	
	Artichokes	Artichokes	
	Lettuce and chicory	Lettuce and chicory	
	Broad beans and horse beans, green	Broad beans and horse beans, green	

Continued on next page

Table C.6: FAO commodities used to compute production and trade for all LCA food categories (Continued)

Other Vegetables	Other beans, green	Other beans, green	
	String beans	String beans	
	Asparagus	Asparagus	
	Chillies and peppers, green (Capsicum spp. and Pimenta spp.)	Chillies and peppers, green (Capsicum spp. and Pimenta spp.)	
	Eggplants (aubergines)	Eggplants (aubergines)	
	Green corn (maize)	Green corn (maize)	
	Green garlic	Green garlic	
	Mushrooms and truffles	Canned mushrooms Dried mushrooms Mushrooms and truffles	
	Okra	Okra	
	Other vegetables, fresh n.e.c.	Other vegetables, fresh n.e.c. Other vegetables provisionally preserved Other vegetable juices Sweet corn, frozen Sweet corn, prepared or preserved Vegetables frozen Vegetables preserved (frozen) Vegetables preserved nes (o/t vinegar) Vegetables, dehydrated Vegetable products, fresh or dry n.e.c. Vegetables, pulses and potatoes, preserved by vinegar or acetic acid	
	Spinach	Spinach	
Citrus Fruit	Oranges	Orange juice Orange juice, concentrated Oranges	
	Lemons and limes	Juice of lemon Lemon juice, concentrated Lemons and limes	
	Tangerines, mandarins, clementines	Juice of tangerine Tangerines, mandarins, clementines	
	Pomelos and grapefruits	Grapefruit juice Grapefruit juice, concentrated Pomelos and grapefruits	
	Other citrus fruit, n.e.c.	Citrus juice, concentrated n.e.c. Juice of citrus fruit n.e.c. Other citrus fruit, n.e.c.	
Bananas	Bananas	Bananas	
	Plantains and cooking bananas	Plantains and cooking bananas	
Apples	Apples	Apple juice Apple juice, concentrated Apples	
Berries Grapes	Strawberries	Strawberries	
	Raspberries	Raspberries	
	Blueberries	Blueberries	
	Cranberries	Cranberries	
	Gooseberries	Gooseberries	
	Other berries and fruits of the genus vaccinium n.e.c.	Other berries and fruits of the genus vaccinium n.e.c.	
	Grapes	Grape juice Grapes	
Wine	Wine	Wine	
	Pears	Pears	
	Peaches and nectarines	Peaches and nectarines	

Continued on next page

Table C.6: FAO commodities used to compute production and trade for all LCA food categories (Continued)

Other Fruit	Plums and sloes	Plums and sloes Plums, dried	Oil converted to oil crops using processing factors Production and trade split between oil crops and oil.
	Apricots	Apricots, Apricots, dried	
	Avocados	Avocados	
	Watermelons	Watermelons	
	Cantaloupes and other melons	Cantaloupes and other melons	
	Kiwi fruit	Kiwi fruit	
	Olives	Olives Olives preserved Olive oil	
	Cashewapple	Cashewapple	
	Dates	Dates	
	Figs	Figs Figs, dried	
	Locust beans (carobs)	Locust beans (carobs)	
	Mangoes, guavas and mangosteens	Juice of mango Mangoes, guavas and mangosteens Mango pulp	
	Other fruits, n.e.c.	Fruit prepared n.e.c. Juice of fruits n.e.c. Other fruit n.e.c., dried Other fruits, n.e.c. Raisins	
	Other tropical fruits, n.e.c.	Other tropical fruit, dried Other tropical fruits, n.e.c.	
	Papayas	Papayas	
	Pineapples	Juice of pineapples, concentrated Pineapple juice Pineapples Pineapples, otherwise prepared or preserved	
	Coconuts, in shell	Coconuts, in shell Coconuts, desiccated Coconut oil	
	Cherries	Cherries	
	Currants	Currants	
	Other pome fruits		
	Other stone fruits	Other stone fruits	
	Persimmons	Persimmons	
	Quinces	Quinces	
	Sour cherries	Sour cherries	
Coffee	Coffee, green	Coffee, green Coffee husks and skins Coffee, decaffeinated or roasted	
Dark Chocolate	Cocoa beans	Cocoa beans	
Bovine Meat (beef herd)	Beef and Buffalo Meat, primary	Bovine meat, salted, dried or smoked Meat of buffalo, fresh or chilled Meat of cattle boneless, fresh or chilled Meat of cattle with the bone, fresh or chilled Sausages and similar products of meat, offal or blood of beef and veal	

Continued on next page

Table C.6: FAO commodities used to compute production and trade for all LCA food categories (Continued)

'Bovine Meat (dairy herd)	Beef and Buffalo Meat, primary	Bovine meat, salted, dried or smoked Meat of buffalo, fresh or chilled Meat of cattle boneless, fresh or chilled Meat of cattle with the bone, fresh or chilled Sausages and similar products of meat, offal or blood of beef and veal	
Lamb Mutton	Sheep and Goat Meat	Meat of goat, fresh or chilled Meat of sheep, fresh or chilled	
Pig Meat	Meat of pig with the bone, fresh or chilled	Meat of pig boneless, fresh or chilled Meat of pig with the bone, fresh or chilled Pig meat, cuts, salted, dried or smoked (bacon and ham) Sausages and similar products of meat, offal or blood of pig	
Poultry Meat	Meat of chickens, fresh or chilled	Meat of chickens, fresh or chilled	
	Meat of turkeys, fresh or chilled	Meat of turkeys, fresh or chilled	
	Meat of sucks, fresh or chilled	Meat of sucks, fresh or chilled	
	Meat of geese, fresh or chilled	Meat of geese, fresh or chilled	
	Meat of pigeons and other birds n.e.c., fresh, chilled or frozen	Meat of pigeons and other birds n.e.c., fresh, chilled or frozen	
Milk	Milk, total	Butter and ghee of sheep milk Butter of cow milk Butter of goat milk Buttermilk, curdled and acidified milk Buttermilk, dry Casein Cheese from milk of goats, fresh or processed Cheese from milk of buffalo, fresh or processed Cheese from milk of sheep, fresh or processed Cheese from skimmed cow milk Cheese from whole cow milk Cream, fresh Dairy products n.e.c. Ghee from buffalo milk Ghee from cow milk Ice cream and other edible ice Processed cheese Raw milk of cattle Raw milk of sheep Reconstituted milk Skim milk and whey powder Skim milk of cows Skim milk, condensed Skim milk, evaporated Standardized milk Whey cheese Whey, condensed Whey, dry Whey, fresh Whole milk powder Whole milk, condensed Whole milk, evaporated Yoghurt Yoghurt, with additives	Production and trade split between milk and cheese.

Continued on next page

Table C.6: FAO commodities used to compute production and trade for all LCA food categories (Continued)

Cheese	Milk, total	Butter and ghee of sheep milk Butter of cow milk Butter of goat milk Buttermilk, curdled and acidified milk Buttermilk, dry Casein Cheese from milk of goats, fresh or processed Cheese from milk of buffalo, fresh or processed Cheese from milk of sheep, fresh or processed Cheese from skimmed cow milk Cheese from whole cow milk Cream, fresh Dairy products n.e.c. Ghee from buffalo milk Ghee from cow milk Ice cream and other edible ice Processed cheese Raw milk of cattle Raw milk of sheep Reconstituted milk Skim milk and whey powder Skim milk of cows Skim milk, condensed Skim milk, evaporated Standardized milk Whey cheese Whey, condensed Whey, dry Whey, fresh Whole milk powder Whole milk, condensed Whole milk, evaporated Yoghurt Yoghurt, with additives	Production and trade split between milk and cheese.
Eggs	Eggs Primary	Hen eggs in shell, fresh Eggs from other birds in shell, fresh, n.e.c. Eggs, dried Eggs, liquid	
Fish	Freshwater Fish Demersal Fish Pelagic Fish Marine Fish, Other	All items in FishStat under SITC codes 34 (Fish, fresh (live or dead), chilled or frozen), 35 (Fish, dried, salted or in brine; smoked fish), 37 (Fish, aqua. invertebrates, prepared, preserved, n.e.s.)	
Crustaceans	Crustaceans Cephalopods Molluscs, Other	All items in FishStat under SITC code 36 (Crustaceans, mollusks and aquatic invertebrates)	

Table C.7: Mapping of countries to geographic regions (restricted to countries with available product or LCA data)

Country	**Intermediate Region Name**	**Sub-region Name**	**Region Name**
Algeria		Northern Africa	Africa
Egypt			
Morocco			
Tunisia			
Kenya	Eastern Africa	Sub-Saharan Africa	
Mauritius			
Reunion			
Uganda			
Cameroon	Middle Africa		
South Africa	Southern Africa		
Benin	Western Africa		
Ghana			
Ivory Coast			
Cuba	Caribbean	Latin America and the Caribbean	Americas
Guadeloupe			
Martinique			
Puerto Rico			
Costa Rica	Central America		
Mexico			
Nicaragua			
Panama			
Argentina	South America		
Bolivia			
Brazil			
Chile			
Colombia			
Ecuador			
Peru			
Venezuela			
Canada		Northern America	
United States			
China		Eastern Asia	Asia
Hong Kong			
Japan			
South Korea			
Indonesia		South-eastern Asia	
Malaysia			
Philippines			
Singapore			
Thailand			
Vietnam			
Bangladesh		Southern Asia	
India			
Iran			

Table C.7: Mapping of countries to geographic regions (restricted to countries with available product or LCA data) (Continued)

Nepal			
Cyprus		Western Asia	
Iraq			
Israel			
Kuwait			
Lebanon			
Qatar			
Saudi Arabia			
Turkey			
United Arab Emirates			
Bulgaria		Eastern Europe	Europe
Czech Republic			
Hungary			
Poland			
Romania			
Russia			
Slovakia			
Ukraine			
Denmark		Northern Europe	
Estonia			
Finland			
Ireland			
Latvia			
Lithuania			
Norway			
Sweden			
United Kingdom			
Croatia		Southern Europe	
Greece			
Italy			
Portugal			
Slovenia			
Spain			
Austria		Western Europe	
Belgium			
France			
Germany			
Luxembourg			
Netherlands			
Switzerland			
Australia		Australia and New Zealand	Oceania
New Zealand			
New Caledonia		Melanesia	
French Polynesia		Polynesia	

Table C.8: Aggregate categories used for analyzing and visualizing estimated environmental impacts

Parent category	**Subcategory**	**Aggregated category**	**Aggregated group**
Cereals and Cereal Products	Pizza	Pizza	Cereals and Cereal Products
Cereals and Cereal Products	Pasta	Pasta	
Cereals and Cereal Products	Rice	Rice	
Cereals and Cereal Products	Other cereals	Other cereals	
Cereals and Cereal Products	Brown, granary and wheatgerm bread	Bread	
Cereals and Cereal Products	Other bread		
Cereals and Cereal Products	White bread (not high fibre, not multiseed bread)		
Cereals and Cereal Products	Wholemeal bread		
Cereals and Cereal Products	High fibre breakfast cereals	Breakfast cereals	
Cereals and Cereal Products	Other breakfast cereals (not high fibre)		
Cereals and Cereal Products	Biscuits	Biscuits	
Cereals and Cereal Products	Buns cakes and pastries	Cakes, pastries and puddings	
Cereals and Cereal Products	Fruit pies		
Cereals and Cereal Products	Cereal based milk puddings		
Cereals and Cereal Products	Other cereal based puddings		
Cereals and Cereal Products	Sponge puddings		
Fruit	Apples and pears not canned	Fresh or canned fruit	Fruits, Vegetables, and Nuts
Fruit	Bananas		
Fruit	Canned fruit in juice		
Fruit	Canned fruit in syrup		
Fruit	Citrus fruit not canned		
Fruit	Other fruit not canned		
Vegetables, Potatoes	Carrots	Vegetables and vegetable dishes	
Vegetables, Potatoes	Green beans		
Vegetables, Potatoes	Leafy green vegetables		
Vegetables, Potatoes	Other vegetables		
Vegetables, Potatoes	Peas		
Vegetables, Potatoes	Tomatoes		
Vegetables, Potatoes	Other vegetable products and dishes		
Vegetables, Potatoes	Chips purchased including takeaway	Potato products and dishes	
Vegetables, Potatoes	Other fried/roast/baked potatoes		
Vegetables, Potatoes	Other potato products and dishes		
Vegetables, Potatoes	Baked beans	Beans and pulses	
Vegetables, Potatoes	Beans and pulses (including ready meal homemade dishes)		
Nuts and Seeds	Nuts and Seeds	Nuts and seeds	
Milk and Milk Products	1% Milk		
Milk and Milk Products	Infant formula		
Milk and Milk Products	Other milk		

Table C.8: Aggregate categories used for analyzing and visualizing estimated environmental impacts (Continued)

Milk and Milk Products	Semi-skimmed milk	Dairy products and dairy alternatives	Meat, Dairy, and Eggs
Milk and Milk Products	Skimmed milk		
Milk and Milk Products	Whole milk		
Milk and Milk Products	Cheddar cheese		
Milk and Milk Products	Cottage cheese		
Milk and Milk Products	Other cheese		
Fat Spreads	Butter		
Fat Spreads	Low fat spread not polyunsaturated		
Fat Spreads	Polyunsaturated low fat spread		
Fat Spreads	Block margarine		
Fat Spreads	Soft margarine not polyunsaturated		
Fat Spreads	Polyunsaturated margarine		
Fat Spreads	Reduced fat spread (not polyunsaturated)		
Fat Spreads	Reduced fat spread (polyunsaturated)		
Milk and Milk Products	Cream (including imitation cream)		
Milk and Milk Products	Yogurt		
Milk and Milk Products	Ice cream		
Milk and Milk Products	Fromage frais and other dairy desserts		
Eggs and Egg Dishes	Manufactured egg products including ready meals	Eggs	
Eggs and Egg Dishes	Other eggs and egg dishes including homemade		
Fish and Fish Dishes	Oily fish	Seafood	
Fish and Fish Dishes	Canned tuna		
Fish and Fish Dishes	Other white fish		
Fish and Fish Dishes	White fish coated or fried		
Fish and Fish Dishes	Shellfish		
Meat and Meat Products	Other chicken and turkey	Poultry and pig meat	
Meat and Meat Products	Manufactured coated chicken/turkey products		
Meat and Meat Products	Bacon and ham		
Meat and Meat Products	Pork		
Meat and Meat Products	Beef and veal	Beef and lamb	
Meat and Meat Products	Lamb		
Meat and Meat Products	Burgers and kebabs purchased	Sausages, burgers and kebabs	
Meat and Meat Products	Sausages		
Meat and Meat Products	Meat pies and pastries	Meat dishes	

Table C.8: Aggregate categories used for analyzing and visualizing estimated environmental impacts (Continued)

Meat and Meat Products	Liver and dishes	Liver and other meat products	
Meat and Meat Products	Other meat products		
Vegetables, Potatoes	Meat alternatives (including ready meals and homemade dishes)	Meat alternatives	
Artificial Sweeteners	Artificial Sweeteners	Sugar, preserves, and spreads	Sugar and Confectionery
Sugar, Preserves and Confectionery	Preserves		
Sugar, Preserves and Confectionery	Sugar		
Sugar, Preserves and Confectionery	Sweet spreads fillings and icing		
Sugar, Preserves and Confectionery	Sugar confectionery	Sugar confectionery	
Sugar, Preserves and Confectionery	Chocolate confectionery	Chocolate confectionery	
Non-Alcoholic Beverages	Fruit juice	Fruit juice	Non-Alcoholic Beverages
Non-Alcoholic Beverages	Smoothies	Smoothies	
Non-Alcoholic Beverages	Soft drinks low calorie carbonated	Water and soft drinks	
Non-Alcoholic Beverages	Soft drinks low calorie concentrated		
Non-Alcoholic Beverages	Soft drinks low calorie, ready to drink, still		
Non-Alcoholic Beverages	Soft drinks not low calorie carbonated		
Non-Alcoholic Beverages	Soft drinks not low calorie concentrated		
Non-Alcoholic Beverages	Soft drinks not low calorie, ready to drink, still		
Non-Alcoholic Beverages	Bottled water still or carbonated		
Non-Alcoholic Beverages	Coffee (made up weight)	Coffee	
Non-Alcoholic Beverages	Herbal tea (made up)	Tea	
Non-Alcoholic Beverages	Tea (made up)		
Miscellaneous	Beverages dry weight	Beverages dry weight	
Fat Spreads	Other cooking fats and oils not polyunsaturated	Cooking fats and oils	Miscellaneous Items
Fat Spreads	Polyunsaturated oils		
Miscellaneous	Savoury sauces pickles gravies condiments	Sauces and condiments	
Savoury Snacks	Savoury Snacks	Savoury snacks	
Commercial Toddlers Foods and Drinks	Commercial Toddlers Foods and Drinks	Soup and toddler foods	
Miscellaneous	Soup		
Dietary Supplements	Dietary Supplements	Nutrition powders and supplements	
Miscellaneous	Nutrition powders and drinks		

Table C.9: Pairwise correlations between different environmental indicators

Metric 1	**Metric 2**	**Correlation**
Land use	GHG emissions	0.62
	Biodiversity loss	0.71
	Eutrophication	0.80
	Water stress	0.24
GHG emissions	Biodiversity loss	0.52
	Eutrophication	0.45
	Water stress	0.31
Biodiversity loss	Eutrophication	0.63
	Water stress	0.10
Eutrophication	Water stress	0.18

Table C.10: Pairwise correlations between impacts computed with vs without accounting for ingredient sourcing.

Food Group	Food Category	Correlation					
		Land use	GHG emissions	Biodiversity loss	Eutrophication	Water stress	Composite
Cereals and Cereal Products	Pizza	0.77	0.93	0.52	0.72	0.81	0.89
	Pasta	0.72	0.93	0.59	0.65	0.75	0.82
	Rice	0.89	0.75	0.74	0.59	0.53	0.58
	Other cereals	0.76	0.84	0.63	0.66	0.77	0.79
	Bread	0.77	0.94	0.56	0.76	0.74	0.83
	Breakfast cereals	0.91	0.61	0.60	0.80	0.86	0.83
	Biscuits	0.98	0.54	0.67	0.88	0.91	0.83
	Cakes, pastries and puddings	0.98	0.66	0.67	0.89	0.93	0.85
Fruits, Vegetables, and Nuts	Fresh or canned fruit	0.95	0.97	0.56	0.89	0.93	0.93
	Vegetables and vegetable dishes	0.84	0.92	0.69	0.79	0.77	0.79
	Potato products and dishes	0.92	0.92	0.61	0.81	0.76	0.86
	Beans and pulses	0.71	0.82	0.33	0.69	0.78	0.67
	Nuts and seeds	0.94	0.42	0.44	0.66	0.97	0.97
Meat, Dairy, and Eggs	Dairy products	0.85	0.93	0.58	0.86	0.91	0.96
	Eggs	0.79	0.76	0.69	0.84	0.68	0.71
	Seafood	0.73	0.87	0.68	0.71	0.91	0.90
	Poultry and pig meat	0.75	0.96	0.61	0.67	0.73	0.84
	Beef and lamb	0.27	0.56	-0.18	0.19	0.89	0.10
	Sausages, burgers and kebabs	0.59	0.84	0.52	0.72	0.73	0.69
	Meat dishes	0.65	0.85	0.44	0.63	0.77	0.71
	Liver and other meat products	0.67	0.84	0.21	0.47	0.74	0.66
	Meat alternatives	0.78	0.92	0.61	0.88	0.84	0.84
	Dairy alternatives	0.97	0.48	0.50	0.92	0.99	0.96
Sugar and Confectionery	Sugar, preserves, and spreads	0.94	0.78	0.65	0.81	0.96	0.90
	Sugar confectionery	0.95	0.57	0.73	0.80	0.93	0.80
	Chocolate confectionery	0.99	0.34	0.53	0.94	0.96	0.64
Non-Alcoholic Beverages	Fruit juice	0.89	0.98	0.56	0.94	0.80	0.85
	Smoothies	0.92	0.94	0.59	0.92	0.96	0.93
	Water and soft drinks	0.98	0.85	0.73	0.90	0.90	0.89
	Coffee	0.97	0.93	0.91	0.97	0.95	0.93
	Tea	0.99	0.99	0.98	0.99	0.87	0.99
	Beverages dry weight	0.98	0.26	0.37	0.93	0.99	0.53
Miscellaneous Items	Cooking fats and oils	0.94	0.96	0.84	0.62	0.92	0.92
	Sauces and condiments	0.69	0.91	0.58	0.75	0.84	0.83
	Savoury snacks	0.84	0.95	0.58	0.87	0.67	0.85
	Soup and toddler foods	0.64	0.91	0.43	0.62	0.83	0.80
	Nutrition powders and supplements	0.87	0.83	0.59	0.62	0.93	0.85
Overall		0.70	0.83	0.57	0.66	0.91	0.80

C.3 Supplementary Methods

C.3.1 Description and Processing of Food Data

Data for retail food products used in this research came from two sources – foodDB (Harrington et al., 2019) and Open Food Facts (homepage). foodDB is a web tool that collects data for food products from food retailer's websites. We used an extract of 262,711 products from 9 food retailers based in the UK and Ireland. About 36,000 of these products did not have any listed ingredients – these products were retained during training of the product categorization models (to increase the representativeness of the training data), but they were dropped before estimating product composition and impacts. From the remaining products, about 5,000 products identified as Alcoholic Beverages and Non-Food were dropped. Another ~10,000 products were removed as their ingredient information only contained allergen advice or other labels, leaving about 212,000 products. Our composition algorithm then excluded ~36,000 products where it could not reliably identify at least 75% of the composition. We further removed ~72,000 products with duplicated names[1], resulting in 104,250 foodDB products.

Open Food Facts is a publicly available dataset, which relies on crowdsourcing to collect information about food products available around the world. We used an extract of over 3 million products from Open Food Facts. Dropping countries with fewer than 1,000 unique products left around 2.5 million products, and filtering out products with no listed ingredients resulted in 961,989 products, for which product categories were predicted. About 550,000 of these products were in languages other than English – the non-English products were first identified using the 'langdetect' module on Python (which is based on Google's language detection), and then translated using Python's 'googletrans' library (which uses the Google Translate API). These language detection and translation libraries are not 100% accurate, but these tools gave us satisfactory results in terms of speed and accuracy, and any

[1]Impact estimates for products with duplicated names were highly correlated (across both foodDB and Open Food Facts). Correlations for the different environmental metrics were as follows – Land use (0.90), GHG emissions (0.93), Eutrophication (0.87), Biodiversity loss (0.90), Water stress (0.91).

inaccuracies were filtered out in the subsequent steps used to clean ingredient strings and to estimate product composition. After categorizing these products, removing Alcoholic Beverages and Non-Food items leaves about 932,000 products. We could not use all these products as the ingredient lists could not be cleaned or formatted into the desired pattern for many products. It was important to bring the ingredient lists into a format that could be parsed by the algorithm that estimates composition. We used the 'regex' library to clean and format ingredient strings as best as possible, and removed products which could not be cleaned, leaving about 642,000 products. Of these, removing products for which the composition algorithm was able to identify less than 75% of the composition (~150,000), and ~106,000 products with duplicated product names, left 385,419 products from Open Food Facts.

Out of 489,669 products from the two databases, we dropped ~6,000 products for which all five environmental indicators (land use, greenhouse gas emissions, biodiversity loss, eutrophication, and water stress) were estimated as 0. This occurred when products consisted only of zero-impact ingredients (e.g., salt or water) or when all their ingredients lacked environmental estimates (e.g., vitamins, minerals, certain food additives). We then removed approximately 8,000 products from the analysis, based on manual checks of estimated composition, for example, if products were classified into categories for seafood, but they had no relevant ingredients identified as such. This resulted in a total of 474,955 products spanning 74 countries, used for comparative analyses of environmental impacts across food types and geographies.

C.3.2 Categorization of Food Products

While both foodDB and Open Food Facts contain some information about categorizations, the categories are not uniform across the two datasets, countries, and stores. It is important to categorize food products as the algorithm to estimate composition relies on the products being sorted into a set of food categories consistent across datasets, countries, and stores.

C. Supplementary Material for "The Environmental Footprint of Retail Foods at Scale: A Multi-Country Analysis"

Manual categorization of food products can be extremely challenging and time consuming. Hence, we developed a machine learning pipeline to automate the categorization of food products. We chose the categories provided by the UK National Diet and Nutrition Survey (NDNS) to sort products into. The primary reason for this choice was the availability of ~60,000 products sorted into these categories, which could be used as labels for training the machine learning model(s). These labels came from a few different sources: i) almost 20,000 of these were obtained using fuzzy matching, ii) almost 40,000 were obtained with the help of Chat GPTs API in combination with manual verification, iii) a few hundred were labelled manually by researchers (Kennedy et al., 2025). Note that these labels could be inaccurate at times, as it wasn't possible to manually verified all labels assigned using fuzzy matching or Chat GPT.

Supplementary Table C.1 shows the categories provided by NDNS. Some categories were modified for relevance and to remove redundancies. A category for 'Not food' was added to identify and filter out non-food products from the food product datasets. Overall, there are 18 parent categories, 53 main categories, and 104 subcategories.

Machine learning models were trained to predict categories based on product descriptions, i.e. product names and the listed ingredients. These product names and listed ingredients were first converted into features using the Sentence-BERT (SBERT) model, specifically the `all-mnet-base-v2` variant (Reimers & Gurevych, 2019). This approach has been validated in previous work classifying food products in Canadian supermarkets (Hu et al., 2023). SBERT is a modification of the Bidirectional Encoder Representations from Transformers (BERT) framework, designed to generate semantically meaningful sentence embeddings while maintaining computational efficiency. SBERT employs a Siamese network architecture to produce fixed-length sentence embeddings that enables direct comparison between sentence vectors. The pre-trained all-mpnet-base-v2 model was readily available for use with the Sentence Transformers module on Python. This model was trained on more than 1 billion training pairs and can be leveraged without extensive domain-specific

fine-tuning. Prior to embedding extraction, the product names and ingredients were converted to lower case and concatenated. The merged string was then fed into the SBERT encoder, yielding 768-dimensional dense vectors that encapsulate the contextual information for each product.

We first focused on categorizing all data in foodDB, with a very high degree of accuracy. This involved an iterative process of training machine learning models, predicting on unlabeled data, and refining labelled data to then train better models (see flowchart in Supplementary Figure C.1). A parent model was used to classify products into parent categories, and sub models were used to further classify products in each parent category into subcategories. This was done to make the classification task easier for the models – instead of classifying products into 104 subcategories with a single model, we divide the task between 12 models, with each model classifying products into at most 18 classes at a time. Products sorted into the following parent categories were not subdivided further – savoury snacks, nuts and seeds, alcoholic beverages, commercial toddlers foods and drinks, dietary supplements, artificial supplements, and not food. Main categories were imputed based on the predicted subcategories.

The model at the parent category level was first refined through several iterations (Supplementary Figure C.1). After each round of training, predictions were manually verified by sampling 100 products randomly from the entire dataset and from subsets of products allotted to each parent category. These sampled products could contain both labelled and unlabeled data, which helps assess performance on unlabeled products too. Products that were misclassified were used to add similar products to the training dataset and to correct any incorrect labels (if present) might be causing the misclassification. Once, we had reached a satisfactory level of confidence in the performance of the parent category classification model, we moved on to the subcategory level models. This choice was not based on model performance on the training data (that remained stable throughout the iterations), but on the quality of predictions on the randomly sampled data used for manual evaluation.

A similar process was followed for each subcategory to refine the quality of labels and hence the trained models. The manual evaluations at the subcategory level modelling were also used to make corrections at the parent category level, when products were incorrectly classified into the wrong parent category. Hence, after several iterations for subcategory level classification model for each parent category, a few rounds of corrections were done on the parent category level. Note, that no model retraining at the parent category was performed at this stage. Instead, products that were still systematically misclassified were manually corrected. Again, once a satisfactory level of performance was observed on the randomly sampled products at both parent category and subcategory levels, we stopped the iterative process of prediction correction and model refinement.

Random Forest classifiers were used for each classification task. The performance on labelled data was comparable across classification models such as random forest, LDA (linear discriminant analysis), and KNN (k-nearest neighbors), but random forest models did better at predicting categories for the non-labelled products. Supplementary Figure C.2 shows a visual representation of the product categorizations. Each point corresponds to a specific food product, and the colors are based on assigned categories. The figure shows distinct clusters where products of the same category are grouped closely together, indicating strong similarities in their feature representations. Areas where different colors overlap may indicate categories with overlapping characteristics.

Supplementary Table C.2 reports the performance metrics of the classification models at the end of all iterations. Hyperparameters of the Random Forest models are also provided in the table. An 80-20 train-test split was used across all classification tasks. The number of products used for training came out to be higher than the original number of available labels due to the addition of labels manually during the iterations. Note that the labels themselves can occasionally be incorrect (despite the many iterations), meaning that performance metrics can be marginally better or worse than those reported here. We report three

performance metrics for both training and testing sets to comprehensively assess model effectiveness and to minimize the risks of overfitting and underfitting:

1. Accuracy measures the fraction of correct predictions out of all predictions made.

2. Balanced accuracy calculates the average recall obtained across all classes, giving equal weight to each class.

3. Weighted F1-score computes the harmonic mean of precision and recall for each class, weighted by the number of true instances in each class.

Precision, for any given class, measures the ratio of correctly predicted positive observations to the total predicted positives. And recall measures the ratio of correctly predicted positive observations to all actual positive instances.

It is important to note, that the reported performance metrics did not vary significantly throughout the multiple iterations, as the models consistently performed well on the labelled data – on both train and test sets. The primary purpose of the iterations was to enhance performance on the unlabelled data, though this improvement could only be assessed manually and, therefore, cannot be reported quantitatively. Initially, without iterations (e.g., adding labels or correcting parent categories), we observed systematic biases in predictions – for instance, brown bread being classified as white bread or spices like turmeric being misclassified into vegetable categories instead of miscellaneous ones. While accuracy on the unlabelled data initially ranged between 70-80% across categorization tasks, iterations raised it to 85-95%. More importantly, precision (assessed by manually sampling products assigned to each class), which was initially below 60% for certain parent or subcategories, improved significantly after iterations, reaching closer to 90%.

Deep learning models were not utilized so far in the categorization process due to their complexity and the extensive hyperparameter tuning they require compared to simpler classification models. The classification of foodDB products was highly iterative and manual, prompting us to adopt simpler machine learning approaches.

However, once we achieved a satisfactory level of accuracy in categorizing the foodDB products, we had developed a large, high-quality labelled training dataset. This dataset enabled us to leverage deep learning models effectively. In the next phase of the categorization process, we trained deep learning models on the entire foodDB dataset of 262,711 products to categorize the Open Food Facts food products. These models needed to be trained only once, as the extensive and high-quality labelled dataset ensured robust performance without requiring further iterative refinement.

Supplementary Table C.3 presents the hyperparameters used in the deep learning classification models and their performance metrics, evaluated using an 80-20 train-test split. These trained models were subsequently applied to categorize the products in the Open Food Facts dataset. Supplementary Table C.4 shows products sourced from foodDB (262,711) and Open Food Facts (961,989), classified into 104 subcategories.

C.3.3 Algorithm to estimate composition of products

We follow the same methodology for estimating composition of products as described by Clark et al. (2022), with a few additional steps to expand the geographic focus of the algorithm to outside the United Kingdom. First, the raw ingredient texts strings underwent extensive cleaning to remove extraneous information. Specifically, any text related to allergen warnings or ingredient sourcing details, such as indications for organic production or fair-trade certification, was removed. This ensured that only the pertinent ingredient information remained for subsequent parsing and analysis. This level of cleaning was sufficient for the data from foodDB, however the data from Open Food Facts was much messier. The ingredient lists in foodDB followed a fixed format, i.e. ingredients were separated by commas, with a percentage, if available, provided in brackets after ingredient name. If an ingredient contains sub-ingredient lists, those follow the same format as the ingredient lists and are placed inside a pair of brackets after the ingredient name and corresponding percentage (if available). This consistent format is crucial for accurate parsing of information provided in back-of-backage ingredient lists.

C. Supplementary Material for "The Environmental Footprint of Retail Foods at Scale: A Multi-Country Analysis"

Open Food Facts text was not always in the same format – i) the order of ingredient names, corresponding percentages, and sub-ingredient list was not always consistent, ii) the lists sometimes used a punctuation mark other than a comma to separate ingredients, iii) some stray non-English words not translated by the translation algorithm were sometimes present in the lists, iv) cooking instructions and several other kinds of information were sometimes concatenated with ingredient lists, v) there were special characters, vi) and incorrect parentheses, vii) and several other formats for allergen warnings, sourcing information, organic labels etc. After some basic cleaning that removed special characters, replaced parentheses, removed different formats of labels, we first identified Open Food Facts products that only contained the types of characters present in foodDB, i.e. alphabets, numbers, percentage signs, parentheses, commas, decimal points. For these products, we performed further cleaning, and then ensured that they were brought into the desired structure. For all other products, we filtered products that only contained a hyphen or a colon in addition to foodDB characters. After removing these undesired characters, we then performed the same cleaning as before to bring these into the desired format. We also identified some non-English words and translated them manually. Finally, products that were too dirty, i.e. they contained too many undesired characters, and followed completely different structures were dropped from the analysis (~30% of products), to avoid introducing noise into our results.

Once the data were cleaned, the next major step was to parse the ingredient lists into their individual components. Each product's ingredient text, originally provided as a single string, was systematically split into discrete ingredients using delimiters such as commas and semi-colons. Moreover, the method was designed to handle compound ingredients that included embedded lists; for example, a fortified wheat flour entry might include additional ingredients listed in parentheses. These embedded lists were extracted separately, and a hierarchical labelling system was employed (e.g., V1 for the first ingredient, V2 for the second ingredient, and V2.1 for the first ingredient within an embedded list under the second ingredient). This structured labelling ensured that both the order and the nested relationships among

ingredients were preserved, which is critical for subsequent estimation procedures that rely on ingredient positioning.

For ingredients with explicit percent composition information provided on the package, the extraction process utilized regular expressions to detect numerical percentages. Specifically, patterns such as *[0-9]{1,3}(\s)?%* or *[0-9]{1,3}(\.)[0-9]{1,2}(\s)?%* were used to extract the percentage values from the text. In instances where multiple percentages were identified for a single ingredient, a series of logical criteria was applied to determine the most appropriate value. These criteria ensured that the percent composition for any ingredient did not exceed the theoretical maximum based on its position in the list, maintained the expected descending order of ingredients, and did not cause the sum of all ingredient percentages to exceed 100%. This methodological approach provided a reliable baseline for ingredients with provided composition data, setting a benchmark for the estimation of missing values.

To estimate ingredient composition when unknown, ingredients were first mapped to a set of 110 agricultural commodities observed in the environmental datasets. This mapping also enabled integration of product composition, once estimated, with the environmental data. A three-step sorting process was employed to map ingredients to agricultural commodities, based on tailored search terms for each commodity. First, the search terms were used to count how many times each ingredient could potentially match each commodity, without yet mapping it to a specific commodity. Next, ingredients were assigned to the commodity with the fewest matches, thus favouring less common but more specific commodity categories. Finally, ingredients were further classified into sub-categories using additional search terms. After completing these steps, ingredients identified as water and salt were mapped to one of these commodities, only if they had not already been sorted into any of the other commodity categories. The tailored search terms and their mappings to environmental-database commodities were the same as those used in Clark et al. (2022).

For ingredients without explicitly reported percent composition, values were estimated using prior knowledge from similar products and known ingredient pro-

portions, informed by product categorization into parent, main, and subcategories. Similar products were defined as those belonging to the same geographic cluster and hierarchical category. To improve comparability, countries with similar food cultures were grouped into geographic clusters (Supplementary Table C.5) so that products within the same category were more likely to share composition patterns. Missing percent composition was then estimated based on the average proportion of that ingredient when appearing in the same position within the ingredient list of other products in the same sub-category, main category, or parent category, in that order of preference, within the relevant country group. If the same ingredient did not occur in the same position within those categories, the average proportion of the nth ingredient from similar products in the same hierarchical group was used instead. When these methods were insufficient, additional techniques such as linear interpolation between known values were applied. For ingredients appearing within embedded lists, estimated proportions were adjusted by multiplying the parent ingredient's estimated percentage by the relative proportion of the embedded ingredient.

The final step in the process involved a series of iterative logic checks designed to ensure that all estimated values were plausible and internally consistent. These checks enforced that the ingredient percentages adhered to the expected ordering (where each ingredient's composition should be equal to or greater than that of any subsequent ingredient), that no single ingredient exceeded the theoretical maximum based on its position, and that the total composition of all ingredients summed precisely to 100%. In cases where certain ingredients' estimates could not be refined further, such as when an ingredient's percentage matched that of its neighbour, the algorithm anchored those values to avoid implausible outcomes like negative percentages or overestimation of the final ingredient's contribution.

Throughout this process, robust quality control measures were implemented to maintain the integrity of the analysis. Only products in which at least 75% of the total mass could be accurately recognized and sorted into predefined food categories were included in the final dataset. This ensured that the conclusions

drawn from the analysis were based on high-quality, well-categorized data. We estimated compositions for roughly 4.81 million of the 5.21 million ingredient entries – covering about 80% of the total ingredient mass in our dataset of 474,955 products. See Supplementary Figure C.3 for the distribution of ingredient counts by food group and geography. For further technical details and nuances of the methodology, please refer to the published work by Clark et al. (2022).

C.3.4 Estimation of product-level environmental impacts

We employed the approach used by Clark et al. (2022) to estimate environmental impacts, with one important modification – the environmental datasets were paired with country level bilateral trade flow data to account for ingredient sourcing.

The environmental data in this analysis were derived primarily from a meta-analysis of life cycle assessments (LCAs) provided by Poore and Nemecek (2018), which cover over 40,000 food production systems. Because the primary LCA database contained limited information on capture fisheries, data from the Blue Foods Assessment were incorporated to better represent seafood production (Gephart et al., 2021). The commodities from these environmental databases were condensed into 110 categories, which were the ones all ingredients were sorted into previously while estimating ingredient composition. We condensed the production systems into categories, such that every category had at least 5 unique observations. Commodities with fewer than 5 unique observations were grouped together to create a larger category, such as 'Other Fruits'. When possible, we paired organic ingredients and organic products with organic life cycle estimates, but only when at least 5 observations of production systems for that ingredient were available. If there were fewer than 5 organic observations for that ingredient, we instead randomly sampled across all production systems during the Monte Carlo analysis (described below).

Trade flow data was obtained from FAOSTAT (FAO, 2023) and FishStat (FAO, 2024b). We used national-level production and bilateral trade data from the FAO. Trade flows were obtained for each food category of interest, as given in the environmental databases. The national-scale data from the FAO requires some

pre-processing to address the following discrepancies – i) the trade volumes reported by the importing countries did not always match those reported by the exporting countries, and ii) the total reported exports from some countries exceeded the volumes produced and imported together, because of misreported transactions or countries reporting re-exported imports as their exports. Discrepancies between the volume of trade reported by the importer and exporter are resolved using a reliability index approach similar to the one outlined by Gehlhar (1996). Furthermore, to resolve the second issue, a re-export algorithm proposed by Croft et al. (2018) is used to obtain 'flows' – the algorithm ensures that the total exports from a country never exceed its production and total imports; and it also links the source of production with the destination of import. For the fisheries data, only the second step was employed, and the imports were used directly without applying the reliability index approach (as FishStat reports exports and re-exports separately, which are not directly comparable with imports). We used data over a few years to remove any year-on-year noise from the data. We averaged the FAOSTAT data over 2017-2021 and the FishStat data over 2019-2022. These were the latest years available at the time of accessing these data.

Supplementary Table C.6 lists the FAO commodities mapped to each LCA category. We matched trade data at the top LCA category level because many fine subcategories were not distinguished in FAO data (e.g., red vs white wine; types of wheat), or were sparsely represented in the LCA dataset (e.g., chickpeas). Aggregating at the top level provided cleaner, more consistent trade weights. Production and trade data for all commodities (except fisheries) were sourced from FAOSTAT's Production and Detailed Trade Matrix datasets. For fisheries, we sourced production figures from FAOSTAT Food Balance Sheets and trade volumes from FishStat. For each produced commodity and year, we implemented the two preprocessing steps, i.e., reconciling import-export discrepancies and then correcting any negative consumption from re-exports. For each produced commodity, such as wheat, we aggregate trade data for both its unprocessed and processed forms (e.g., wheat grain, wheat germ, and wheat and meslin flour). For fisheries, we

split the production and trade data into two groups – Fish and Crustaceans – and aggregated production and trade within each group. Finally, we sum the resolved data for all FAO commodities in each LCA category by year, then average those annual totals across all years. Note that some miscellaneous cereal and oil crops are included in the Wheat and Rye (Bread) LCA category – this is because their LCA values are calculated by scaling Wheat and Rye (Bread) LCA data using predefined ratios (Clark et al., 2022; Poore & Nemecek, 2018). Similarly, LCA values for animal fats, certain cheese types, and some other categories are derived from other LCA categories using predefined ratios (e.g., pig meat, cheese) and are therefore not mapped separately to FAO commodities.

For most processed commodities that are traded, we assume that the main products and their by-products balance each other – so no conversion factors are applied, e.g. wheat germ and flour, cheese and whey, soybean oil and cake. For certain traded items, however, we apply conversion factors to align them with their produced counterparts. For example, dry cassava, cassava flour, cassava starch and tapioca are converted to fresh cassava using factors of 2.5, 4, 5, and 5, respectively (Chisenga et al., 2019; Elisabeth et al., 2022; Mejía-Agüero et al., 2012), and potato tapioca is converted to fresh potato with a factor of 5 (Robertson et al., 2018). We also derived global average conversion factors for oils and sugars (excluding soybean oil, since its cake by-product is also traded, which offsets the oil conversion) using FAOSTAT Food Balance Sheets (FBS) and Supply Utilization Accounts (SUA). For each oil, the factor equals the ratio of global oil + cake supply to oil supply (as given by SUA). For sugars, it is the ratio of globally processed sugar crops to total supply of sugars and sweeteners (as given by FAO Food Balance Sheets).

Finally, to avoid double counting across overlapping LCA categories, we used FAOSTAT Supply Utilization Accounts (SUA) to split production and trade between processed and unprocessed products for the following commodities – olives, coconuts, groundnuts, linseed, hempseed, sunflower seed, safflower seed, sesame seed, soya beans, and milk. For each producing country, we calculated the share of each commodity processed into oil or cheese and applied those shares to the country's

production and exports. The processed shares became the volumes for products such as soybean oil or cheese, and the remainder represented the unprocessed commodity (e.g., soybeans or milk). We did not perform this split for soybeans versus tofu or for beef from beef versus dairy herds, since FAOSTAT lacks distinct identifiers for those pairs. Instead, we used the same country-level production and trade data to identify sourcing for soybeans and tofu, and for beef from beef and dairy herds, assuming comparable sourcing patterns. Finally, because FAOSTAT trade data does not distinguish between raw and refined sugar from sugar cane vs sugar beet, we split raw and refined sugar exports in proportion to each country's sugar cane and sugar beet production.

For each country, we used the trade flow data to estimate the share of each ingredient, i.e., LCA food category, sourced from every origin country. Then, for each source country, we reweighted its LCA production systems so that their total matches that country's sourcing share, while preserving the systems' relative proportions in global production. For example, if Country A sources 50% of an ingredient from Country B, and Country B has three production systems with global shares of 10%, 8%, and 7%, we scaled those to 20%, 16%, and 14% for Country A's consumption. When no LCA data was available for a given ingredient in a source country (e.g. Brazil), we used other data in its place, in this order: the country's intermediate geographic region (South America), its sub-region (Latin America), its broader region (Americas), and finally global production systems. Supplementary Table C.7 shows this mapping from countries to geographic regions. Finally, if reweighting by all source countries left us with fewer than five production-system entries for any ingredient, we reverted to the original global-weighted data to avoid introducing bias. This procedure produced environmental datasets specific to each country, that accurately reflect each ingredient's true sourcing profile.

To estimate the environmental impact of each food product, the composition estimates were then integrated with production system-level environmental performance data via a Monte Carlo analysis. In this analysis, for each commodity, production system data were randomly selected – with the selections weighted

by the production systems' weights as determined using the trade flows data earlier. This process was repeated 3,000 times to generate mean impact estimates, variance, and range for five environmental indicators: greenhouse gas emissions, land use, scarcity weighted water use, eutrophication potential, and biodiversity loss. For seafood products, a 50:50 split between capture fisheries and aquaculture systems was assumed, with slight variations between fish types, to reflect FAO estimates (FAO, 2020).

Ingredient-level shares of each product's impact were computed by pooling across the 3,000 Monte Carlo draws. For each indicator, we summed each ingredient's impact over all draws and divided by the summed product-level total. For interpretability, shares were calculated for 55 top-level LCA commodity categories rather than the finer set of 110 commodities.

Additionally, another set of impacts were computed, without taking ingredient sourcing into account, to help assess the influence of ingredient sourcing on product impacts. These calculations were also performed using a Monte Carlo analysis, but for these calculations, the environmental data was not weighted by ingredient sourcing, but rather based on the production systems' share in global production.

Each environmental indicator was then scaled from 0 (no impact) to 100 (highest observed impact across all products), and these scaled scores were averaged to create a composite environmental impact score for each product. This composite score was further normalized so that all products could be directly compared on a 0-100 scale. For the sourcing-agnostic analysis, indicators and scores were normalized using the minimum and maximum values from the sourcing-informed results. Consequently, the lowest and highest composite scores of the sourcing-agnostic impacts could mathematically be different from 0 and 100.

For further details on the specific search terms used or the Monte Carlo analysis, please refer to the original published work by Clark et al. (2022).

C.3.5 Reliability index approach

The reliability index approach outlined by (Gehlhar, 1996) is used to resolve discrepancies between the volume of trade reported by the importer and exporter in the bilateral trade dataset. An accuracy level (Supplementary Equation C.3.5.1) is computed for each bilateral trading pair, and this captures the quality of match between the importer and exporter reported quantities. The value of AL should be closer to 0 for the match to be more accurate, and a threshold of 0.2 is used to separate accurate from non-accurate matches, i.e. a match is accurate only if the difference between the reported imports and exports is less than 20%. Then, for each country, it becomes possible to construct an importer reliability index (RIM), and an exporter reliability index (RIX), which are given by Supplementary Equations C.3.5.2 and C.3.5.3 respectively. An importer's reliability is measured by the proportion of total imports it reports accurately, and similarly an exporter's reliability is measured by the proportion of its total exports it reports reliably. Finally, for each bilateral trading pair, the value reported by the more reliable partner is accepted as the trade flow between those countries.

Equation C.3.5.1 calculates the accuracy level (AL) of a transaction from region r to region s, for which the value of trade reported by the importer is $M_{r,s}$ and that reported by the exporter is $X_{r,s}$:

$$AL_{r,s} = 2 \times \frac{|M_{r,s} - X_{r,s}|}{M_{r,s} + X_{r,s}} \tag{C.3.5.1}$$

Equation C.3.5.2 calculates the reliability index of import region s as:

$$RIM_s = \frac{M_s^A}{M_s^T} \tag{C.3.5.2}$$

where $M_s^T = \sum_r M_{r,s}\ \forall s$, and $M_s^A = \sum_r M_{r,s}\ \forall s$ where $AL_{r,s} \leq 0.2$.

Equation C.3.5.3 calculates the reliability index of export region r as:

$$RIX_r = \frac{X_r^A}{X_r^T} \tag{C.3.5.3}$$

where $X_r^T = \sum_s X_{r,s}\ \forall r$, and $X_r^A = \sum_s X_{r,s}\ \forall r$ where $AL_{r,s} \leq 0.2$.

C.3.6 Re-export algorithm

The bilateral trade dataset harmonized using the reliability index approach is fed into a re-export algorithm along with the production dataset from the FAO. The re-export algorithm proposed by Croft et al. (2018) ensures that the total exports from a country never exceed its production and total imports; and it also links the source of production with the destination of import. The algorithm uses the production and export matrices P and E, and applies an iterative approach to produce a domestic supply matrix D.

$$P = \begin{bmatrix} p_1 \\ p_2 \\ \vdots \\ p_n \end{bmatrix}, \quad E = \begin{bmatrix} 0 & e_{12} & \cdots & e_{1n} \\ e_{21} & 0 & \cdots & e_{2n} \\ \vdots & \vdots & \ddots & \vdots \\ e_{n1} & e_{n2} & \cdots & 0 \end{bmatrix}, \quad D = \begin{bmatrix} d_{11} & d_{12} & \cdots & d_{1n} \\ d_{21} & d_{22} & \cdots & d_{2n} \\ \vdots & \vdots & \ddots & \vdots \\ d_{n1} & d_{n2} & \cdots & d_{nn} \end{bmatrix}$$

where, p_i is the production in country i; e_{ij} are the exports from country i to j; and d_{ij} is the quantity of country j's domestic supply that originates from country i. The sum of rows of matrix D equals the countries' production, and the sum of columns equals the countries' domestic supply (or consumption). The diagonal elements correspond to the produce that stays within the countries. The non-diagonal elements of matrix D are referred to as 'flows' in this study, i.e., $d_{ij|i\neq j}$ gives the food flow from i to j. Croft et al. (2018) list all the algorithm steps and also provide MATLAB code for implementing it to obtain the domestic supply matrix D.

C.3.7 Aggregate Food Categories Used in Figures

To prepare our results for visualization, we consolidated the original 102 categories (Supplementary Table C.8) into 37 broader groups using many-to-one mappings. In most cases, similar items were merged – so all types of bread became a single bread category. However, dairy alternatives were carved out from the broader dairy group – any product with no dairy ingredients but containing plant-based ingredients (coconut, nut, soy, oat, etc.) was reassigned into the dairy alternatives category. We also recategorized some mixed dishes based on composition, e.g., cereal based dishes such as pasta or pizza containing more than 20% of an animal

product (such as seafood, poultry) were moved into one of the meat categories, and specific meat products (e.g., poultry or pork) with less than 40% of the named animal ingredient (e.g., Thai red chicken curry) were reassigned into the meat dishes category. We used a quick manual review to flag obvious misclassifications, like a meat dish with no animal ingredients, or coffee beans classified into beans and pulses, and corrected them when the true composition was clear; otherwise, those items were dropped. In total, this recategorization process removed about 8,000 products from our analysis set.

In this consolidated view, meat, dairy, and eggs (25.3%) and cereal products (23.9%) together account for nearly half the sample. The rest breaks down into fruits, vegetables, and nuts (16.4%), miscellaneous items (14.2%), sugar and confectionery (10.9%), and non-alcoholic beverages (9.3%). Note that these categories can overlap, for example, some cereal products include meat and vegetables, and certain vegetable-based products contain grains like rice.

C.3.8 Confidence in Environmental Impact Estimates Across Geographies and Categories

We quantified confidence in each product's environmental-footprint estimate as the product of three scores: classification certainty, composition completeness, and LCA-data coverage.

Classification certainty reflects how confidently a product was assigned to its food category. All foodDB entries, which have been extensively validated, received a 95% certainty. For Open Food Facts, we started at 95% and adjusted based on model probabilities: if only the parent-category probability ≥ 0.5, certainty dropped to 90%; if only the subcategory probability ≥ 0.5, it dropped to 85%; and if both probabilities are below 0.5, it was 80%. These probabilities are the classification models' likelihood scores for each possible class, with the highest-scoring class chosen as the product's category.

Composition completeness measures how much of a product's ingredient breakdown comes directly from back-of-package data. We calculated it as: 50% + 0.5

× (% of ingredients by weight identified on the label), so that more complete labels yield higher confidence.

LCA-data coverage captures the extent to which each ingredient's source country has LCA data, with fallbacks to broader regions as needed. For each ingredient, we computed coverage as: (% supply covered by country LCA data × 1) + (% supply estimated using intermediate regional LCA data × 0.9) + (% supply estimated using sub-regional LCA data × 0.8) + (% supply estimated using regional LCA data × 0.7) + (% supply estimated using global LCA data × 0.6). For seafood ingredients, we calculated coverage as 0.5 × standard calculation + 0.5 × 70, to reflect wild-caught versus farmed sources. We then averaged these LCA-coverage scores across all ingredients, weighting by their identified composition share (so unidentified composition further lowered this score).

Finally, overall confidence for each product was calculated as the product of its three component scores. Figure 3.2 presents the average confidence by geography and food category – the colour bar in the figure is qualitative because the computed absolute scores are not interpretable on their own, but their relative ordering is. Supplementary Figure C.4 displays each component score separately, with numerical colour bars reflecting the actual calculated values. Classification scores remain high across all regions and categories. In contrast, composition scores are particularly low in the USA and Canada and exhibit substantial variation across categories worldwide. LCA coverage scores peak in Europe and are lowest in Africa. Although the absolute numbers depend on our scoring method and are not inherently meaningful, their relative ordering provides valuable insights into the disaggregated scores.

D

Supplementary Material for "The Impact of Dietary Transitions, Trade Policy and Climate Change on Food Production and Import-dependence through to 2050"

Contents

D.1 Supplementary Figures

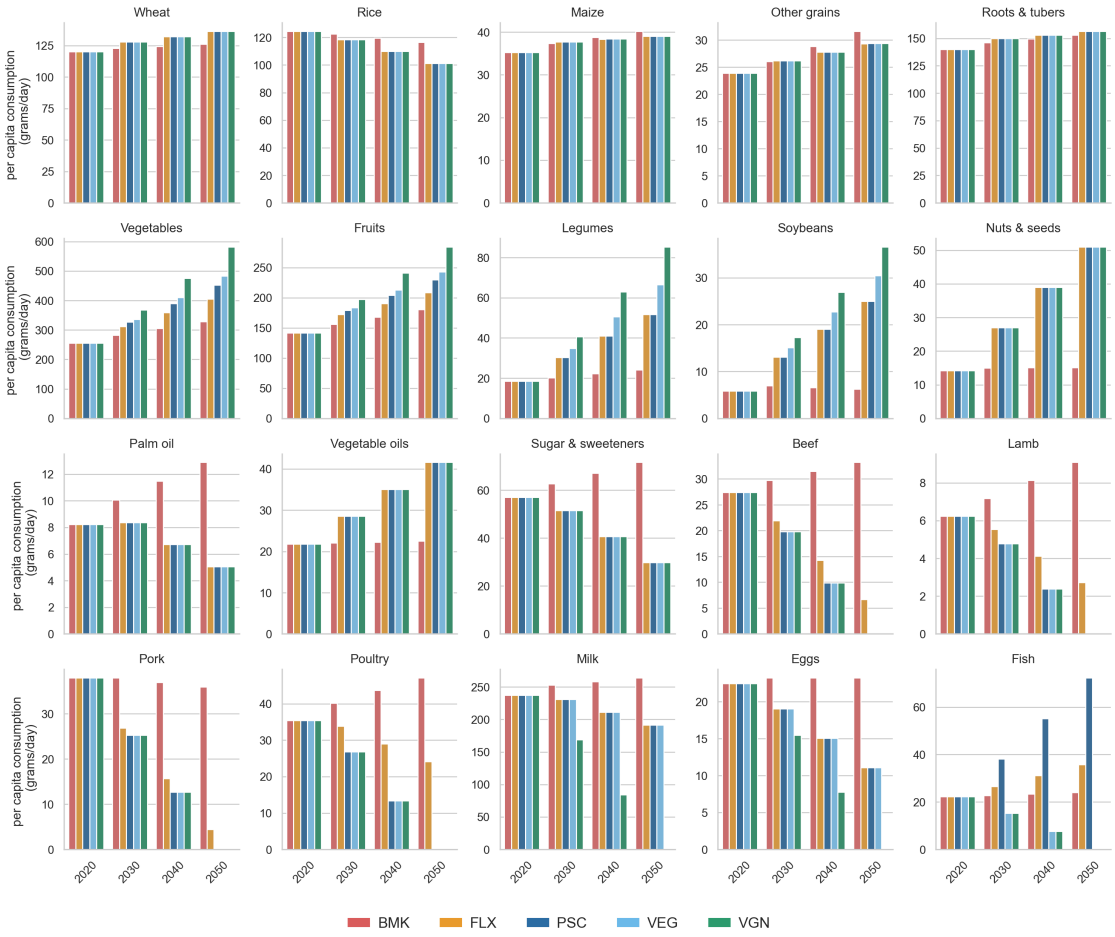

Figure D.1: Global average per-capita consumption of 20 food groups (plant and animal-based), under five dietary scenarios at a total energy intake of 2500 kcal/day. A 100% benchmark diet is assumed in 2020, with alternate diets phasing in to 100% adoption by 2050.

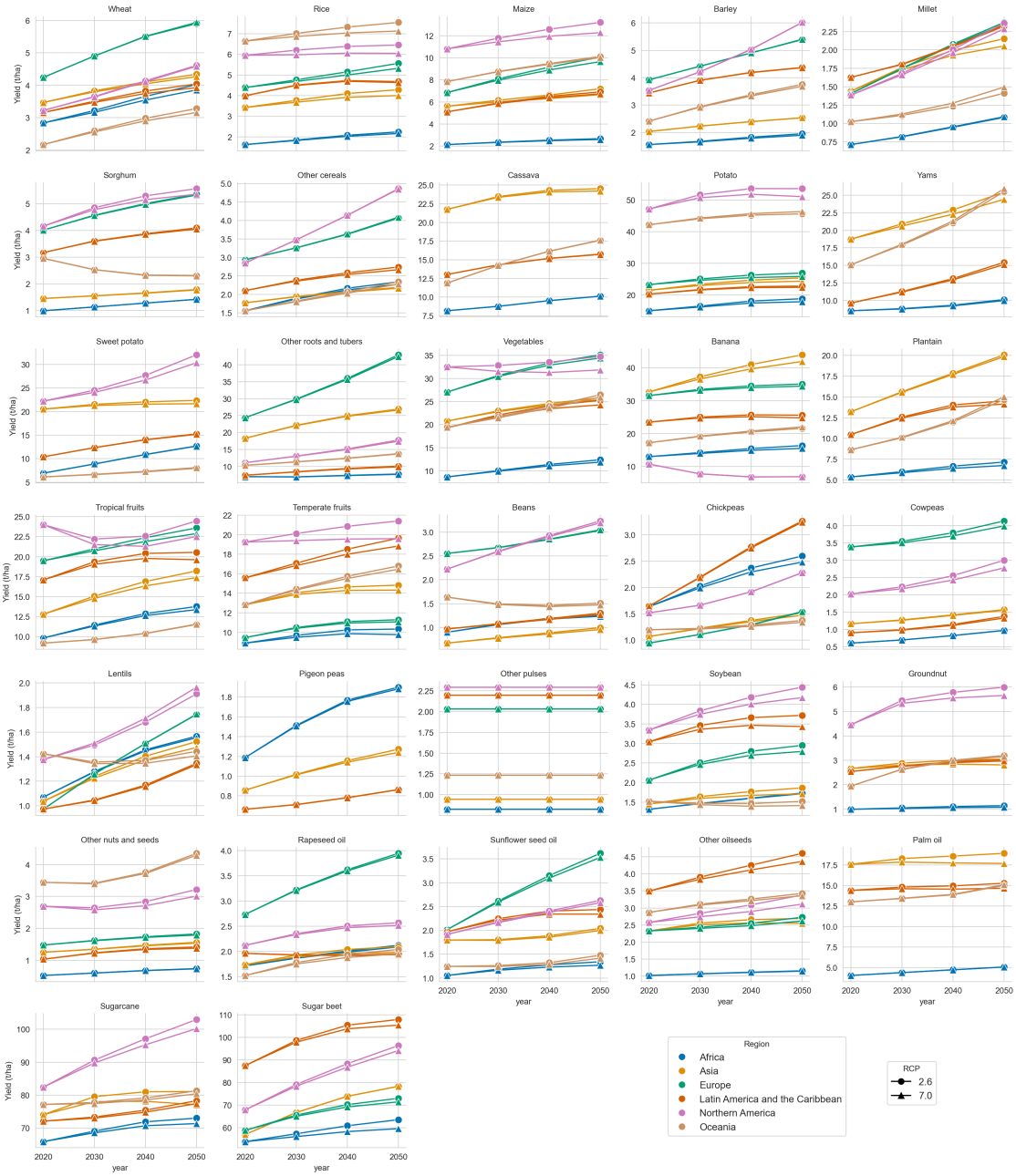

Figure D.2: Projected yield trajectories by crop category under RCP 2.6 and RCP 7.0, 2020–2050. Trajectories incorporate climate impacts and technological progress from the IMPACT model.

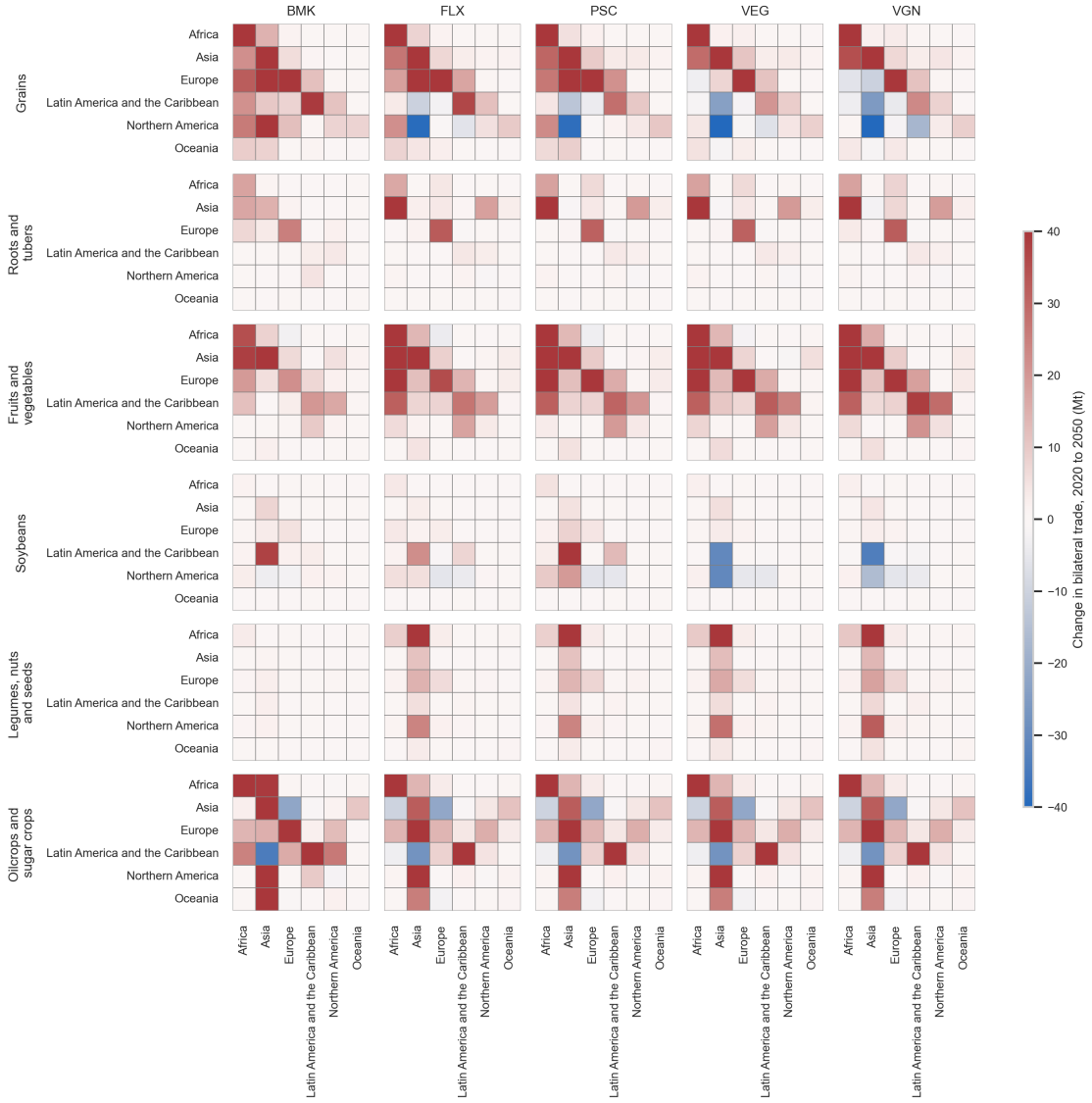

Figure D.3: Change in bilateral trade by 2050 relative to 2020 under high trade liberalization and RCP 2.6. Panels are organized by crop group and diet scenario, and values are aggregated to regions. In each panel, rows are exporting regions and columns are importing regions.

Figure D.4: Regional import dependence versus supplier concentration by crop group in 2050. Concentration is measured using HHI over imports, weighted by importer size. Points represent dietary and trade liberalization scenarios under RCP 2.6; 2020 baseline shown for comparison.

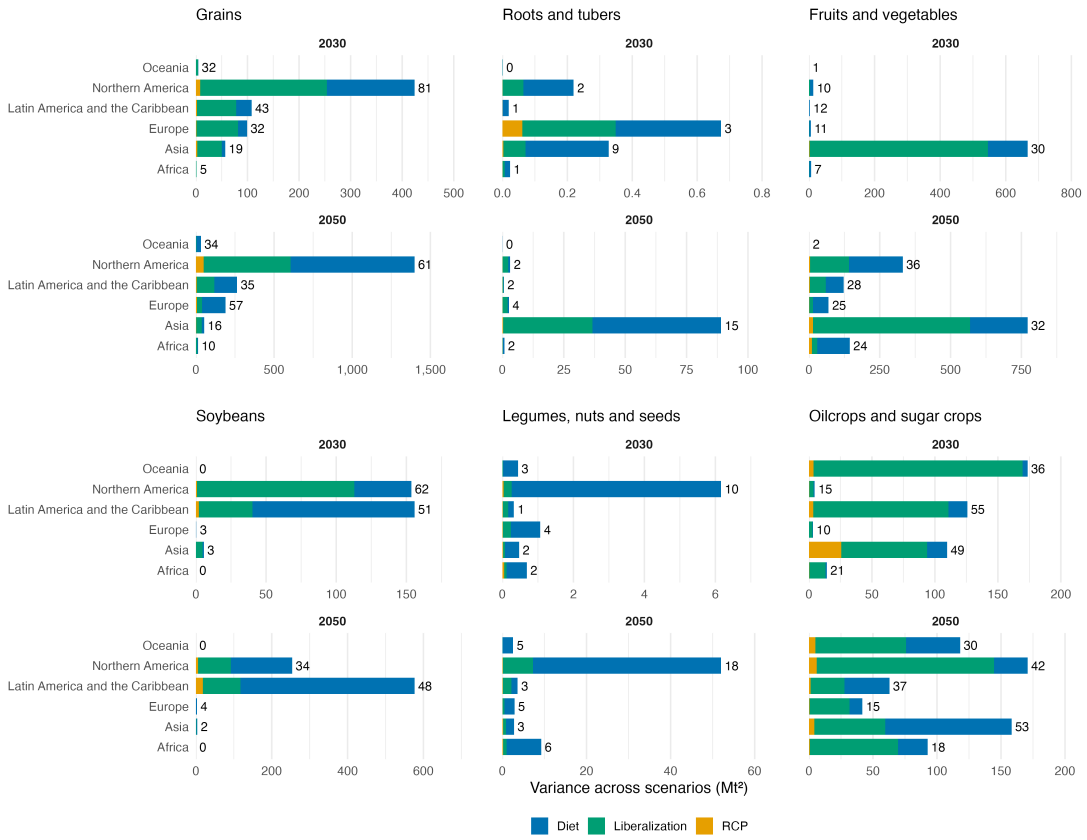

Figure D.5: Variance decomposition of projected exports by crop group for 2035 (top) and 2050 (bottom). Bars show the total variance across scenarios (Mt²) partitioned by dietary, trade, and climate drivers. Annotations show regional mean exports (Mt). Regional statistics are computed as variance-weighted averages of country-level values.

D.2 Supplementary Tables

Table D.1: Mapping between EAT-Lancet food groups, IMPACT crop categories, and FAO commodities for production and trade data.

Lancet food group	**IMPACT crop category**	**Production**	**Trade**	**Notes**
wheat	wheat	Wheat	Wheat, Germ of wheat, Wheat and meslin flour	
rice	rice	Rice	Rice, paddy (rice milled equivalent), Flour of rice	
maize	maize	Maize (corn)	Maize (corn), Germ of maize, Flour of maize, Bran of maize, Cake of maize, Forage and silage, maize	
other grains	barley	Barley	Barley, Barley flour and grits, Barley, pearled, Bran of barley, Pot barley	
	sorghum	Sorghum	Sorghum, Flour of sorghum, Bran of sorghum	
	millet	Millet	Millet, Flour of millet, Bran of millet	
	other cereals	Rye	Rye, Flour of rye, Bran of rye	
		Buckwheat	Buckwheat, Flour of buckwheat	
		Oats	Oats, Oats, rolled, Bran of oats	
		Quinoa	Quinoa	
		Canary seed	Canary seed	
		Fonio	Fonio	
		Mixed grain	Mixed grain, Flour of mixed grain, Bran of mixed grain	
		Triticale	Triticale	
		Cereals N.E.C.	Cereals n.e.c., Flour of cereals n.e.c., Bran of cereals n.e.c.	
roots	cassava	Cassava, fresh	Cassava, dry, Cassava, fresh, Flour of cassava, Starch of cassava, Tapioca of cassava	Processing factors applied to convert traded commodities into equivalent quantities of crops. Cassava dry: 2.5 Flour of cassava: 4 Starch of cassava: 5 Tapioca of cassava: 5 Tapioca of potatoes: 5
	potatoes	Potatoes	Potatoes, Potatoes, frozen, Tapioca of potatoes	
	sweet potatoes	Sweet potatoes	Sweet potatoes	
	yams	Yams	Yams	

Table D.1: Mapping between EAT-Lancet food groups, IMPACT crop categories, and FAO commodities for production and trade data. (Continued)

	other roots	Taro	Taro	
		Edible roots and tubers with high starch or inulin content, n.e.c., fresh	Edible roots and tubers with high starch or inulin content, n.e.c., fresh	
vegetables	vegetables	Artichokes	Artichokes	
		Asparagus	Asparagus	
		Broad beans and horse beans, green	Broad beans and horse beans, green	
		Cabbages	Cabbages	
		Carrots and turnips	Carrots and turnips	
		Cauliflowers and broccoli	Cauliflowers and broccoli	
		Chillies and peppers, green (Capsicum spp. and Pimenta spp.)	Chillies and peppers, green (Capsicum spp. and Pimenta spp.)	
		Cucumbers and gherkins	Cucumbers and gherkins	
		Eggplants (aubergines)	Eggplants (aubergines)	
		Green corn (maize)	Green corn (maize)	
		Green garlic	Green garlic	
		Leeks and other alliaceous vegetables	Leeks and other alliaceous vegetables	
		Lettuce and chicory	Lettuce and chicory	
		Mushrooms and truffles	Canned mushrooms, Dried mushrooms, Mushrooms and truffles	
		Okra	Okra	
		Onions and shallots, dry (excluding dehydrated)	Onions and shallots, dry (excluding dehydrated)	
		Onions and shallots, green	Onions and shallots, green	
		Other beans, green	Other beans, green	
		Other vegetables, fresh n.e.c.	Other vegetables, fresh n.e.c., Other vegetables provisionally preserved, Other vegetable juices, Sweet corn, frozen, Sweet corn, prepared or preserved, Vegetables frozen, Vegetables preserved (frozen), Vegetables preserved nes (o/t vinegar), Vegetables, dehydrated, Vegetable products, fresh or dry n.e.c., Vegetables, pulses and potatoes, preserved by vinegar or acetic acid	
		Peas, green	Peas, green	
		Pumpkins, squash and gourds	Pumpkins, squash and gourds	
		Spinach	Spinach	
		String beans	String beans	

Table D.1: Mapping between EAT-Lancet food groups, IMPACT crop categories, and FAO commodities for production and trade data. (Continued)

		Tomatoes	Paste of tomatoes, Tomato juice, Tomatoes, Tomatoes, peeled (o/t vinegar)	
fruits	bananas	Bananas	Bananas	For olives and coconuts: Production and trade split between fruits and oils. Oil converted to oil crops using processing factors.
	plantains	Plantains and cooking bananas	Plantains and cooking bananas	
	sub-tropical fruits	Apricots	Apricots, Apricots, dried	
		Avocados	Avocados	
		Cantaloupes and other melons	Cantaloupes and other melons	
		Cashewapple	Cashewapple	
		Dates	Dates	
		Figs	Figs, Figs, dried	
		Kiwi fruit	Kiwi fruit	
		Lemons and limes	Juice of lemon, Lemon juice, concentrated, Lemons and limes	
		Locust beans (carobs)	Locust beans (carobs)	
		Mangoes, guavas and mangosteens	Juice of mango, Mangoes, guavas and mangosteens, Mango pulp	
		Oranges	Orange juice, Orange juice, concentrated, Oranges	
		Other citrus fruit, n.e.c.	Citrus juice, concentrated n.e.c., Juice of citrus fruit n.e.c., Other citrus fruit, n.e.c.	
		Other fruits, n.e.c.	Fruit prepared n.e.c., Juice of fruits n.e.c., Other fruit n.e.c., dried, Other fruits, n.e.c., Raisins	
		Other tropical fruits, n.e.c.	Other tropical fruit, dried, Other tropical fruits, n.e.c.	
		Papayas	Papayas	
		Pineapples	Juice of pineapples, concentrated, Pineapple juice, Pineapples, Pineapples, otherwise prepared or preserved	
		Pomelos and grapefruits	Grapefruit juice, Grapefruit juice, concentrated, Pomelos and grapefruits	
		Tangerines, mandarins, clementines	Juice of tangerine, Tangerines, mandarins, clementines	
		Watermelons	Watermelons	
		Coconuts, in shell	Coconuts, in shell, Coconuts, desiccated, Coconut oil	
		Apples	Apple juice, Apple juice, concentrated, Apples	
		Blueberries	Blueberries	

Table D.1: Mapping between EAT-Lancet food groups, IMPACT crop categories, and FAO commodities for production and trade data. (Continued)

	temperate fruits	Cherries	Cherries	
		Cranberries	Cranberries	
		Currants	Currants	
		Grapes	Grape juice, Grapes	
		Gooseberries	Gooseberries	
		Other berries and fruits of the genus vaccinium n.e.c.	Other berries and fruits of the genus vaccinium n.e.c.	
		Other pome fruits		
		Other stone fruits	Other stone fruits	
		Peaches and nectarines	Peaches and nectarines	
		Pears	Pears	
		Persimmons	Persimmons	
		Plums and sloes	Plums and sloes, Plums, dried	
		Quinces	Quinces	
		Raspberries	Raspberries	
		Sour cherries	Sour cherries	
		Strawberries	Strawberries	
		Olives	Olives, Olives preserved, Olive oil	
legumes	beans	Bambara beans, dry	Bambara beans, dry	
		Beans, dry	Beans, dry	
		Broad beans and horse beans, dry	Broad beans and horse beans, dry	
	chickpeas	Chick peas, dry	Chick peas, dry	
	cowpeas	Cow peas, dry	Cow peas, dry	
	lentils	Lentils, dry	Lentils, dry	
	pigeon peas	Pigeon peas, dry	Pigeon peas, dry	
	other pulses	Other pulses n.e.c.	Flour of pulses, Other pulses n.e.c.	
		Peas, dry	Peas, dry	
		Lupins		
		Vetches		
soybeans		Soya beans	Cake of soya beans, Soya beans, Soya curd, Soya paste, Soya sauce, Soya bean oil	
nuts and seeds	groundnuts	Groundnuts, excluding shelled	Groundnuts, excluding shelled, Groundnuts, shelled, Prepared groundnuts, Groundnut oil	For groundnuts, linseed, hempseed, sunflower seed, safflower seed, sesame seed: Production and trade split between nuts seeds and oils. Oil converted to oil crops using processing factors.
	other	Almonds, in shell	Almonds, in shell, Almonds, shelled	
		Brazil nuts, in shell	Brazil nuts, in shell, Brazil nuts, shelled	
		Cashew nuts, in shell	Cashew nuts, in shell, Cashew nuts, shelled	
		Chestnuts, in shell	Chestnuts, in shell	
		Hazelnuts, in shell	Hazelnuts, in shell, Hazelnuts, shelled	
		Other nuts (excluding wild edible nuts and groundnuts), in shell, n.e.c.	Other nuts (excluding wild edible nuts and groundnuts), in shell, n.e.c.	

Table D.1: Mapping between EAT-Lancet food groups, IMPACT crop categories, and FAO commodities for production and trade data. (Continued)

		Pistachios, in shell	Pistachios, in shell	
		Walnuts, in shell	Walnuts, in shell, Walnuts, shelled	
		Linseed	Linseed, Oil of linseed	
		Hempseed	Hempseed	
		Sunflower seed	Sunflower seed, Sunflower-seed oil, crude	
		Safflower seed	Safflower seed, Safflower-seed oil, crude	
		Poppy seed	Poppy seed	
		Sesame seed	Sesame seed, Oil of sesame seed	
vegetable oil	rapeseed	Rape or colza seed	Rape or colza seed, Rapeseed or canola oil, crude	For olives, coconuts, groundnuts, linseed, hempseed, sunflower seed, safflower seed, sesame seed: Production and trade split between oils and fruits/nuts seeds. Oil converted to oil crops using processing factors.
	sunflower seed	Sunflower seed	Sunflower seed, Sunflower-seed oil, crude	
	other oilcrops	Groundnuts, excluding shelled	Groundnuts, excluding shelled, Groundnuts, shelled, Prepared groundnuts, Groundnut oil	
		Linseed	Linseed, Oil of linseed	
		Hempseed	Hempseed	
		Safflower seed	Safflower seed, Safflower-seed oil, crude	
		Sesame seed	Sesame seed, Oil of sesame seed	
		Castor oil seeds	Castor oil seeds, Oil of castor beans	
		Cotton seed	Cottonseed oil	
		Coconuts, in shell	Coconuts, in shell, Coconuts, desiccated, Coconut oil	
		Mustard seed	Mustard seed, Mustard seed oil, crude	
		Olives	Olives, Olives preserved, Olive oil	
palm oil	palm oil	Oil palm fruit	Palm oil	Oil converted to oil crops using processing factors.
sugar	sugar beet	Sugar beet	Sugar beet, Refined sugar, Raw cane or beet sugar (centrifugal only)	Sugar converted to sugar crops using processing factors. Refined sugar and raw sugar flows split between sugar cane and sugar beet.
	sugarcane	Sugar cane	Sugar cane, Refined sugar, Raw cane or beet sugar (centrifugal only)	

Table D.2: Mapping of IMPACT regions to FAO countries and aggregated regional groupings.

IMPACT region code	IMPACT region name	Country	Intermediate Region Name	Sub-region Name	Region Name
DZA	Algeria	Algeria			
EGY	Egypt	Egypt			
LBY	Libya	Libya		Northern Africa	Africa
MOR	Morocco	Morocco			
SDN	Sudan	Sudan			
TUN	Tunisia	Tunisia			
BDI	Burundi	Burundi			
DJI	Djibouti	Djibouti			
ERI	Eritrea	Eritrea			
ETH	Ethiopia	Ethiopia			
KEN	Kenya	Kenya			
MDG	Madagascar	Madagascar			
MOZ	Mozambique	Mozambique			
MWI	Malawi	Malawi			
OIO	Other Indian Ocean	Comoros			
OIO	Other Indian Ocean	Mauritius	Eastern Africa	Sub-Saharan Africa	Africa
OIO	Other Indian Ocean	Seychelles			
RWA	Rwanda	Rwanda			
SOM	Somalia	Somalia			
SSD	Southern Sudan	South Sudan			
TZA	United Republic of Tanzania	United Republic of Tanzania			
UGA	Uganda	Uganda			
ZMB	Zambia	Zambia			
ZWE	Zimbabwe	Zimbabwe			
AGO	Angola	Angola			
CAF	Central African Republic	Central African Republic			
CMR	Cameroon	Cameroon			
COD	Democratic Republic of the Congo	Democratic Republic of the Congo			
COG	Congo	Congo	Middle Africa	Sub-Saharan Africa	Africa
GAB	Gabon	Gabon			
GNQ	Equatorial Guinea	Equatorial Guinea			
OAO	Other Atlantic Ocean	Sao Tome and Principe			
TCD	Chad	Chad			
BWA	Botswana	Botswana			
LSO	Lesotho	Lesotho			
NAM	Namibia	Namibia	Southern Africa	Sub-Saharan Africa	Africa
SWZ	Swaziland	Eswatini			
ZAF	South Africa	South Africa			

Continued on next page

Table D.2: Mapping of IMPACT regions to FAO countries and aggregated regional groupings. (Continued)

BEN	Benin	Benin	Western Africa	Sub-Saharan Africa	Africa
BFA	Burkina Faso	Burkina Faso			
CIV	Côte d'Ivoire	Côte d'Ivoire			
GHA	Ghana	Ghana			
GIN	Guinea	Guinea			
GMB	Gambia	Gambia			
GNB	Guinea-Bissau	Guinea-Bissau			
LBR	Liberia	Liberia			
MLI	Mali	Mali			
MRT	Mauritania	Mauritania			
NER	Niger	Niger			
NGA	Nigeria	Nigeria			
OAO	Other Atlantic Ocean	Cabo Verde			
SEN	Senegal	Senegal			
SLE	Sierra Leone	Sierra Leone			
TGO	Togo	Togo			
CRB	Other Caribbean	Antigua and Barbuda	Caribbean	Latin America and the Caribbean	Americas
CRB	Other Caribbean	Bahamas			
CRB	Other Caribbean	Barbados			
CRB	Other Caribbean	Dominica			
CRB	Other Caribbean	Grenada			
CRB	Other Caribbean	Puerto Rico			
CRB	Other Caribbean	Saint Kitts and Nevis			
CRB	Other Caribbean	Saint Lucia			
CRB	Other Caribbean	Saint Vincent and the Grenadines			
CRB	Other Caribbean	Trinidad and Tobago			
CUB	Cuba	Cuba			
DOM	Dominican Republic	Dominican Republic			
HTI	Haiti	Haiti			
JAM	Jamaica	Jamaica			
BLZ	Belize	Belize	Central America	Latin America and the Caribbean	Americas
CRI	Costa Rica	Costa Rica			
GTM	Guatemala	Guatemala			
HND	Honduras	Honduras			
MEX	Mexico	Mexico			
NIC	Nicaragua	Nicaragua			
PAN	Panama	Panama			
SLV	El Salvador	El Salvador			

Continued on next page

Table D.2: Mapping of IMPACT regions to FAO countries and aggregated regional groupings. (Continued)

ARG	Argentina	Argentina	South America	Latin America and the Caribbean	Americas
BOL	Bolivia	Bolivia			
BRA	Brazil	Brazil			
CHL	Chile	Chile			
COL	Colombia	Colombia			
ECU	Ecuador	Ecuador			
GSA	Guyanas South America	Guyana			
GSA	Guyanas South America	Suriname			
PER	Peru	Peru			
PRY	Paraguay	Paraguay			
URY	Uruguay	Uruguay			
VEN	Venezuela	Venezuela			
CAN	Canada	Canada		Northern America	Americas
USA	United States of America	United States of America			
KAZ	Kazakhstan	Kazakhstan		Central Asia	Asia
KGZ	Kyrgyzstan	Kyrgyzstan			
TJK	Tajikistan	Tajikistan			
TKM	Turkmenistan	Turkmenistan			
UZB	Uzbekistan	Uzbekistan			
CHM	China	China		Eastern Asia	Asia
CHM	China	Hong Kong			
CHM	China	Macao			
CHM	China	Taiwan			
JPN	Japan	Japan			
KOR	Republic of Korea	Republic of Korea			
MNG	Mongolia	Mongolia			
PRK	Democratic People's Republic of Korea	Democratic People's Republic of Korea			
IDN	Indonesia	Indonesia		South-eastern Asia	Asia
KHM	Cambodia	Cambodia			
LAO	Lao People's Democratic Republic	Lao People's Democratic Republic			
MMR	Myanmar	Myanmar			
MYS	Malaysia	Malaysia			
OSA	Other Southeast Asia	Brunei Darussalam			
OSA	Other Southeast Asia	Singapore			
PHL	Philippines	Philippines			
THA	Thailand	Thailand			
TLS	Timor-Leste	Timor-Leste			
VNM	Viet Nam	Viet Nam			

Continued on next page

Table D.2: Mapping of IMPACT regions to FAO countries and aggregated regional groupings. (Continued)

AFG	Afghanistan	Afghanistan		Southern Asia	Asia
BGD	Bangladesh	Bangladesh			
BTN	Bhutan	Bhutan			
IND	India	India			
IRN	Iran	Iran			
LKA	Sri Lanka	Sri Lanka			
NPL	Nepal	Nepal			
OIO	Other Indian Ocean	Maldives			
PAK	Pakistan	Pakistan			
ARM	Armenia	Armenia		Western Asia	Asia
AZE	Azerbaijan	Azerbaijan			
CYP	Cyprus	Cyprus			
GEO	Georgia	Georgia			
IRQ	Iraq	Iraq			
ISR	Israel	Israel			
JOR	Jordan	Jordan			
LBN	Lebanon	Lebanon			
PSE	State of Palestine	State of Palestine			
RAP	Rest of Arab Peninsula	Bahrain			
RAP	Rest of Arab Peninsula	Kuwait			
RAP	Rest of Arab Peninsula	Oman			
RAP	Rest of Arab Peninsula	Qatar			
RAP	Rest of Arab Peninsula	United Arab Emirates			
SAU	Saudi Arabia	Saudi Arabia			
SYR	Syrian Arap Republic	Syrian Arab Republic			
TUR	Turkey	Turkey			
YEM	Yemen	Yemen			
BGR	Bulgaria	Bulgaria		Eastern Europe	Europe
BLR	Belarus	Belarus			
CZE	Czech Republic	Czechia			
HUN	Hungary	Hungary			
MDA	Moldova	Republic of Moldova			
POL	Poland	Poland			
ROU	Romania	Romania			
RUS	Russian Federation	Russian Federation			
SVK	Slovakia	Slovakia			
UKR	Ukraine	Ukraine			

Continued on next page

Table D.2: Mapping of IMPACT regions to FAO countries and aggregated regional groupings. (Continued)

BLT	Baltic States	Estonia		Northern Europe	Europe
BLT	Baltic States	Latvia			
BLT	Baltic States	Lithuania			
DNK	Denmark	Denmark			
DNK	Denmark	Faroe Islands			
FNP	Finland	Finland			
IRL	Ireland	Ireland			
ISL	Iceland	Iceland			
NOR	Norway	Norway			
SWE	Sweden	Sweden			
UKP	United Kingdom	United Kingdom			
ALB	Albania	Albania		Southern Europe	Europe
GRC	Greece	Greece			
HRV	Croatia	Croatia			
ITP	Italy	Italy			
ITP	Italy	Malta			
OBN	Other Balkans	Bosnia and Herzegovina			
OBN	Other Balkans	Montenegro			
OBN	Other Balkans	North Macedonia			
OBN	Other Balkans	Serbia			
PRT	Portugal	Portugal			
SPP	Spain	Spain			
SVN	Slovenia	Slovenia			
AUT	Austria	Austria		Western Europe	Europe
BLX	Belgium and Luxembourg	Belgium			
BLX	Belgium and Luxembourg	Luxembourg			
CHP	Switzerland	Switzerland			
DEU	Germany	Germany			
FRP	France	France			
NLD	Netherlands	Netherlands			
AUS	Australia	Australia		Australia and New Zealand	Oceania
NZL	New Zealand	New Zealand			
FJI	Fiji	Fiji		Melanesia	Oceania
OPO	Other Pacific Ocean	New Caledonia			
PNG	Papua New Guinea	Papua New Guinea			
SLB	Solomon Islands	Solomon Islands			
VUT	Vanuatu	Vanuatu			
OPO	Other Pacific Ocean	Kiribati		Micronesia	Oceania
OPO	Other Pacific Ocean	Marshall Islands			
OPO	Other Pacific Ocean	Micronesia			
OPO	Other Pacific Ocean	Nauru			

Continued on next page

Table D.2: Mapping of IMPACT regions to FAO countries and aggregated regional groupings. (Continued)

OPO	Other Pacific Ocean	Cook Islands		Polynesia	Oceania
OPO	Other Pacific Ocean	French Polynesia			
OPO	Other Pacific Ocean	Niue			
OPO	Other Pacific Ocean	Samoa			
OPO	Other Pacific Ocean	Tokelau			
OPO	Other Pacific Ocean	Tonga			
OPO	Other Pacific Ocean	Tuvalu			

Table D.3: FAO Commodities used to compute production and trade of animal products for allocation of feed.

Lancet Food group	**Production**	**Trade**	**Notes**
beef	Beef and Buffalo Meat, primary	Bovine meat, salted, dried or smoked Meat of buffalo, fresh or chilled Meat of cattle boneless, fresh or chilled Meat of cattle with the bone, fresh or chilled Sausages and similar products of meat, offal or blood of beef and veal	
milk	Milk, total	Butter and Ghee Buttermilk, curdled and acidified milk Buttermilk, dry Cheese from whole cow milk Cream, fresh Evaporated & Condensed Milk Ghee from cow milk Processed cheese Raw milk of cattle Skim Milk & Buttermilk, Dry Skim milk and whey powder Skim milk of cows Whey, fresh and dry (milk equivalent) Whole milk powder Whole milk, evaporated Butter of cow milk Cheese from skimmed cow milk Skim milk, condensed Whey cheese Whole milk, condensed Cheese from milk of sheep, fresh or processed Skim milk, evaporated	No processing factors were applied to processed items, and by-products weren't removed resulting in approximate milk equivalent in total amounts
poultry	Meat, Poultry	Meat of chickens, fresh or chilled Meat of ducks, fresh or chilled Meat of geese, fresh or chilled Meat of pigeons and other birds n.e.c., fresh, chilled or frozen Meat of turkeys, fresh or chilled Poultry meat preparations	
eggs	Eggs, Primary	Hen eggs in shell, fresh Eggs from other birds in shell, fresh, n.e.c. Eggs, dried Eggs, liquid	
pork	Meat of pig with the bone, fresh or chilled	Meat of pig boneless, fresh or chilled Meat of pig with the bone, fresh or chilled Pig meat, cuts, salted, dried or smoked (bacon and ham) Sausages and similar products of meat, offal or blood of pig	
lamb	Sheep and Goat Meat	Meat of goat, fresh or chilled Meat of sheep, fresh or chilled	

Table D.4: Mapping between EAT-Lancet food groups and FAOSTAT sources (FBS or SUA) used for computing demand for 'other' uses.

EAT-Lancet food group	**FAOSTAT source**	**Commodity name**	**Notes**
wheat	FBS	Wheat and products	Processing included in the food category
rice	FBS	Rice and products	
maize	FBS	Maize and products	
other grains	FBS	Barley and products	
		Sorghum and products	
		Rye and products	
		Oats	
		Millet and products	
		Cereals, Other	
roots	FBS	Starchy Roots	
vegetables	FBS	Vegetables	
fruits	FBS	Fruits	
legumes	FBS	Pulses	
soybeans	SUA	Soya beans	Processing for beans equals total supply for other soy products (curd, paste, sauce, oil, cake). Hence, processing for beans ignored. Food, feed, and other aggregated for the 4 soy categories.
		Soya curd	
		Soya paste	
		Cake of soya beans	
		Soya bean oil	
		Soya sauce	
nuts and seeds	FBS	Nuts and products	This includes treenuts. Processing already 0.
	SUA	Groundnuts, excluding shelled	Processing from unshelled groundnuts ignored (it approximately equals the total supply of all groundnut-based commodities, i.e. shelled, prepared, cake, and oil). Processing from shelled groundnuts included in food.
		Groundnuts, shelled	
		Prepared groundnuts	
		Linseed	Processing ignored for all (as it approximately equals the total supply for the oils and cakes produced from these seeds). Melon seeds not included here, as they are not specifically produced for the purpose of seeds.
		Hempseed	
		Sunflower seed	
		Safflower seed	
		Poppy seed	
		Sesame seed	
vegetable oil	SUA	Groundnut oil	All these oils have a corresponding SUA commodity for 'cake'. Total supply for oil and cake together gives an estimate for the required supply of these oil crops.
		Oil of linseed	
		Oil of hempseed	
		Sunflower seed oil, crude	
		Safflower seed oil, crude	
		Oil of sesame seed	
		Cottonseed oil	
		Mustard seed oil, crude	
		Rapeseed or canola oil, crude	
		Oil of castor beans	Processing for castor oil seeds gives the estimated oil crop supply
		Castor oil, hydrogenated	

Table D.4: Mapping between EAT-Lancet food groups and FAOSTAT sources (FBS or SUA) used for computing demand for 'other' uses. (Continued)

		Olive oil	Processing for olives, ignoring the processed amount going towards preserved olives, gives the estimated oil crop supply.
		Coconut oil	No clear commodity to estimate by-products. Oil crop supply assumed to be the same as oil supply. Processing included in the food category.
			Other uses for oil crops before processing ignored, unless there is an overlap with other food groups, in which case other uses for the crops in those other food groups considered.
palm oil	SUA	Palm Oil	Processing included in the food category. Processing for oil palm fruit gives the estimated oil crop supply. Kernels not included separately to compute oil crop supply (as they are by-products of palm fruit). Other uses for palm oil crops before processing ignored.
		Oil of palm kernel	
sugar	FBS	Sugar crops	Processing included in the food category (for both). Domestic supply of sugar and sweeteners / Processing for sugar crops gives the conversion factor between sugar and sugar crops. Other calculated for both, i.e. other uses for sugar crops before processing also considered.
		Sugar and sweeteners	

Table D.5: Mapping between Harmonized System (HS) codes and IMPACT crop categories for bilateral tariff data.

Lancet Food group	**IMPACT food group**	**HS codes**	**Notes**
wheat	wheat	100111, 100119, 100191, 100199	Flour, starch, gluten, groats, bran etc. not considered.
rice	rice	100610, 100620, 100630, 100640	
maize	maize	100510, 100590	Flour, starch, groats, bran etc. not considered.
other grains	barley	100310, 100390	
	sorghum	100710, 100790	
	millet	100821, 100829	
	other cereals	100210, 100290, 100410, 100490, 100810, 100830, 100840, 100850, 100860, 100890	
roots	cassava	071410	
	potatoes	070110, 070190, 071010	
	sweet potatoes	071420	
	yams	071430	
	other roots	071440, 071450, 071490	
vegetables	vegetables	070200, 070310, 070320, 070390, 070410, 070420, 070490, 070511, 070519, 070521, 070529, 070610, 070690, 070700, 070810, 070820, 070890, 070920, 070930, 070940, 070951, 070959, 070960, 070970, 070991, 070992, 070993, 070999, 071021, 071029, 071030, 071040, 071080, 071140, 071151, 071159, 071190, 071220, 071231, 071232, 071233, 071239, 071290	Vegetable preparations not considered
fruits	bananas	080390	Fruit preparations not considered
	plantains	080310	
	sub-tropical fruits	080410, 080420, 080430, 080440, 080450, 080510, 080521, 080522, 080529, 080540, 080550, 080590, 080711, 080719, 080720, 080910, 081050, 081060, 081090, 081310, 080111, 080112, 080119	
	temperate fruits	071120, 080610, 080620, 080810, 080830, 080840, 080921, 080929, 080930, 080940, 081010, 081020, 081030, 081040, 081070, 081110, 081120, 081190, 081210, 081290, 081320, 081330, 081340	
legumes	beans	071331, 071332, 071333, 071334, 071350	
	chickpeas	071320	
	cowpeas	071335	
	lentils	071340	
	pigeon peas	071360	
	other pulses	071310, 071339, 071390, 110610	
soybeans	soybeans	120110, 120190, 120810, 150710, 150790, 210310, 230400	
nuts and seeds	groundnuts	120230, 120241, 120242	
	other	081350, 080121, 080122, 080131, 080132, 080211, 080212, 080231, 080232, 080241, 080242, 080251, 080252, 080261, 080262, 080270, 080280, 080290, 120400, 120600, 120740, 120760, 120791, 120799	

Continued on next page

Table D.5: Mapping between Harmonized System (HS) codes and IMPACT crop categories for bilateral tariff data. (Continued)

vegetable oil	rapeseed	100510, 120590, 151411, 151419, 151491, 151499	Includes both oils and oil crops
	sunflower seed	120600, 151211, 151219	
	other oilcrops	120230, 120241, 120242, 120400, 120721, 120729, 120730, 120740, 120750, 120760, 120799, 150810, 150890, 150910, 150990, 151000, 151221, 151229, 151311, 151319, 151511, 151519, 151530, 151550, 151590	
palm oil	palm oil	120710, 151110, 151190, 151321, 151329	Includes both oils and oil crops
sugar	sugar beet	121291, 170112	Includes both sugar and sugar crops. Sugar confectionary not considered.
	sugarcane	121293, 170113, 170114	

Table D.6: Calibration performance for the baseline Spatial Price Equilibrium Model (SPEM).

Crop	Trade links			Trade flows		Demand R2	Supply R2	Producer price R2	Transport cost R2
	Accuracy	Precision	Recall	R2	RMSE (tonnes)				
wheat	0.90	0.87	0.73	0.99	1184	0.99	0.99	0.78	0.98
rice	0.90	0.93	0.46	0.99	1041	0.99	0.99	0.97	0.99
maize	0.89	0.86	0.60	0.99	1034	0.99	0.99	0.97	0.98
barley	0.92	0.59	0.58	0.99	1006	0.99	0.99	0.93	0.99
millet	0.95	0.32	0.27	0.99	307	0.99	0.99	0.99	0.99
sorghum	0.87	0.20	0.70	0.99	1057	0.99	0.99	0.90	0.99
other cereals	0.90	0.87	0.44	0.99	624	0.99	0.99	0.96	0.99
cassava	0.94	0.69	0.38	0.99	760	0.99	0.99	0.97	0.99
potato	0.87	0.86	0.43	0.99	998	0.99	0.99	0.91	0.99
yams	0.98	0.30	0.38	0.99	201	0.99	0.99	0.99	0.99
sweet potato	0.96	0.61	0.35	0.99	309	0.99	0.99	0.99	0.99
other roots and tubers	0.97	0.37	0.29	0.99	478	0.99	0.99	0.99	0.99
vegetables	0.66	0.95	0.31	0.99	1212	0.99	0.99	0.77	0.98
bananas	0.96	0.75	0.56	0.99	520	0.99	0.99	0.97	0.99
plantains	0.97	0.34	0.53	0.99	486	0.99	0.99	0.81	0.99
sub-tropical fruits	0.68	0.94	0.32	0.99	1167	0.99	0.99	0.93	0.98
temperate fruits	0.80	0.88	0.31	0.99	2197	0.99	0.99	0.96	0.98
beans	0.83	0.59	0.25	0.99	909	0.99	0.99	0.92	0.99
chickpeas	0.95	0.65	0.31	0.99	432	0.99	0.99	0.96	0.99
cowpeas	0.97	0.31	0.19	0.99	323	0.99	0.99	0.99	0.99
lentils	0.96	0.67	0.37	0.99	209	0.99	0.99	0.99	0.99
pigeon peas	0.98	0.30	0.32	0.99	267	0.99	0.99	0.99	0.99
other pulses	0.87	0.75	0.24	0.99	1101	0.99	0.99	0.99	0.99
soybeans	0.89	0.72	0.56	0.99	853	0.99	0.99	0.84	0.99
groundnuts	0.93	0.80	0.37	0.99	910	0.99	0.99	0.99	0.99
other nuts	0.76	0.86	0.24	0.99	2521	0.99	0.99	0.99	0.96
rapeseed	0.90	0.76	0.41	0.99	392	0.99	0.99	0.90	0.99
sunflower seed oil	0.90	0.84	0.42	0.99	457	0.99	0.99	0.97	0.99
other oilseeds	0.80	0.84	0.42	0.99	1640	0.99	0.99	0.96	0.99
palm oil fruit	0.88	0.49	0.62	0.99	1061	0.99	0.99	0.86	0.99
sugar beet	0.92	0.77	0.65	0.99	446	0.99	0.99	0.95	0.99
sugarcane	0.89	0.68	0.57	0.99	4332	0.99	0.99	0.92	0.99

D.3 Supplementary Methods

D.3.1 Trade data processing

We obtained national-level production and bilateral trade data from the FAO. The raw data requires pre-processing to address two key discrepancies: i) the trade volumes reported by the importing countries did not always match those reported by the exporting countries, and ii) the total reported exports from some countries exceeded the volumes produced and imported together, because of misreported transactions or countries reporting re-exported imports as their exports.

Reliability index approach

Discrepancies between the volume of trade reported by the importer and exporter are resolved using a reliability index approach (Gehlhar, 1996). An accuracy level (AL) is computed for each bilateral trading pair, capturing the quality of match between importer and exporter reported quantities. A threshold of 0.2 is used to separate accurate from non-accurate matches (i.e., a match is accurate only if the difference between reported imports and exports is less than 20%).

The accuracy level for a transaction from region r to region s is calculated as:

$$AL_{r,s} = 2 \times \frac{|M_{r,s} - X_{r,s}|}{M_{r,s} + X_{r,s}} \tag{D.3.1.1}$$

where $M_{r,s}$ is the value of trade reported by the importer and $X_{r,s}$ is that reported by the exporter.

For each country, an importer reliability index (RIM), and an exporter reliability index (RIX), are constructed. An importer's reliability is measured by the proportion of total imports it reports accurately:

$$RIM_s = \frac{M_s^A}{M_s^T} \tag{D.3.1.2}$$

where M_s^T equals total imports to country s, and M_s^A equals the sum of imports to country s where $AL_{r,s} \leq 0.2$.

Similarly, an exporter's reliability is:

$$RIX_r = \frac{X_r^A}{X_r^T} \tag{D.3.1.3}$$

where X_r^T equals total exports from country r, and X_r^A equals the sum of exports from country r where $AL_{r,s} \leq 0.2$.

For each bilateral trading pair, the value reported by the more reliable partner is accepted as the trade flow between those countries.

Re-export algorithm

The bilateral trade dataset harmonized using the reliability index approach is fed into a re-export algorithm along with the production dataset from the FAO. The re-export algorithm proposed by (Croft et al., 2018) ensures that the total exports from a country never exceed its production and total imports; and it also links the source of production with the destination of import. The algorithm uses the production vector P and export matrix E, and applies an iterative approach to produce a domestic supply matrix D.

$$P = \begin{bmatrix} p_1 \\ p_2 \\ \vdots \\ p_n \end{bmatrix}, \qquad E = \begin{bmatrix} 0 & e_{12} & \dots & e_{1n} \\ e_{21} & 0 & \dots & e_{2n} \\ \vdots & \vdots & \ddots & \vdots \\ e_{n1} & e_{n2} & \dots & 0 \end{bmatrix}, \qquad D = \begin{bmatrix} d_{11} & d_{12} & \dots & d_{1n} \\ d_{21} & d_{22} & \dots & d_{2n} \\ \vdots & \vdots & \ddots & \vdots \\ d_{n1} & d_{n2} & \dots & d_{nn} \end{bmatrix}$$

where, p_i is the production in country i; e_{ij} are the exports from country i to j; and d_{ij} is the quantity of country j's consumption that originates from country i. The sum of rows of matrix D equals the countries' production, and the sum of columns equals the countries' consumption. The diagonal elements correspond to the produce that stays within the countries. The non-diagonal elements of matrix D ($d_{ij|i\neq j}$) represent trade flow from i to j.

Commodity mapping

Supplementary Table D.1 provides the complete mapping between 13 EAT-Lancet food groups, 32 IMPACT crop categories, and FAO commodities (~120 produced, over 150 traded). The reliability index and re-export preprocessing

steps were implemented separately for each FAO commodity and year. For each commodity, we aggregated trade data across both unprocessed and processed forms (e.g., for wheat: wheat grain, wheat germ, and wheat and meslin flour). The harmonized data for all FAO commodities within each IMPACT crop category were summed by year, then averaged across 2013-2017 and 2018-2022. The calibration uses the earlier period to initialize trade patterns and the later period as the calibration target.

For most processed commodities that are traded, we assume that the main products and their by-products balance each other – so no conversion factors are applied, e.g. wheat germ and flour, soybean oil and cake. For certain traded items, however, we apply conversion factors to align them with their produced counterparts. For example, dry cassava, cassava flour, cassava starch and tapioca are converted to fresh cassava using factors of 2.5, 4, 5, and 5, respectively (Chisenga et al., 2019; Elisabeth et al., 2022; Mejía-Agüero et al., 2012), and potato tapioca is converted to fresh potato with a factor of 5 (Robertson et al., 2018). We also derived global average conversion factors for oils and sugars (excluding soybean oil, since its cake by-product is also traded, which offsets the oil conversion) using FAOSTAT Food Balance Sheets (FBS) and Supply Utilization Accounts (SUA). For each oil, the factor equals the ratio of global oil + cake supply to oil supply (as given by SUA). For sugars, it is the ratio of globally processed sugar crops to total supply of sugars and sweeteners (as given by FBS). Processing factors are calculated as global averages to avoid inconsistencies arising from differential trade patterns for raw versus processed commodities.

To avoid double counting across overlapping EAT-Lancet food groups, we used FAOSTAT Supply Utilization Accounts (SUA) to split production and trade between processed and unprocessed products for the following commodities – olives, coconuts, groundnuts, linseed, hempseed, sunflower seed, safflower seed, and sesame seed. For each producing country, we calculated the share of each commodity processed into oil and applied those shares to the country's production and exports. The processed shares became the volumes for products such as coconut oil or groundnut

oil, and the remainder represented the unprocessed commodity (e.g., coconuts or groundnuts). Finally, because FAOSTAT trade data does not distinguish between raw and refined sugar from sugar cane vs sugar beet, we split raw and refined sugar exports in proportion to each country's sugar cane and sugar beet production.

Region mapping

The IMPACT model uses 158 regions identified by three-letter abbreviations. Of these, 157 are covered in the EAT-Lancet dataset, and 153 have corresponding data in FAOSTAT. Our analysis therefore covers 153 regions for which data are available across all three sources. FAO countries were mapped to IMPACT regions using ISO 3166-1 alpha-3 codes (Supplementary Table D.2). Some IMPACT regions aggregate multiple countries (e.g., BLX includes Belgium and Luxemburg; CRB includes Caribbean island nations). UN M49 geographic classifications are used for regional aggregation in figures.

D.3.2 Dietary scenario construction

Dietary scenarios are derived from the EAT-Lancet dataset (Willett et al., 2019), which provides consumption estimates (per person per day) by food group, country, and year under seven dietary scenarios: benchmark (BMK), flexitarian (FLX), flexitarian with high milk consumption (FLX_hmilk), flexitarian with high meat consumption (FLX_hredmeat), pescetarian (PSC), vegetarian (VEG), and vegan (VGN); and two calorie scenarios: 2100 and 2500 kcal/day. The dataset covers 157 countries, 21 food groups, and three years (2010, 2030, 2050). We use five dietary scenarios (BMK, FLX, PSC, VEG, VGN) and the 2500 kcal scenario in this analysis.

Dietary change time trends

The EAT-Lancet data assume 100% adoption under each dietary scenario across years. We process this to impose a gradual time trend and interpolate consumption at 5-year intervals. We assume 100% benchmark diet composition through 2020, with 2050 as the target year for complete transition to alternate diets. The transition proceeds linearly in equal increments every 5 years. This means that in 2030,

countries would have adopted 33% of the dietary shift, in 2040 67%, and by 2050 100%. Supplementary Figure D.1 shows the resulting dietary change time trends.

Per capita consumption (g/person/day) is multiplied by population projections and scaled to annual totals to obtain food demand by country, year, food group, and dietary scenario. Although our analysis is limited to vegetal commodities, we track animal-product consumption under each dietary scenario to derive feed requirements.

Feed requirement estimation

Feed requirements are estimated using feed conversion ratios (FCRs) that specify the amount of feed required to produce a unit of animal product, along with the crop composition of feed rations. For example, 1 gram of beef requires approximately 19.27 grams of feed, of which 43% comes from maize, 9% from other cereals, 15% from pulses, and so on.

Terrestrial animal products. For beef, milk, lamb, poultry, eggs, and pork, we use country-specific feed conversion ratios from Herrero et al. (2013). Where country FCRs are unavailable, we impute sequentially using the mean for (i) the country's intermediate geographic region, (ii) its sub-region, (iii) its broader region, and (iv) global production systems. Supplementary Table D.2 shows the mapping from countries to geographic regions. We incorporate trade in animal products when computing feed requirements: production and trade data for animal products are processed from FAOSTAT using the same reliability index and re-export pipeline as for crops. Supplementary Table D.3 provides a description of commodities from the FAO used for estimating trade flows for animal products. We assume animal product trade patterns remain constant across years and dietary scenarios, and use the processed flows to estimate, for each country, the shares of animal product demand met by domestic production vs imports. For each scenario and animal product, feed demand is assigned to the producing country, using post-trade supply allocations and that country's FCRs.

Seafood and aquaculture. Feed conversion ratios for seafood products are from Tilman and Clark (2014), which provide FCRs grouped by eight economic groups.

Countries are assigned to economic groups based on 2030 GDP projections in the EAT-Lancet dataset. We assume 50% of seafood is farmed globally and compute feed requirements accordingly (FAO, 2020). Trade in seafood is not incorporated in feed allocation.

Crops used for feed. Feed requirements are computed for the following crop groups: wheat, rice, maize, other grains, roots, legumes, and soybeans. Feed demand for vegetables, fruits, nuts and seeds, palm oil, other oil crops, and sugar crops is assumed to be zero, as these are primarily by-products rather than primary feed crops.

Other uses estimation

'Other uses' includes industrial uses, seed, and waste. These are obtained from FAOSTAT food balance sheets (FBS) and supply utilization accounts (SUA), depending on the food group. For each country and food group, 'other' quantities are obtained from FAOSTAT, and averaged over 2018-2022. Supplementary Table D.4 provides the mapping between EAT-Lancet food groups and FAOSTAT sources (FBS or SUA) used for computing other uses. For crops processed into oils or sugar (e.g., oilseeds, sugar crops), processing factors are applied to convert between raw crop and processed product equivalents, as described in D.3.1.

Total quantity demanded

Total quantity demanded is calculated as the sum of demand for food, feed, and other uses, as estimated above. For each food group, diet, country, and year, we compute a demand change ratio from the EAT-Lancet projections, i.e. projected demand divided by its 2020 level. These ratios are applied to each of the 32 crop categories in the analysis according to the mapping between EAT-Lancet food groups and IMPACT crop categories (Supplementary Table D.1). These ratios are used to parametrize the demand-side scenarios for forward modelling.

In cases where the demand change ratio is excessively large (i.e. greater than 2000), typically because the EAT-Lancet-based 2020 demand is close to zero, we

do not scale the calibrated 2020 demand by the ratio. Instead, the ratio itself is applied directly as the future demand level. This approach prevents implausibly large future demand values that would otherwise arise from multiplying non-zero calibrated baseline quantities by large ratios. This adjustment affects two countries for nuts and seeds and four countries for vegetable oil crops.

D.3.3 IMPACT Model Outputs

The supply-side analysis covers 32 vegetal food crops modelled in IFPRI's IMPACT model (Robinson et al., 2015). We exclude animal products, coffee, tea, cocoa, spices, and fiber crops from the analysis. For animal products, we assume that trade patterns and domestic supply shares remain constant at their 2020 values throughout the projection period (as described in D.3.2).

We use yield and supply projections under two different Representative Concentration Pathways, RCP 2.6 and RCP 7.0, accounting for projected technological progress. Yield impacts under different climate scenarios show relatively modest variation across RCPs (Supplementary Figure D.2), reflecting that these trajectories assume continued technological progress offsetting climate-induced yield losses through 2050. Supply changes in our projection period are a function of both area expansion and yield changes, and are modelled by IMPACT assuming benchmark demand. For each crop category, RCP, country, and year, we compute a supply change ratio and a yield change ratio from the IMPACT projections, i.e. projected supply/yield divided by their 2020 level. These ratios are used to parameterize the supply-side scenarios for forward modelling.

Additionally, we use demand and supply elasticities given by the IMPACT model. Demand elasticities vary by region, crop and year, while supply elasticities vary by region and crop.

D.3.4 Producer price gap-filling

Producer prices are obtained from FAOSTAT. These represent prices received by farmers at the farm gate and do not include post-farm costs (transportation,

warehousing, processing, marketing). For most crops, 45-75% of producing countries have at least one reported value since 2010. Where available, we average the 1-3 most recent available producer prices (since 2010).

Missing producer prices are gap-filled using a linear regression model. We first convert producer prices to prices per hectare (price/tonne × yield) as this variable exhibits a better fit with available covariates. For each crop we use the regression specification given by:

$$\log price = \beta_0 + \beta_1 \log GDP + \beta_2 \log production + \beta_3 \log yield + region\ FE \tag{D.3.4.1}$$

For each crop, the model is fitted on data from the 25 largest producers (among countries with available price data) to avoid introducing noise from many small producers. The fitted model is used to predict producer prices for countries where the crop is produced but price information is missing. If the 25 largest producers do not cover all regions, a second model is fitted on all countries with available price data to provide predictions for countries outside the regions covered by top producers. For countries in regions with no price data at all, producer prices are estimated using a global average of available prices. For crops with fewer than 25 observations, gaps are filled using intermediate regional, sub-regional, regional, and global averages in sequence.

For non-producing countries, both yields and producer prices are imputed using the same geographical hierarchy. Gap-filled producer prices per hectare are then converted back to prices per tonne. Finally, producer prices for each IMPACT crop category are computed as production-weighted averages of the producer prices for all commodities in the category.

D.3.5 Trade cost data

Bilateral transport costs are obtained from Verschuur et al. (2023), which provides estimates of the cost to ship agricultural commodities between any pair of countries. These costs incorporate hinterland transportation from farm to port or border, port

handling and fees, maritime transport cost, intermodal transfers, and custom and border compliance.

Bilateral ad valorem tariff rates are obtained from the MAcMap-HS6 database (Guimbard et al., 2012), which provides tariff data at the HS6 product level. For each IMPACT crop category, we compute simple averages of tariff rates across relevant HS codes. Supplementary Table D.5 provides the HS code mapping for each crop category.

D.3.6 Spatial price equilibrium model

We use a spatial price equilibrium model (SPEM) based on the Enke-Samuelson-Takayama-Judge formulation for homogeneous goods (Takayama, 1971; Takayama & Judge, 1964). Below, we describe the trade cost formulation used, the calibration process, and the model setup for projecting forward. The reference period (t) for the model is the 2018-2022 average trade network, to smooth out inter-year trade fluctuations, while the previous period referred to throughout is the 2013-2017 average trade network ($t-1$). A separate SPEM is set up for each of the 32 crops (c) considered, without considering cross-commodity substitution effects.

Trade cost formulation

Total trade costs (TTC) comprise transport costs ($C^{transport}$), tariff costs $\left(C^{tariff}\right)$, market entry costs (C^{entry}), and a calibrated trade cost term (C^{calib}). We distinguish between trade costs at the intensive margin (for region pairs that already trade) and at the extensive margin (for region pairs that do not currently trade).

$$TTC_{int} = \left(C^{tariff}_{i,j,t,c} + C^{calib}_{i,j,c}\right) \times T_{i,j,t,c} + \left[\frac{\varepsilon}{1+\varepsilon}\right] \times C^{transport}_{i,j,c} \times \left(\frac{T_{i,j,t,c}}{T_{i,j,t-1,c}}\right)^{\frac{1+\varepsilon}{\varepsilon}} \times T_{i,j,t,c} \tag{D.3.6.1}$$

$$TTC_{ext} = \left(C^{tariff}_{i,j,t,c} + C^{calib}_{i,j,c} + C^{transport}_{i,j,c} + C^{entry}_{i,j,t,c}\right) \times T_{i,j,t,c} + 0.5 \times \sigma \times T^2_{i,j,t,c} \tag{D.3.6.2}$$

where $T_{i,j,t,c}$ is the bilateral trade flow from region i to region j for crop c at time t, and $T_{i,j,t-1,c}$ is the trade flow in the previous period. The parameters ε and σ reflect non-linear trade expansion costs that capture the logistics costs of expanding trade beyond existing capacity and enable persistence in existing supply networks (Janssens et al., 2022). Higher σ and lower ε make it costlier to increase trade from existing suppliers (intensive) to source from new suppliers (extensive), respectively.

Transport costs ($C^{transport}$) are time-invariant and include hinterland transport, border compliance, intermodal handling, port fees, maritime transport, and customs compliance (Verschuur et al., 2023). Tariff costs are calculated using the ad-valorem tariff rate ($adv_{i,j,c}$).

$$C^{tariff}_{i,j,t,c} = adv_{i,j,c} \times (P^{producer}_{i,t,c} + C^{transport}_{i,j,c}) \tag{D.3.6.3}$$

Market entry costs for new trade links are set at 20% of producer prices, following Verschuur et al. (2024).

$$C^{entry}_{i,j,t,c} = 0.2 \times P^{producer}_{i,t,c} \tag{D.3.6.4}$$

The time-invariant calibration cost $\left(C^{calib}\right)$ captures any trade cost components not explicitly modelled, as well as non-cost trade frictions (e.g., geopolitics, trade agreements).

Trade between regions occurs when the sum of producer price and trade costs equals the consumer price in the destination region.

Intensive margin:

$$\left(P^{producer}_{i,t,c} + C^{tariff}_{i,j,t,c} + C^{calib}_{i,j,c}\right) + C^{transport}_{i,j,c} \times \left(\frac{T_{i,j,t,c}}{T_{i,j,t-1,c}}\right)^{\frac{1}{\varepsilon}} = P^{consumer}_{j,t,c} \tag{D.3.6.5}$$

Extensive margin:

$$\left(P^{producer}_{i,t,c} + C^{tariff}_{i,j,t,c} + C^{calib}_{i,j,c} + C^{transport}_{i,j,c} + C^{entry}_{i,j,t,c}\right) + \sigma T_{i,j,t,c} = P^{consumer}_{j,t,c} \tag{D.3.6.6}$$

D. Supplementary Material for "The Impact of Dietary Transitions, Trade Policy and Climate Change on Food Production and Import-dependence through to 2050"

Baseline calibration

Following the approach used by Verschuur et al. (2024), the model is calibrated using a bi-level programming procedure introduced by Jansson and Heckelei (2009) and advanced by Mosnier (2014). The calibration uses two time periods: 2013–2017 $(t-1)$ to initialize trade patterns and 2018–2022 (t) as the calibration target.

The inner problem (first calibration) serves as the input to the outer problem (second calibration), and minimizes total trade costs across all bilateral flows.

$$\text{minimize} \sum_{i,j} TTC_{i,j,t,c}$$

subject to market equilibrium and non-negativity constraints:

$$e_{i,j,c} + \sum_{j} \left(T_{i,j,t,c} - T_{j,i,t,c}\right) = 0; T_{i,j,t,c} \geq 0 \tag{D.3.6.7}$$

where e is the excess demand (consumption − domestic production). This results in trade flows based on minimum trade costs, assuming homogenous producer price across countries. These flows are then used as inputs to the outer problem.

The outer problem then jointly minimizes the total deviations from observed trade flows, producer prices, and transport costs, plus a price chain residual penalty (pen).

The total deviation is calculated as follows. Variables with hats denote observed values, and w_t, w_p, and w_{tr} are the weights associated with the errors from trade flows, producer prices, and transport costs, respectively.

$$z = w_t \sum_{ij} \left(T_{i,j,t,c} - \widehat{T}_{i,j,t,c}\right)^2 + w_p \sum_{i} \left(P_{i,t,c} - \widehat{P}_{i,t,c}\right)^2 + w_{tr} \sum_{ij} \left(C^{transport}_{i,j,t,c} - \widehat{C}^{transport}_{i,j,t,c}\right)^2 \tag{D.3.6.8}$$

The price chain residual (π) is added to the price chain formula at the intensive and extensive margin as follows.

Intensive margin:

$$\left(P_{i,t,c}^{producer} + C_{i,j,t,c}^{tariff} + C_{i,j,c}^{calib}\right) + C_{i,j,c}^{transport} \times \left(\frac{T_{i,j,t,c}}{T_{i,j,t-1,c}}\right)^{\frac{1}{\epsilon}} = P_{j,t,c}^{consumer} + \pi_{i,j,t,c} \tag{D.3.6.9}$$

Extensive margin:

$$\left(P_{i,t,c}^{producer} + C_{i,j,t,c}^{tariff} + C_{i,j,c}^{calib} + C_{i,j,c}^{transport} + C_{i,j,t,c}^{entry}\right) + \sigma T_{i,j,t,c} = P_{j,t,c}^{consumer} + \pi_{i,j,t,c} \tag{D.3.6.10}$$

The total penalty is calculated as:

$$pen = \mu \sum_{ij} \left(\pi_{i,j,t,c} \times T_{i,j,t,c}\right) \tag{D.3.6.11}$$

where μ is the weight associated with the price chain residual penalty. Finally, the objective function that the outer problem minimizes becomes:

$$\text{minimize } zz = z + pen, \text{with } \pi_{i,j,t,c} \geq 0 \tag{D.3.6.12}$$

The outer problem is solved iteratively, with the penalty weight μ increasing to force *pen* to go towards zero. Calibration is achieved once zz converges, yielding calibrated values of producer prices, consumer prices, trade flows, transport costs, and the calibration constant C^{calib}.

Supplementary Table D.6 reports calibration performance for all 32 crop categories.

Projection framework

To project future trade patterns, we shift country-level demand and supply curves to reflect scenario-specific changes in food demand and agricultural production. Our long-term framework assumes markets fully adjust to structural changes over decadal timescales. Stocks are not modelled, and each year (2025, 2030, 2035, 2040, 2045, 2050) is solved sequentially, with each period initialized from the previous period's solution.

For projection years $t > 2020$, we initialize quantities and prices from the previous period's equilibrium solution $(t-5)$, adjusted by scenario-specific scaling factors.

Quantity demanded D is scaled using demand change ratios:

$$D_{i,t,c} = D_{i,t-5,c} \times \left(\frac{r^{demand}_{i,t,c}}{r^{demand}_{i,t-5,c}} \right) \tag{D.3.6.13}$$

where $r^{demand}_{i,t,c}$ is the demand scaling factor for region i, crop c, in year t relative to 2020.

Quantity supplied S is scaled using supply change ratios:

$$S_{i,t,c} = S_{i,t-5,c} \times \left(\frac{r^{supply}_{i,t,c}}{r^{supply}_{i,t-5,c}} \right) \tag{D.3.6.14}$$

where $r^{supply}_{i,t,c}$ is the supply scaling factor for region i, crop c, in year t relative to 2020.

Producer prices are adjusted to reflect both supply expansion (movement along the supply curve) and yield changes (shift of the supply curve):

$$P^{producer}_{i,t,c} = P^{producer}_{i,t-5,c} \times \frac{\left[1 + \frac{1}{\zeta_{i,c}} \times \left(\frac{r^{supply}_{i,t,c}}{r^{supply}_{i,t-5,c}} - 1 \right) \right]}{\left(\frac{r^{yield}_{i,t,c}}{r^{yield}_{i,t-5,c}} \right)} \tag{D.3.6.15}$$

where $\zeta_{i,c}$ is the (time-invariant) supply elasticity. The numerator captures the price change associated with movements along the supply curve as quantities expand or contract. The denominator captures the price change resulting from shifts of the supply curve driven by yield improvements or declines.

Consumer prices are initialized from the previous period's equilibrium values.

Demand elasticities are updated for time period t, based on IMPACT.

Using the initialized values, we compute demand and supply curves for the new time period. Consumer prices follow the demand curve.

$$\alpha_{i,t,c} - \beta_{i,t,c} \times D_{i,t,c} \leq P^{consumer}_{i,t,c} \tag{D.3.6.16}$$

where the slope and intercept are derived from the initialized values:

$$\beta_{i,t,c} = \frac{P_{i,t,c}^{consumer}}{D_{i,t,c} \times \eta_{i,t,c}} \tag{D.3.6.17}$$

$$\alpha_{i,t,c} = P_{i,t,c}^{consumer} + \beta_{i,t,c} \times D_{i,t,c} \tag{D.3.6.18}$$

Producer prices follow the supply curve:

$$\gamma_{i,t,c} + \delta \times S_{i,t,c} \geq P_{i,t,c}^{producer} \tag{D.3.6.19}$$

where the slope and intercept are derived from the initialized values:

$$\gamma_{i,t,c} = \frac{P_{i,t,c}^{producer}}{S_{i,t,c} \times \zeta_{i,c}} \tag{D.3.6.20}$$

$$\delta_{i,t,c} = P_{i,t,c}^{producer} - \gamma_{i,t,c} \times S_{i,t,c} \tag{D.3.6.21}$$

Trade policy constraints

Trade policy scenarios impose constraints on self-sufficiency and supplier concentration. For each projection year t > 2020, minimum domestic supply must satisfy:

$$T_{i,i,t,c} \geq \lambda^{SS} \times \left(\frac{T_{i,i,2020,c}}{D_{i,2020,c}} \right) \times D_{i,t,c} \tag{D.3.6.22}$$

where λ^{SS} is the self-sufficiency preservation parameter. This ensures domestic supply maintains at least λ^{SS} of its 2020 share of demand.

Maximum imports from any single trading partner are constrained by:

$$T_{j,i,t,c} \ \leq \ max \left(\lambda^{SD}, \frac{T_{j,i,2020,c}}{D_{i,2020,c}} \right) \times D_{i,t,c} \tag{D.3.6.23}$$

where λ^{SD} is the supplier diversification parameter. This limits dependence on any single foreign supplier to either λ^{SD} of demand or the 2020 share, whichever is larger.

For the low trade liberalization scenario: $\lambda^{SS} = 0.7$, $\lambda^{SD} = 0.3$

For the high trade liberalization scenario: $\lambda^{SS} = 0.3$, $\lambda^{SD} = 0.7$

Model solution

The model solves for equilibrium by finding bilateral trade flows, prices, and quantities that satisfy the following conditions.

Interregional trade must be constrained by supply and demand.

$$S_{i,t,c} = \sum_{j} T_{i,j,t,c} \tag{D.3.6.24}$$

$$D_{i,t,c} = \sum_{j} T_{j,i,t,c} \tag{D.3.6.25}$$

In addition, the price chain relationship at the intensive and extensive margin must hold.

Intensive margin:

$$\left(P_{i,t,c}^{producer} + C_{i,j,t,c}^{tariff} + C_{i,j,c}^{calib}\right) + C_{i,j,c}^{transport} \times \left(\frac{T_{i,j,t,c}}{T_{i,j,t-1,c}}\right)^{\frac{1}{\varepsilon}} \geq P_{j,t,c}^{consumer} \tag{D.3.6.26}$$

Extensive margin:

$$\left(P_{i,t,c}^{producer} + C_{i,j,t,c}^{tariff} + C_{i,j,c}^{calib} + C_{i,j,c}^{transport} + C_{i,j,t,c}^{entry}\right) + \sigma T_{i,j,t,c} \geq P_{j,t,c}^{consumer} \tag{D.3.6.27}$$

D.3.7 Outcome metrics

For presentation of results, the 32 individual crops are aggregated into six categories: grains (wheat, rice, maize, barley, millet, sorghum, other cereals), roots and tubers (cassava, potatoes, yams, sweet potatoes, other roots), fruits and vegetables (vegetables, bananas, plantains, subtropical fruits, temperate fruits), soybeans (soybeans), legumes, nuts and seeds (beans, chickpeas, cowpeas, lentils, pigeon peas, other pulses, groundnuts, other nuts and seeds), oilcrops and sugar crops (rapeseed, sunflower seed, other oilseeds, palm oil, sugarcane, sugar beet).

Supplier concentration for importing region i and crop c is measured using the Herfindahl-Hirschman Index:

$$HHI_{i,c} = \sum_j \left(\frac{T_{j,i,c}}{\sum_k T_{k,i,c}} \right)^2 \tag{D.3.7.1}$$

where $T_{j,i,c}$ are the imports from exporter j. The HHI measures the relative size of firms within an industry and serves as an indicator of market competitiveness. It ranges from nearly 0 (perfectly diversified) to 1 (monopoly). An $HHI < 0.15$ indicates a competitive market, and HHI between 0.15 and 0.25 indicates moderate concentration, and an $HHI > 0.25$ indicates high levels of market concentration. Higher values here indicate greater concentration of imports and potential vulnerability from individual trading partners, especially when self-sufficiency is low.

Changes between 2020 and 2050 are summarized using means across scenarios, with uncertainty characterized by the interquartile range (IQR) spanning the 25th to 75th percentiles across the scenario ensemble. This captures the central tendency and spread of outcomes across dietary, climate, and trade policy combinations.

To attribute variation in outcomes to different scenario dimensions, we decompose the total across-scenario variance using an ANOVA formulation based on cell means (Montgomery, 2017). Specifically, for each country we compute main-effect and interaction sums of squares for diet, liberalization, and RCP directly from scenario averages. Interaction sums of squares are then allocated to individual drivers using the Shapley-Owen attribution, whereby two-way interactions are split equally between the two contributing factors, and the three-way interaction is split equally among all three (Owen, 2014; Shapley, 1953). This yields additive contributions that sum to 100% of the explained across-scenario variance for each country. Country-level contributions are subsequently aggregated to regional and global levels by summing the underlying sums of squares (equivalently, using weights proportional to each country's explained variance), ensuring that countries with larger scenario-driven variability contribute proportionally more to aggregate results.

D.3.8 Methodological notes and limitations

Cropland area implications

Because supply is modelled independently for each crop, the model does not enforce aggregate land constraints, and implied cropland requirements may exceed biophysical availability in some countries. At the global level, change in total cropland in 2050 ranges from -20 million hectares (-1.5%) under 'VEG, RCP 2.6, trade low' to +162 million hectares (+11.9%) under 'PSC, RCP 7.0, trade low'. At the country level, area differences range from -56 million hectares (-31%) in China under 'VEG, RCP 2.6, trade low' to +48 million hectares (+25%) in India under 'PSC, RCP 7.0, trade low', with a median difference of +0.07 million hectares across all country-scenario combinations.

One potential source of additional cropland not captured in our model is the conversion of pastureland currently used for livestock grazing. Globally, pastureland covers approximately 3.2 billion hectares – more than twice the area of cropland (FAO, 2024a). Under plant-forward dietary scenarios that substantially reduce consumption of animal products, a fraction of this pastureland could potentially be freed converted to crop production or restored to natural ecosystems (Kozicka et al., 2023; Poore & Nemecek, 2018). While two-thirds of current pastureland is unsuitable for crop cultivation (Poore & Nemecek, 2018), the remaining one-third represents a potential reserve for cropland expansion, though conversion would depend on local infrastructure, investment, and the trade-offs with ecosystem restoration objectives (Schneider et al., 2022). This land use flexibility is not endogenously modelled in our framework.

Demand projection differences

For some crop categories and scenarios, particularly fruits and vegetables, the equilibrium quantities produced by the model fall short of the 2050 EAT-Lancet target demands, especially under more plant-forward dietary scenarios. For example, global fruits and vegetables demand in 2050 ranges from 2,900 million tonnes (BMK) to 4,800 million tonnes (VGN) based on EAT-Lancet targets, but modelled quantities reach only around 2,700 to 3,700 million tonnes respectively – a gap of 7% under BMK widening to 23% under VGN. The largest absolute gaps occur in major

consuming countries: India and China show gaps of 35% and 21% for fruits and vegetables under VGN scenarios in 2050.

This gap reflects the constraints of projecting radical dietary transitions using elasticities and model parameters calibrated to benchmark policy environments. The supply and demand elasticities in our model are derived from IMPACT and reflect historical responsiveness of agricultural systems. Meeting the full EAT-Lancet targets, particularly for plant-forward diets, would require substantially more elastic supply responses, through accelerated technological change, land use conversion, or policy interventions. Similarly, our trade policy constraints (self-sufficiency and supplier diversification bounds) reflect plausible evolutions of current trade regimes rather than the transformative policy changes that might accompany a global dietary transition.

References

Amoutzopoulos, B., Mulligan, A., Swan, G., Roberts, C., Abraham, S., Farooq, A., Collins, D., Steer, T., & Page, P. (2025). A new updated food grouping system for the uk national diet and nutrition survey. *Journal of Food Composition and Analysis*, 107986.

Arita, S., Grant, J., Sydow, S., & Beckman, J. (2022). Has global agricultural trade been resilient under coronavirus (covid-19)? findings from an econometric assessment of 2020. *Food Policy*, *107*, 102204.

Awika, J. M. (2011). Major cereal grains production and use around the world. In *Advances in cereal science: Implications to food processing and health promotion* (pp. 1–13). ACS Publications.

Baas, S., Trujillo, M., & Lombardi, N. (2015). *Impact of disasters on agriculture and food security*.

Baldos, U. L. C., Fuglie, K. O., & Hertel, T. W. (2020). The research cost of adapting agriculture to climate change: A global analysis to 2050. *Agricultural Economics*, *51*(2), 207–220.

Béné, C. (2020). Resilience of local food systems and links to food security–a review of some important concepts in the context of covid-19 and other shocks. *Food security*, *12*(4), 805–822.

Bentéjac, C., Csörgő, A., & Martínez-Muñoz, G. (2021). A comparative analysis of gradient boosting algorithms. *Artificial Intelligence Review*, *54*, 1937–1967.

Brown, M. E., Carr, E. R., Grace, K. L., Wiebe, K., Funk, C. C., Attavanich, W., Backlund, P., & Buja, L. (2017). Do markets and trade help or hurt the global food system adapt to climate change? *Food policy*, *68*, 154–159.

Centeno, M. A., Nag, M., Patterson, T. S., Shaver, A., & Windawi, A. J. (2015). The emergence of global systemic risk. *Annual Review of Sociology*, *41*, 65–85.

Chisenga, S. M., Workneh, T. S., Bultosa, G., & Alimi, B. A. (2019). Progress in research and applications of cassava flour and starch: A review. *Journal of food science and technology*, *56*, 2799–2813.

Clark, M., Domingo, N. G., Colgan, K., Thakrar, S. K., Tilman, D., Lynch, J., Azevedo, I. L., & Hill, J. D. (2020). Global food system emissions could preclude achieving the 1.5 and 2 c climate change targets. *Science*, *370*(6517), 705–708.

Clark, M., Springmann, M., Rayner, M., Scarborough, P., Hill, J., Tilman, D., Macdiarmid, J. I., Fanzo, J., Bandy, L., & Harrington, R. A. (2022). Estimating the environmental impacts of 57,000 food products. *Proceedings of the National Academy of Sciences*, *119*(33), e2120584119.

Commission, E. (n.d.). The common agricultural policy at a glance. https://agriculture.ec.europa.eu/common-agricultural-policy/cap-overview/cap-glance_en

Cottrell, R. S., Nash, K. L., Halpern, B. S., Remenyi, T. A., Corney, S. P., Fleming, A., Fulton, E. A., Hornborg, S., Johne, A., & Watson, R. A. (2019). Food production shocks across land and sea. *Nature Sustainability*, *2*(2), 130–137.

Crippa, M., Solazzo, E., Guizzardi, D., Monforti-Ferrario, F., Tubiello, F. N., & Leip, A. (2021). Food systems are responsible for a third of global anthropogenic ghg emissions. *Nature food*, *2*(3), 198–209.

Croft, S. A., West, C. D., & Green, J. M. (2018). Capturing the heterogeneity of sub-national production in global trade flows. *Journal of Cleaner Production*, *203*, 1106–1118.

Davis, K. F., Downs, S., & Gephart, J. A. (2021). Towards food supply chain resilience to environmental shocks. *Nature Food*, *2*(1), 54–65. https://www.nature.com/articles/s43016-020-00196-3.pdf

Deconinck, K., Jansen, M., & Barisone, C. (2023). Fast and furious: The rise of environmental impact reporting in food systems. *European Review of Agricultural Economics*, *50*(4), 1310–1337.

Denicoff, M., Jessup, E., Taylor, A., & Nibarger, D. (2010). Chapter 2: The importance of freight transportation to agriculture. *Study of rural transportation issues*, 110–246.

Devadoss, S., & Ridley, W. (2024). Impacts of the russian invasion of ukraine on the global wheat market. *World Development*, *173*, 106396.

Dietrich, J. P., Bodirsky, B. L., Humpenöder, F., Weindl, I., Stevanović, M., Karstens, K., Kreidenweis, U., Wang, X., Mishra, A., & Klein, D. (2019). Magpie 4–a modular open-source framework for modeling global land systems. *Geoscientific Model Development*, *12*(4), 1299–1317.

Distefano, T., Laio, F., Ridolfi, L., & Schiavo, S. (2018). Shock transmission in the international food trade network. *PloS one*, *13*(8), e0200639.

El Bilali, H., & Allahyari, M. S. (2018). Transition towards sustainability in agriculture and food systems: Role of information and communication technologies. *Information Processing in Agriculture*, *5*(4), 456–464.

Elisabeth, D. A. A., Utomo, J. S., Byju, G., & Ginting, E. (2022). Cassava flour production by small scale processors, its quality and economic feasibility. *Food Science and Technology*, *42*, e41522.

Esteve-Llorens, X., Darriba, C., Moreira, M. T., Feijoo, G., & González-García, S. (2019). Towards an environmentally sustainable and healthy atlantic dietary pattern: Life cycle carbon footprint and nutritional quality. *Science of the Total Environment*, *646*, 704–715.

Fanelli, R. M., & Giglio, A. (2021). The 'similarity'of agri-food trade flows between the eu-28 and the asia-50. *The International Trade Journal*, *35*(6), 558–586.

FAO. (2020). The state of world fisheries and aquaculture. sustainability in action.

FAO. (2022). *The state of agricultural commodity markets 2022. the geography of food and agricultural trade: Policy approaches for sustainable development,* https://doi.org/https://doi.org/10.4060/cc0471en

FAO. (2023). Faostat.

FAO. (2024a). Land statistics 2001–2022—global, regional and country trends.

FAO. (2024b, 23 January, 2025). Fishstat.

Fischer, G., Nachtergaele, F. O., Van Velthuizen, H., Chiozza, F., Franceschini, G., Henry, M., Muchoney, D., & Tramberend, S. (2021). *Global agro-ecological zones v4–model documentation*. Food & Agriculture Org.

Fisher, G., Shah, M., & van Velthuizen, H. (2002). Climate change and agricultural vulnerability. special report prepared by the international institute for applied systems analysis under un contract agreement no. 1113 as contribution to the world summit on sustainable development, johannesburg, 2002. *IIASA, Laxenburg, Austria*.

Foley, J. A., Ramankutty, N., Brauman, K. A., Cassidy, E. S., Gerber, J. S., Johnston, M., Mueller, N. D., O'Connell, C., Ray, D. K., & West, P. C. (2011). Solutions for a cultivated planet. *Nature*, *478*(7369), 337–342.

Frolking, S., Wisser, D., Grogan, D., Proussevitch, A., & Glidden, S. (2020a). Gaez+$_2$015*cropharvestarea*. https://doi.org/doi/10.7910/DVN/KAGRFI

Frolking, S., Wisser, D., Grogan, D., Proussevitch, A., & Glidden, S. (2020b). Gaez+$_2$015*cropproduction*. https://doi.org/doi/10.7910/DVN/KJFUO1

Gaupp, F., Hall, J., Hochrainer-Stigler, S., & Dadson, S. (2020). Changing risks of simultaneous global breadbasket failure. *Nature Climate Change*, *10*(1), 54–57.

Gaupp, F., Hall, J., Mitchell, D., & Dadson, S. (2019). Increasing risks of multiple breadbasket failure under 1.5 and 2 c global warming. *Agricultural Systems*, *175*, 34–45.

Gaupp, F., Pflug, G., Hochrainer-Stigler, S., Hall, J., & Dadson, S. (2017). Dependency of crop production between global breadbaskets: A copula approach for the assessment of global and regional risk pools. *Risk Analysis*, *37*(11), 2212–2228.

Gehlhar, M. (1996). Reconciling bilateral trade data for use in gtap. *GTAP Technical papers*, 11.

Gephart, J. A., Henriksson, P. J., Parker, R. W., Shepon, A., Gorospe, K. D., Bergman, K., Eshel, G., Golden, C. D., Halpern, B. S., & Hornborg, S. (2021). Environmental performance of blue foods. *Nature*, *597*(7876), 360–365.

Gilbert, M., Cinardi, G., Da Re, D., Wint, W. G. R., Wisser, D., & Robinson, T. P. (2022a). Global buffaloes distribution in 2015 (5 minutes of arc). https://doi.org/doi/10.7910/DVN/I1WCAB

Gilbert, M., Cinardi, G., Da Re, D., Wint, W. G. R., Wisser, D., & Robinson, T. P. (2022b). Global cattle distribution in 2015 (5 minutes of arc). https://doi.org/doi/10.7910/DVN/LHBICE

Gilbert, M., Cinardi, G., Da Re, D., Wint, W. G. R., Wisser, D., & Robinson, T. P. (2022c). Global chickens distribution in 2015 (5 minutes of arc). https://doi.org/doi/10.7910/DVN/SXHLF3

Gilbert, M., Cinardi, G., Da Re, D., Wint, W. G. R., Wisser, D., & Robinson, T. P. (2022d). Global ducks distribution in 2015 (5 minutes of arc). https://doi.org/doi/10.7910/DVN/S9ONXV

Gilbert, M., Cinardi, G., Da Re, D., Wint, W. G. R., Wisser, D., & Robinson, T. P. (2022e). Global goats distribution in 2015 (5 minutes of arc). https://doi.org/doi/10.7910/DVN/YYG6ET

Gilbert, M., Cinardi, G., Da Re, D., Wint, W. G. R., Wisser, D., & Robinson, T. P. (2022f). Global horses distribution in 2015 (5 minutes of arc). https://doi.org/doi/10.7910/DVN/JJGCTX

Gilbert, M., Cinardi, G., Da Re, D., Wint, W. G. R., Wisser, D., & Robinson, T. P. (2022g). Global pigs distribution in 2015 (5 minutes of arc). https://doi.org/doi/10.7910/DVN/CIVCPB

Gilbert, M., Cinardi, G., Da Re, D., Wint, W. G. R., Wisser, D., & Robinson, T. P. (2022h). Global sheep distribution in 2015 (5 minutes of arc). https://doi.org/doi/10.7910/DVN/VZOYHM

Godfray, H. C. J., Beddington, J. R., Crute, I. R., Haddad, L., Lawrence, D., Muir, J. F., Pretty, J., Robinson, S., Thomas, S. M., & Toulmin, C. (2010). Food security: The challenge of feeding 9 billion people. *science*, *327*(5967), 812–818.

Gouel, C., & Guimbard, H. (2019). Nutrition transition and the structure of global food demand. *American Journal of Agricultural Economics*, *101*(2), 383–403.

Gouel, C., & Laborde, D. (2021). The crucial role of domestic and international market-mediated adaptation to climate change. *Journal of Environmental Economics and Management*, *106*, 102408.

Grassia, M., Mangioni, G., Schiavo, S., & Traverso, S. (2022). Insights into countries' exposure and vulnerability to food trade shocks from network-based simulations. *Scientific Reports*, *12*(1), 4644.

Grogan, D., Frolking, S., Wisser, D., Prusevich, A., & Glidden, S. (2022). Global gridded crop harvested area, production, yield, and monthly physical area data circa 2015. *Scientific data*, *9*(1), 15.

Guimbard, H., Jean, S., Mimouni, M., & Pichot, X. (2012). Macmap-hs6 2007, an exhaustive and consistent measure of applied protection in 2007. *International Economics*, *130*, 99–121.

Hale, G., Oncescu, V., & Bhangale, R. (2025). Pace of adoption of alternatives to animal-source foods is an important factor in reaching climate goals. *Scientific Reports*, *15*(1), 22643.

Harrington, R. A., Adhikari, V., Rayner, M., & Scarborough, P. (2019). Nutrient composition databases in the age of big data: Fooddb, a comprehensive, real-time database infrastructure. *BMJ open*, *9*(6), e026652.

Harris, F., Dalin, C., Cuevas, S., NR, L., Adhya, T., Joy, E. J., Scheelbeek, P. F., Kayatz, B., Nicholas, O., & Shankar, B. (2020). Trading water: Virtual water flows through interstate cereal trade in india. *Environmental Research Letters*, *15*(12), 125005.

Havlík, P., Valin, H., Herrero, M., Obersteiner, M., Schmid, E., Rufino, M. C., Mosnier, A., Thornton, P. K., Böttcher, H., & Conant, R. T. (2014). Climate change mitigation through livestock system transitions. *Proceedings of the National Academy of Sciences*, *111*(10), 3709–3714.

Headey, D. (2011). Rethinking the global food crisis: The role of trade shocks. *Food Policy*, *36*(2), 136–146.

Hélias, A., van Der Werf, H. M., Soler, L.-G., Aggeri, F., Dourmad, J.-Y., Julia, C., Nabec, L., Pellerin, S., Ruffieux, B., & Trystram, G. (2022). Implementing environmental labelling of food products in france. *The International Journal of Life Cycle Assessment*, *27*(7), 926–931.

Hernández, M. A., Espinoza, A., Berrospi, M. L., Deconinck, K., Swinnen, J., & Vos, R. (2023). *The role of market concentration in the agrifood industry* (Vol. 2168). Intl Food Policy Res Inst.

Herrero, M., Havlík, P., Valin, H., Notenbaert, A., Rufino, M. C., Thornton, P. K., Blümmel, M., Weiss, F., Grace, D., & Obersteiner, M. (2013). Biomass use, production, feed efficiencies, and greenhouse gas emissions from global livestock systems. *Proceedings of the National Academy of Sciences*, *110*(52), 20888–20893.

Hu, G., Ahmed, M., & L'Abbé, M. R. (2023). Natural language processing and machine learning approaches for food categorization and nutrition quality prediction compared with traditional methods. *The American Journal of Clinical Nutrition*, *117*(3), 553–563.

Hultgren, A., Carleton, T., Delgado, M., Gergel, D. R., Greenstone, M., Houser, T., Hsiang, S., Jina, A., Kopp, R. E., Malevich, S. B., et al. (2025). Impacts of climate change on global agriculture accounting for adaptation. *Nature*, *642*(8068), 644–652.

Humpenöder, F., Popp, A., Merfort, L., Luderer, G., Weindl, I., Bodirsky, B. L., Stevanović, M., Klein, D., Rodrigues, R., & Bauer, N. (2024). Food matters: Dietary shifts increase the feasibility of 1.5° c pathways in line with the paris agreement. *Science Advances*, *10*(13), eadj3832.

Ingram, J., & Zurek, M. (2019). Food systems approaches for the future. In *Agriculture & food systems to 2050: Global trends, challenges and opportunities* (pp. 547–567). World Scientific.

Janssens, C., Havlík, P., Boere, E., Palazzo, A., Mosnier, A., Leclère, D., Balkovič, J., & Maertens, M. (2022). A sustainable future for africa through continental free trade and agricultural development. *Nature Food*, *3*(8), 608–618.

Janssens, C., Havlík, P., Krisztin, T., Baker, J., Frank, S., Hasegawa, T., Leclère, D., Ohrel, S., Ragnauth, S., & Schmid, E. (2020). Global hunger and climate change adaptation through international trade. *Nature Climate Change*, *10*(9), 829–835.

Jansson, T., & Heckelei, T. (2009). A new estimator for trade costs and its small sample properties. *Economic Modelling*, *26*(2), 489–498.

Jin, Z., Azzari, G., You, C., Di Tommaso, S., Aston, S., Burke, M., & Lobell, D. B. (2019). Smallholder maize area and yield mapping at national scales with google earth engine. *Remote sensing of environment*, *228*, 115–128.

Karakoc, D. B., & Konar, M. (2024). Optimization of national grain imports to balance risk and return: A portfolio theory approach. *Environmental Research: Food Systems*, *1*(1), 011001.

Karakoc, D. B., Wang, J., & Konar, M. (2022). Food flows between counties in the united states from 2007 to 2017. *Environmental Research Letters*, *17*(3), 034035.

Kearney, J. (2010). Food consumption trends and drivers. *Philosophical transactions of the royal society B: biological sciences*, *365*(1554), 2793–2807.

Kennedy, J., Clark, M., Stewart, C., Runions, R., Vonderschmidt, A., Frank, S., Scarborough, P., Comrie, F., McDonald, A., & McNeill, G. (2025). Impact of reducing meat and dairy consumption on nutrient intake, health, cost of diets and the environment: A simulation among adults in scotland.

Kinnunen, P., Guillaume, J. H., Taka, M., D'odorico, P., Siebert, S., Puma, M. J., Jalava, M., & Kummu, M. (2020). Local food crop production can fulfil demand for less than one-third of the population. *Nature food*, *1*(4), 229–237.

Kluger, D. M., Wang, S., & Lobell, D. B. (2021). Two shifts for crop mapping: Leveraging aggregate crop statistics to improve satellite-based maps in new regions. *Remote Sensing of Environment*, *262*, 112488.

Konar, M., Lin, X., Ruddell, B., & Sivapalan, M. (2018). Scaling properties of food flow networks. *PloS one*, *13*(7), e0199498. https://journals.plos.org/plosone/article/file?id=10.1371/journal.pone.0199498&type=printable

Kotavaara, O., Ala-Hulkko, T., Toivanen, M., Poturalska, A., Magyar, M., & Kinnunen, P. (2021). Mapping the balance between grain supply and demand globally–gis-based transport accessibility. *Abstracts of the ICA*, *3*, 1–2.

Kozicka, M., Havlík, P., Valin, H., Wollenberg, E., Deppermann, A., Leclère, D., Lauri, P., Moses, R., Boere, E., & Frank, S. (2023). Feeding climate and biodiversity goals with novel plant-based meat and milk alternatives. *Nature Communications*, *14*(1), 5316.

Kummu, M., Kinnunen, P., Lehikoinen, E., Porkka, M., Queiroz, C., Röös, E., Troell, M., & Weil, C. (2020). Interplay of trade and food system resilience: Gains on supply diversity over time at the cost of trade independency. *Global Food Security*, *24*, 100360.

Laborde, D., Martin, W., Swinnen, J., & Vos, R. (2020). Covid-19 risks to global food security. *Science*, *369*(6503), 500–502.

Lang, T., & McKee, M. (2022). The reinvasion of ukraine threatens global food supplies.

LaValley, M. P. (2008). Logistic regression. *Circulation*, *117*(18), 2395–2399.

Leng, G., & Hall, J. (2019). Crop yield sensitivity of global major agricultural countries to droughts and the projected changes in the future. *Science of the Total Environment*, *654*, 811–821.

Lesk, C., Rowhani, P., & Ramankutty, N. (2016). Influence of extreme weather disasters on global crop production. *Nature*, *529*(7584), 84–87.

Li, M., Jia, N., Lenzen, M., Malik, A., Wei, L., Jin, Y., & Raubenheimer, D. (2022). Global food-miles account for nearly 20% of total food-systems emissions. *Nature food*, *3*(6), 445–453.

Lin, X., Ruess, P. J., Marston, L., & Konar, M. (2019). Food flows between counties in the united states. *Environmental Research Letters*, *14*(8), 084011.

Liu, W., Antonelli, M., Kummu, M., Zhao, X., Wu, P., Liu, J., Zhuo, L., & Yang, H. (2019). Savings and losses of global water resources in food-related virtual water trade. *Wiley Interdisciplinary Reviews: Water*, *6*(1), e1320.

Lopes, M. S., de Araújo, M. L., & Lopes, A. C. S. (2019). National general truck drivers' strike and food security in a brazilian metropolis. *Public health nutrition*, *22*(17), 3220–3228.

Martin, W., & Laborde Debucquet, D. (2018). Trade: The free flow of goods and food security and nutrition. *IFPRI book chapters*, 20–29.

McCance, R. A., & Widdowson, E. M. (2014). *Mccance and widdowson's the composition of foods*. Royal Society of Chemistry.

Mejía-Agüero, L. E., Galeno, F., Hernández-Hernández, O., Matehus, J., & Tovar, J. (2012). Starch determination, amylose content and susceptibility to in vitro amylolysis in flours from the roots of 25 cassava varieties. *Journal of the Science of Food and Agriculture*, *92*(3), 673–678.

Montgomery, D. C. (2017). *Design and analysis of experiments*. John wiley & sons.

Mosnier, A. (2014). Tracking indirect effects of climate change mitigation and adaptation strategies in agriculture and land use change with a bottom-up global partial equilibrium model. *University of Natural Resources and Life Sciences*.

Nations, U. (n.d.). Sustainable development goals: 17 goals to transform our world. https://www.un.org/en/exhibits/page/sdgs-17-goals-transform-world

Nelson, G. C., Valin, H., Sands, R. D., Havlík, P., Ahammad, H., Deryng, D., Elliott, J., Fujimori, S., Hasegawa, T., & Heyhoe, E. (2014). Climate change effects on agriculture: Economic responses to biophysical shocks. *Proceedings of the National Academy of sciences*, *111*(9), 3274–3279.

Nguyen, H. (2018). Sustainable food systems: Concept and framework.

Nkonya, E. M. (2019). Climate change and land: An ipcc special report on climate change, desertification, land degradation, sustainable land management, food security, and greenhouse gas fluxes in terrestrial ecosystems.

Ortiz-Bobea, A., Chambers, R. G., He, Y., & Lobell, D. B. (2025). Large increases in public r&d investment are needed to avoid declines of us agricultural productivity. *Proceedings of the National Academy of Sciences*, *122*(11), e2411010122.

Owen, A. B. (2014). Sobol'indices and shapley value. *SIAM/ASA Journal on Uncertainty Quantification*, *2*(1), 245–251.

Paillard, S., Dorin, B., Le Cotty, T., Ronzon, T., & Treyer, S. (2011). Food security by 2050: Insights from the agrimonde project. *European Foresight Platform*, Brief 196.

Pandit, A., Karakoc, D. B., & Konar, M. (2023). Spatially detailed agricultural and food trade between china and the united states. *Environmental Research Letters*, *18*(8), 084031.

Pang, B., Nijkamp, E., & Wu, Y. N. (2020). Deep learning with tensorflow: A review. *Journal of Educational and Behavioral Statistics*, *45*(2), 227–248.

Parmar, A., Katariya, R., & Patel, V. (2019). A review on random forest: An ensemble classifier. *International conference on intelligent data communication technologies and internet of things (ICICI) 2018*, 758–763.

Pingali, P. (2007). Westernization of asian diets and the transformation of food systems: Implications for research and policy. *Food policy*, *32*(3), 281–298.

Poore, J., & Nemecek, T. (2018). Reducing food's environmental impacts through producers and consumers. *Science*, *360*(6392), 987–992.

Porkka, M., Guillaume, J. H., Siebert, S., Schaphoff, S., & Kummu, M. (2017). The use of food imports to overcome local limits to growth. *Earth's Future*, *5*(4), 393–407.

Potts, J., Lynch, M., Wilkings, A., Huppé, G. A., Cunningham, M., & Voora, V. A. (2014). *The state of sustainability initiatives review 2014: Standards and the green economy*. International Institute for Sustainable Development Winnipeg, MB.

Prettenhofer, P., & Louppe, G. (2014). Gradient boosted regression trees in scikit-learn. *PyData 2014*.

Puma, M. J., Bose, S., Chon, S. Y., & Cook, B. I. (2015). Assessing the evolving fragility of the global food system. *Environmental Research Letters*, *10*(2), 024007.

Qamer, F. M., Abbas, S., Ahmad, B., Hussain, A., Salman, A., Muhammad, S., Nawaz, M., Shrestha, S., Iqbal, B., & Thapa, S. (2023). A framework for multi-sensor satellite data to evaluate crop production losses: The case study of 2022 pakistan floods. *Scientific Reports*, *13*(1), 4240.

Reimers, N., & Gurevych, I. (2019). Sentence-bert: Sentence embeddings using siamese bert-networks. *arXiv preprint arXiv:1908.10084*.

Rezaei, E. E., Webber, H., Asseng, S., Boote, K., Durand, J. L., Ewert, F., Martre, P., & MacCarthy, D. S. (2023). Climate change impacts on crop yields. *nature reviews earth & environment*, *4*(12), 831–846.

Robertson, T. M., Alzaabi, A. Z., Robertson, M. D., & Fielding, B. A. (2018). Starchy carbohydrates in a healthy diet: The role of the humble potato. *Nutrients*, *10*(11), 1764.

Robinson, S., Mason-D'Croz, D., Sulser, T., Islam, S., Robertson, R., Zhu, T., Gueneau, A., Pitois, G., & Rosegrant, M. W. (2015). The international model for policy analysis of agricultural commodities and trade (impact): Model description for version 3.

Rosenzweig, C., Elliott, J., Deryng, D., Ruane, A. C., Müller, C., Arneth, A., Boote, K. J., Folberth, C., Glotter, M., & Khabarov, N. (2014). Assessing agricultural risks of climate change in the 21st century in a global gridded crop model intercomparison. *Proceedings of the national academy of sciences*, *111*(9), 3268–3273.

Rosenzweig, C., Iglesius, A., Yang, X.-B., Epstein, P. R., & Chivian, E. (2001). Climate change and extreme weather events-implications for food production, plant diseases, and pests.

Sala, S., McLaren, S. J., Notarnicola, B., Saouter, E., & Sonesson, U. (2017). In quest of reducing the environmental impacts of food production and consumption. *Journal of cleaner production*, *140*, 387–398.

Salih, A. A., Baraibar, M., Mwangi, K. K., & Artan, G. (2020). Climate change and locust outbreak in east africa. *Nature Climate Change*, *10*(7), 584–585.

Sartori, M., & Schiavo, S. (2015). Connected we stand: A network perspective on trade and global food security. *Food Policy*, *57*, 114–127.

Schiavina, M., Melchiorri, M., Pesaresi, M., Politis, P., Freire, S., Maffenini, L., Florio, P., Ehrlich, D., Goch, K., & Tommasi, P. (2022). Ghsl data package 2022. *Publications Office of the European Union: Luxembourg*.

Schlindwein, S. L., & Ison, R. (2020). Confronting total systemic failure? the may 2018 truckers' strike in brazil. *Systems Research and Behavioral Science*, *37*(1), 119–127.

Schneider, J. M., Zabel, F., & Mauser, W. (2022). Global inventory of suitable, cultivable and available cropland under different scenarios and policies. *Scientific Data*, *9*(1), 527.

Seekell, D., Carr, J., Dell'Angelo, J., D'Odorico, P., Fader, M., Gephart, J., Kummu, M., Magliocca, N., Porkka, M., & Puma, M. (2017). Resilience in the global food system. *Environmental Research Letters*, *12*(2), 025010.

Segal, M. R. (2004). Machine learning benchmarks and random forest regression.

Shapley, L. S. (1953). A value for n-person games.

Skea, J., Shukla, P. R., Reisinger, A., Slade, R., Pathak, M., Al Khourdajie, A., van Diemen, R., Abdulla, A., Akimoto, K., & Babiker, M. (2022). Summary for policymakers. In *Climate change 2022: Mitigation of climate change: Contribution of working group iii to the sixth assessment report of the intergovernmental panel on climate change*. Cambridge University Press.

Springmann, M., Clark, M., Mason-D'Croz, D., Wiebe, K., Bodirsky, B. L., Lassaletta, L., De Vries, W., Vermeulen, S. J., Herrero, M., & Carlson, K. M. (2018). Options for keeping the food system within environmental limits. *Nature*, *562*(7728), 519–525.

Springmann, M., Godfray, H. C. J., Rayner, M., & Scarborough, P. (2016). Analysis and valuation of the health and climate change cobenefits of dietary change. *Proceedings of the National Academy of Sciences*, *113*(15), 4146–4151.

Springmann, M., Mason-D'Croz, D., Robinson, S., Garnett, T., Godfray, H. C. J., Gollin, D., Rayner, M., Ballon, P., & Scarborough, P. (2016). Global and regional health effects of future food production under climate change: A modelling study. *The Lancet*, *387*(10031), 1937–1946.

Stehl, J., Vonderschmidt, A., Vollmer, S., Alexander, P., & Jaacks, L. M. (2025). Gap between national food production and food-based dietary guidance highlights lack of national self-sufficiency. *Nature Food*, 1–6.

Stokeld, E., Croft, S. A., Green, J. M., & West, C. D. (2020). Climate change, crops and commodity traders: Subnational trade analysis highlights differentiated risk exposure. *Climatic change*, *162*, 175–192.

Sun, Q., Hou, M., Shi, S., Cui, L., & Xi, Z. (2022). The influence of country risks on the international agricultural trade patterns based on network analysis and panel data method. *Agriculture*, *12*(3), 361.

Sun, Z., Scherer, L., Tukker, A., & Behrens, P. (2020). Linking global crop and livestock consumption to local production hotspots. *Global food security*, *25*, 100323.

Sun, Z., Scherer, L., Zhang, Q., & Behrens, P. (2022). Adoption of plant-based diets across europe can improve food resilience against the russia–ukraine conflict. *Nature Food*, *3*(11), 905–910.

Suweis, S., Carr, J. A., Maritan, A., Rinaldo, A., & D'Odorico, P. (2015). Resilience and reactivity of global food security. *Proceedings of the National Academy of Sciences*, *112*(22), 6902–6907.

Takayama, T., Hashimoto, H., & Uri, N. (1984). Spatial and temporal price and allocation modeling: Some extensions. *Socio-Economic Planning Sciences*, *18*(4), 227–234.

Takayama, T. (1971). Spatial and temporal price and allocation models.

Takayama, T., & Judge, G. G. (1964). An intertemporal price equilibrium model. *Journal of Farm Economics*, *46*(2), 477–484.

Tendall, D. M., Joerin, J., Kopainsky, B., Edwards, P., Shreck, A., Le, Q. B., Kruetli, P., Grant, M., & Six, J. (2015). Food system resilience: Defining the concept. *Global food security*, *6*, 17–23.

Thøgersen, J., & Nielsen, K. S. (2016). A better carbon footprint label. *Journal of Cleaner Production*, *125*, 86–94.

Tilman, D., Balzer, C., Hill, J., & Befort, B. L. (2011). Global food demand and the sustainable intensification of agriculture. *Proceedings of the national academy of sciences*, *108*(50), 20260–20264.

Tilman, D., & Clark, M. (2014). Global diets link environmental sustainability and human health. *Nature*, *515*(7528), 518–522.

Torero, M. (2021). The state of food and agriculture 2021. making agrifood systems more resilient to shocks and stresses.

Traverso, S., & Schiavo, S. (2020). Fair trade or trade fair? international food trade and cross-border macronutrient flows. *World Development*, *132*, 104976.

Tubiello, F. N., Soussana, J.-F., & Howden, S. M. (2007). Crop and pasture response to climate change. *Proceedings of the National Academy of Sciences*, *104*(50), 19686–19690.

Union, A. (n.d.). Comprehensive african agricultural development programme (caadp). https://caadp.org/

Van Berkum, S., Dengerink, J., & Ruben, R. (2018). The food systems approach: Sustainable solutions for a sufficient supply of healthy food.

Venkatramanan, S., Wu, S., Shi, B., Marathe, A., Marathe, M., Eubank, S., Sah, L. P., Giri, A., Colavito, L. A., & Nitin, K. (2017). Towards robust models of food flows and their role in invasive species spread. *2017 IEEE International Conference on Big Data (Big Data)*, 435–444.

Verschuur, J., Murgatroyd, A., Vittis, Y., Mosnier, A., Obersteiner, M., Godfray, C., & Hall, J. (2024). The impacts of polycrises on global grain availability and prices.

Verschuur, J., Vittis, Y., Obersteiner, M., & Hall, J. (2023). Cost drivers of international grains and oilseeds trade.

Vishwakarma, S., Zhang, X., & Lyubchich, V. (2022). Wheat trade tends to happen between countries with contrasting extreme weather stress and synchronous yield variation. *Communications Earth & Environment*, *3*(1), 261.

Wang, T., & Sun, F. (2022). Global gridded gdp data set consistent with the shared socioeconomic pathways, sci. data, 9, 221.

Weber, C. L., & Matthews, H. S. (2008). Food-miles and the relative climate impacts of food choices in the united states.

Weisberg, S. (2005). *Applied linear regression* (Vol. 528). John Wiley & Sons.

Wellesley, L., Preston, F., Lehne, J., & Bailey, R. (2017). Chokepoints in global food trade: Assessing the risk. *Research in transportation business & management*, *25*, 15–28.

Westlake, M. J. (2005). *Addressing marketing and processing constraints that inhibit agrifood exports: A guide for policy analysts and planners*. Food & Agriculture Org.

Willett, W., Rockström, J., Loken, B., Springmann, M., Lang, T., Vermeulen, S., Garnett, T., Tilman, D., DeClerck, F., & Wood, A. (2019). Food in the anthropocene: The eat–lancet commission on healthy diets from sustainable food systems. *The lancet*, *393*(10170), 447–492.

Wood, A., Queiroz, C., Deutsch, L., González-Mon, B., Jonell, M., Pereira, L., Sinare, H., Svedin, U., & Wassénius, E. (2023). Reframing the local–global food systems debate through a resilience lens. *Nature Food*, *4*(1), 22–29.

Woodhill, J., & Quak, E.-j. (2019). Changing food systems: Implications for dfid priorities. *contexts*, *7*, 5.

WorldPop. (n.d.). The spatial distribution of population in 2020. https://hub.worldpop.org/geodata/summary?id=24777

Zhang, C., Yang, Y., Feng, Z., Xiao, C., Lang, T., Du, W., & Liu, Y. (2021). Risk of global external cereals supply under the background of the covid-19 pandemic: Based on the perspective of trade network. *Foods*, *10*(6), 1168.

Zhang, Y.-T., & Zhou, W.-X. (2022). Structural evolution of international crop trade networks. *Frontiers in Physics*, *10*, 926764.

Zurek, M., Ingram, J., Sanderson Bellamy, A., Goold, C., Lyon, C., Alexander, P., Barnes, A., Bebber, D. P., Breeze, T. D., & Bruce, A. (2022). Food system resilience: Concepts, issues, and challenges. *Annual Review of Environment and Resources*, *47*(1), 511–534.